frontiers | Research Topics

# The essential role of multidisciplinary teams in breast cancer surgery: collaboration for superior patient outcomes

**Edited by**
Piero Fregatti, Raquel Diaz, Francesca Poggio and Alessandra Fozza

**Coordinated by**
Letizia Cuniolo and Irene Giannubilo

**Published in**
Frontiers in Oncology

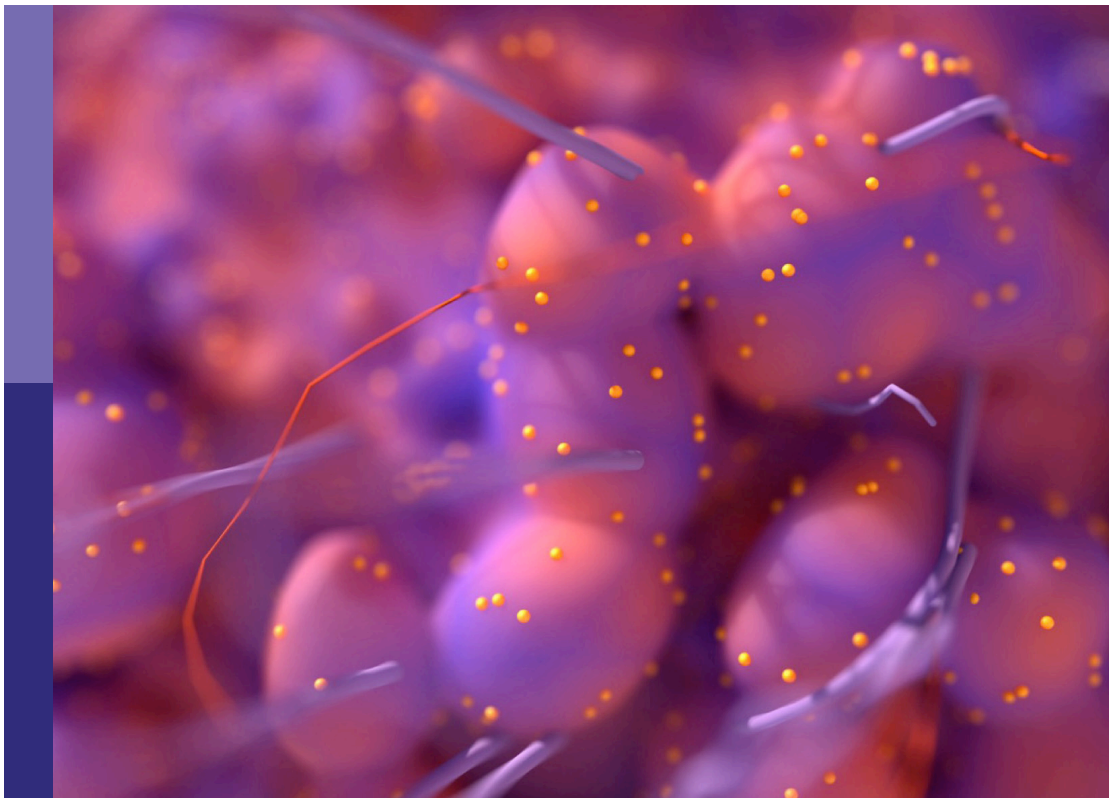

ISSN 1664-8714
ISBN 978-2-8325-7386-0
DOI 10.3389/978-2-8325-7386-0

**Generative AI statement**
Any alternative text (Alt text) provided alongside figures in the articles in this ebook has been generated by Frontiers with the support of artificial intelligence and reasonable efforts have been made to ensure accuracy, including review by the authors wherever possible. If you identify any issues, please contact us.

## About Frontiers

Frontiers is more than just an open access publisher of scholarly articles: it is a pioneering approach to the world of academia, radically improving the way scholarly research is managed. The grand vision of Frontiers is a world where all people have an equal opportunity to seek, share and generate knowledge. Frontiers provides immediate and permanent online open access to all its publications, but this alone is not enough to realize our grand goals.

## Frontiers journal series

The Frontiers journal series is a multi-tier and interdisciplinary set of open-access, online journals, promising a paradigm shift from the current review, selection and dissemination processes in academic publishing. All Frontiers journals are driven by researchers for researchers; therefore, they constitute a service to the scholarly community. At the same time, the *Frontiers journal series* operates on a revolutionary invention, the tiered publishing system, initially addressing specific communities of scholars, and gradually climbing up to broader public understanding, thus serving the interests of the lay society, too.

## Dedication to quality

Each Frontiers article is a landmark of the highest quality, thanks to genuinely collaborative interactions between authors and review editors, who include some of the world's best academicians. Research must be certified by peers before entering a stream of knowledge that may eventually reach the public - and shape society; therefore, Frontiers only applies the most rigorous and unbiased reviews. Frontiers revolutionizes research publishing by freely delivering the most outstanding research, evaluated with no bias from both the academic and social point of view. By applying the most advanced information technologies, Frontiers is catapulting scholarly publishing into a new generation.

## What are Frontiers Research Topics?

Frontiers Research Topics are very popular trademarks of the *Frontiers journals series*: they are collections of at least ten articles, all centered on a particular subject. With their unique mix of varied contributions from Original Research to Review Articles, Frontiers Research Topics unify the most influential researchers, the latest key findings and historical advances in a hot research area.

Find out more on how to host your own Frontiers Research Topic or contribute to one as an author by contacting the Frontiers editorial office: frontiersin.org/about/contact

# The essential role of multidisciplinary teams in breast cancer surgery: collaboration for superior patient outcomes

**Topic editors**
Piero Fregatti — University of Genoa, Italy
Raquel Diaz — University of Genova, Italy
Francesca Poggio — San Martino Hospital (IRCCS), Italy
Alessandra Fozza — San Martino Hospital (IRCCS), Italy

**Topic coordinators**
Letizia Cuniolo — University of Genoa, Italy
Irene Giannubilo — University of Genoa, Italy

**Citation**
Fregatti, P., Diaz, R., Poggio, F., Fozza, A., Cuniolo, L., Giannubilo, I., eds. (2026). *The essential role of multidisciplinary teams in breast cancer surgery: collaboration for superior patient outcomes*. Lausanne: Frontiers Media SA.
doi: 10.3389/978-2-8325-7386-0

# Table of contents

frontiers | Frontiers in Oncology

TYPE Editorial
PUBLISHED 07 January 2026
DOI 10.3389/fonc.2025.1754900



OPEN ACCESS

EDITED AND REVIEWED BY
Kara Britt,
Peter MacCallum Cancer Centre, Australia

*CORRESPONDENCE
Raquel Diaz
raqueldiaz.ge@gmail.com

RECEIVED 26 November 2025
ACCEPTED 15 December 2025
PUBLISHED 07 January 2026

CITATION
Diaz R, Poggio F, Fozza A, Giannubilo I, Cuniolo L and Fregatti P (2026) Editorial: The essential role of multidisciplinary teams in breast cancer surgery: collaboration for superior patient outcomes. *Front. Oncol.* 15:1754900. doi: 10.3389/fonc.2025.1754900



# Editorial: The essential role of multidisciplinary teams in breast cancer surgery: collaboration for superior patient outcomes

Raquel Diaz[1]*, Francesca Poggio[2], Alessandra Fozza[3], Irene Giannubilo[2], Letizia Cuniolo[1] and Piero Fregatti[1]

[1]Department of Surgical and Diagnostic Integrated Sciences (DISC), University of Genova, Genova, Italy, [2]Medical Oncology Unit 2, Istituto di Ricovero e Cura a Carattere Scientifico (IRCCS) Ospedale Policlinico San Martino, Genoa, Italy, [3]Department of Radiation Oncology, IRCCS Ospedale Policlinico San Martino, Genova, Italy

KEYWORDS

**breast cancer surgery, collaborative care, multidisciplinary team (MDT), patient-centered approach, precision medicine**

Editorial on the Research Topic
The essential role of multidisciplinary teams in breast cancer surgery: collaboration for superior patient outcomes

## Introduction

Breast cancer remains one of the most common and complex diseases affecting women worldwide, and its management increasingly depends on the integration of multiple medical disciplines. In recent years, advances in imaging, genetics, and surgical techniques have significantly changed our approach, but the most important element has been the development of multidisciplinary teamwork. The idea that no single specialty can fully address the needs of breast cancer patients has evolved from concept to reality. Today, successful treatment is not only about the precision of surgery or the accuracy of diagnosis, but about the coordination, dialogue, and shared expertise that bring those elements together.

This Research Topic, "*The Essential Role of Multidisciplinary Teams in Breast Cancer Surgery: Collaboration for Superior Patient Outcomes*" was designed to explore how collaboration drives progress in breast cancer care. The eleven papers gathered in this Research Topic reflect the remarkable range of perspectives that define modern practice, from the operating room to the radiology suite, from pathology and oncology to psychology and rehabilitation. Together, they illustrate that true innovation arises when disciplines meet around the same patient.

## The value of collaboration

Multidisciplinary care has become the cornerstone of comprehensive breast cancer management. Team discussions allow for individualized treatment planning, the alignment of oncologic and reconstructive goals, and improved communication with patients and

their families. Beyond the practical aspects, these meetings foster a shared culture of decision-making where every professional contributes their expertise to a common purpose.

The articles included in this Research Topic demonstrate this principle in different but complementary ways. Some highlight how close collaboration between radiologists and pathologists prevents misdiagnosis in rare entities, as in the reports of mucinous carcinoma in a male patient or adenoid cystic carcinoma with multiple metastases. Others, such as those describing benign lesions initially suspected as malignancies, remind us how dialogue between specialists can prevent unnecessary procedures and anxiety for patients.

Technological advances also play a growing role within multidisciplinary settings. Two studies in this Topic explore the use of artificial intelligence and radiomics in ultrasound evaluation, showing how computational models can assist clinicians in predicting therapeutic response and improving diagnostic accuracy. However, these studies also show that technological progress reaches its real potential only when embedded in multidisciplinary collaboration.

Surgical innovation is another area where collaboration proves essential. Papers addressing complex postoperative complications, such as refractory seroma, or describing multidisciplinary management of chemotherapy extravasation, provide tangible examples of how teamwork translates into better outcomes. Similarly, the study exploring combined lung biopsy and microwave ablation for suspected metastases expands the boundaries of breast surgery, integrating thoracic expertise into oncologic care.

Finally, the human dimension of multidisciplinary care is powerfully represented by the study on pain management from the ARISE project. By involving anesthesiologists, oncologists, psychologists, and rehabilitation specialists, it underscores that addressing pain is not merely a technical issue but a holistic challenge requiring shared responsibility.

Reading across all these papers, several lessons emerge. Communication itself is therapeutic: regular, structured discussion among specialists leads to earlier and more accurate decisions. Innovation thrives on integration: new technologies, from AI to image-guided surgery, succeed only when evaluated through collective expertise. True personalization of breast cancer treatment depends on teamwork, combining clinical, molecular, and psychosocial insights. And sustained education in interdisciplinary collaboration ensures that these advances endure across generations.

Taken together, this Research Topic goes beyond the technical or academic level. It captures a shift in mindset: from isolated excellence to collective intelligence, showing that progress in breast cancer surgery is built on communication and trust between disciplines.

## Conclusion

The contributions gathered in this Research Topic collectively affirm that multidisciplinary teamwork is no longer optional in breast cancer surgery: it is essential. Each article illustrates a different facet of collaboration, whether in diagnosis, operative strategy, complication management, or supportive care. Together, they provide a snapshot of a field that continues to evolve toward integration, precision, and humanity.

As Guest Editors, we are deeply grateful to the authors and reviewers who have contributed to this project. Their commitment and expertise reflect the very principles this Topic celebrates: communication, cooperation, and shared purpose. We hope this Research Topic will serve as both a scientific reference and an inspiration for future endeavors, reminding us all that in breast cancer surgery, the best outcomes are achieved when we work together across disciplines, across institutions, and always in partnership with our patients.

## Author contributions

RD: Conceptualization, Data curation, Investigation, Methodology, Project administration, Supervision, Validation, Writing – original draft, Writing – review & editing. FP: Conceptualization, Data curation, Investigation, Methodology, Project administration, Supervision, Validation, Writing – original draft, Writing – review & editing. AF: Conceptualization, Data curation, Investigation, Methodology, Project administration, Supervision, Validation, Writing – original draft, Writing – review & editing. IG: Data curation, Investigation, Methodology, Writing – original draft, Writing – review & editing. LC: Data curation, Investigation, Methodology, Writing – original draft, Writing – review & editing. PF: Conceptualization, Data curation, Investigation, Methodology, Project administration, Supervision, Validation, Writing – original draft, Writing – review & editing.

## Conflict of interest

The authors declared that this work was conducted in the absence of any commercial or financial relationships that could be construed as a potential conflict of interest.

## Generative AI statement

The author(s) declared that generative AI was used in the creation of this manuscript. During the preparation of this work the authors used ChatGPT in order to improve the readability and language of the manuscript. After using this tool, the authors reviewed and edited the content as needed and take full responsibility for the content of the published article.

Any alternative text (alt text) provided alongside figures in this article has been generated by Frontiers with the support of artificial intelligence and reasonable efforts have been made to ensure accuracy, including review by the authors wherever possible. If you identify any issues, please contact us.

## Publisher's note

frontiers | Frontiers in Oncology

TYPE Case Report
PUBLISHED 06 February 2025
DOI 10.3389/fonc.2025.1521704



OPEN ACCESS

EDITED BY
Raquel Diaz,
University of Genova, Italy

REVIEWED BY
Francesca Combi,
University of Modena and Reggio Emilia, Italy
Cherry Bansal,
Tantia University, India

*CORRESPONDENCE
Jie Ma
cjr.majie@vip.163.com

RECEIVED 02 November 2024
ACCEPTED 17 January 2025
PUBLISHED 06 February 2025

CITATION
Lin X, Liao T, Yang Y, Zhou J and Ma J (2025) Mucinous carcinoma in a male breast with skin ulcer: a case report.
*Front. Oncol.* 15:1521704.
doi: 10.3389/fonc.2025.1521704



# Mucinous carcinoma in a male breast with skin ulcer: a case report

Xiaohui Lin, Tingting Liao, Yuting Yang, Jingzhi Zhou and Jie Ma*

Department of Radiology, Shenzhen People's Hospital, The Second Clinical Medical College of Jinan University, Shenzhen, China

A case of pure mucinous carcinoma of the male breast presenting with skin ulceration was reported. The patient, a 67-year-old male, inadvertently discovered a subcutaneous mass with the size of a soybean near the areola on the right side of his chest. Pathological analysis identified the mass as mucinous adenocarcinoma. Differentiating between primary mucinous carcinoma of the skin and mucinous carcinoma of the breast was challenging due to their overlapping histological and immunohistochemical features. Ultimately, the tumor was diagnosed as pure mucinous carcinoma of the male breast based on the primary site and clinical history.

KEYWORDS

**male breast tumor, magnetic resonance imaging, cutaneous mucinous carcinoma, breast mucinous carcinoma, skin ulcer**

## Introduction

Male breast cancer is a rare disease, accounting for less than 1% of all breast cancer cases worldwide (1, 2). Mucinous carcinoma, also known as colloid or gelatinous carcinoma, is extremely rare in males. Differentiating between breast mucinous carcinoma and cutaneous mucinous carcinoma (e.g., primary mucinous degeneration of the skin or mucinous skin cancer) in males through radiological and histopathological examinations can be challenging, particularly when the skin is ulcerated. This study aimed to report a case of pure mucinous adenocarcinoma of the male breast with skin ulceration and review the clinical and imaging features of this exceptionally rare tumor, providing valuable information for the differential diagnosis of cutaneous mucinous carcinoma.

## Case presentation

### Patient's information

The patient is a 67-year-old male who inadvertently discovered a subcutaneous nodule, about the size of a soybean, near the areola on the right side of his chest in 2020. The patient reported undergoing ultrasound and CT scans at a local hospital, although the specific

details were unclear. The nodule was initially suspected to be a dermatofibroma and was left untreated. Recently, the patient noticed rapid growth of the nodule into a mass accompanied by skin erythema and ulceration. Seeking further treatment, he was admitted to the breast surgery department of our hospital on July 28, 2022. He had no family history of breast cancer or other malignancies.

## Clinical finding

Physical examination revealed a large mass behind the nipple on the right side of his chest, about 5.0 cm × 4.0 cm in size, with an uneven surface, soft texture, unclear boundaries, poor mobility, and no adhesion to the chest wall. The surface skin was dark red and ulcerated (Figure 1). Enlarged lymph nodes, about 1.5 cm in size, were palpable in the right axilla.

## Imaging examinations

Ultrasound examination was performed on July 28, 2022. A heterogeneous isoechoic mass was observed behind the right nipple, approximately 60 mm × 43 mm in size, with a lobulated shape, smooth edges, a distinct capsule, and slightly increased posterior echoes. No lateral acoustic shadows were found (Figure 2A). Color Doppler flow imaging (CDFI) displayed no significant blood flow signals in the mass, while a small amount of blood flow signals was visible around the periphery. The mass was classified as BI-RADS 4B.

To further confirm the diagnosis, breast magnetic resonance imaging (MRI) was performed on August 8, 2022. The MRI showed the right breast exhibited increased volume, with a lobulated mass of approximately 48 mm × 56 mm × 56 mm in size and clear boundaries. The mass showed low signal intensity on T1-weighted image (T1WI) (Figure 2B), and high signal intensity on T2-weighted image (T2WI) (Figure 2C) and fat-suppressed T2WI (Figure 2D). Diffusion-weighted imaging (DWI) with a b-value of 800 s (Figure 2E) and apparent diffusion coefficients (ADCs) (Figure 2F) demonstrated high signal intensity. The dynamic contrast-enhanced scan revealed heterogeneous enhancement, with slow and progressive enhancement gradually filling the center of the lesion (Figure 2G). The time-signal intensity curve (TIC) was type III (slow-persistent) (Figure 2H). The right nipple displayed abnormal morphology, with indistinct boundaries near the tumor and evidence of adjacent skin invasion. The lesion was categorized as BI-RADS 6.

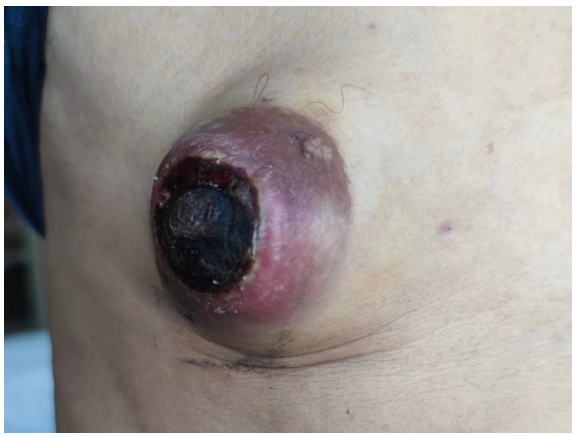

FIGURE 1
A mass on the right side of the male patient's chest.

## Pathological and immunohistochemical results

Ultrasound-guided core needle biopsy (CNB) of the right breast mass was performed on August 4, 2022. The biopsy indicated three tissue strips with a mucinous appearance on the cut surface, revealing atypical cells in a mucus-rich background. The findings suggested the possibility of mucinous carcinoma.

The patient underwent breast surgery on August 11, 2022. Postoperative pathology: Gross pathology showed that the tumor's cut surface was gray-white, gray-yellow, gel-like, with moderate texture and unclear boundaries. Microscopically, the tumor cells were trabecular, ribbon-like, and micropapillary, containing a large amount of extracellular mucus (Figure 2I). The cells had low-grade nuclei with rare nuclear division. Immunohistochemical results were summarized as follows: ER (approximately 70%, 2+), PR (approximately 60%, 2+), HER2 (1+), KI67 (approximately 5%+), E-Ca (+), P120 (+), P63 (-), Calponin (-), CK5-6 (-), EMA B (+), Syn (-), WY-1 (+). Based on the postoperative pathological results, the final diagnosis was mucinous carcinoma, classic type, grade II. The tumor invaded the skin of the areola papilla. Sentinel lymph node biopsy of the right axilla showed no signs of metastasis (0/3).

## Multidisciplinary expert consultation

A multidisciplinary consultation involving the departments of breast surgery, oncology, radiology, ultrasound, and pathology confirmed the diagnosis of primary mucinous carcinoma of the male breast based on histopathological examination and immunohistochemistry analysis of the excised tissue.

## Final diagnosis

The patient was diagnosed with pure mucinous adenocarcinoma of the male breast.

## Therapeutic intervention and follow-up

The patient underwent modified radical mastectomy (Figure 3), followed by tamoxifen hormone therapy. He was monitored for two years, and no evidence of tumor recurrence was found.

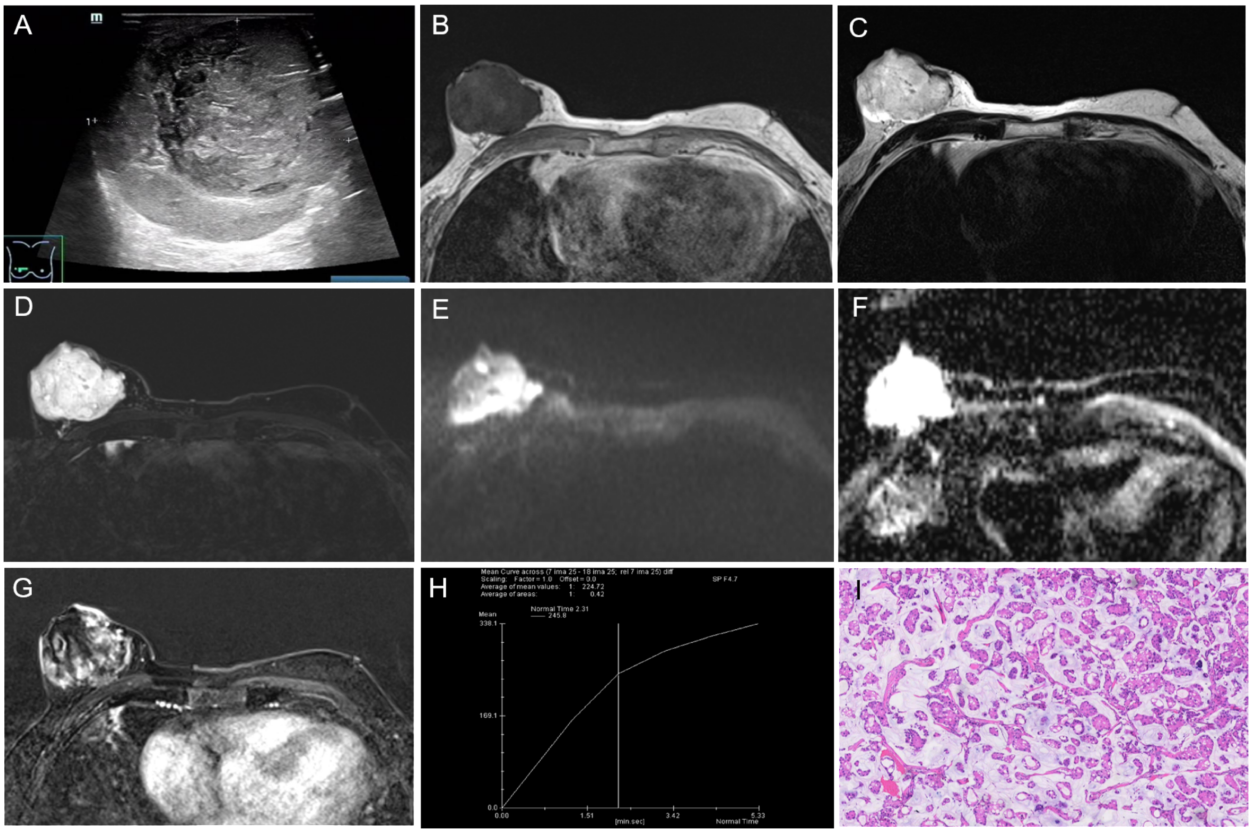


FIGURE 2
The results of imaging and pathological examinations. **(A)** Ultrasound showing a heterogeneous isoechoic mass behind the right breast nipple, with a lobulated shape and smooth edges. Breast MR images: **(B)** T1-weighted image (T1WI) demonstrating the mass with low signal intensity, **(C)** T2-weighted image (T2WI) and **(D)** fat-suppressed T2WI showing significantly high signal intensity. **(E)** Diffusion-weighted imaging (DWI) with a b-value of 800s showed high signal intensity. **(F)** the apparent diffusion coefficient (ADC) both showed high signal intensity. **(G)** The dynamic contrast-enhanced scan revealed the mass with heterogeneous, slow, and progressive enhancement. **(H)** The time-signal intensity curve (TIC) indicated type III (slow-persistent) enhancement. **(I)** Photomicrograph of histological image showing the tumor cells in trabecular, ribbon-like, and micropapillary shapes, containing a large amount of extracellular mucus (HE × 100). T1WI, T1-weighted image; T2WI, T2 weighted image; MRI, magnetic resonance imaging; DWI, diffusion-weightedimaging; TIC, time-signal intensity curve; ADC, apparent diffusion coefficient; HE, hematoxylin and eosin.

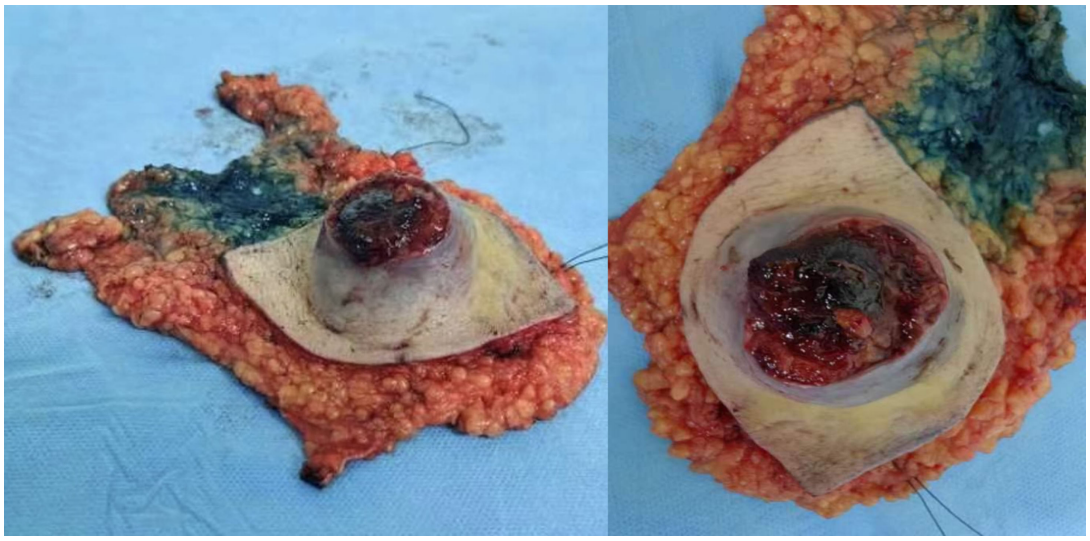

FIGURE 3
Right breast specimen.

## Discussion

Mucinous carcinoma, also referred to as colloid or gelatinous carcinoma, is among the rarest types of breast cancer, accounting for less than 2% of female breast carcinomas (3). Its occurrence in the male breast is extremely rare. Histopathologically, mucinous carcinoma is characterized by the presence of clusters of neoplastic cells suspended in extensive extracellular mucin, and it can be subclassified into pure and mixed types. Pure mucinous carcinoma type contains mucinous carcinoma components, accounting for more than 90% of the tumor, while the mixed type has both mucinous and invasive ductal carcinoma components (4). In the present case, diagnosis of pure mucinous carcinoma was made as no conventional invasive ductal carcinoma component was present. Pure mucinous carcinoma grows slowly, accompanying by relatively favorable prognosis, low recurrence rate, and low incidence of lymph node metastasis (5, 6). Its pathogenesis remains elusive, however, studies suggested its link with genetics and hormones (7, 8). Prior research demonstrated that gynecomastia is not a risk factor for male breast cancer (9).

Pure mucinous carcinoma is typically associated with favorable prognosis, and it is mainly misdiagnosed as a benign tumor on imaging examination (10). Even in female breasts, metastasis and invasion of contiguous structures are rare, typically presenting as a solitary breast mass without skin involvement or noticeable changes. However, in the present case, the tumor was found both in the skin and at the base of the areola and nipple. This could be attributed to the lower amount of fat in male breast tissue, which positions the tumor closer to the skin and increases the likelihood of dermal and basal infiltration. The histological and immunohistochemical characteristics of primary mucinous carcinoma of the skin and mucinous carcinoma of the breast overlap, complicating differential diagnosis. According to previous studies, three-quarters of mucinous carcinoma cases affecting the skin were found on the head, primarily on the eyelid (44%), with only a small proportion (5%) occurring on the chest (11, 12). Comparing the morphology and immune markers of the tumor in this case, it was difficult to determine whether it originated from the breast or chest wall skin. The primary site of the tumor indicates tissue origin: if the tumor begins on the skin surface, ruptures early, and then gradually grows into the breast, it is considered to originate from the skin appendages of the chest wall. Conversely, if the tumor originates deep within the breast tissue and subsequently involves the skin, it suggests a more typical breast origin. In the present case, the tumor was finally diagnosed as primary mucinous carcinoma of the male breast based on its primary site.

Pure mucinous carcinoma has imaging characteristics that may mimic benign lesions. On mammography, it mainly presents as a round or microlobulated, well-circumscribed high-density mass without microcalcification (10). On ultrasound, it appears as an isoechogenic mass with well-defined margins, relative to the surrounding fat, accompanying by posterior echo enhancement (13). MRI findings exhibit distinctive characteristics: on T1WI, signal intensity varies from low to high based on protein concentrations in the tumors. Mucinous carcinoma, owing to its abundant mucin content, typically demonstrates high signal intensity on T2WI (14). Early enhancement reveals gradual circular enhancement surrounding the tumor periphery, indicating that tumor cells are clustered around a central pool of mucin. The TICs from dynamic contrast-enhanced MRI exhibit a gradually enhancing pattern (15). Mucinous carcinoma needs to be distinguished from myxoid fibroadenoma, mucocele-like lesions, and encapsulated papillary carcinoma. Myxoid fibroadenoma and mucocele-like lesions present as distinct high-signal masses on T2WI, while they are mainly accompanied by coarse or amorphous calcification on mammograms. Encapsulated papillary carcinoma appears as a mixed solid and cystic mass with no enhancement of the cystic component and obvious enhancement of the solid component on enhanced scans. This case also needed differentiation of metastasis from mucinous adenocarcinoma of other sites, while no primary malignancy was found in this patient.

Although breast mucinous carcinoma and cutaneous mucinous carcinoma both belong to the category of mucinous carcinomas, there are some differences in their treatment methods. Primary mucinous carcinoma of the skin, a rare malignancy of the sweat glands, is characterized by low metastatic potential but a high recurrence rate. Lymph node dissection is typically unnecessary, as regional lymph node metastasis is rare in this type of carcinoma (16). Treatment concentrates on wide excision of the lesion, which may include standard local excision or Mohs micrographic surgery (17). Radiotherapy and chemotherapy are generally not utilized due to the resistance of cutaneous mucinous carcinoma to these modalities (18). In contrast, the standard treatment for male breast mucinous carcinoma involves modified radical mastectomy with sentinel lymph node biopsy, followed by adjuvant therapy. Hormonal therapy plays a pivotal role in treatment, given the high prevalence of hormone receptor positivity in male breast carcinomas (19). Patients with either type of carcinoma are recommended to undergo regular follow-up to monitor for local tumor recurrence or regional lymphadenopathy. However, standardized guidelines for the duration and frequency of follow-up sessions have not yet been provided (16, 20). The specific follow-up strategy should be based on the patient's individual circumstances and physician's advice.

Male breast mucinous carcinoma is rare and exhibits imaging characteristics similar to those of mucinous adenocarcinoma in female breast. However, distinguishing between breast mucinous carcinoma and primary mucinous carcinoma of skin on imaging is difficult due to overlapping histopathological features. Therefore, a definitive diagnosis mainly requires consideration of clinical history. Given the differences in clinical behavior and treatment strategies between mucinous carcinoma of the breast and primary mucinous carcinoma of the skin, it is crucial to ensure an accurate diagnosis.

## Data availability statement

The original contributions presented in the study are included in the article/supplementary material. Further inquiries can be directed to the corresponding author.

## Ethics statement

Written informed consent was obtained from the individual(s) for the publication of any potentially identifiable images or data included in this article.

## Author contributions

XL: Investigation, Writing – original draft, Writing – review & editing, Conceptualization, Supervision. TL: Conceptualization, Formal analysis, Investigation, Writing – review & editing. YY: Conceptualization, Formal analysis, Investigation, Resources, Writing – review & editing. JZ: Formal analysis, Investigation, Writing – review & editing. JM: Formal analysis, Funding acquisition, Methodology, Writing – review & editing.

## Funding

The author(s) declare financial support was received for the research, authorship, and/or publication of this article. This study was supported by Shenzhen Science and Technology Research and Development Fund (Grant No.GJHZ20220913142613025), which was critical to the successful completion of this study.

## Conflict of interest

The authors declare that the research was conducted in the absence of any commercial or financial relationships that could be construed as a potential conflict of interest.

## Generative AI statement

The author(s) declare that no Generative AI was used in the creation of this manuscript.

## Publisher's note



## References

1. Fox S, Speirs V, Shaaban AM. Male breast cancer: an update. *Virchows Arch*. (2022) 480:85–93. doi: 10.1007/s00428-021-03190-7

2. McClurg DP, Urquhart G, McGoldrick T, Chatterji S, Miedzybrodzka Z, Speirs V, et al. Analysis of the clinical advancements for BRCA-related Malignancies highlights the lack of treatment evidence for BRCA-positive male breast cancer. *Cancers (Basel)*. (2022) 14(13):3175. doi: 10.3390/cancers14133175

3. Bray F, et al. Global cancer statistics 2022: GLOBOCAN estimates of incidence and mortality worldwide for 36 cancers in 185 countries. *CA: Cancer J Clin*. (2024) 74:229–63. doi: 10.3322/caac.21834

4. Kashiwagi S, Onoda N, Asano Y, Noda S, Kawajiri H, Takashima T, et al. Clinical significance of the sub-classification of 71 cases mucinous breast carcinoma. *Springerplus*. (2013) 2:481. doi: 10.1186/2193-1801-2-481

5. Emiroglu S, Tukenmez M, Karakus S, Karanlik H, Onder S, Ozmen V, et al. Pure mucinous breast carcinoma with a favorable tumor biology and clinical outcomes. *Eur J Breast Health*. (2022) 18(4):353–9. doi: 10.4274/ejbh.galenos.2022.2022-8-1

6. Yang M, Li X, Chun-Hong P, Lin-Ping H. Pure mucinous breast carcinoma: a favorable subtype. *Breast Care (Basel)*. (2013) 8:56–9. doi: 10.1159/000346828

7. Khan NAJ, Tirona M. An updated review of epidemiology, risk factors, and management of male breast cancer. *Med Oncol*. (2021) 38:39. doi: 10.1007/s12032-021-01486-x

8. Rizzolo P, Silvestri V, Tommasi S, Pinto R, Danza K, Falchetti M, et al. Male breast cancer: genetics, epigenetics, and ethical aspects. *Ann Oncol*. (2013) 24 Suppl 8:viii75–82. doi: 10.1093/annonc/mdt316

9. Coopey SB, Kartal K, Li C, Yala A, Barzilay R, Faulkner HR, et al. Atypical ductal hyperplasia in men with gynecomastia: what is their breast cancer risk? *Breast Cancer Res Treat*. (2019) 175(1):1–4. doi: 10.1007/s10549-018-05117-4

10. Kuzmiak CM, Calhoun BC. Pure mucinous carcinoma of the breast: radiologic-pathologic correlation. *J Breast Imaging*. (2023) 5:180–7. doi: 10.1093/jbi/wbac084

11. Boynton JR, Markowitch W Jr. Mucinous eccrine carcinoma of the eyelid. *Arch Ophthalmol*. (1998) 116:1130–1. doi: 10.1001/archopht.116.8.1130

12. Mardi K, Diwana VK. Primary cutaneous mucinous carcinoma: a rare entity. *Indian Dermatol Online J*. (2011) 2:82–4. doi: 10.4103/2229-5178.85997

13. Memis A, Ozdemir N, Parildar M, Ustun EE, Erhan Y. Mucinous (colloid) breast cancer: mammographic and US features with histologic correlation. *Eur J Radiol*. (2000) 35(1):39–43. doi: 10.1016/s0720-048x(99)00124-2

14. Monzawa S, Yokokawa M, Sakuma T, Takao S, Hirokaga K, Hanioka K, et al. Mucinous carcinoma of the breast: MRI features of pure and mixed forms with histopathologic correlation. *AJR Am J Roentgenol*. (2009) 192(3):W125–31. doi: 10.2214/AJR.07.4021

15. Bitencourt AG, Graziano L, Osório CA, Guatelli CS, Souza JA, Mendonça MH, et al. MRI features of mucinous cancer of the breast: correlation with pathologic findings and other imaging methods. *AJR Am J Roentgenol*. (2016) 206(2):238–46. doi: 10.2214/AJR.15.14851

16. Javaid H, Raza N, Ejaz U, Sarfraz T. Unusual skin mass (primary cutaneous mucinous carcinoma). *BMJ Case Rep*. (2018) 2018:bcr2017222546. doi: 10.1136/bcr-2017-222546

17. Beteddini OS, Sheikh S, Shareefi F, Shahab R. Primary mucinous adenocarcinoma in the oscalp: a case report and literature review. *Int J Surg Case Rep*. (2015) 10:241–4. doi: 10.1016/j.ijscr.2015.02.006

18. Breiting L, Dahlstrøm K, Christensen L, Winther Jeanette F, Breiting Vibeke M. Primary mucinous carcinoma of the skin. *Am J Dermatopathol*. (2007) 29(6):595–6. doi: 10.1097/DAD.0b013e318158d878

19. Gupta K, Sharma S, Kudva R, Kumar S. Mixed mucinous and infiltrating carcinoma occurring in male breast-study of clinico-pathological features: A rare case report. *J Clin Diagn Res*. (2015) 9(6):ED07–ED8. doi: 10.7860/JCDR/2015/12209.6090

20. Ishida M, Umeda T, Kawai Y, Mori T, Kubota Y, et al. Mucinous carcinoma occurring in the male breast. *Oncol Lett*. (2014) 7(2):378–80. doi: 10.3892/ol.2013.1730

frontiers | Frontiers in Oncology

TYPE Original Research
PUBLISHED 12 March 2025
DOI 10.3389/fonc.2025.1536709



OPEN ACCESS

EDITED BY
Sharon R Pine,
University of Colorado, United States

REVIEWED BY
Shinya Suzuki,
National Cancer Center Hospital East, Japan
Yumeng Lin,
Chengdu University of Traditional Chinese Medicine, China

*CORRESPONDENCE
Arina A. Zamfir
arinaalexandra.zamfir@aosp.bo.it

†These authors have contributed equally to this work and share senior authorship

RECEIVED 29 November 2024
ACCEPTED 24 February 2025
PUBLISHED 12 March 2025

CITATION
Donati CM, Zamagni A, Zamfir AA, Aristei C, Cammelli S, Zamagni C, Paolinelli S, Buwenge M, Rossi R, Maltoni M, Morganti AG and Cilla S (2025) Exploring pain management in breast cancer: key findings from the ARISE study. *Front. Oncol.* 15:1536709. doi: 10.3389/fonc.2025.1536709



# Exploring pain management in breast cancer: key findings from the ARISE study

Costanza M. Donati[1,2], Alice Zamagni[2,3], Arina A. Zamfir[1*], Cynthia Aristei[4], Silvia Cammelli[1,2], Claudio Zamagni[5], Silvia Paolinelli[1,2], Milly Buwenge[2], Romina Rossi[6], Marco Maltoni[7], Alessio G. Morganti[1,2†] and Savino Cilla[8†]

[1]Radiation Oncology, Istituti di Ricovero e Cura a Carattere Scientifico (IRCCS) Azienda Ospedaliero-Universitaria di Bologna, Bologna, Italy, [2]Department of Medical and Surgical Sciences (DIMEC), Alma Mater Studiorum University of Bologna, Bologna, Italy, [3]Radiation Oncology Unit, Clinical Cancer Centre, AUSL-Istituti di Ricovero e Cura a Carattere Scientifico (IRCCS) di Reggio Emilia, Reggio Emilia, Italy, [4]Radiation Oncology Section, University of Perugia and Perugia General Hospital, Perugia, Italy, [5]Addarii Medical Oncology, Istituti di Ricovero e Cura a Carattere Scientifico (IRCCS) Azienda Ospedaliero-Universitaria di Bologna, Bologna, Italy, [6]Palliative Care Unit, Istituti di Ricovero e Cura a Carattere Scientifico (IRCCS) Istituto Romagnolo per lo Studio dei Tumori (IRST) "Dino Amadori", Meldola, Italy, [7]Medical Oncology Unit, Department of Medical and Surgical Sciences (DIMEC), University of Bologna, Bologna, Italy, [8]Medical Physics Unit, Responsible Research Hospital, Campobasso, Italy

**Aims:** This ARISE study secondary analysis aims to delve into the complexities of pain management in breast cancer patients undergoing radiotherapy (RT) in Italy. It aims to identify and analyze predictive variables for pain management adequacy and establish the relationship between these variables and the effectiveness of pain control.

**Materials and methods:** This observational study engaged 2,104 participants from 13 Italian RT departments, focusing on 426 breast cancer patients reporting pain. Advanced statistical methods, were employed to identify significant predictive variables for pain management adequacy. Data collection involved a standardized form capturing personal, health-related information, specifics about cancer, pain intensity, and medication. The Pain Management Index (PMI) was used to evaluate pain management adequacy, where negative PMI values indicate inadequate or suboptimal pain management.

**Results:** The analysis showed that 61.7% of patients experienced inadequate pain management (PMI<0). Factors identified as influencing pain management adequacy included the type of pain, patient age, the objective of RT, and the geographical location of the RT center. Notably, patients undergoing curative RT exhibited a higher incidence of inadequate pain management (PMI<0) compared to those undergoing palliative RT (82.9% versus 31.4%). Geographical variations were evident, with patients treated in northern Italy showing better pain management compared to those in central-southern Italy (72.0% versus 85.6%).

**Conclusion:** The ARISE study underscores a significant inadequacy in pain management among breast cancer patients undergoing RT in Italy, influenced

by a complex interplay of treatment-related, demographic, and regional factors. The study findings emphasize the need for enhanced, personalized pain management strategies and highlight the importance of considering a multifaceted approach.

KEYWORDS

**breast cancer, pain management, radiotherapy, patient outcomes, predictive variables, ARISE study, healthcare disparities, pain measurement**

# Introduction

Pain significantly reduces the quality of life (QoL) in cancer patients, impacting their physical, psychological, and spiritual well-being (1–3). Furthermore, a negative impact on the QoL in cancer patients can also be caused by pain of non-neoplastic origin (4). Therefore, also proper treatment of this pain is relevant as managing cancer-related pain. However, it has been repeatedly observed that non-neoplastic pain therapy in cancer patients is frequently inadequate (4–6). Challenges to effective pain control encompass both the healthcare system and patient perspectives (7). These include a lack of knowledge and skills among healthcare professionals (8), and a hesitancy among patients to communicate their pain (9). Recognizing the critical role of pain management is vital for enhancing patient outcomes (10).

The widespread issue of pain has led to efforts to bolster educational programs in universities and ongoing professional training, focusing on supportive treatments (11, 12). Moreover, educating patients about pain has become increasingly recognized as a key component of effective pain management (13, 14). Nevertheless, pain associated with breast cancer (BCa) often receives insufficient attention, resulting in subpar management outcomes compared to other cancers (5, 15, 16). Our prior ARISE studies corroborate this pattern, showing a marked link between BCa and suboptimal pain management (6).

To address the unclear reasons behind the generally less effective pain management in BCa patients, we undertook a detailed sub analysis of the ARISE study (6), focusing on BCa patients dealing with pain in Italian radiotherapy (RT) centers. Utilizing advanced statistical techniques, we sought to unravel the connection between the adequacy of pain management and various factors, such as the geographic site of the RT center, the demographics of patients, and the characteristics of pain. Moreover, our study seeks to fill this gap by systematically analyzing pain management practices and outcomes, utilizing patient-reported data to ensure a comprehensive assessment. Unlike previous research, which often focuses on broad oncological populations or singular interventions, our work integrates a multifaceted approach to the quality of pain management.

Finally, Italy is conventionally divided into three macro-regions: North, Center, and South, which differ for cultural, economic, and social reasons. Our previous analysis on the ARISE study (6) had shown that the geographic location of the RT center had a very significant impact on the adequacy of pain therapy. Therefore, in the present analysis we wanted to verify whether this phenomenon was also recorded in the subgroup of patients affected by BCa.

# Materials and methods

## Study design

Our investigation was set up as a cross-sectional, observational study aimed at evaluating the prevalence of pain and the adequacy of its management in RT departments (6, 17). This analysis focused specifically on BCa patients reporting pain or those taking analgesic drugs regardless of reported pain.

## Setting

The study was conducted across 13 Italian RT departments (Table 1). Patients were evaluated during their RT visits in October and November 2019.

## Participants

Inclusion criteria were as follows: (1) BCa cancer patients (regardless of tumor stage and RT aim), (2) treated in RT departments, and (3) aged ≥ 18 years. Patients with comorbidities (psychiatric disorders or neurosensory deficits) preventing data collection or informed consent were excluded. Eligible participants were those using analgesic drugs solely for pain management, excluding those on medications for non-pain-related purposes (e.g., opioids for cough sedation or dyspnea) (18).

## Variables

The primary outcome of the study was the adequacy of pain management, assessed using the previously validated Pain Management Index (PMI) (4, 5, 15, 16, 20–27). Predictive

TABLE 1 Participating centers in the ARISE study, categorized by geographic area, along with the number of patients enrolled in the analysis.

| | Location of the radiotherapy center | Radiotherapy center | Number of patients |
|---|---|---|---|
| 1 | North of Italy | Bologna | 50 |
| 2 | | Verona | 10 |
| 3 | | Forlì | 10 |
| 4 | Center of Italy | Campobasso | 15 |
| 5 | | Roma | 29 |
| 6 | South of Italy | Rionero in Vulture | 30 |
| 7 | | Cosenza | 34 |
| 8 | | Chieti | 43 |
| 9 | | Messina | 38 |
| 10 | | San Giovanni Rotondo | 61 |
| 11 | | Bari | 34 |
| 12 | | Brindisi | 30 |
| 13 | | Napoli | 42 |

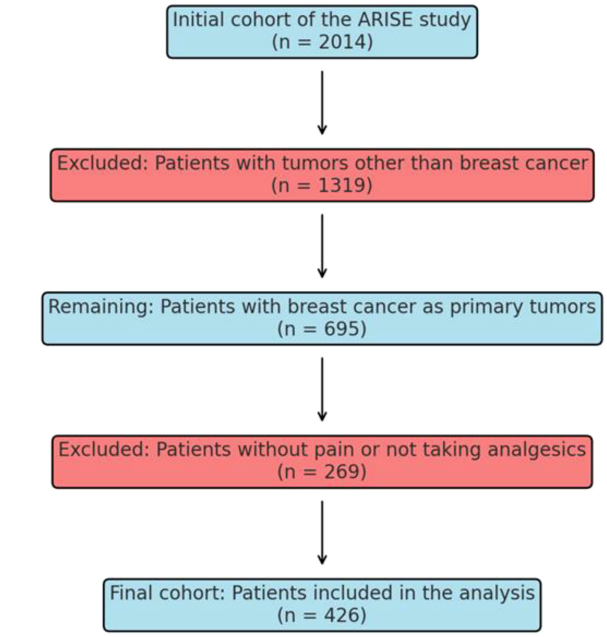


FIGURE 1
Flowchart of study cohort selection in the ARISE study.

variables analyzed included patient demographics (age, ECOG-PS), cancer stage (metastatic vs. non-metastatic), nature of pain (cancer-related, non-neoplastic, or mixed), aim of RT, geographic location of the RT facility (North, Central, or South Italy), and timing of the visit (during RT or at the end of RT).

## Data sources/measurement

All patients who met the enrollment criteria and who underwent a clinical visit at least once in the RT departments of participating centers in the period October–November 2019 were included. The evaluation was performed regardless of the visit timing (ongoing RT visits or clinical evaluation at the end of treatment). However, each patient was evaluated only once. Data collection utilized a standardized form (Supplementary Material 1) capturing personal and health-related information, cancer specifics, pain intensity (measured using the Numeric Rating Scale, NRS), and medication details. The Pain Management Index (PMI) was used to evaluate pain management adequacy, where negative PMI values indicate inadequate pain management. Pain was categorized as cancer-related, non-cancer-related, or mixed based on clinical evaluation and diagnostic imaging. The intensity of pain was recorded as the average experienced by patients during the week before their assessment.

## Bias

Selection bias may have been introduced as participation was voluntary, potentially underrepresenting patients with more severe pain or those less engaged in care. Recall bias is also a possibility due to reliance on patient-reported data for pain intensity.

## Study size

The study engaged 2,104 participants across all RT departments, focusing on 426 BCa patients reporting pain (Figure 1). The sample size was deemed sufficient for statistical analysis and predictive modeling but may limit the ability to detect smaller clinically relevant effects.

## Quantitative variables

We assigned a pain score by using the following values: 0 (NRS: 0, no pain), 1 (NRS: 1–4, mild pain), 2 (NRS: 5–6, moderate pain), and 3 (NRS: 7–0, intense pain). In addition, based on the therapy the patients took, we defined an analgesic score as follows: no analgesics: 0, non-opioid analgesics: 1, "weak"opioids: 2, and "strong" opioids: 3. The Pain Management Index (PMI) was calculated by subtracting the pain score from the analgesic score, considering prescriptions with a negative value as inadequate (6, 17–19).

## Statistical methods

The Least Absolute Shrinkage and Selection Operator (LASSO) algorithm and Classification and Regression Tree (CART) analysis were employed to identify predictive variables and construct predictive models. LASSO filtered variables for inclusion in the

model, and CART was used for decision tree-based modeling. Model robustness was ensured through cross-validation (5-fold, repeated 100 times), and predictive performance was evaluated using Receiver Operating Characteristic (ROC) curves and the Area Under the Curve (AUC) statistic.

## Results

The ARISE study encompassed 2,104 participants across 13 Italian RT departments, with 1,387 individuals reporting pain or on analgesic medication. Among the latter, this analysis centered on 426 BCa patients, with demographic and clinical specifics outlined in Table 2. The PMI served as the tool to evaluate pain management effectiveness, indicating that 61.7% of the patients experienced suboptimal management. Employing LASSO analysis, we identified crucial determinants for a PMI below zero. Particularly, we identified the following variables as related to the study endpoint (PMI): type of pain, patient age, RT aim, and geographical location of the RT center (Figure 2). On the contrary, ECOG-PS, tumor stage, and timing of the assessment were not correlated with negative PMI values. In fact, the PMI assessment of pain management adequacy revealed significant disparities among patients and varied depending on the characteristics of the treatment.

Specifically, patients receiving curative RT exhibited a higher incidence of PMI<0 compared to those undergoing palliative RT (82.9% versus 31.4%). Additionally, within the curative RT group, a lower incidence of PMI<0 was observed in patients treated in northern Italian centers than in those from central-southern Italy (72.0% versus 85.6%). Within this latter group, patients experiencing non-neoplastic pain had a higher frequency of PMI<0 compared to those with neoplastic pain (86.9% versus 76.9%). Conversely, in the palliative RT cohort, a greater incidence of PMI<0 was noted in patients older than 70 years compared to their younger counterparts (54.4% versus 27.9%). Within this younger subgroup, those with mixed pain (both neoplastic and non-neoplastic) exhibited a lower rate of PMI<0 in contrast to those with solely neoplastic or non-neoplastic pain (12.9% versus 32.1%).

Furthermore, acknowledging the evidence of inferior pain management in cancer patients with non-neoplastic pain (4–6), a specialized analysis was conducted focusing solely on BCa patients with non-neoplastic pain. This analysis resulted in a model highlighting the geographical location of the RT center and age as significant factors influencing pain management adequacy (Figure 3). Specifically, patients treated in northern Italy demonstrated a lower incidence of PMI<0 in comparison to those in central-southern Italy (67.7% versus 86.6%). Within the latter group, patients younger than 50 years experienced a higher rate of PMI<0 relative to their older counterparts (92.9% versus 85.4%). However, among patients treated in northern Italy, those older than 70 years exhibited a lower incidence of PMI<0 compared to younger patients (54.5% versus 75.0%).

TABLE 2 Patients characteristics (426).

| | | Number | (%) |
|---|---|---|---|
| **Age, years** | | | |
| ≤ 70 | | 315 | 74.0 |
| 71-80 | | 90 | 21.0 |
| > 80 | | 21 | 5.0 |
| **ECOG-PS** | | | |
| 0-1 | | 307 | 72.0 |
| 2 | | 82 | 19.0 |
| 3 | | 34 | 8.0 |
| 4 | | 3 | 1.0 |
| **Aim of treatment** | | | |
| Curative | | 251 | 59.0 |
| Palliative | | 175 | 41.0 |
| **Tumor stage** | | | |
| Metastatic | | 190 | 45.0 |
| Non-Metastatic | | 236 | 55.0 |
| **Type of Pain** | | | |
| Cancer Pain or mixed pain | | 216 | 51.0 |
| Non-cancer Pain | | 210 | 49.0 |
| **Pain score** | | | |
| (NRS: 0) | 0 | 4 | 1.0 |
| (NRS: 1 – 4) | 1 | 198 | 46.5 |
| (NRS: 5 – 6) | 2 | 155 | 36.5 |
| (NRS: 7 – 10) | 3 | 69 | 16.0 |
| **Analgesic score** | | | |
| (No therapy) | 0 | 156 | 37.0 |
| (Analgesics) | 1 | 180 | 42.0 |
| (Weak Opioids) | 2 | 44 | 10.0 |
| (Strong Opioids) | 3 | 46 | 11.0 |
| **Location of the radiotherapy center** | | | |
| Nord of Italy | | 70 | 16.0 |
| Center of Italy | | 44 | 10.0 |
| South of Italy | | 312 | 74.0 |
| **Timing of visit** | | | |
| During Therapy | | 209 | 49.0 |
| End of Therapy | | 217 | 51.0 |

The classification performances of the CART models are reported in Figure 4 in terms of AUCs with 95% confidence intervals, demonstrating excellent generalizability. Considering all

10.3389/fonc.2025.1536709

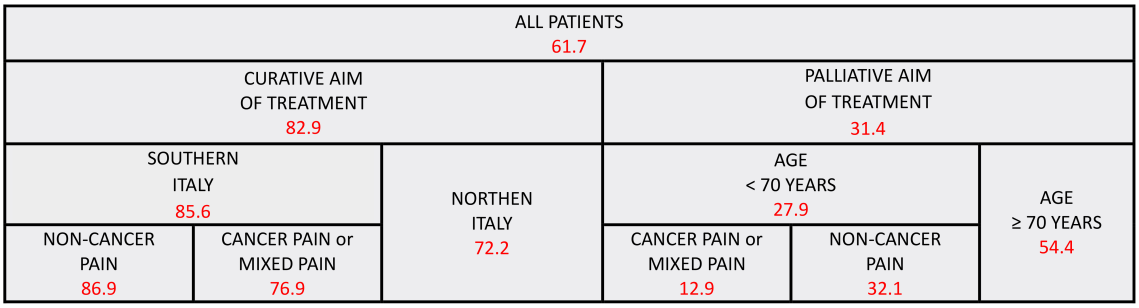


FIGURE 2
Predictive model for inadequate pain management: red numbers represent the proportion of patients with inadequate pain management (PMI < 0); all patients with breast cancer were included.

patients, the CART model showed AUC values of 79.1% (95%CI: 0.767-0.815) and 77.1% (95% CI: 0.695-0.847) in the training and validation datasets, respectively. With respect to BCa patients with non-neoplastic pain, the CART model showed AUC values of 68.8% (95% CI: 0.643-0.732) and 65.6% AUC: 0.656 (95% CI: 0.589-0.723) in the training and validation datasets, respectively.

## Discussion

The ARISE study comprehensive examination of pain management in BCa patients undergoing RT in Italy reveals a nuanced landscape of pain control efficacy. Despite the recognition of pain multifaceted impact on cancer patients' lives, our findings underscore a prevalent inadequacy in pain management, with 61.7% of the studied cohort experiencing suboptimal care. The application of advanced statistical methods, including LASSO and CART analysis, has brought to light significant disparities in pain management adequacy.

The LASSO algorithm was chosen for its ability to perform both variable selection and regularization, which is critical in avoiding overfitting in datasets with high-dimensional predictors. By shrinking some coefficients to zero, LASSO identifies the most relevant variables influencing pain management adequacy, enhancing model interpretability. CART analysis complements LASSO by providing an intuitive and visual decision-making framework, allowing for the exploration of interactions between variables and the identification of thresholds critical for clinical decisions.

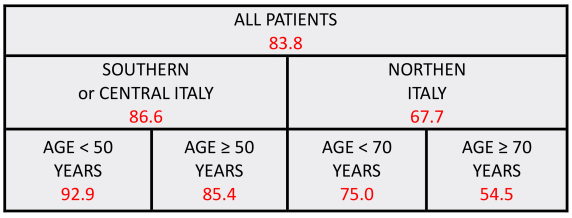


FIGURE 3
Predictive model for inadequate pain management: red numbers represent the proportion of patients with inadequate pain management (PMI < 0); only patients with breast cancer and non-neoplastic pain were included.

However, we acknowledge certain limitations of these methods. LASSO assumes linear relationships and may struggle to capture complex, non-linear interactions without appropriate transformation or feature engineering. CART, while interpretable, is prone to overfitting, particularly in the presence of noisy data. To mitigate these issues, we utilized cross-validation and pruning techniques to ensure model robustness and generalizability. These methods were selected to balance interpretability and predictive accuracy, aligning with the study's goals to provide actionable insights for clinical practice.

The disparities recorded in our analysis are not random but are closely associated with age, nature of pain, RT aim, and geographical location of RT centers.

The lesser adequacy in the management of non-neoplastic pain may derive from concerns that treatment of chronic-benign pain with opioids could result in drug addiction, as well as from potentially less attention by physicians to symptoms not directly caused by cancer. We acknowledge the complexity in quantifying how these two factors specifically impacted our results. However, it is noteworthy to mention the stark contrast in inadequacy of non-neoplastic pain management between patients undergoing curative and palliative RT (86.9% vs 32.1%, respectively). Nevertheless, also this difference may stem both from greater physician attention to patients with advanced disease, irrespective of the pain origin, and from differing risks of opioid drug addiction in these two distinct patient populations.

Particularly striking is the difference in pain management effectiveness between patients undergoing curative and palliative RT, and the further influence of regional practices, as evidenced by the variations between northern and central-southern Italian centers.

Our analysis aligns with existing literature in several aspects, confirming the suboptimal pain management in BCa patients (5, 16, 20), particularly in those undergoing curative therapy compared to palliative therapy (6, 25), the inferior management of non-neoplastic pain (4–6), geographic disparities in pain management effectiveness (5, 6), and the adverse influence of

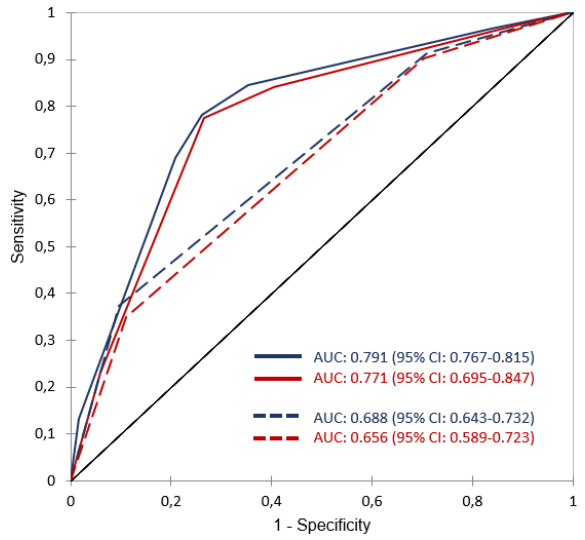


FIGURE 4
ROC curves and AUC values of the two CART models. The solid blue and red curves are the average ROC for the training and validation sets in the model including all patients. Dotted blue and red curves are the average ROC for the training and validation sets in the model including only patients with non-neoplastic pain.

younger age on pain management adequacy (6, 16). However, our findings indicate a complex relationship between age and PMI<0, differing from previous reports. While earlier studies suggested poorer pain management among younger patients (6, 16), our analysis across all pain types shows a higher incidence of PMI<0 among older patients (>70 years) receiving palliative RT. This could imply that healthcare professionals might prioritize pain management more in younger, symptomatic BCa patients, or it may reflect younger patients' greater likelihood to report pain symptoms compared to their older counterparts. Additionally, it is important to consider that clinicians might often exhibit reluctance in prescribing opioids to older patients due to potential adverse effects, particularly cognitive impairment and increased risk of falls. These concerns can heavily influence prescribing practices, especially in contexts where the risk of these side effects might outweigh the benefits of pain relief.

Moreover, the complexity of pain management in patients under 70 years undergoing palliative RT is highlighted by the finding that pain management is more adequate in patients with mixed pain compared to those with only neoplastic or non-neoplastic pain. This contrasts with previous studies, which generally found an intermediate quality of pain management in patients with mixed pain (6).

Regarding the differential adequacy of pain management in patients undergoing palliative versus curative RT, we propose the following hypotheses: Firstly, it is plausible that in palliative care settings, clinicians prioritize quality of life, thereby focusing more attentively on symptom relief, including the provision of adequate pharmacological therapy. In contrast, the focus in curative treatment settings might lean more towards clinical outcomes, potentially at the expense of optimal symptom management. Secondly, patients receiving palliative RT might more frequently be under the care of clinicians specialized in supportive and palliative therapies, who are perhaps better experienced in prescribing effective pain management regimens.

The intricacies of pain management in BCa are further underscored by our secondary analysis focusing exclusively on patients with non-neoplastic pain. In fact, this study confirms better symptomatic treatment in patients in northern Italy, possibly due to superior clinical management by northern healthcare professionals or a reluctance among southern patients to report pain. This reluctance could be related to different psychological profiles shaped by varying socio-economic conditions (28–30).

In younger patient groups from both northern and central-southern Italy, poorer pain management was noted. The age threshold for this disparity was 70 years in the north and 50 years in the south, suggesting regional differences in pain management effectiveness between younger or middle-aged patients and older adults. This raises questions about whether these variations are due to different sensitivities of healthcare professionals towards patient age or if they reflect regional influences on patients' psychological profiles, affecting their likelihood to report pain. Undoubtedly, additional research is needed to enhance the current unsatisfactory state of pain management in BCa patients. Specifically, it is crucial to discern the extent to which the documented disparities stem from the attitudes of healthcare providers versus those of the patients themselves. Pursuing this line of inquiry, future studies could incorporate the utilization of well-designed questionnaires. These instruments should be capable of differentiating between pain that patients spontaneously report during routine clinical interactions with their oncology healthcare providers, and pain revealed in response to specific, direct inquiries about the intensity and nature of pain posed by interviewers. This approach would provide a more nuanced understanding of the dynamics influencing pain reporting and management in the clinical setting.

The ARISE-breast study, with its extensive cohort of 426 participants across 13 Italian RT departments, offers a robust, observational insight into the complexities of pain management in BCa patients. A notable strength of our study is the application of advanced statistical methods, such as LASSO and CART analysis, which enabled the identification of significant predictive variables for pain management adequacy. This methodological rigor offers a comprehensive understanding of the multifactorial nature of pain management, encompassing patient demographics, pain characteristics, treatment objectives, and even geographical discrepancies in treatment practices.

However, the study is not without limitations. The observational nature of the study, while offering real-world insights, limits our ability to infer causality. The reliance on patient-reported outcomes for pain intensity and management adequacy may introduce subjective biases, potentially influenced by individual pain thresholds and communication barriers. Furthermore, the study utilized a single definition of pain (average pain). Additionally, the opioids prescribed were not categorized as long-acting or short-acting. The specific pharmacological agents used in the analgesic

drugs were not documented, and there is no available information regarding which clinician or specialist prescribed the analgesic therapy. Moreover, the study focuses on a single country, Italy, which, while providing in-depth regional insights, may limit the generalizability of our findings to other healthcare systems with different cultural, socio-economic, and medical practice landscapes. In fact, to the best of our knowledge, this is the first study dedicated to the analysis of pain adequacy in BCa patients. This has limited our ability to compare with studies conducted in other settings (other than RT) or in other countries. Additionally, our study assessment was based on a single time point, evaluating a single pain score, which may not fully capture the dynamic nature of pain management across different stages of treatment. The number of radiation therapy fractions varied among patients, introducing another layer of complexity and potential variability in pain outcomes. We acknowledge that these factors, along with the exclusion of certain patient groups and variations in healthcare provider training and experience across regions, could have influenced the results. These elements should be carefully considered when interpreting the findings and their application to broader contexts. Finally, our study was based on the analysis of the PMI, the limitations of which have been previously recognized and discussed (6). In particular, although this tool was previously used in analyses of non-neoplastic pain (4–6), it must be recognized that in this context this tool is not entirely suitable. In fact, for patients with pain that is related to active treatment, even in the curative setting, contemporary guidelines (31) stress the importance of using opioids for the management of strong pain. In stark contrast, the guidelines for survivorship pain emphasize the risk of aberrant behaviors and strongly suggest using opioids only as a last resort, and even then, only in patients who have a low risk of abuse behaviors (31).

Therefore, we hypothesize that the percentage of patients with a negative PMI may be influenced, at least in part, by a reluctance to prescribe opioids for non-cancer pain. Unfortunately, our dataset does not enable us to quantify this percentage. Additionally, it is important to consider that this percentage might be higher in countries where, unlike Italy, there is a significant concern regarding an 'opioid epidemic.' This factor could affect opioid prescription practices and consequently the management of pain across different healthcare settings.

To further address the limitations of this study, we acknowledge that the sample size, while sufficient for our analyses, may limit the statistical power to detect smaller but clinically relevant effects. Future studies with larger, more diverse cohorts would be valuable in validating and extending our findings. We also recognize the potential for selection bias, as participation was voluntary, and patients with more severe pain or those less engaged in their care may have been underrepresented. Lastly, while our study design provides a snapshot of current practices, a longitudinal approach would better capture the evolution of pain management strategies over time and their outcomes at different treatment stages. These additional considerations further underscore the need for cautious interpretation and the importance of follow-up research to build upon our findings.

Future research should aim to address these limitations, potentially incorporating more objective pain measurement tools and considering multi-national cohorts to enhance the generalizability and applicability of the findings. Furthermore, integrating qualitative methods could provide a more nuanced understanding of the interplay between healthcare provider approaches, patient attitudes, and systemic healthcare factors in the context of pain management in BCa care.

From a practical point of view, considering the availability of national guidelines for the management of cancer pain in Italy (32), largely based on WHO guidelines, the poor adequacy of pain management recorded in this and previous analyses suggests the need to improve the education and continuing training of physicians on this topic, especially in the setting of RT. Furthermore, considering that the worse results demonstrated by our and other studies (5, 15, 16) regarding BCa cancer patients can hardly be justified by a different respect of guidelines by physicians in these subjects, our analysis should stimulate greater attention to this patient population, since we cannot exclude that they have a lower propensity to report to physicians the intensity of their pain.

## Data availability statement

The original contributions presented in the study are included in the article/Supplementary Material. Further inquiries can be directed to the corresponding author.

## Ethics statement

The studies involving humans were approved by Comitato Etico Area Vasta Emilia Centro (AVEC) - Ethics Committee of IRCCS Azienda Ospedaliero-Universitaria di Bologna. The studies were conducted in accordance with the local legislation and institutional requirements. The participants provided their written informed consent to participate in this study.

## Author contributions

CD: Writing – original draft, Writing – review & editing. AZ: Writing – original draft, Writing – review & editing. AAZ: Writing – review & editing. CA: Writing – original draft, Writing – review & editing. SCa: Writing – original draft, Writing – review & editing. CZ: Writing – original draft, Writing – review & editing. SP: Writing – review & editing. MB: Writing – original draft, Writing – review & editing. RR: Writing – review & editing. MM: Writing – original draft, Writing – review & editing. AM: Writing – original draft, Writing – review & editing. SCi: Writing – original draft.

## Funding

The author(s) declare that financial support was received for the research and/or publication of this article. The work reported in this

publication was funded by the Italian Ministry of Health, RC-2024-2790151 Project.

## Acknowledgments

We would like to express our gratitude to all those who helped us during the writing of this manuscript. Furthermore, we are grateful to AGEOP (Associazione Genitori Ematologia Oncologia Pediatrica) Ricerca Odv, which supports our research.

## Conflict of interest

AM reports personal fees from Astellas and Alfa-Sigma, and grants from Elekta, Tema Sinergie, Janssen, Bayer, and Igea outside the submitted work.

The remaining authors declare that the research was conducted in the absence of any commercial or financial relationships that could be construed as a potential conflict of interest.

## Generative AI statement

The author(s) declare that no Generative AI was used in the creation of this manuscript.

## Publisher's note



## Supplementary material

The Supplementary Material for this article can be found online at: https://www.frontiersin.org/articles/10.3389/fonc.2025.1536709/full#supplementary-material

## References

1. Tavoli A, Montazeri A, Roshan R, Tavoli Z, Melyani M. Depression and quality of life in cancer patients with and without pain: the role of pain beliefs. *BMC Cancer*. (2008) 8:177. doi: 10.1186/1471-2407-8-177

2. Rodriguez C, Ji M, Wang HL, Padhya T, McMillan SC. Cancer pain and quality of life. *J Hosp Palliat Nurs*. (2019) 21:116–23. doi: 10.1097/NJH.0000000000000507

3. Katz N. The impact of pain management on quality of life. *J Pain Symptom Manage*. (2002) 24:S38–47. doi: 10.1016/S0885-3924(02)00411-6

4. Massaccesi M, Deodato F, Caravatta L, Macchia G, Padula GD, Di Rito S, et al. Incidence and management of noncancer pain in cancer patients referred to a radiotherapy center. *Clin J Pain*. (2013) 29:944–7. doi: 10.1097/AJP.0b013e31827eb5e6

5. Shen WC, Chen JS, Shao YY, Lee KD, Chiou TJ, Sung YC, et al. Impact of undertreatment of cancer pain with analgesic drugs on patient outcomes: A nationwide survey of outpatient cancer patient care in Taiwan. *J Pain Symptom Manage*. (2017) 54:55–65.e1. doi: 10.1016/j.jpainsymman.2017.02.018

6. Donati CM, Nardi E, Zamagni A, Siepe G, Mammini F, Cellini F, et al. Adequacy of pain treatment in radiotherapy departments: results of a multicenter study on 2104 patients (Arise). *Cancers*. (2022) 14:4660. doi: 10.3390/cancers14194660

7. Pargeon KL, Hailey BJ. Barriers to effective cancer pain management: a review of the literature. *J Pain Symptom Manage*. (1999) 18:358–68. doi: 10.1016/S0885-3924(99)00097-4

8. Al-Ghabeesh SH, Bashayreh IH, Saifan AR, Rayan A, Alshraifeen AA. Barriers to effective pain management in cancer patients from the perspective of patients and family caregivers: A qualitative study. *Pain Manag Nurs*. (2020) 21:238–44. doi: 10.1016/j.pmn.2019.07.011

9. Kwon JH. Overcoming barriers in cancer pain management. *J Clin Oncol*. (2014) 32:1727–33. doi: 10.1200/JCO.2013.52.4827

10. Adam R, de Bruin M, Burton CD, Bond CM, Giatsi Clausen M, Murchie P. What are the current challenges of managing cancer pain and could digital technologies help? *BMJ Support Palliat Care*. (2018) 8:204–12. doi: 10.1136/bmjspcare-2016-001232

11. Obaid A, Hroub AA, Rifai AA, Alruzzieh M, Radaideh M, Tantawi Y. Barriers to effective cancer pain management, comparing the perspectives of physicians, nurses, and patients. *Pain Manag Nurs*. (2023) 24:498–505. doi: 10.1016/j.pmn.2023.07.003

12. Miró J, Castarlenas E, Solé E, Martí L, Salvat I, Reinoso-Barbero F. Pain curricula across healthcare professions undergraduate degrees: a cross-sectional study in Catalonia, Spain. *BMC Med Educ*. (2019) 19:307. doi: 10.1186/s12909-019-1741-5

13. Briggs E. Evaluating the impact of pain education: how do we know we have made a difference? *Br J Pain*. (2012) 6:85–91. doi: 10.1177/2049463712449961

14. Lee BH, Wu CL. Educating patients regarding pain management and safe opioid use after surgery: A narrative review. *Anesth Analg*. (2020) 130:574–81. doi: 10.1213/ANE.0000000000004436

15. Mitera G, Zeiadin N, Kirou-Mauro A, DeAngelis C, Wong J, Sanjeevan T, et al. Retrospective assessment of cancer pain management in an outpatient palliative radiotherapy clinic using the Pain Management Index. *J Pain Symptom Manage*. (2010) 39:259–67. doi: 10.1016/j.jpainsymman.2009.07.005

16. Thronæs M, Balstad TR, Brunelli C, Torbjørn Løhre E, Klepstad P, Vagnildhaug OM, et al. Pain management index (PMI)-does it reflect cancer patients' wish for focus on pain? *Support Care Cancer*. (2020) 28:1675–84.

17. Donati CM, Maggiore CM, Maltoni M, Rossi R, Nardi E, Zamagni A, et al. Adequacy of pain management in patients referred for radiation therapy: A subanalysis of the multicenter ARISE-1 study. *Cancers (Basel)*. (2023) 16:109. doi: 10.3390/cancers16010109

18. Anekar AA, Hendrix JM, Cascella M. WHO analgesic ladder. [Updated 2023 apr 23]. In: *StatPearls*. StatPearls Publishing, Treasure Island (FL (2024). Available at: https://www.ncbi.nlm.nih.gov/books/NBK554435/.

19. Cleeland CS, Gonin R, Hatfield AK, Edmonson JH, Blum RH, Stewart JA, et al. Pain and its treatment in outpatients with metastatic cancer. *N Engl J Med*. (1994) 330:592–6. doi: 10.1056/NEJM199403033300902

20. Mitera G, Fairchild A, DeAngelis C, Emmenegger U, Zurawel-Balaura L, Zhang L, et al. A multicenter assessment of the adequacy of cancer pain treatment using the pain management index. *J Palliat Med*. (2010) 13:589–93. doi: 10.1089/jpm.2009.0342

21. Gonçalves F, Almeida A, Antunes C, Cardoso M, Carvalho M, Claro M, et al. A cross-sectional survey of pain in palliative care in Portugal. *Support Care Cancer*. (2013) 21:2033–9. doi: 10.1007/s00520-013-1746-2

22. Vuong S, Pulenzas N, DeAngelis C, Torabi S, Ahrari S, Tsao M, et al. Inadequate pain management in cancer patients attending an outpatient palliative radiotherapy clinic. *Support Care Cancer*. (2016) 24:887–92. doi: 10.1007/s00520-015-2858-7

23. Singh H, Singh Banipal RP, Singh B. Assessment of adequacy of pain management and analgesic use in patients with advanced cancer using the brief pain inventory and pain management index calculation. *J Glob Oncol*. (2016) 3:235–41. doi: 10.1200/JGO.2016.004663

24. Reis-pina P, Lawlor PG, Barbosa A. Adequacy of cancer-related pain management and predictors of undertreatment at referral to a pain clinic. *J Pain Res*. (2017) 10:2097–107. doi: 10.2147/JPR.S139715

25. Fujii A, Yamada Y, Takayama K, Nakano T, Kishimoto J. Longitudinal assessment of pain management with the pain management index in cancer outpatients receiving chemotherapy. *Support Care Cancer*. (2017) 25:925–32. doi: 10.1007/s00520-016-3482-x

26. Sakakibara N, Higashi T, Yamashita I, Yoshimoto T, Matoba M. Negative pain management index scores do not necessarily indicate inade-quate pain management: A cross-sectional study. *BMC Palliat Care*. (2018) 17:102. doi: 10.1186/s12904-018-0355-8

27. Tuem KB, Gebremeskel L, Hiluf K, Arko K, Haftom Gebregergs H. Adequacy of cancer-related pain treatments and factors affecting proper management in ayder comprehensive specialized hospital, Mekelle, Ethiopia. *J Oncol*. (2020) 2020:2903542. doi: 10.1155/2020/2903542

28. Zeilinger EL, Oppenauer C, Knefel M, Kantor V, Schneckenreiter C, Lubowitzki S, et al. Prevalence of anxiety and depression in people with different types of cancer or haematologic Malignancies: a cross-sectional study. *Epidemiol Psychiatr Sci*. (2022) 31: e74. doi: 10.1017/S2045796022000592

29. Yeom JW, Yeom IS, Park HY, Lim SH. Cultural factors affecting the self-care of cancer survivors: An integrative review. *Eur J Oncol Nurs*. (2022) 59:102165. doi: 10.1016/j.ejon.2022.102165

30. Patrick DL, Ferketich SL, Frame PS, Harris JJ, Hendricks CB, Levin B, et al. National institutes of health state-of-the-science conference statement: symptom management in cancer: pain, depression, and fatigue, July 15-17, 2002. *J Natl Cancer Inst*. (2003) 95:1110–7. doi: 10.1093/jnci/djg014

31. Dowell D, Ragan KR, Jones CM, Baldwin GT, Chou R. Prescribing opioids for pain - the new CDC clinical practice guideline. *N Engl J Med*. (2022) 387:2011–3. doi: 10.1056/NEJMp2211040

32. Available online at: https://www.aiom.it/linee-guida-aiom-2021-terapia-del-dolore-in-oncologia/ (Accessed January 21, 2025).

frontiers | Frontiers in Oncology

TYPE Case Report
PUBLISHED 22 April 2025
DOI 10.3389/fonc.2025.1565175



OPEN ACCESS

EDITED BY
Giuseppe Giaccone,
Cornell University, United States

REVIEWED BY
Nektarios I. Koufopoulos,
University General Hospital Attikon, Greece
Vitor Marques,
Universidade Federal de Goiás, Brazil

*CORRESPONDENCE
Miduo Tan
tanmiduo123@163.com
Fengxian An
anfengxian2021@163.com

†These authors have contributed equally to this work and share first authorship

RECEIVED 22 January 2025
ACCEPTED 31 March 2025
PUBLISHED 22 April 2025

CITATION
Zhang Y, Li X, Xue Y, Huang X, An F and Tan M (2025) Solid subtype of adenoid cystic carcinoma of the breast with multiple distant metastases: a case report and literature review.
*Front. Oncol.* 15:1565175.
doi: 10.3389/fonc.2025.1565175



# Solid subtype of adenoid cystic carcinoma of the breast with multiple distant metastases: a case report and literature review

Yibo Zhang[1†], Xidie Li[2†], Yaxi Xue[3], Xiaohui Huang[4], Fengxian An[5*] and Miduo Tan[1,4*]

[1]Department of Ultrasonography, The Hunan Province Directly Affiliated TCM Hospital, Zhuzhou, Hunan, China, [2]Department of Obstetrics and Gynecology, Zhuzhou Hospital Affiliated to Xiangya School of Medicine, Central South University, Zhuzhou, Hunan, China, [3]Department of Cardiology, Zhuzhou Hospital Affiliated to Xiangya School of Medicine, Central South University, Zhuzhou, Hunan, China, [4]Department of Breast Surgery, Zhuzhou Hospital Affiliated to Xiangya School of Medicine, Central South University, Zhuzhou, Hunan, China, [5]Department of Pathology, Liaocheng People's Hospital, Liaocheng, Shandong, China

**Objective:** To present a rare case of adenoid cystic carcinoma of the breast (ACCB), solid subtype, with multiple distant metastases, and to analyze its clinical management and differentiation from typical triple-negative breast cancer (TNBC), highlighting the lack of standardized guidelines for this rare entity and providing insights for future therapeutic strategies.

**Methods:** A 46-year-old female with ACCB was followed for 9 years, documenting metastatic progression, treatment responses, and survival outcomes. A literature review was conducted to compare ACCB and TNBC in terms of clinicopathological features, immunohistochemical profiles, metastatic patterns, and therapeutic strategies.

**Results:** The patient exhibited aggressive behavior with metastases to the brain, lungs, liver, and kidneys. Systemic chemotherapy (albumin-bound paclitaxel and capecitabine) combined with radiotherapy stabilized the disease, achieving a 9-year survival with preserved quality of life.

**Conclusion:** ACCB requires differentiation from TNBC due to its unique biological behavior and favorable prognosis. Breast-conserving surgery with radiotherapy may be preferable for localized disease, while systemic chemotherapy should be considered for metastatic solid subtypes. This case underscores the urgent need for consensus guidelines and further research on molecular profiling to refine therapeutic approaches.

KEYWORDS

**adenoid cystic carcinoma of the breast, triple-negative breast cancer, distant metastasis, treatment, follow-up**

# 1 Introduction

For Adenoid cystic carcinoma of the breast (ACCB) is a rare subtype of invasive breast cancer, with an incidence of approximately 0.92 per million people (1), that accounts for less than 0.1% of all breast cancer cases (2). ACCB primarily occurs in postmenopausal women, although cases in men have also been reported (3, 4). Its histopathological features are similar to those of adenoid cystic carcinoma (ACC) found in other tissues, such as the salivary glands and skin. However, ACCB is typically characterized by local growth and low invasiveness, with rare metastasis to axillary lymph nodes or distant organs (5). Classic ACCB typically exhibits favorable biological behavior, whereas the solid and high-grade transformation types are more prone to local recurrence and distant metastasis (6–8). Therefore, it is crucial to recognize these more aggressive forms of ACCB. ACCB is associated with a favorable prognosis, with 5-year, 10-year, and 15-year survival rates of 98%, 95%, and 91%, respectively (9). Surgery is the mainstay of treatment for ACCB, followed by radiotherapy, while the role of adjuvant chemotherapy remains controversial.

This article presents a case of ACCB with widespread systemic metastasis and shares our experience with its treatment and follow-up. Followed by a review of the previous literature, we discuss the clinical presentation, histological features, immunohistochemical results, treatment strategies, and prognosis of ACCB, aiming to provide a deeper understanding of the disease and offer evidence to guide clinical management. Due to the rarity of ACCB and the lack of consensus guidelines, clinicians often extrapolate treatment strategies from TNBC, risking overtreatment. This case highlights the need for tailored management and underscores the importance of distinguishing ACCB from conventional TNBC.

# 2 Case description

A 46-year-old Han Chinese female, with a BMI of 24.24 kg/m$^2$ (height 156 cm, weight 59 kg), was admitted to the hospital in December 2021 due to intermittent headaches for one week. She had no family history of breast cancer and completed high school education. In January 2016, she underwent radical surgery for a breast mass, and the postoperative pathological diagnosis was adenoid cystic carcinoma of the breast (ACCB), solid type (Figure 1A). After surgery, she received three cycles of adjuvant chemotherapy with docetaxel (75 mg/m$^2$) and cyclophosphamide (600 mg/m$^2$). Upon admission, relevant examinations were performed. MRI of the head revealed an intracranial mass (Figure 1B), and CT of the chest revealed a left lung mass (Figure 1C), both of which were suspected to be metastatic tumors.

In December 2021, we resected the left frontal lobe tumor. The histopathological report described the tumor as being composed of two cell types: basaloid cells (nonluminal cells) and glandular epithelial cells (luminal cells). The tumor primarily showed a solid arrangement, with some areas exhibiting tubular, trabecular, and sieve-like patterns of growth. The basaloid tumor cells were round or oval, with scant cytoplasm and prominent mitotic figures (Figure 1D). Immunohistochemical profile: ER, PR, HER-2, and GATA3 were all negative, while CD117, P63, CK7, CK, P40, and SOX10 were positive, and Ki67 was 30% positive. Postoperatively, the patient received whole-brain radiotherapy.

In January 2022, we performed a CT-guided biopsy of the left lung mass. Microscopic examination revealed basaloid tumor cells arranged in a solid pattern, with areas of sieve-like structures. The tumor cells had large, deeply stained nuclei with marked atypia and mitotic figures (Figure 1E). The immunohistochemical profile was negative for ER, PR, and HER-2 but positive for CD117, P63, CK7, and PAS. On the basis of the histological morphology, immunohistochemical findings, and history of breast cancer, the diagnosis was confirmed as ACCB metastasis to the brain and lungs. After diagnosis, the patient received six cycles of systemic chemotherapy with albumin-bound paclitaxel and capecitabine, with follow-up indicating stable disease.

In February 2024, the patient was readmitted due to right upper abdominal pain. A follow-up CT scan revealed multiple low-density lesions in both the kidney (Figure 1F) and the liver (Figure 1G), suggestive of metastatic tumors. The patient received ten cycles of systemic chemotherapy with albumin-bound paclitaxel and carboplatin. After completing chemotherapy, the patient was maintained on daily oral capecitabine. As of January 2025, the patient has survived 9 years since the diagnosis of ACCB, with satisfactory quality of life, and is still under follow-up.

# 3 Discussion

ACCB is a rare subtype of TNBC, accounting for approximately 0.1% of all breast cancer cases (2). It predominantly affects postmenopausal women, with a median age of onset between 50 and 60 years (10, 11). ACCB differs from other forms of TNBC in both clinical characteristics and prognosis. Typically, ACCB is characterized by local growth and low invasiveness, with rare metastasis to the axillary lymph nodes or distant organs. The prognosis is generally favorable, with 5-year, 10-year, and 15-year survival rates of 98%, 95%, and 91%, respectively (9).

ACCB often presents as a palpable, solitary breast mass, with a minority of patients experiencing breast pain (12, 13). Symptoms such as nipple inversion, nipple discharge, and skin retraction may also rarely occur (1). The disease typically exhibits slow, indolent growth, with an average diameter of 2–3 cm, although it can reach up to 15 cm (12, 14). A case of giant ACCB with a diameter of 30 cm has been reported, where the mass gradually increased over a span of more than 20 years. Despite the lack of treatment, there are no regional lymph node or distant metastases (15). Although pain is not a typical feature of ACCB, it can serve as an important diagnostic clue (13, 16). Studies have shown that approximately 14% of ACCB patients experience breast pain associated with the mass, possibly due to nerve invasion by tumor cells and the contraction of myoepithelial cells (17). The radiological findings of ACCB lack specificity, and CT scans play an essential role in the follow-up of ACCB patients, as the lungs are the most common site of distant metastasis (16). In the present case, a routine follow-up chest CT revealed a pulmonary mass, and a biopsy confirmed ACCB metastasis to the lungs.

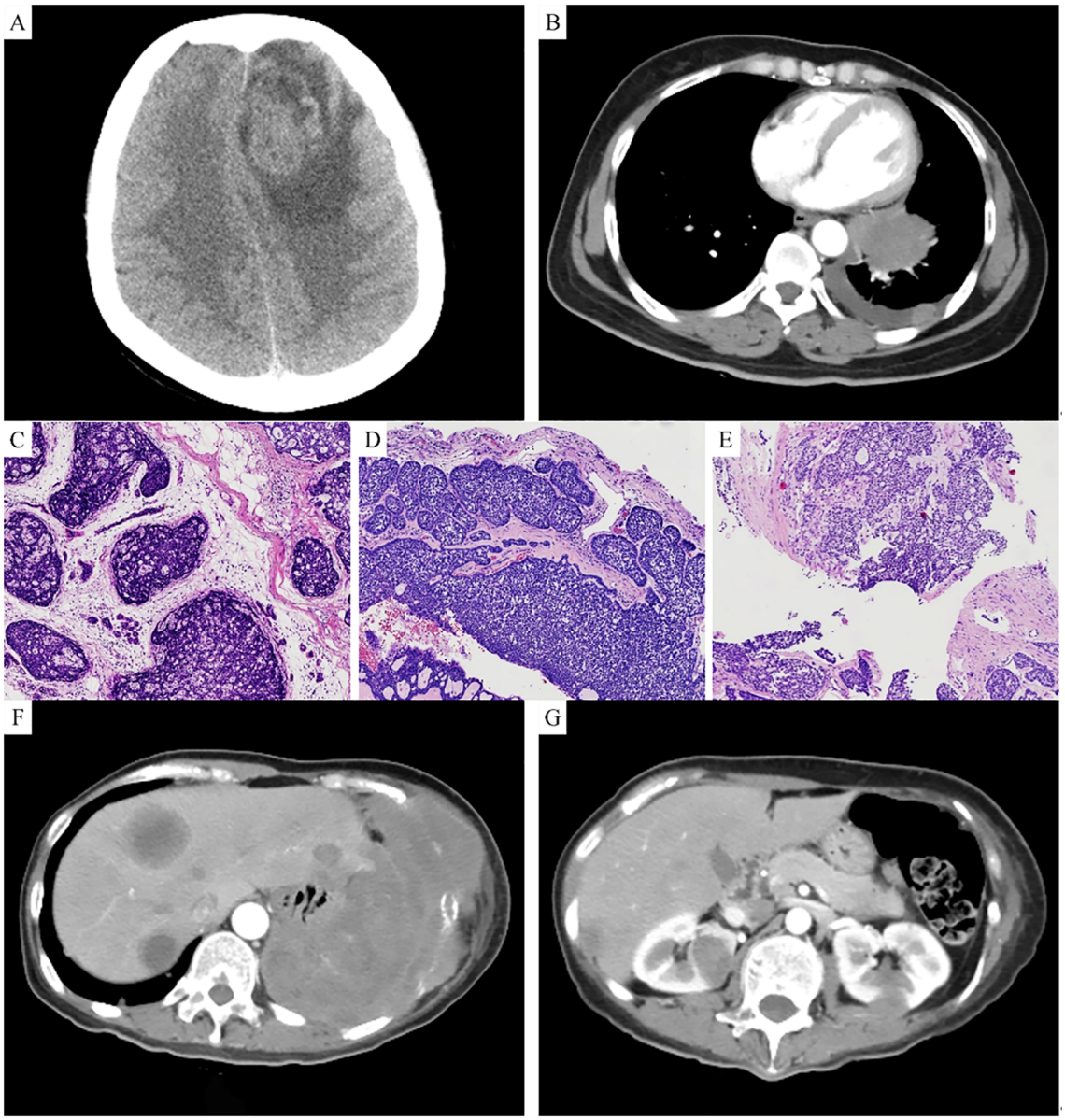


FIGURE 1
**(A)** MRI shows an intracranial space-occupying lesion. **(B)** CT shows a space-occupying lesion in the left lung. **(C)** Hematoxylin and eosin (HE) staining of the breast tumor shows basaloid cells with deeply stained nuclei. **(D)** HE staining of the brain tumor shows a mixture of basaloid cells and glandular epithelial cells, primarily arranged in a solid pattern. **(E)** HE staining of the lung tumor shows basaloid tumor cells arranged in a solid pattern, with focal sieve-like structures. **(F)** CT shows multiple space-occupying lesions in the liver. **(G)** CT shows multiple space-occupying lesions in both kidneys.

ACCB is primarily composed of glandular epithelial, myoepithelial, and basaloid cells arranged in classic tubular, sieve-like, or solid structures. Invasive growth is commonly observed under a microscope, and some tumors exhibit perineural invasion (12). According to the fifth edition of the WHO classification of breast tumors, ACCB is divided into three histological subtypes: classic, solid, and high-grade transformation. The classic type of ACCB is characterized by glandular epithelial and myoepithelial cells surrounding true and pseudoglandular lumens, with pseudoglandular lumens containing basement membrane-like material. The solid type of ACCB builds upon the classic type, featuring solid cell nests made of basaloid cells, marked cytologic atypia, frequent mitoses, and necrosis. The high-grade transformation type develops further from the classic type and is characterized by high-grade malignant tumor components (4, 18).

ACCB typically does not express ER, PR, or HER-2. Unlike other TNBCs, ACCB displays a unique immunophenotype. Glandular epithelial cells commonly express CK7, CK8, CK18, and CD117, whereas myoepithelial and basaloid cells typically express p63, S-100, CK5, CK6, CK14, and CK17 (4, 18, 19). The expression of p63 and CD117 via immunohistochemistry can help distinguish ACC from invasive cribriform carcinoma and ductal carcinoma in situ (19). Ki-67 expression is relatively low in ACCB (8, 20), with increased expression only in the solid subtype with

basaloid cell features, which is consistent with the findings of this study (21). Although ACCB is classified as TNBC, some studies have reported rare cases of hormone receptor-positive ACCB (11).

Surgery is the primary treatment for ACCB. In a single-center study with a follow-up period of 17 years, all ACCB patients underwent surgical treatment (1). Gomez et al. (22) evaluated the benefits of radiotherapy in ACCB patients and reported that postoperative radiotherapy could improve overall survival (OS). Fewer studies have evaluated the value of adjuvant chemotherapy in ACCB. Some studies suggest that ACCB patients do not benefit from adjuvant chemotherapy (23). However, Liu et al. (12) indicated that adjuvant chemotherapy may be beneficial for ACCB patients with distant metastasis. In the present case, the patient underwent radical surgery and adjuvant chemotherapy, which was in accordance with the recommended treatment protocol for TNBC. Further studies with larger sample sizes are needed to better define the treatment strategy for ACCB. Wenig et al. (24) reported two ACCB patients with IDH2 and FGFR2 mutations who were treated with enasidenib and erdafitinib targeted therapies, both of which showed clinical benefit, suggesting that genetic testing plays an important role in the treatment of rare malignant tumors. This case reinforces the importance of differentiating ACCB from conventional TNBC and adopting individualized treatment. It also highlights the potential role of genetic testing in guiding targeted therapies for metastatic ACCB.

Distant metastasis is rare in ACCB, with an incidence of 2.2% (25). Even after metastasis occurs, the disease tends to progress slowly, allowing for long-term follow-up. Classic ACCB generally has a better prognosis than solid and high-grade transformed ACCB. Li et al. (26) found that tumor size, regional lymph node metastasis, histological grade, AJCC stage, and radiotherapy are important prognostic factors for ACCB patients. Additionally, Tang et al. (3) reported nine male ACCB patients, three of whom developed distant metastasis, suggesting that male ACCB patients may have more aggressive behavior and a greater tendency for distant metastasis.

## 4 Conclusion

In conclusion, ACCB is a distinct subtype of TNBC with a favorable prognosis, and its clinical characteristics differ from those of other pathological types of TNBC. Therefore, treatment strategies should be differentiated from those used for TNBC. Clinicians must recognize and distinguish ACCB from other types of TNBC to avoid misclassifying and treating ACCB as TNBC. Breast-conserving surgery followed by postoperative radiotherapy may be a suitable treatment option for ACCB. This case highlights the necessity of genetic profiling in metastatic ACCB. Recent studies identified IDH2 and FGFR2 mutations in ACCB, suggesting potential targeted therapies such as enasidenib or erdafitinib. Collaborative efforts through platforms like the Adenoid Cystic Carcinoma Research Foundation (ACCRF) are critical to accelerate clinical trials for rare cancers. Regular imaging follow-up is essential to exclude distant metastasis. Our findings support the use of breast-conserving surgery combined with radiotherapy for localized ACCB, as it achieves comparable survival to mastectomy while preserving quality of life. However, for solid subtypes with high Ki-67 (e.g., 30% in this case), adjuvant chemotherapy may be warranted despite limited evidence. Furthermore, larger sample studies are needed to identify the most appropriate treatment strategies for ACCB.

## Data availability statement

The original contributions presented in the study are included in the article/supplementary material. Further inquiries can be directed to the corresponding authors.

## Ethics statement

Written informed consent was obtained from the individual(s) for the publication of any potentially identifiable images or data included in this article. Written informed consent was obtained from the participant/patient(s) for the publication of this case report.

## Author contributions

YZ: Writing – original draft. XL: Writing – original draft. YX: Writing – review & editing. XH: Writing – review & editing. FA: Writing – original draft, Writing – review & editing. MT: Writing – original draft, Writing – review & editing.

## Funding

The author(s) declare that financial support was received for the research and/or publication of this article. This work was supported by the Hunan Provincial Natural Science Foundation (Grant No. 2024JJ7654). The funder had no role in study design, data collection/analysis, or publication decisions.

## Acknowledgments

We are appreciative of Dr. TaoLi Wang for the interpretation of the pathological diagnosis. We appreciate the patient's active cooperation.

## Conflict of interest

The authors declare that the research was conducted in the absence of any commercial or financial relationships that could be construed as potential conflicts of interest.

## Generative AI statement

The author(s) declare that no Generative AI was used in the creation of this manuscript.

## Publisher's note



## References

1. Zhang W, Fang Y, Zhang Z, Wang J. Management of adenoid cystic carcinoma of the breast: a single-institution study. *Front Oncol*. (2021) 11:621012. doi: 10.3389/fonc.2021.621012

2. Treitl D, Radkani P, Rizer M, El Hussein S, Paramo JC, Mesko TW. Adenoid cystic carcinoma of the breast, 20 years of experience in a single center with review of literature. *Breast Cancer*. (2018) 25:28–33. doi: 10.1007/s12282-017-0780-1

3. Tang P, Yang S, Zhong X, Yao J, Zhang Y, Dong H, et al. Breast adenoid cystic carcinoma in a 19-year-old man: a case report and review of the literature. *World J Surg Oncol*. (2015) 13:19. doi: 10.1186/s12957-015-0442-8

4. Wan D, Zhou H, Zhang Y. Adenoid cystic carcinoma of the breast in a male patient: a case report and literature review. *Front Oncol*. (2022) 12:905997. doi: 10.3389/fonc.2022.905997

5. Thomas DN, Asarian A, Xiao P. Adenoid cystic carcinoma of the breast. *J Surg Case Rep*. (2019) 2019:rjy355. doi: 10.1093/jscr/rjy355

6. Hara Y, Yamaguchi R, Yano H, Iwasaki K. Adenoid cystic carcinoma, solid-basaloid subtype of the breast: a Case Report. *Int J Surg Pathol*. (2023) 31:460–3. doi: 10.1177/10668969221102548

7. Sołek JM, Braun M, Kalwas M, Jesionek-Kupnicka D, Romańska H. Adenoid cystic carcinoma of the breast–an uncommon Malignancy with unpredictable clinical behavior. A case series of three patients. *Contemp Oncology/Współczesna Onkologia*. (2020) 24(4):263–5. doi: 10.5114/wo.2020.99025

8. Zhang M, Liu Y, Yang H, Jin F, Zheng A. Breast adenoid cystic carcinoma: a report of seven cases and literature review. *BMC surg*. (2022) 22:113. doi: 10.1186/s12893-022-01560-9

9. Thompson K, Grabowski J, Saltzstein SL, Sadler GR, Blair SL. Adenoid cystic breast carcinoma: is axillary staging necessary in all cases? Results from the California Cancer Registry. *Breast J*. (2011) 17:485–9. doi: 10.1111/j.1524-4741.2011.01117.x

10. Khanfir K, Kallel A, Villette S, Belkacémi Y, Vautravers C, Nguyen T, et al. Management of adenoid cystic carcinoma of the breast: a Rare Cancer Network study. *Int J Radiat Oncol Biol Physics*. (2012) 82:2118–24. doi: 10.1016/j.ijrobp.2010.12.008

11. Welsh JL, Keeney MG, Hoskin TL, Glazebrook KN, Boughey JC, Shah SS, et al. Is axillary surgery beneficial for patients with adenoid cystic carcinoma of the breast? *J Surg Oncol*. (2017) 116(6):690–5. doi: 10.1002/jso.24702

12. Liu Z, Wang M, Wang Y, Shen X, Li C. Diagnosis of adenoid cystic carcinoma in the breast: a case report and literature review. *Arch Med Science: AMS*. (2022) 18:279. doi: 10.5114/aoms/144321

13. Meng M, Xie LJ, Qiu X. A case of adenoid cystic carcinoma of the breast. *Asian J surg*. (2024) 47:2415–6. doi: 10.1016/j.asjsur.2024.01.046

14. Boujelbene N, Khabir A, Sozzi WJ, Mirimanoff R, Khanfir K. Clinical review–breast adenoid cystic carcinoma. *Breast*. (2012) 21:124–7. doi: 10.1016/j.breast.2011.11.006

15. Liu Y, Zhu L, Guo L, Yang H, Wang S, Sun G, et al. Tremendous and infrequently adenoid cystic carcinoma of the breast without any metastasis for more than 20 years: A case report. *Medicine*. (2024) 103:e39461. doi: 10.1097/MD.0000000000039461

16. Guldogan N, Esen G, Kayadibi Y, Taskin F, Alfatli AO, Boy FNS, et al. Adenoid cystic carcinoma of the breast: multimodality imaging findings and review of the literature. *Acad Radiol*. (2023) 30:1107–17. doi: 10.1016/j.acra.2022.10.003

17. Kashiwagi S, Asano Y, Ishihara S, Morisaki T, Takashima T, Tanaka S, et al. Adenoid cystic carcinoma of the breast: a case report. *Case Rep Oncol*. (2020) 12:698–703. doi: 10.1159/000502949

18. Gillie B, Kmeid M, Asarian A, Xiao P. Adenoid cystic carcinoma of the breast with distant metastasis to the liver and spleen: a case report. *J Surg Case Rep*. (2020) 2020:rjaa483. doi: 10.1093/jscr/rjaa483

19. Burusapat C, Buarabporn N, Wongchansom K, Chanapai P, Parinyanut P, Supaporn S. Mammary adenoid cystic carcinoma presenting with Ductal carcinoma in situ and axillary lymph node metastasis. *J Surg Case Rep*. (2020) 2020:rjz362. doi: 10.1093/jscr/rjz362

20. de Gregorio A, Friedl TWP, Hering E, Widschwendter P, de Gregorio N, Bekes I, et al. Ki67 as proliferative marker in patients with early breast cancer and its association with clinicopathological factors. *Oncology*. (2021) 99:780–9. doi: 10.1159/000517490

21. Mastropasqua MG, Maiorano E, Pruneri G, Orvieto E, Mazzarol G, Vento AR, et al. Immunoreactivity for c-kit and p63 as an adjunct in the diagnosis of adenoid cystic carcinoma of the breast. *Modern pathol*. (2005) 18:1277–82. doi: 10.1038/modpathol.3800423

22. Gomez-Seoane A, Davis A, Oyasiji T. Treatment of adenoid cystic carcinoma of the breast: Is postoperative radiation getting its due credit? *Breast*. (2021) 59:358–66. doi: 10.1016/j.breast.2021.08.001

23. Yang L, Wang C, Liu M, Wang S. Evaluation of adjuvant treatments for adenoid cystic carcinoma of the breast: A population-based, propensity score matched cohort study from the SEER database. *Diagnostics*. (2022) 12:1760. doi: 10.3390/diagnostics12071760

24. Wenig E, Birhiray RE. *Novel treatment options in advanced adenoid cystic carcinoma of the breast*. Wolters Kluwer Health (2021). doi: 10.1200/jco.2021.39.15_suppl.e13071

25. Macias J, Sales Nogueira Amorim Canedo F, Lu S-E, Chen C, Heleno CT, Bridgeman M, et al. Treatment patterns of adenoid cystic carcinoma of the breast: A systematic review. *J Clin Oncol*. (2024) 42:e13147–e. doi: 10.1200/JCO.2024.42.16_suppl.e13147

26. Li L, Zhang D, Ma F. Adenoid cystic carcinoma of the breast may be exempt from adjuvant chemotherapy. *J Clin Med*. (2022) 11:4477. doi: 10.3390/jcm11154477

frontiers | Frontiers in Oncology

TYPE Original Research
PUBLISHED 05 June 2025
DOI 10.3389/fonc.2025.1525285



OPEN ACCESS

EDITED BY
Sharon R. Pine,
University of Colorado Anschutz Medical Campus, United States

REVIEWED BY
Sriroop Reddy Ramireddy,
The Apollo University, India
Cherry Bansal,
Tantia University, India

*CORRESPONDENCE
Ma Ziqian
419090291@qq.com
Zhu Yiwen
1628461616@qq.com
Gan Ling
xyyycsgl@163.com

†These authors have contributed equally to this work and share first authorship

RECEIVED 09 November 2024
ACCEPTED 16 May 2025
PUBLISHED 05 June 2025

CITATION
Tenghui W, Xinyi L, Ziyi S, Yanting Z, Ziqian M, Yiwen Z and Ling G (2025) Combination of ultrasound-based radiomics and deep learning with clinical data to predict response in breast cancer patients treated with neoadjuvant chemotherapy.
*Front. Oncol.* 15:1525285.
doi: 10.3389/fonc.2025.1525285



# Combination of ultrasound-based radiomics and deep learning with clinical data to predict response in breast cancer patients treated with neoadjuvant chemotherapy

Wu Tenghui[1†], Liu Xinyi[2†], Si Ziyi[2], Zhang Yanting[2], Ma Ziqian[3*], Zhu Yiwen[2*] and Gan Ling[2*]

[1]Department of Nuclear Medicine, Xiangyang No. 1 People's Hospital, Hubei University of Medicine, Xiangyang, China, [2]Department of Ultrasound, Xiangyang No.1 People's Hospital, Hubei University of Medicine, Xiangyang, China, [3]Department of Oncology, The People's Hospital of Zouping City, Zouping, China

**Objectives:** Accurate assessment of NAC efficacy is crucial for determining appropriate surgical strategies and guiding the extent of surgical resection in breast cancer. Therefore, this study aimed to design an integrated predictive model combining ultrasound imaging, deep learning features, and clinical characteristics to predict pCR in breast cancer patients undergoing NAC.

**Methods:** A retrospective study was conducted, including 643 pathologically confirmed breast cancer patients who underwent NAC between January 2022 to February 2024 from two institutions (Center 1: 372 cases; Center 2: 271 cases). Ultrasound images before and after NAC were collected for each patient. A total of 2,920 radiomics features and 4,096 deep learning features were extracted from the ultrasound images. Multiple machine learning algorithms were employed to model and validate the diagnostic performance of different types of features. Finally, clinical data, radiomics, and deep learning features were integrated to form a fusion model, which was evaluated using receiver operating characteristic (ROC) analysis.

**Results:** The combined model achieved the highest predictive performance for pathological complete response (pCR) across both cohorts. In the internal validation cohort, it reached an accuracy of 0.892 (95% CI: 0.862–0.912) and an AUC of 0.901 (95% CI: 0.854–0.948). In the external cohort, it maintained strong performance with an accuracy of 0.857 (95% CI: 0.822–0.928) and an AUC of 0.891 (95% CI: 0.848–0.934), significantly outperforming the individual models (DeLong test, $p < 0.01$).The deep learning model showed solid performance with accuracies of 0.875 and 0.833 in the internal and external cohorts, respectively, and AUCs of 0.870 and 0.874. The radiomics model displayed moderate accuracy and AUC in both cohorts, while the clinical model showed the lowest predictive capability among the models, with accuracy and AUC values around 0.67 in both cohorts.

**Conclusions:** The combined model, integrating clinical, radiomics, and deep learning features, demonstrated superior predictive accuracy for pCR following neoadjuvant chemotherapy (NAC) in breast cancer patients, outperforming individual models. This integrated approach highlights the value of combining diverse data types to improve prediction, offering a promising tool for guiding NAC response assessment and personalized treatment planning.

KEYWORDS

**ultrasound, deep learning, breast cancer, neoadjuvant chemotherapy, radiomics**

## 1 Introduction

Breast cancer remains one of the most prevalent malignancies among women worldwide and is a leading cause of cancer-related mortality (1). Neoadjuvant chemotherapy (NAC) is widely employed as a first-line treatment strategy to downstage tumors before surgical intervention. Achieving a pathological complete response (pCR) following NAC is considered an effective surrogate endpoint for predicting long-term prognosis in breast cancer patients. Those who attain pCR have reported 5-year survival rates as high as 85–90% (2, 3).

Despite its benefits, the effectiveness of NAC varies significantly due to tumor heterogeneity, leading to considerable differences in pCR rates among different molecular subtypes of breast cancer, especially in advanced stages or in patients resistant to therapy (4–6). Approximately 30–50% of breast cancer patients achieve pCR after completing NAC, as defined by postoperative pathology (ypT0/is ypN0). Conversely, about 29% of patients exhibit no response to NAC, and 7.9% experience disease progression post-treatment, which adversely affects prognosis and increases mortality rates in advanced cases (2, 3). These disparities not only affect individual prognoses but also complicate treatment planning and decision-making processes. Consequently, there is a pressing need to understand the factors influencing NAC responsiveness and to develop reliable methods for predicting pCR in order to tailor individualized treatment strategies effectively.

The choice of surgical options after NAC largely depends on whether the patient achieves pCR. Some researchers suggest that patients who reach pCR may opt for breast-conserving surgery to improve quality of life and outcomes, with some even proposing the possibility of completely avoiding mastectomy. However, accurately identifying which patients are suitable for such conservative treatments remains a challenge in clinical practice. Currently, the assessment of NAC efficacy in clinical practice predominantly relies on subjective evaluations using ultrasound (US) and magnetic resonance imaging (MRI). While these imaging modalities provide valuable information, they have limitations in accurately predicting pCR due to factors like inter-observer variability and limited sensitivity and specificity. Moreover, the gold standard for determining pCR remains the pathological examination of surgical specimens obtained after NAC, which is invasive and only available postoperatively. This highlights a critical gap in preoperative assessment tools that can non-invasively and accurately predict NAC outcomes, enabling clinicians to optimize treatment plans before surgical intervention.

The emergence of deep learning and radiomics has opened new avenues for developing such predictive tools. Radiomics involves extracting a vast array of high-dimensional features from medical images, capturing subtle textural and spatial characteristics that are often imperceptible to traditional manual analysis (7). By modeling and integrating these features, robust predictive models can be established. Deep learning, with its powerful automated learning capability, effectively handles complex non-linear data relationships, further enhancing the model's ability to capture abstract and spatial features, thereby improving the model's predictive accuracy and robustness. With advancements in computational power and the accumulation of large-scale datasets, deep learning–based radiomics models have demonstrated substantial potential for clinical applications. The significance of this integration is that the two can play their relative advantages to describe different types of texture features, and finally achieve more accurate diagnostic efficiency through feature combination.

Several studies have demonstrated the feasibility of such approaches using other imaging modalities. For instance, Huang et al. (8) developed a predictive model using multimodal longitudinal MRI images for different pathological subtypes of breast cancer, achieving excellent diagnostic performance (AUC = 0.89), Song et al. also verified the feasibility of the method in prostate cancer (9). However, the reliance on MRI images across multiple time points limits the model's applicability, given the higher cost, longer scanning time, and reduced accessibility of MRI compared to other imaging modalities.In clinical practice, ultrasound is the most commonly used and recommended modality for monitoring and evaluating NAC response in breast cancer due to its accessibility, cost-effectiveness, and real-time imaging capabilities. Despite these advantages, the quality of evidence for using ultrasound data to predict the efficacy of NAC in different pathological subtypes is still poor, and the method using radiomics combined with deep learning has not been explored (10). Therefore, the aim of this study is to develop a predictive model based on

radiomics and deep learning using US images to predict patients' pCR status. This model seeks to provide a non-invasive, practical tool that can assist clinicians in making more informed decisions regarding surgical planning and personalized treatment strategies.

# 2 Materials and methods

## 2.1 Patient information and clinical data

This retrospective study adhered to the Declaration of Helsinki and received ethical approval from Xiangyang First People's Hospital and Zou Ping Hospital, with informed consent waived due to its retrospective nature. Data collection at Xiangyang First People's Hospital involved 372 patients between January 2022 and February 2024, including 146 patients who achieved pathological complete response (pCR) and 226 patients who did not. These patients were divided into a training cohort and an internal validation cohort in a 7:3 ratio using stratified random sampling. Zou Ping Hospital collected data from 271 patients between March 2022 and February 2024, comprising 107 pCR and 164 non-pCR patients, which served as an external test cohort.

Inclusion criteria were as follows: (a) confirmed diagnosis of invasive breast cancer; (b) completion of NAC treatment followed by surgery; (c) availability of US data both before and at the midpoint of NAC; and (d) comprehensive clinical and pathological data. Although histological subtyping (e.g., ductal vs. lobular carcinoma) was not explicitly used as an inclusion criterion, the vast majority of patients were diagnosed with invasive ductal carcinoma.

Exclusion criteria included: (a) diagnosis of bilateral breast cancer; (b) incomplete or non-standardized NAC treatment or surgery; (c) poor US quality or absence of US data; and (d) presence of metastatic disease or a secondary malignancy.

Patient demographic data, including age and clinical symptoms, were obtained from medical records. Collected clinical data included: (a) age; (b) clinical stage; (c) estrogen receptor (ER) status; (d) progesterone receptor (PR) status; (e) HER-2 status; and (f) Ki-67 status. The comprehensive data screening and collection workflow is illustrated in Figure 1.

## 2.2 Experimental methods

### 2.2.1 Data processing

Breast ultrasound examinations were conducted by five radiologists with over 10 years of experience in breast ultrasound imaging, both prior to intervention and at the midpoint of NAC. Imaging was performed using four different ultrasound systems (Resona 7, Mindray, China; Philips Healthcare, USA; LOGIQ E20, GE, USA; and Samsung, Korea), each equipped with a linear array transducer. To ensure consistency, all images were acquired at the largest cross-sectional area of the tumor.

To reduce variability introduced by different ultrasound machines, all images were rescaled to a uniform resolution of 512 × 512 pixels using linear interpolation. The 3-sigma method was applied to remove outlier pixel values. All segmentation was manually performed by two radiologists under the supervision of a senior breast imaging expert using 3D Slicer software. Radiologists were blinded to outcomes, and delineation was performed in

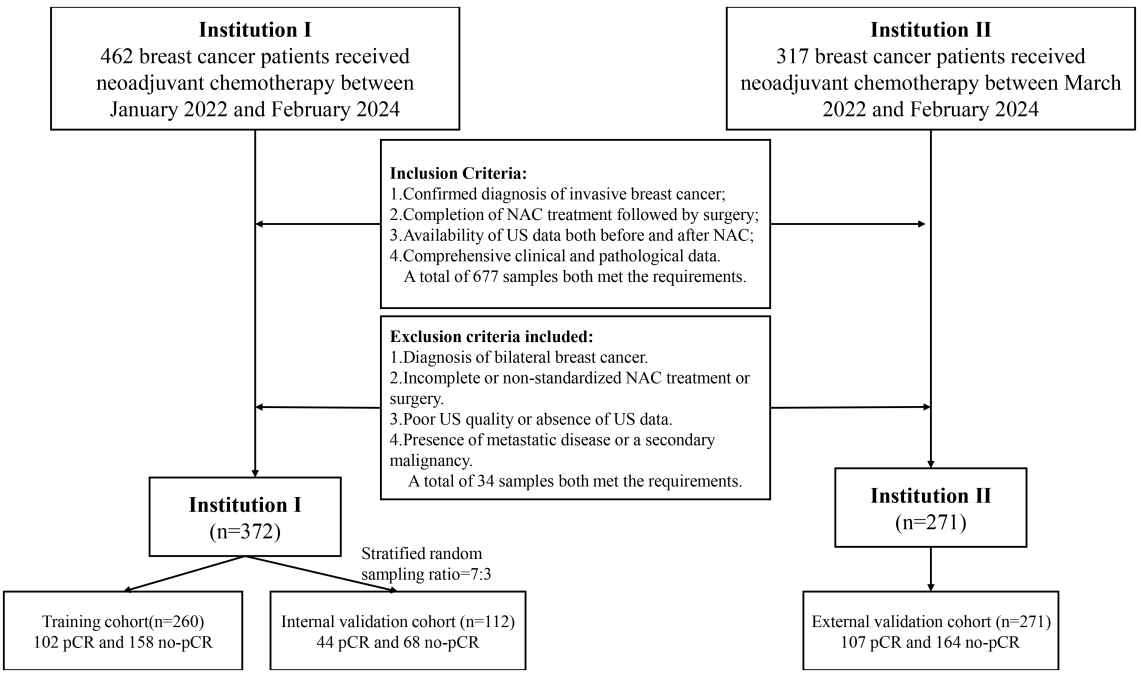


FIGURE 1
Diagram of the experimental inclusion-exclusion criteria.

consensus. The largest cross-sectional images from both pre-NAC and mid-NAC were used for segmentation and saved as ROI-original images.

To train the deep learning model, ROI-original images were further resampled to 128 × 128 pixels to generate a uniform dataset (ROI-resample) for input. This standardization ensured a consistent representation of tumor morphology and enhanced model generalizability.

### 2.2.2 pCR prediction model

To construct the clinical model, clinical variables showing statistical significance ($p < 0.05$) in univariate analysis of the training cohort were selected and input into eight supervised machine learning algorithms. The radiomics model was developed by extracting features from the ROI-original images using the PyRadiomics library. Filters such as Laplacian of Gaussian and wavelets were applied to generate derivative images, from which 1,216 features per ROI were extracted. Categories included shape-based, first-order, GLCM, GLRLM, GLSZM, GLDM, and NGTDM features. Each patient contributed two ROIs (pre- and mid-NAC), resulting in 2,438 radiomics features per patient.

To construct the deep learning model, a ResNet-50 architecture was trained using the ROI-resample dataset. Probability-based predictions were generated through a softmax activation function in the final layer. The model with the best internal validation performance was selected. Deep features were extracted from the final fully connected layer for further integration.

To address class imbalance between pCR and non-pCR groups (~39% vs. ~61%), the Synthetic Minority Oversampling Technique (SMOTE) was applied to the training cohort. For algorithms that support class weighting, such as logistic regression and XGBoost, balanced class weights were also utilized.

The composite (Combine) model was constructed by integrating clinical, radiomics, and deep learning features using early feature-level fusion. Eight machine learning algorithms were employed for model building. All models were trained on the training cohort and evaluated on both internal and external test sets. Model calibration was assessed using calibration curves and Brier scores. Clinical utility was evaluated using decision curve analysis (DCA). The complete experimental workflow is summarized in Figure 2.

### 2.2.3 Statistical analysis

Statistical analysis and model construction were performed using R (version 4.1.3) and Python (version 3.6.2). For continuous variables, the Kolmogorov-Smirnov test was employed to assess normality. Depending on the distribution, either the t-test or the Mann-Whitney U test (using SciPy version 1.7.0) was used to compare differences between the two cohorts. For multivariate analysis, logistic regression was applied to evaluate associations between clinical variables and outcomes. The p-values were adjusted using the Benjamini-Hochberg correction to control for multiple comparisons, ensuring statistical rigor. Categorical variables were analyzed with the chi-square test to identify significant associations.

To assess the agreement between predicted probabilities and actual outcomes, model calibration was evaluated using calibration curves and Brier scores. Calibration curves were generated by plotting the predicted probabilities against observed event rates. The optimal classification threshold was determined based on the Youden index, maximizing the sum of sensitivity and specificity on the ROC curve. To further explore the clinical value of the model across different probability thresholds, DCA was performed, which estimates the net benefit of using the model in clinical decision-making compared to treating all or no patients.

To evaluate model performance, 95% confidence intervals (CIs) for the AUC were calculated using a bootstrapping approach with 1,000 iterations, providing robust interval estimates. Using the selected clinical features, a predictive model was developed using machine learning algorithms optimized for diagnostic accuracy.ROC curves were used to visually demonstrate the predictive ability of each model—the clinical, deep learning, radiomics, and composite models. Each model was tested on both internal and external validation sets to assess generalizability and predictive performance across different datasets. The DeLong test was conducted to compare the AUCs between models, allowing for statistical validation and comparison of their predictive capabilities.

## 3 Results

### 3.1 Baseline characteristics of patients

Between January 2022 and February 2024, a total of 372 patients were included in the primary cohort from Xiangyang First People's Hospital, and 271 patients were included in the external validation cohort from Zou Ping Hospital (March 2022 to February 2024). In the primary cohort, 146 patients (39.2%) achieved pathological complete response (pCR), while 226 patients (60.8%) did not. Similarly, in the validation cohort, the pCR rate was 39.5% (107 out of 271), with the remaining 164 patients (60.5%) not achieving pCR.

Table 1 summarizes the clinical characteristics of all patients in this study. The primary and validation cohorts exhibited similar baseline characteristics, with no significant differences observed in age or clinical stage between pCR and non-pCR patients across both cohorts ($p = 0.631$ and $p = 0.682$ in the primary cohort; $p = 0.317$ and $p = 0.231$ in the validation cohort, respectively). However, significant differences were noted in several molecular markers, including estrogen receptor (ER), progesterone receptor (PR), human epidermal growth factor receptor 2 (HER2), and Ki-67 status.

ER and PR positivity were more prevalent among non-pCR patients. In the primary cohort, ER positivity was observed in 69.9% of non-pCR patients compared to 44.5% in pCR patients ($p < 0.01$). Conversely, HER2 positivity was significantly higher in the pCR group, with rates of 67.8% in the primary cohort and 72.9% in the validation cohort ($p < 0.01$). Additionally, Ki-67 positivity, an indicator of cellular proliferation, was more common among pCR patients, showing significant differences in both cohorts ($p = 0.036$ in the primary cohort and $p = 0.01$ in the validation cohort).

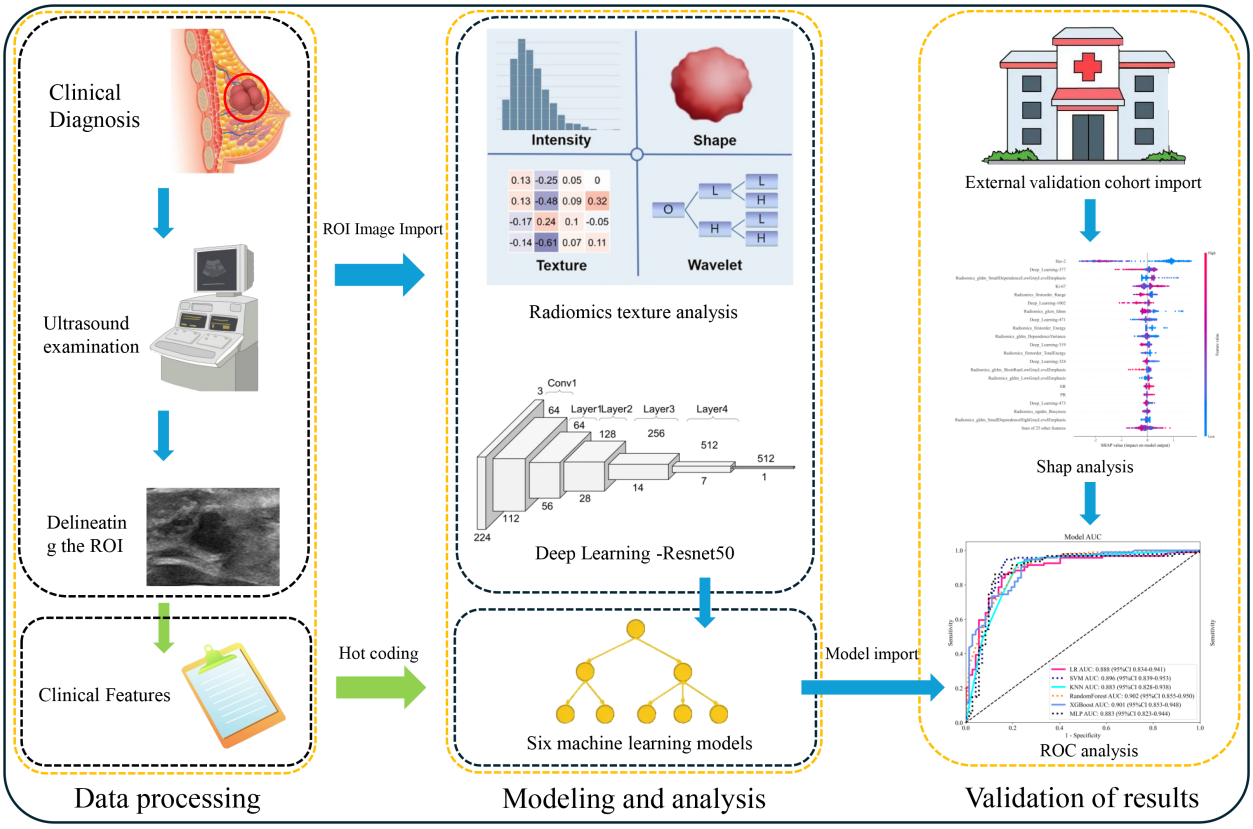


FIGURE 2
Flow chart. The flowchart shows the study design.

Regarding molecular subtypes, the HER2-positive subtype had the highest pCR rate, with 66.4% of pCR patients in the primary cohort belonging to this subtype, whereas the hormone receptor-positive/HER2-negative (HR+/HER2−) subtype had the lowest pCR rate, accounting for only 11.6% of pCR patients ($p < 0.01$). These findings highlight significant associations between ER, PR, HER2, and Ki-67 status with pCR, underscoring the importance of these biomarkers in predicting NAC response.

## 3.2 Model performance

Achieved an accuracy (ACC) of 0.892 (95% CI: 0.862–0.912) and an area under the curve (AUC) of 0.901 (95% CI: 0.854–0.948). This model consistently outperformed the individual models. The deep learning model recorded an ACC of 0.875 (95% CI: 0.818–0.932) and an AUC of 0.870 (95% CI: 0.833–0.907), while the radiomics model had an ACC of 0.797 (95% CI: 0.791–0.913) and an AUC of 0.831 (95% CI: 0.788–0.873). The clinical model showed the lowest predictive capability, with an ACC of 0.674 (95% CI: 0.628–0.741) and an AUC of 0.682 (95% CI: 0.629–0.736).

In the external validation cohort, the combined model maintained high performance, achieving an ACC of 0.857 (95% CI: 0.822–0.928) and an AUC of 0.891 (95% CI: 0.848–0.934). The deep learning model demonstrated robust external generalizability with an ACC of 0.833 (95% CI: 0.791–0.875) and an AUC of 0.874 (95% CI: 0.838–0.909). The radiomics model also performed well, with an ACC of 0.801 (95% CI: 0.788–0.859) and an AUC of 0.822 (95% CI: 0.778–0.866). However, the clinical model recorded the lowest external validation performance, with an ACC of 0.655 (95% CI: 0.601–0.709) and an AUC of 0.666 (95% CI: 0.612–0.721).

DCA was also conducted to assess the net clinical benefit across a range of threshold probabilities. The combined model provided the highest net benefit in both validation cohorts, supporting its clinical utility in decision-making contexts (Figure 3). To evaluate the reliability of probability-based predictions, calibration analysis was performed using calibration curves (Figure 4). The combined and deep learning models demonstrated good calibration performance, with curves closely aligned to the ideal diagonal and low Brier scores in both internal and external validation sets (see Supplementary File S1).

For final model comparisons, DeLong's test was used to compare the AUCs among the clinical, ResNet50, radiomics, and combined models. The results showed that the combined model significantly outperformed the clinical model ($p < 0.01$), and also demonstrated superiority over the radiomics and standalone deep learning models (see Figure 5, Table 2).

10.3389/fonc.2025.1525285

TABLE 1 Characteristics of patients in the training and test cohort.

| Characteristics | Primary cohort (N=372) | | | Validation cohort 1 (N=271) | | |
|---|---|---|---|---|---|---|
| | pCR (n=146) | N-pCR (n=226) | P Value | pCR (n=107) | N-pCR (n=164) | P Value |
| Age | 48.93 ± 8.73 | 49.21 ± 9.66 | 0.631 | 47.91 ± 10.31 | 49.13.39 ± 9.78 | 0.317 |
| Clinical Stage (%) | | | 0.682 | | | 0.231 |
| I | 2 (1.37%) | 1 (0.44%) | | 1 (0.9%) | 2 (1.2%) | |
| II | 97 (66.4%) | 152 (67.3%) | | 67 (62.6%) | 108 (65.9%) | |
| III | 47 (32.2%) | 73 (32.3%) | | 39 (36.4%) | 54 (32.9%) | |
| ER Status (%) | | | <0.01 | | | <0.01 |
| Positive | 65 (44.5%) | 158 (69.9%) | | 63 (58.9%) | 121 (73.8%) | |
| Negative | 67 (45.9%) | 82 (36.3%) | | 44 (41.1%) | 43 (26.2%) | |
| PR status (%) | | | <0.01 | | | <0.01 |
| Positive | 71 (48.6%) | 159 (70.4%) | | 61 (57.0%) | 122 (74.4%) | |
| Negative | 68 (46.6%) | 74 (32.7%) | | 46 (43.0%) | 42 (25.6%) | |
| HER-2status (%) | | | <0.01 | | | <0.01 |
| Positive<br>Negative | 99 (67.8%)<br>33 (22.6%) | 71 (31.4%)<br>169 (74.8%) | | 78 (72.9%)<br>29 (27.1%) | 47 (28.7%)<br>117 (71.3%) | |
| Ki-67 Status (%) | | | 0.036 | | | 0.01 |
| Positive | 106 (72.6%) | 172 (76.1%) | | 86 (80.4%) | 118 (72.0%) | |
| Negative | 26 (17.8%) | 68 (23.9%) | | 21 (19.6%) | 46 (28.0%) | |
| Cancer subtype (%) | | | <0.01 | | | <0.01 |
| HR+/Her2- | 17 (11.6%) | 131 (58.0%) | | 13 (12.1%) | 94 (57.3%) | |
| Her2+ | 97 (66.4%) | 69 (30.5%) | | 78 (72.9%) | 50 (30.5%) | |
| TN | 21 (14.4%) | 37 (16.4%) | | 16 (14.9%) | 20 (12.2%) | |

P-value is derived from the univariable association analyses between the clinicopathologic variables and Bone status. The data marked with * are averaged.

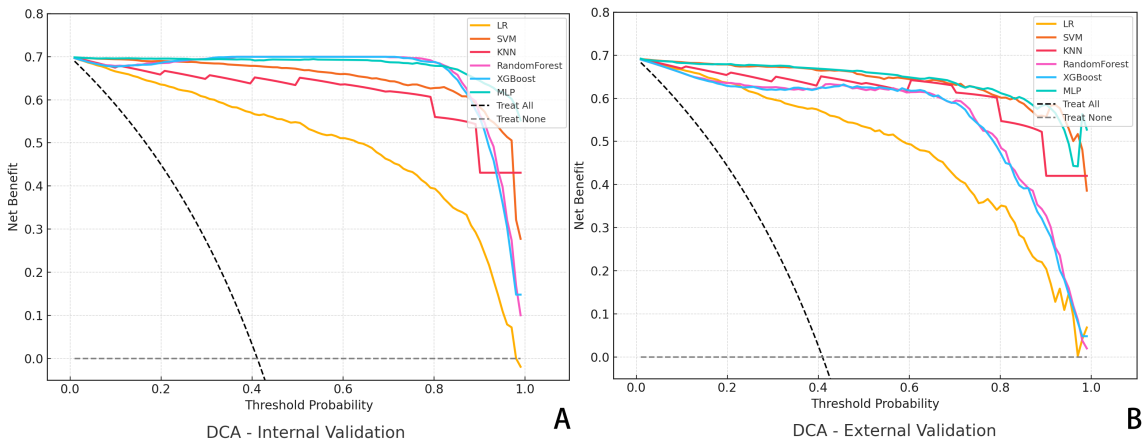


FIGURE 3
Decision Curve Analysis (DCA) for Predictive Models. **(A)** DCA curves of six algorithms in the internal validation cohort; **(B)** DCA results in the external validation cohort. The y-axis represents the net benefit, and the x-axis denotes the threshold probability.

10.3389/fonc.2025.1525285

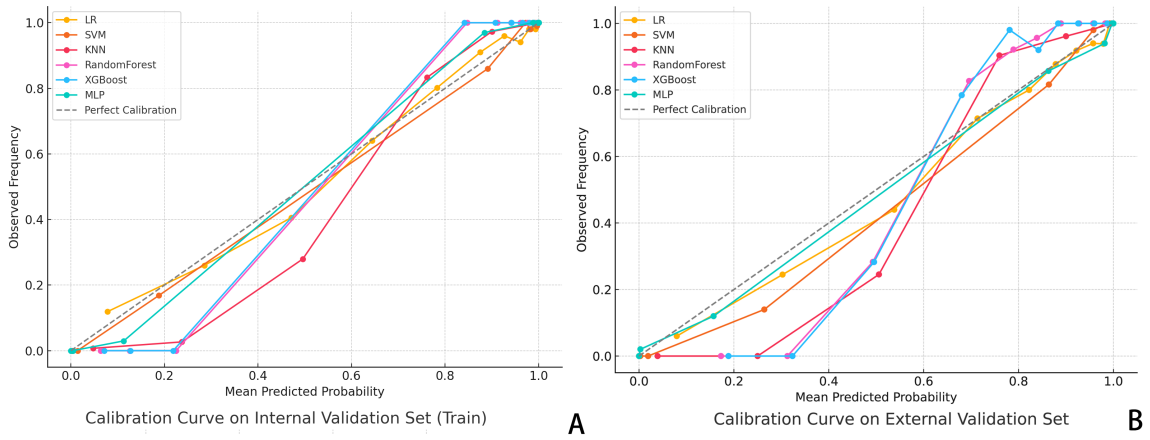


FIGURE 4
Calibration Curve Analysis. **(A)** Calibration curves for six classifiers in the internal validation set; **(B)** Dashed diagonal line indicates perfect calibration. A curve closer to the diagonal suggests better agreement between predicted probability and actual observed frequency of pCR. The XGBoost and MLP models showed the highest calibration accuracy across both datasets.

## 4 Discussion

Accurate prediction of pathological complete response (pCR) following neoadjuvant chemotherapy (NAC) is essential for optimizing surgical planning and improving outcomes for breast cancer patients. Reliable pCR prediction enables clinicians to make informed decisions about the feasibility of breast-conserving surgery, potentially avoiding unnecessary mastectomies and their associated morbidity (11–13). However, traditional reliance on imaging modalities like MRI and postoperative pathological examination presents limitations, including limited accessibility, high costs, and delayed diagnostic timing. Therefore, developing a convenient, non-invasive, and accurate method to assess pCR before surgery is a crucial objective in current breast cancer treatment strategies.

Recent advances in radiomics and deep learning have opened new avenues for enhancing the prediction of treatment response. Radiomics involves extracting high-dimensional quantitative features from medical images, capturing subtle textural, spatial, and morphological characteristics that may not be discernible through conventional imaging analyses (7). Deep learning, particularly convolutional neural networks (CNNs), can model complex non-linear relationships within imaging data, thereby improving predictive accuracy and robustness (14). Integrating these technologies with ultrasound imaging—a widely available, cost-effective, and non-invasive modality—offers a practical solution to overcome the limitations of traditional methods. Despite this potential, few studies have focused on using ultrasound-based radiomics models for predicting pCR in breast cancer.

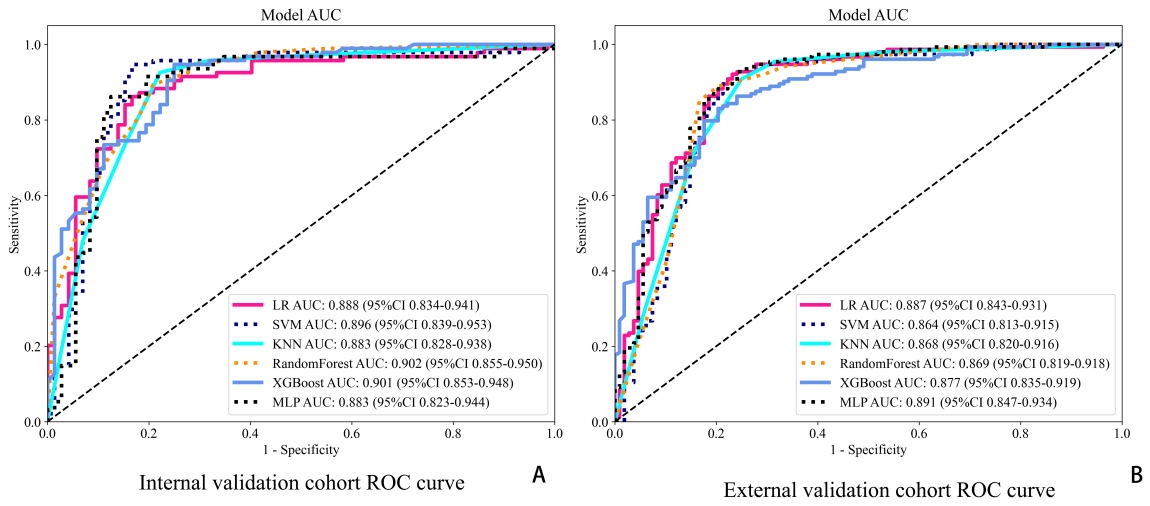


FIGURE 5
ROC curves for six classification models in both cohorts. **(A)** ROC curves in the internal validation cohort. **(B)** ROC curves in the external validation cohort.

TABLE 2 Predictive model performance effectiveness.

| Model | Accuracy | | AUC | | Delong test* | |
|---|---|---|---|---|---|---|
| | Internal validation cohort | External Validation | Internal validation cohort | External Validation | Internal validation cohort | External Validation |
| Combine | 0.892 (0.862,0.912) | 0.857 (0.822,0.928) | 0.901 (0.854,0.948) | 0.877 (0.834,0.919) | 0.002 | 0.003 |
| Deep learning | 0.875 (0.818,0.932) | 0.833 (0.791,0.875) | 0.870 (0.833,0.907) | 0.834 (0.808,0.889) | 0.002 | 0.014 |
| Radiomics | 0.797 (0.791,0.913) | 0.801 (0.788,0.859) | 0.831 (0.788,0.873) | 0.822 (0.778,0.866) | 0.019 | 0.029 |
| Clinic | 0.674 (0.628,0.741) | 0.655 (0.601,0.709) | 0.682 (0.629,0.736) | 0.666 (0.612,0.721) | – | – |

1. DeLong test is performed with Clinic as the benchmark, and the 95% confidence interval is listed for AUC and ACC, respectively. 2. All results show the best model results in internal validation cohort AUC.

In our study, we aimed to address this gap by developing a predictive model based on ultrasound images, leveraging the strengths of deep learning and radiomics to offer a practical and accessible tool for clinicians. Our model demonstrated strong performance in predicting pCR, with area under the curve (AUC) values of 0.907 and 0.862 across different validation cohorts. The use of ultrasound expands the applicability of predictive models to a broader patient population, including those in resource-limited environments or with contraindications to MRI. Beyond its accessibility, ultrasound's real-time imaging capability enables dynamic monitoring of treatment response, further enhancing its clinical utility. By focusing on a widely available and user-friendly modality, our approach simplifies the predictive process, reduces methodological complexity, and facilitates more efficient clinical implementation. This not only improves workflow efficiency but also increases the likelihood of broader adoption in clinical practice, where ease of use is a critical factor for integrating new technologies.

In our cohort, the pCR rate following NAC was approximately 38%, which is slightly higher than the 26–35% typically reported in previous studies. This discrepancy may be attributed to the retrospective nature of our study, where patients were selected based on real-world clinical decisions. As a result, individuals with more favorable baseline characteristics—such as earlier-stage disease or molecular subtypes known to be more responsive to NAC—were more likely to be included. Moreover, the relatively limited sample size may have contributed to this deviation through statistical variability.Despite this potential selection bias, the reliability of our ultrasound-based radiomics model remains robust, as it leverages high-dimensional imaging features that are less influenced by subjective clinical judgment. This objectivity supports the model's potential for broader clinical applicability and generalizability.

Currently, clinical evaluation of NAC response often includes biomarkers such as estrogen receptor (ER), progesterone receptor (PR), and human epidermal growth factor receptor 2 (HER2) status, which significantly influence treatment outcomes. Research has shown that molecular subtypes like triple-negative and HER2-positive breast cancers are more likely to achieve pCR compared to hormone receptor-positive tumors (15–20). Accordingly, our study incorporated these molecular subtypes as key clinical variables in the model development process. Univariate and multivariate logistic regression analyses revealed significant associations between molecular subtype, tumor grade, and the likelihood of achieving pCR ($P < 0.05$, Table 1), aligning with findings from previous research. However, predictive models based solely on traditional clinical indicators demonstrated limited accuracy (AUC of clinical feature model = 0.73, 0.69). This limitation could be due to the inherent complexity of tumor biology, where molecular and imaging markers alone may not fully capture the heterogeneity of treatment response. Additionally, certain clinical parameters, such as Ki-67 proliferation index and histological grade, may not always be reliably assessed due to sampling errors or variability in pathological interpretation (21, 22). These challenges underscore the necessity for advanced imaging-based models that integrate both clinical and imaging data to enhance predictive accuracy.

Radiomics research, leveraging high-throughput data and advancements in CNN-based deep learning, has significantly enhanced the non-invasive prediction of tumor biological behavior. Traditional radiomics approaches have demonstrated promise in identifying imaging features correlated with treatment outcomes, such as predicting pCR following NAC (10, 23, 24). However, our study introduces several methodological and clinical innovations that improve predictive accuracy and applicability beyond prior efforts.

Firstly, our model utilizes ultrasound imaging instead of MRI, which many existing models rely upon. Ultrasound offers substantial practical advantages due to its widespread availability, cost-effectiveness, and non-invasive nature, making it highly suitable for routine clinical practice. By integrating radiomics with deep learning, our model captures high-dimensional imaging features that are often undetectable through conventional analyses, enhancing the precision of pCR prediction in breast cancer patients undergoing NAC. The model's strong performance metrics, with AUC values of 0.907 and 0.862 across different validation cohorts, underscore its effectiveness and potential for clinical application.

Secondly, we address the limitations of traditional radiomics models in capturing abstract and non-linear relationships within

imaging data by incorporating CNNs. CNNs have the unique ability to extract complex spatial features from medical images through convolutional and pooling operations, analyzing relationships between distant pixels (25, 26). This capability provides deeper insights into tumor heterogeneity—a significant challenge in predicting treatment response in breast cancer. Furthermore, we enhanced the robustness and reliability of our predictive model through ensemble learning by combining radiomics and deep learning-derived features. In performing ensemble learning, we tested a variety of model structures, and the results showed that the XGBoost algorithm model had the highest accuracy in the internal validation set (Supplementary File S1). Employing the XGBoost algorithm, known for effectively handling non-linear and complex data interactions (27, 28), we developed the combined model. This ensemble model achieved impressive AUCs of 0.901 and 0.891 across two independent centers, demonstrating both its generalizability and clinical strength. The multicenter validation significantly enhances the external validity of our results. The DeLong test ($P < 0.05$) revealed significant differences between our ultrasound-based model and traditional clinical risk models, emphasizing the necessity of incorporating advanced imaging techniques into predictive modeling.

To address the "black box" nature of deep learning, we incorporated Gradient-weighted Class Activation Mapping (Grad-CAM) into our study to visually interpret which tumor regions the model prioritized for prediction (Figure 6). This technique generates heatmaps that indicate the areas most influential in the model's decision-making. For interpretability, we further utilized SHAP plots (Figure 7) to reveal the decision-making process of the optimal model (internal validation set). As a novel visualization tool, SHAP showed that among the top 20 features, clinical features were all considered and prioritized by the model, with molecular phenotypes like Ki-67 and HER2 positively correlated with pCR probability, consistent with previous research. Notably, both deep learning and radiomic features were among the top 20, validating our integrated learning strategy that combines different types of features. Importantly, clinical reviewers who evaluated the SHAP plots confirmed not only the intuitive alignment of high-impact variables—such as HER2 and Ki-67—with their clinical expectations, but also found the explanations actionable in supporting individualized treatment discussions. Feedback indicated that the clear ranking and directionality of feature contributions could help reinforce clinical decision-making, particularly when used alongside other interpretable tools like Grad-CAM.

In addition to evaluating discriminative performance via AUC, we assessed the calibration of our model's predicted probabilities. Calibration curves showed a strong agreement between predicted

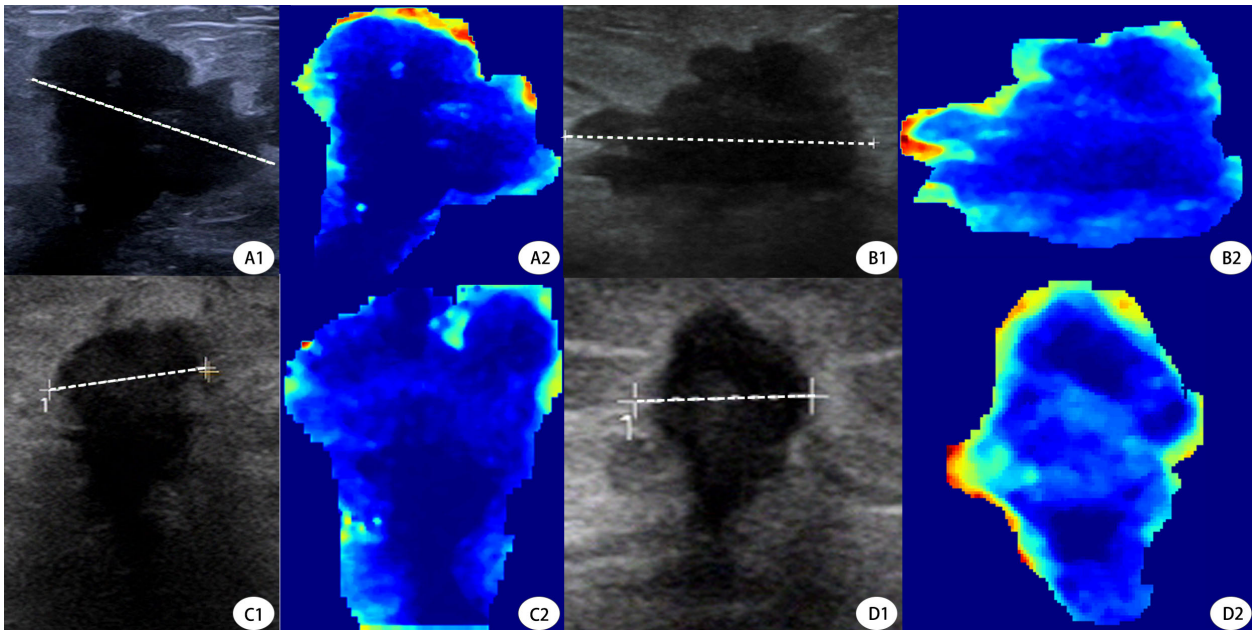


FIGURE 6
Grad-CAM Visualization of Deep Learning Model Attention in Pre- and Post-NAC Ultrasound Images. This figure demonstrates the deep learning model's attention maps using Gradient-weighted Class Activation Mapping (Grad-CAM) on tumor ultrasound images before and after neoadjuvant chemotherapy (NAC). (A1, A2) Pre- and post-NAC ultrasound and Grad-CAM images, respectively, of a 53-year-old patient who did not achieve pCR. The Grad-CAM heatmap (A2) highlights strong peripheral activations, particularly on the upper tumor border.B1, B2 Corresponding post-NAC ultrasound and Grad-CAM images of the same non-pCR patient. The attention remains at the edge but appears more diffuse, indicating persistent residual tumor.C1, C2 Pre-NAC ultrasound and Grad-CAM visualization of a 49-year-old patient who achieved pCR. The heatmap (C2) shows dispersed and weak activations across the tumor, suggesting limited model attention toward aggressive patterns.(D1, D2) Post-NAC ultrasound and Grad-CAM of the same pCR patient. The model's attention in D2 is minimal and centrally located, aligning with radiologic signs of tumor regression.Dashed lines represent the maximal tumor diameters measured during routine clinical evaluation. Tumor sizes were A = 2.24 cm, B = 2.61 cm (non-pCR case), and C = 1.08 cm, D = 0.68 cm (pCR case), respectively. These measurements further validate model attention correlates with tumor shrinkage patterns.

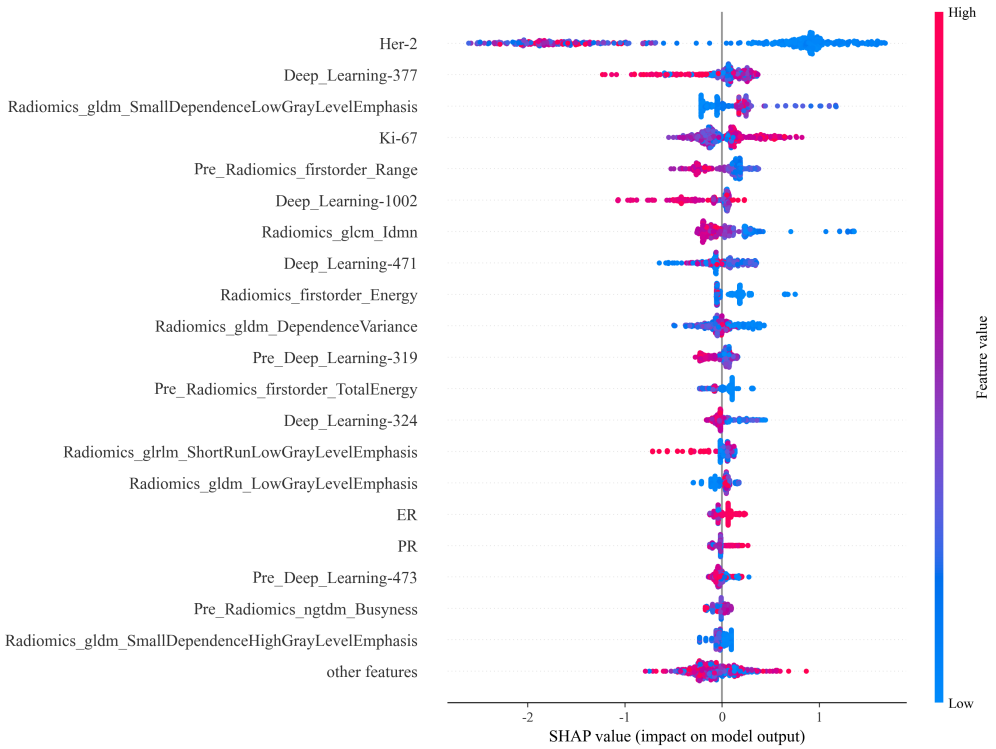


FIGURE 7
SHAP Plot. The SHAP values illustrate each feature's contribution to the prediction outcome, providing insight into feature importance and the model's interpretability.

and actual pCR probabilities across both internal and external cohorts, suggesting that the model not only distinguishes outcomes effectively but also provides reliable probability estimates. Furthermore, DCA demonstrated that our integrated model yielded a greater net clinical benefit across a wide range of threshold probabilities, compared with models based solely on clinical or radiomic features. These findings underscore the practical value of our approach, indicating that the model's high discriminative power is matched by strong calibration and tangible clinical utility.

In addition to visual interpretability, we conducted calibration curve analyses (Figure 4) and decision curve analysis (DCA, Figure 7) to further evaluate the clinical reliability and practical value of our model. Calibration curves demonstrated that the predicted probabilities aligned well with the actual outcomes in both internal and external validation sets, as reflected by Brier scores of 0.102 and 0.109, respectively, supporting the model's reliability. Moreover, DCA showed that the combined model consistently provided the highest net benefit across a wide range of threshold probabilities, confirming its strong clinical utility in decision-making scenarios. Notably, the optimal probability threshold for distinguishing pCR from non-pCR cases may vary depending on the clinical context. In our analysis, threshold values between 0.4 and 0.7 offered the best balance between sensitivity and specificity, as observed from DCA performance, and corresponded to the range where net clinical benefit was maximized across most patient scenarios. This range was selected based on maximizing clinical utility while maintaining interpretability for real-world application.

Our model demonstrated excellent performance in predicting pCR, providing a more accessible and cost-effective alternative to MRI-based models. This is particularly important in routine clinical settings where resource constraints or contraindications to MRI may limit its use. Additionally, the use of ultrasound imaging has the potential to expand the applicability of predictive models to a broader patient population, including those in resource-limited settings. Beyond its accessibility, ultrasound enables clinicians to monitor treatment response dynamically, further enhancing its clinical utility.

Furthermore, our model demonstrates not only excellent performance in terms of discrimination and calibration but also delivers consistent net benefit and clinical interpretability through robust visual explanation tools. This positions the model as a promising, scalable, and user-friendly solution for preoperative pCR prediction, particularly in resource-limited or MRI-constrained clinical environments. By focusing on ultrasound—a widely accessible and low-cost modality, we further simplify model deployment and enhance feasibility for routine integration into clinical workflows.

Despite the promising results of our study, several limitations should be acknowledged. First, the model relies on manual tumor segmentation for feature extraction, which introduces potential variability due to operator dependency. In this study, all segmentations were performed in consensus by two experienced

radiologists to mitigate inter-observer variability. However, we acknowledge that inter-observer agreement was not formally quantified, which may impact reproducibility. This limitation has been noted, and future studies will incorporate quantitative evaluation of segmentation consistency using standard metrics such as the Dice Similarity Coefficient. Moreover, although manual delineation remains common in radiomics research, the development of automatic or semi-automatic segmentation methods will be critical to improve reproducibility, reduce labor, and enhance clinical applicability. We plan to explore these approaches in subsequent work.

Second, while our use of ultrasound imaging offers practical advantages such as accessibility and cost-effectiveness, ultrasound is inherently operator-dependent, and variations in image acquisition and quality could affect radiomic feature extraction and model performance. This variability underscores the importance of standardizing ultrasound scanning protocols and ensuring adequate training across institutions to promote consistency and reduce noise in future multicenter implementations. Notably, in our preprocessing, we implemented uniform image resampling and pixel normalization strategies to reduce inter-equipment variability, thus improving the consistency of feature extraction.

Third, although our cohort included only patients with confirmed invasive breast cancer who underwent NAC, we did not further stratify cases based on molecular subtypes such as hormone receptor (HR) or HER2 status. Certain subtypes—such as HER2-negative Luminal A—are less responsive to NAC and are often not recommended for such treatment. However, since this was a retrospective study, all patients had already received NAC based on clinical judgment and established treatment guidelines. This real-world selection process likely excluded low-response subtypes and reduced potential molecular-level bias. This is supported by our data: while HR+/HER2− patients accounted for approximately 38.5% of the total cohort, they represented only 11.6% of the pCR group, consistent with their known lower chemosensitivity. In contrast, HER2-positive and triple-negative breast cancer (TNBC) patients accounted for 46.8% and 15.0% of the cohort, respectively, and demonstrated significantly higher pCR rates, in alignment with existing clinical evidence. These distributions are highly consistent with real-world NAC-treated populations, suggesting that our cohort is representative and clinically relevant. Nevertheless, future studies should consider incorporating molecular subtyping more explicitly into model development to further improve performance across heterogeneous tumor biology.

Finally, while our model demonstrated strong predictive performance across two independent centers, the relatively limited sample size and geographic diversity may restrict its generalizability to broader populations. To address this, we plan to expand our external validation to include geographically and ethnically diverse cohorts across multiple clinical centers. Preliminary collaborations have already been initiated with two additional tertiary hospitals outside our current regional network, and ethics approval processes are underway. This will ensure the robustness and scalability of our model in real-world applications. Additionally, future research should continue to explore strategies that enhance interpretability—such as explainable artificial intelligence (XAI)—and develop intuitive clinical decision support tools that facilitate seamless integration into clinical workflows.

## 5 Conclusions

In this study, we developed a deep learning-based radiomics model using ultrasound imaging to predict pCR in breast cancer patients undergoing NAC. Integrating CNN allowed for the extraction of complex, non-linear imaging features, addressing the limitations of traditional radiomics approaches in capturing tumor heterogeneity. By employing ultrasound, we ensured that our model is both accessible and cost-effective, making it suitable for widespread clinical application. Additionally, ensemble learning, through the combination of radiomics and deep learning-derived features, further enhanced the predictive accuracy and robustness of the model. The multicenter validation demonstrated strong generalizability across independent datasets, confirming the potential of our model in clinical practice.

## Data availability statement

The raw data supporting the conclusions of this article will be made available by the authors, without undue reservation.

## Ethics statement

The studies involving humans were approved by Ethics committees of Xiangyang First People's Hospital and Ethics committees of Zou Ping Hospital. The studies were conducted in accordance with the local legislation and institutional requirements. The ethics committee/institutional review board waived the requirement of written informed consent for participation from the participants or the participants' legal guardians/next of kin because In retrospective studies, relevant study data were derived in the case system, and all samples were hidden from the original patient information.

## Author contributions

WT: Conceptualization, Data curation, Formal analysis, Investigation, Methodology, Project administration, Supervision, Writing – original draft, Writing – review & editing. LX: Conceptualization, Data curation, Formal analysis, Investigation, Methodology, Project administration, Software, Supervision, Visualization, Writing – original draft, Writing – review & editing. SZ: Conceptualization, Data curation, Methodology, Writing – review & editing, Validation, Writing – original draft. ZYa: Conceptualization, Methodology, Validation, Writing – original draft, Writing – review & editing, Formal analysis, Software,

Visualization. MZ: Methodology, Software, Validation, Visualization, Writing – original draft, Writing – review & editing, Funding acquisition, Investigation. ZYi: Funding acquisition, Investigation, Software, Validation, Visualization, Writing – original draft, Writing – review & editing, Conceptualization, Formal analysis. GL: Conceptualization, Formal analysis, Funding acquisition, Visualization, Writing – review & editing, Data curation, Methodology, Resources, Supervision.

## Funding

The author(s) declare that financial support was received for the research and/or publication of this article. This study has received funding from the "323" Public Health Project of the Hubei health commission and the Xiangyang No.1 People's Hospital (XYY2022-323).

## Acknowledgments

The study was designed and conducted following the Declaration of Helsinki and approved by the ethics committees of Xiangyang First People's Hospital and Zou Ping Hospital. Since this experiment was a retrospective study, the ethics committee of Xiangyang First People's Hospital and Zou Ping Hospital approved the patient informed consent waiver.

## Conflict of interest

The authors declare that the research was conducted in the absence of any commercial or financial relationships that could be construed as a potential conflict of interest.

## Generative AI statement

The author(s) declare that no Generative AI was used in the creation of this manuscript.

## Publisher's note



## Supplementary material

The Supplementary Material for this article can be found online at: https://www.frontiersin.org/articles/10.3389/fonc.2025.1525285/full#supplementary-material

## References

1. Sung H, Ferlay J, Siegel RL, Laversanne M, Soerjomataram I, Jemal A, et al. Global cancer statistics 2020: GLOBOCAN estimates of incidence and mortality worldwide for 36 cancers in 185 countries. *CA: A Cancer J Clin*. (2021) 71:209–49. doi: 10.3322/caac.21660

2. Harbeck N, Nitz UA, Christgen M, Kümmel S, Braun M, Schumacher C, et al. De-escalated neoadjuvant trastuzumab-emtansine with or without endocrine therapy versus trastuzumab with endocrine therapy in HR+/HER2+ Early breast cancer: 5-year survival in the WSG-ADAPT-TP trial. *J Clin Oncol: Off J Am Soc Clin Oncol*. (2023) 41:3796–804. doi: 10.1200/JCO.22.01816

3. Göker E, Hendriks MP, van Tilburg M, Barcaru A, Mittempergher L, van Egmond A, et al. Treatment response and 5-year distant metastasis-free survival outcome in breast cancer patients after the use of MammaPrint and BluePrint to guide preoperative systemic treatment decisions. *Eur J Cancer (Oxford England: 1990)*. (2022) 167:92–102. doi: 10.1016/j.ejca.2022.03.003

4. de Nonneville A, Houvenaeghel G, Cohen M, Sabiani L, Bannier M, Viret F, et al. Pathological complete response rate and disease-free survival after neoadjuvant chemotherapy in patients with HER2-low and HER2–0 breast cancers. *Eur J Cancer (Oxford England: 1990)*. (2022) 176:181–8. doi: 10.1016/j.ejca.2022.09.017

5. Chen JH, Bahri S, Mehta RS, Carpenter PM, McLaren CE, Chen WP, et al. Impact of factors affecting the residual tumor size diagnosed by MRI following neoadjuvant chemotherapy in comparison to pathology. *J Surg Oncol*. (2014) 109:158–67. doi: 10.1002/jso.23470

6. Wolf DM, Yau C, Wulfkuhle J, Brown-Swigart L, Gallagher RI, Lee PRE, et al. Redefining breast cancer subtypes to guide treatment prioritization and maximize response: Predictive biomarkers across 10 cancer therapies. *Cancer Cell*. (2022) 40:609–623.e6. doi: 10.1016/j.ccell.2022.05.005

7. Lambin P, Rios-Velazquez E, Leijenaar R, Carvalho S, van Stiphout RG, Granton P, et al. Radiomics: extracting more information from medical images using advanced feature analysis. *Eur J Cancer (Oxford England: 1990)*. (2012) 48:441–6. doi: 10.1016/j.ejca.2011.11.036

8. Huang Y, Zhu T, Zhang X, Li W, Zheng X, Cheng M, et al. Longitudinal MRI-based fusion novel model predicts pathological complete response in breast cancer treated with neoadjuvant chemotherapy: a multicenter, retrospective study. *EClinicalMedicine*. (2023) 58:101899. doi: 10.1016/j.eclinm.2023.101899

9. Song X, Zhang S, Shi T, Huang X, Wang Y, Du M, et al. A machine learning radiomics model based on bpMRI to predict bone metastasis in newly diagnosed prostate cancer patients. *Magnetic Resonance Imaging*. (2024) 107:15–23. doi: 10.1016/j.mri.2023.12.009

10. Li Z, Liu X, Gao Y, Lu X, Lei J. Ultrasound-based radiomics for early predicting response to neoadjuvant chemotherapy in patients with breast cancer: a systematic review with meta-analysis. *Radiol Med*. (2024) 129:934–44. doi: 10.1007/s11547-024-01783-1

11. Jannusch K, Dietzel F, Bruckmann NM, Morawitz J, Boschheidgen M, Minko P, et al. Prediction of therapy response of breast cancer patients with machine learning based on clinical data and imaging data derived from breast [18F]FDG-PET/MRI. *Eur J Nucl Med Mol Imaging*. (2024) 51:1451–61. doi: 10.1007/s00259-023-06513-9

12. Sella T, Simor B, Adler-Levy Y, Maly B, Kadouri L, Carmon E, et al. MRI prediction of neoadjuvant chemotherapy response is equivalent in patients with or without mammographic calcifications: a step towards adapting surgical approach? *Eur Radiol*. (2023) 33:7168–77. doi: 10.1007/s00330-023-09640-x

13. Zhou J, Lu J, Gao C, Zeng J, Zhou C, Lai X, et al. Predicting the response to neoadjuvant chemotherapy for breast cancer: wavelet transforming radiomics in MRI. *BMC Cancer*. (2020) 20:100. doi: 10.1186/s12885-020-6523-2

14. Dayarathna S, Islam KT, Uribe S, Yang G, Hayat M, Chen Z, et al. Deep learning based synthesis of MRI, CT and PET: Review and analysis. *Med Image Anal*. (2024) 92:103046. doi: 10.1016/j.media.2023.103046

15. Wu HY, Lin CY, Tzeng YD, Hung CC, Liu SI, Yin CH, et al, et al. Preoperative systemic inflammation response index: Clinicopathologic predictor of pathological complete response in HER2-positive breast cancer patients receiving neoadjuvant systemic therapy. *J Chin Med Assoc*. (2024) 87:226–35. doi: 10.1097/JCMA.0000000000001034

16. Curigliano G, Burstein HJ, Gnant M, Loibl S, Cameron D, Regan MM, et al. Understanding breast cancer complexity to improve patient outcomes: The St Gallen International Consensus Conference for the Primary Therapy of Individuals with Early Breast Cancer 2023. *Ann Oncol*. (2023) 34:970–86. doi: 10.1016/j.annonc.2023.08.017

17. Loibl S, Poortmans P, Morrow M, Denkert C, Curigliano G. Breast cancer [published correction appears in Lancet. *Lancet*. (2021) 397:1750–69. doi: 10.1016/S0140-6736(20)32381-3

18. Encinas G, Maistro S, Pasini FS, Katayama ML, Brentani MM, Bock GH, et al. Ki-67 index after neoadjuvant endocrine therapy as a prognostic biomarker in patients with ER-positive/HER2-negative early breast cancer: a systematic review and meta-analysis. *Eur J Cancer*. (2023) 194:113358. doi: 10.1016/j.ejca.2023.113358

19. Hong R, Xu B. Breast cancer: an up-to-date review and future perspectives. *Cancer Commun (Lond)*. (2022) 42:913–36. doi: 10.1002/cac2.12358

20. van den Ende NS, Nguyen AH, Jager A, Kok M, Debets R, van Deurzen CHM. Triple-negative breast cancer and predictive markers of response to neoadjuvant chemotherapy: A systematic review. *Int J Mol Sci*. (2023) 24:2969. doi: 10.3390/ijms24032969

21. Gown AM. The biomarker ki-67: promise, potential, and problems in breast cancer. *Appl Immunohistochem Mol Morphol*. (2023) 31:478–84. doi: 10.1097/PAI.0000000000001087

22. Whelan TJ, Smith S, Parpia S, Fyles AW, Bane A, Liu FF, et al. Omitting radiotherapy after breast-conserving surgery in luminal A breast cancer. *N Engl J Med*. (2023) 389:612–9. doi: 10.1056/NEJMoa2302344

23. Zhu T, Huang YH, Li W, Zhang YM, Lin YY, Cheng MY, et al. Multifactor artificial intelligence model assists axillary lymph node surgery in breast cancer after neoadjuvant chemotherapy: multicenter retrospective cohort study. *Int J Surg*. (2023) 109:3383–94. doi: 10.1097/JS9.0000000000000621

24. Jiang W, Deng X, Zhu T, Fang J, Li J. ABVS-based radiomics for early predicting the efficacy of neoadjuvant chemotherapy in patients with breast cancers. *Breast Cancer (Dove Med Press)*. (2023) 15:625–36. doi: 10.2147/BCTT.S418376

25. Lenharo M. An AI revolution is brewing in medicine. What will it look like? *Nature*. (2023) 622:686–8. doi: 10.1038/d41586-023-03302-0

26. Wang H, Pujos-Guillot E, Comte B, de Miranda JL, Spiwok V, Chorbev I, et al. Deep learning in systems medicine. *Brief Bioinform*. (2021) 22:1543–59. doi: 10.1093/bib/bbaa237

27. Fan Z, Jiang J, Xiao C, Chen Y, Xia Q, Wang J, et al. Construction and validation of prognostic models in critically Ill patients with sepsis-associated acute kidney injury: interpretable machine learning approach. *J Transl Med*. (2023) 21:406. doi: 10.1186/s12967-023-04205-4

28. Zheng J, Zhang Z, Wang J, Zhao R, Liu S, Yang G, et al. Metabolic syndrome prediction model using Bayesian optimization and XGBoost based on traditional Chinese medicine features. *Heliyon*. (2023) 9:e22727. doi: 10.1016/j.heliyon.2023.e22727

frontiers | Frontiers in Oncology

TYPE Original Research
PUBLISHED 06 June 2025
DOI 10.3389/fonc.2025.1536365



OPEN ACCESS

EDITED BY
Sharon R. Pine,
University of Colorado Anschutz Medical Campus, United States

REVIEWED BY
Jaber H. Jaradat,
Mutah University, Jordan
Stephen Afrifa,
Tianjin University, China

*CORRESPONDENCE
Wei Zhang
zhwdetom@163.com
Xinying Shen
shenxinying0755@126.com

†These authors have contributed equally to this work and share first authorship

RECEIVED 28 November 2024
ACCEPTED 07 May 2025
PUBLISHED 06 June 2025
CORRECTED 17 June 2025

CITATION
Yin Y, Fang J, Zhang W and Shen X (2025) Optimizing breast cancer ultrasound diagnosis: a comparative study of AI model performance and image resolution. *Front. Oncol.* 15:1536365. doi: 10.3389/fonc.2025.1536365



# Optimizing breast cancer ultrasound diagnosis: a comparative study of AI model performance and image resolution

Yunqing Yin[1†], Junkui Fang[1†], Wei Zhang[2*] and Xinying Shen[2*]

[1]The Second Clinical Medical College, Jinan University, Shenzhen, China, [2]Department of Interventional Radiology, Shenzhen People's Hospital, Shenzhen, China

**Objectives:** To determine the optimal combination of artificial intelligence (AI) models and ultrasound (US) image resolutions for breast cancer diagnosis and evaluate whether this combination surpasses the diagnostic accuracy of senior radiologists.

**Materials and methods:** We systematically compared lightweight (MobileNet, Xception) and dense neural networks (ResNet50, DenseNet121) using three image resolutions (224 × 224, 320 × 320, 448 × 448 pixels). A retrospective cohort of 4,998 patients was divided into training/validation (8:2 ratio, $n$ = 3,578) and independent testing sets ($n$ = 1,410). Diagnostic performance was assessed via AUC, sensitivity, specificity, and analysis speed, with direct comparisons against senior radiologists.

**Results:** MobileNet with 224 × 224 input achieved the highest AUC (0.924, 95% CI: 0.910–0.938) and accuracy (87.3%) outperforming senior US (AUC: 0.820, accuracy: 79.1%) and mammography doctors (AUC: 0.819, accuracy: 83.6%) ($p < 0.05$). After excluding BI-RADS 4c and 5 nodules, the diagnostic efficacy of MobileNet_224 is better than that of senior doctors ($p < 0.05$), can reduce 60.1% false positives of US, and 46.6% of mammography. MobileNet_224 and MobileNet_320 had the fastest analysis speed.

**Conclusion:** MobileNet_224 represents a novel, efficient AI framework for breast cancer diagnosis demonstrating superior accuracy and speed compared to both complex AI models and experienced clinicians. This work highlights the critical role of optimizing model architecture and resolution to enhance diagnostic workflows and reduce unnecessary biopsies.

KEYWORDS

**artificial intelligence, breast cancer, diagnosis, mammography, ultrasound**

# Introduction

Breast cancer (BC) has emerged as the most prevalent malignancy worldwide and is a leading cause of death among women (1, 2). Surpassing lung cancer, it now accounts for over 2.3 million new cases annually representing 30% of all female cancers and 11.7% of all cancers. This malignancy increasingly affects a younger demographic posing a serious threat to women's health (3).

Currently, clinical diagnosis of BC incorporates various methods, including palpation, digital mammography (DM), magnetic resonance imaging (MRI), and ultrasound (US). Mammography, while widely used, often suffers from high rates of false positives and negatives, particularly in women with dense breast tissue, leading to missed diagnoses (4, 5). MRI is recommended for high-risk BC patients, but its high cost, false-positive rate, and time intensity limit its use to a supplementary role in mammography. US, an important tool for BC screening, is not constrained by mammary gland tissue types and has been shown to increase BC detection rates by 17% while reducing unnecessary biopsies (6, 7). However, US is limited by its reliance on the acoustic impedance difference in tumor tissues making it challenging to differentiate diagnoses, especially in cases of non-mass BC (8). The operator-dependent nature of US also means that diagnostic outcomes can vary significantly based on the experience of the practitioner (9).

The Breast Imaging Reporting and Data System (BI-RADS) has significantly improved the standardization and accuracy of breast tumor diagnosis (10). However, BI-RADS classification relies on visual recognition, which can miss subtle image features. Thus, there is an urgent need for an objective method that minimizes operator dependence and accurately reflects tumor characteristics for BC screening and diagnosis (11).

Advances in AI-driven breast cancer classification have demonstrated significant potential in reducing diagnostic variability and improving clinical workflows. Recent studies, such as those employing convolutional neural network for ultrasound-based classification (12–14), underscore the feasibility of AI in standardizing diagnoses. Furthermore, ensemble machine learning techniques (15, 16) demonstrate improved accuracy through model aggregation. However, these works often lack systematic comparisons across model architectures limiting insights into optimal computational frameworks. While capsule networks (17) show promise in capturing spatial hierarchies within tumor morphology, their computational inefficiency hinders real-time clinical deployment compared to lightweight CNNs. Lightweight architectures, like MobileNet variants (18, 19) have emerged as efficient alternatives in cancer classification, yet prior investigations rarely explore resolution-specific trade-offs or benchmark against both complex models [e.g., ShuffleNet (20), EfficientNet (21)] and human expertise. Concurrently, multi-resolution approaches for medical image segmentation (22, 23) highlight the importance of scale optimization, though their focus remains isolated from end-to-end diagnostic pipelines.

Our study addresses these gaps by systematically comparing lightweight and dense neural networks across resolutions to identify the optimal AI–image combination for breast cancer detection, while directly benchmarking diagnostic efficiency against senior radiologists—thereby advancing clinical standards through technically validated innovation.

# Materials and methods

## Study population

This retrospective study was conducted following approval from the institutional review board of Shenzhen People's Hospital, with a waiver for informed consent due to its retrospective nature. The Na-exclusion criteria for this study were as follows:

***Inclusion criteria:*** (1) Breast tumors were detected by US, which were classified as 0, 3, 4a, 4b, 4c, or 5 according to BI-RADS. (2) At least 3.0-mm breast tissue can be displayed around the nodule. (3) No intervention or operation was performed on the nodule to be evaluated before ultrasonic examination. (4) Patients underwent surgery or biopsy within 1 week of ultrasonic data collection and obtained pathological results.

***Exclusion criteria:*** (1) BIRADS 1 and 2; (2) Have a history of breast surgery or intervention; (3) Poor image quality; (4) The clinical data of cases are incomplete, and the pathological results are not tracked.

In this study, following the inclusion and exclusion criteria, a cohort of 4,998 patients with breast tumors was established. These patients were then randomly divided into the following three groups: a training set, a test set, and an independent validation set. The training and validation sets were allocated in an 8:2 ratio, with the training set comprising 2,778 patients (774 with malignant tumors) and the validation set including 800 patients (217 with malignant tumors). The independent test set consisted of 1,410 patients of whom 579 had malignant tumors (Table 1). All patients underwent biopsy or surgical procedures for pathological diagnosis (Figure 1).

## Human examination

The US and mammography diagnosis were made by two senior doctors, with more than 10 years of experience in mammography diagnosis, who made the classification diagnosis of benign and malignant tumors under the condition of independent double blind, and gave the BI-RADS classification of tumors. In case of inconsistency, the third chief physician shall be invited for arbitration (Supplementary Material). In a comparison of diagnostic performance, BI-RADS classifications 3 and 4A are defined as benign lesions, and 4B, 4C, and 5 are defined as malignant lesions. Diagnostic results from ultrasound doctors and mammography doctors are based on the doctor's experience.

TABLE 1 Patient information in this study.

| Characteristics | Training set | | Validation set | | Testing set | |
|---|---|---|---|---|---|---|
| | Benign | Malignant | Benign | Malignant | Benign | Malignant |
| Patients | 2,004 | 774 | 583 | 217 | 831 | 579 |
| Tumor size (mm) | 22.88 ± 9.88 | | 23.17 ± 9.89 | | 22.44 ± 10.07 | |
| Age (year) | | | | | | |
| <40 | 372 | 106 | 131 | 30 | 154 | 68 |
| 40–49 | 619 | 157 | 203 | 50 | 315 | 135 |
| 50–59 | 602 | 182 | 171 | 52 | 279 | 100 |
| 60–69 | 557 | 150 | 179 | 48 | 338 | 143 |
| ≥70 | 628 | 179 | 116 | 37 | 324 | 133 |

## AI model construction

Model selection was guided by (1) computational efficiency for clinical deployment, (2) prior evidence in medical imaging, and (3) architectural diversity to benchmark lightweight against dense networks. MobileNet and Xception were prioritized for their parameter efficiency and validated performance in resource-constrained tasks. DenseNet121 and ResNet50 served as benchmarks for hierarchical feature extraction.

These models employ architectural innovations like depthwise separable convolutions to minimize computational burden while retaining diagnostic accuracy. Conversely, dense models, like DenseNet121 and ResNet50—known for their complex hierarchical

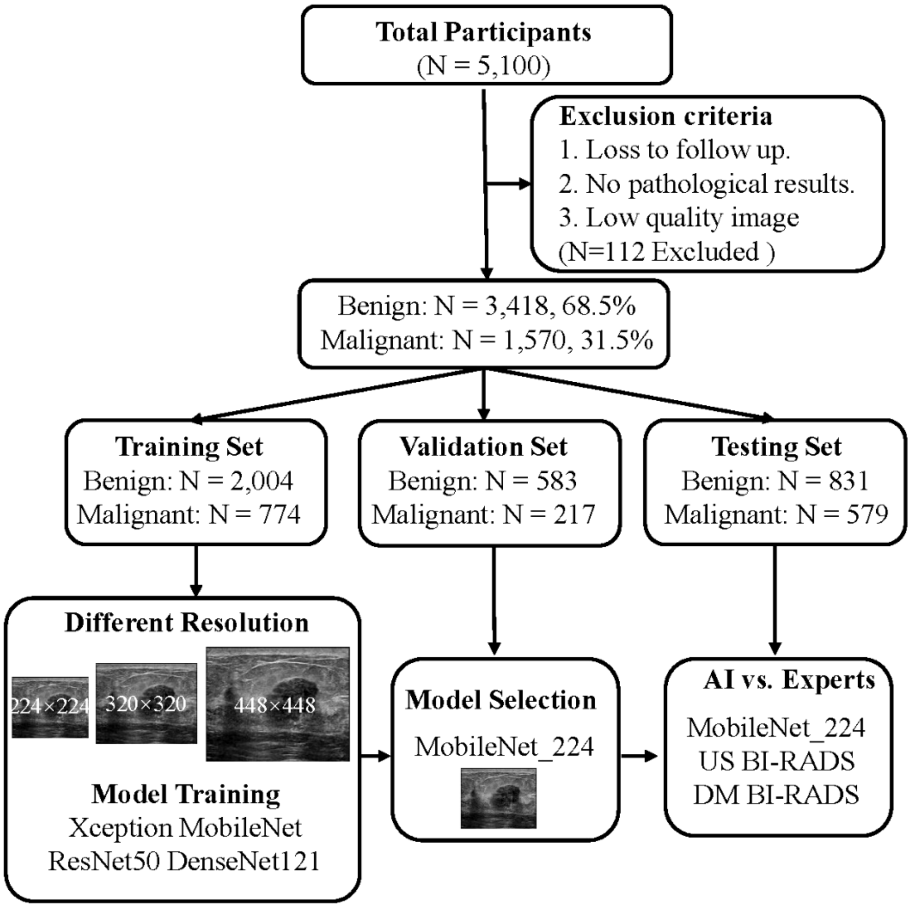


FIGURE 1
Flow chart and results of this study. The optimal model: MobileNet_224, senior ultrasound doctors, senior mammography doctors. MobileNet_224, MobileNet with 224 × 224-pixel image input; US_BI-RADS, senior ultrasound doctors' diagnostic results; DM_BI-RADS, senior mammography doctors' diagnostic results.

structures (e.g., residual blocks in ResNet50, dense connectivity in DenseNet121)—were included to evaluate their ability to capture nuanced tumor features in ultrasound images. By comparing these fundamentally distinct architectures, we aimed to identify the optimal balance between computational efficiency and diagnostic precision for breast cancer detection. By comparing these models, we aimed to assess which architecture is more effective for the task of diagnosing BC from US images.

We employed the following three different image resolutions: 224 × 224, 320 × 320, and 448 × 448 pixels (illustrated in Figure 2). This variation in resolution was intended to examine the impact of image quality on the diagnostic accuracy of the AI models. Higher-resolution images typically provide more detailed information but also require more computational resources to process. Conversely, lower-resolution images are faster to process but may lack some detailed information. Understanding the trade-off between resolution and diagnostic accuracy is crucial for the practical application of AI in medical imaging, particularly in settings where computational resources are limited.

## Training protocol

Models were implemented in TensorFlow 2.5.0, trained on an NVIDIA RTX 3090 GPU, and evaluated on an edge-computing device (Jetson AGX Xavier) to simulate clinical deployment. Images were standardized to 224 × 224, 320 ×3 20, or 448 × 448 pixels. Training employed AdamW optimization (lr = 1e−4) with cosine annealing, and cross-entropy loss weighted for class imbalance (Supplementary Material).

To ensure the integrity and non-overlapping nature of our data, we carefully allocated images from the same patient exclusively to one dataset—either the training set or the validation set. This approach was critical to prevent data leakage and ensure that the models were tested on completely unseen data, thereby providing a reliable assessment of their generalizability.

The independent testing set was crucial for evaluating the real-world applicability of the AI models. It consisted of the following three main components: 1) Comparative Evaluation: We assessed the diagnostic effectiveness between different AI models to identify the optimal model and image resolution combination. 2) Comparison with Senior Doctors: The optimal AI model's diagnostic efficacy was compared with that of experienced senior US and mammography doctors. This comparison aimed to benchmark the AI models against the current gold standard in clinical practice. 3) Exclusion of Certain Tumor Types: We specifically excluded BI-RADS 4c and 5 tumors to focus on challenging cases where AI models could potentially offer the most significant benefit. This step was crucial to understand the potential of AI in improving diagnostic specificity and reducing false positives.

## Statistical analysis

Continuous variable data are expressed as mean ± standard deviation. Categorical variable data are expressed as a percentage. The paired-sample t-test was used to compare the differences within the group. R 3.6.3 was used for the statistical analysis. Diagnostic performance was evaluated using receiver operating characteristic (ROC) curves generated in R 3.6.3 (pROC package). The area under the curve (AUC), reflecting overall discriminative ability, was calculated via the non-parametric DeLong method, with 95% confidence intervals (95% CI) derived from 2,000 stratified bootstrap replicates to account for variability. Sensitivity, specificity, and accuracy were computed from confusion matrices. Statistical significance of AUC differences between models and radiologists was assessed via DeLong's test ($p < 0.05$).

# Code availability

The updated code repository and Jupyter notebook was hosted on GitHub—https://github.com/wukaiyeah/ultrasound_breast_malignant_classification.git.

# Results

## Diagnostic performance of AI models vs. radiologists

MobileNet_224 demonstrated superior diagnostic accuracy compared to both other AI models and senior radiologists. In the independent testing set, MobileNet_224 achieved an AUC of 0.924 (95% CI: 0.910–0.938) significantly outperforming senior ultrasound radiologists (AUC: 0.820, $p < 0.001$) and mammography specialists (AUC: 0.819, $p < 0.001$). Its accuracy (87.3%) surpassed radiologists' performance by 8.2% (ultrasound) and 3.7% (mammography). Dense networks, such as DenseNet121_448, showed lower efficacy (AUC: 0.890; accuracy: 82.8%) highlighting the advantage of lightweight architectures (Tables 2, 3, Figures 2, 3).

The interpretability analysis (Figure 4) demonstrates MobileNet_224's alignment with radiological diagnostic criteria. For benign lesions (A), SHAP values identified smooth margins and homogeneous echotexture as primary contributors to classification, while Grad-CAM heatmaps (C) confirmed focused attention on lesion boundaries. In malignant cases (B), SHAP attributed high malignancy probability to spiculated margins and heterogeneous internal echoes corroborated by Grad-CAM's emphasis on irregular tumor peripheries (D).

## Impact of image resolution on model performance

Lower-resolution inputs (224 × 224 pixels) consistently outperformed higher resolutions (320 × 320, 448 × 448) across all models. MobileNet_224 achieved the highest AUC (0.924) at 224 × 224, while its performance declined at 448 × 448 (AUC: 0.909). Similarly, Xception_224 (AUC: 0.918) surpassed Xception_448 (AUC: 0.909), despite the latter utilizing more detailed imaging data. This suggests that lower resolutions prioritize clinically decisive features over extraneous textures optimizing both accuracy and computational efficiency (Table 2).

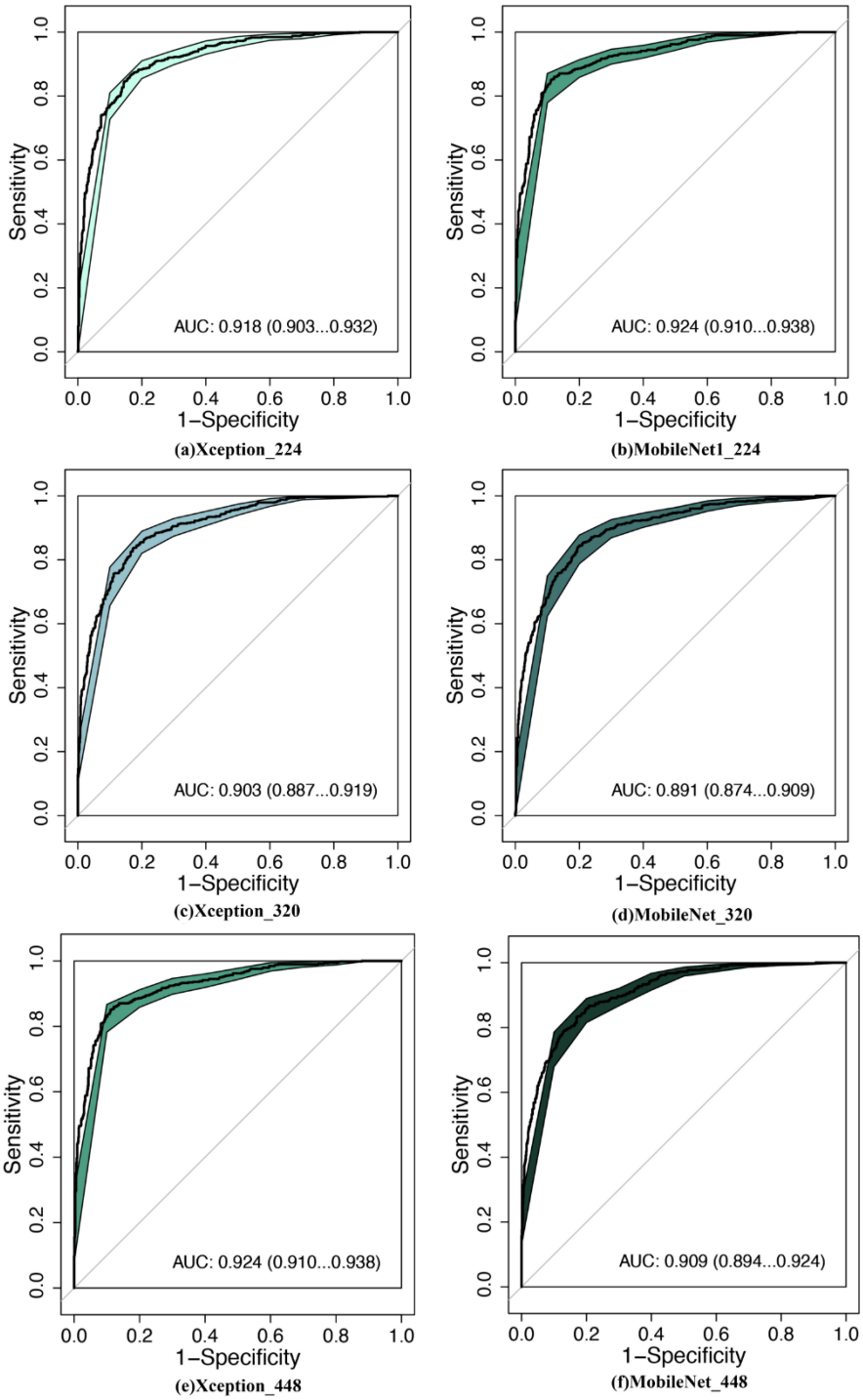


FIGURE 2
Comparison of diagnostic efficacy between LW-CNNs in the testing set. AUC, area under the curve; 95% CI: 95% confidence interval. **(a)** Xception_224: Xception with 224 × 224-pixel image input, **(b)** MobileNet_224, **(c)** Xception_320, **(d)** MobileNet_320, **(e)** Xception_448, **(f)** MobileNet_448.

## Reduction of false positives and clinical implications

MobileNet_224 significantly reduced false-positive diagnoses compared to radiologists: False positives decreased from 286 to 114 cases (60.1% reduction) for ultrasound, and false positives dropped from 204 to 109 cases (46.6% reduction) for mammography. Notably, after excluding BI-RADS 4c/5 cases (high malignancy likelihood), the model maintained superior specificity (88.8% vs. radiologists' 65.6%, $p < 0.001$) demonstrating its ability to resolve diagnostically challenging lesions (Figures 5, 6).

TABLE 2 Comparison of the efficacy of AI model in the independent testing set.

| Modality | AUC (95% CI) | Cut-off | Sensitivity (%) | Specificity (%) | Accuracy (%) | p-Value |
|---|---|---|---|---|---|---|
| Xception_224 | 0.918 (0.903–0.932) | 0.483 | 84.6 | 85.4 | 85.1 | 0.230 |
| Xception_320 | 0.903 (0.887–0.919) | 0.290 | 83.6 | 82.8 | 83.1 | 0.003 |
| Xception_448 | 0.909 (0.893–0.925) | 0.518 | 82.2 | 86.5 | 84.8 | 0.013 |
| MobileNet_224 | 0.924 (0.910–0.938) | 0.555 | 85.1 | 88.8 | 87.3 | NA |
| MobileNet_320 | 0.891 (0.874–0.909) | 0.209 | 84.1 | 80.4 | 81.9 | 0.000 |
| MobileNet_448 | 0.909 (0.894–0.924) | 0.670 | 83.2 | 83.0 | 83.1 | 0.033 |
| ResNet50_224 | 0.801 (0.778–0.825) | 0.214 | 74.8 | 71.5 | 72.8 | 0.000 |
| ResNet50_320 | 0.867 (0.848–0.886) | 0.466 | 80.1 | 78.1 | 78.9 | 0.000 |
| ResNet50_448 | 0.862 (0.843–0.881) | 0.319 | 80.8 | 76.5 | 78.3 | 0.000 |
| DenseNet121_224 | 0.862 (0.843–0.881) | 0.406 | 80.3 | 84.0 | 82.5 | 0.000 |
| DenseNet121_320 | 0.870 (0.851–0.890) | 0.462 | 77.9 | 83.5 | 81.2 | 0.000 |
| DenseNet121_448 | 0.890 (0.872–0.907) | 0.460 | 81.9 | 83.4 | 82.8 | 0.000 |

AUC, area under the curve, 95% CI, 95% confidence interval; MobileNet_224, MobileNet with 224 × 224-pixel image input, others the same; p, p-value of MobileNet_ 224 compared with other models; NA, not applicable.

TABLE 3 Results of MobileNet_224 and ultrasound/mammography in testing set.

| Modality | AUC (95% CI) | Cut-off | Sensitivity (%) | Specificity (%) | Accuracy (%) | p-Value |
|---|---|---|---|---|---|---|
| Model | 0.924 (0.910–0.938) | 0.555 | 85.1 | 88.8 | 87.3 | NA |
| Ultrasound | 0.820 (0.803–0.837) | NA | 98.4 | 65.6 | 79.1 | 0.000 |
| Mammography | 0.819 (0.799–0.838) | NA | 79.7 | 85.1 | 83.6 | 0.000 |
| Model | 0.886 (0.854–0.917) | 0.467 | 78.9 | 86.3 | 85.2 | 0.000 |
| US_BI-RADS | 0.820 (0.803–0.837) | NA | 98.4 | 65.6 | 79.1 | |
| Model | 0.915 (0.892–0.937) | 0.467 | 84.1 | 86.7 | 86.2 | 0.000 |
| DM_BI-RADS | 0.745 (0.714–0.777) | NA | 73.9 | 75.2 | 74.9 | |

AUC, area under the curve; AUC, area under the curve; 95% CI, 95% confidence interval; MobileNet_224, MobileNet with 224 × 224-pixel image input; US_BI-RADS, senior ultrasound doctors' diagnostic results; DM_BI-RADS, senior mammography doctors' diagnostic results; p, p-value of MobileNet_ 224 compared with other models; NA, not applicable.

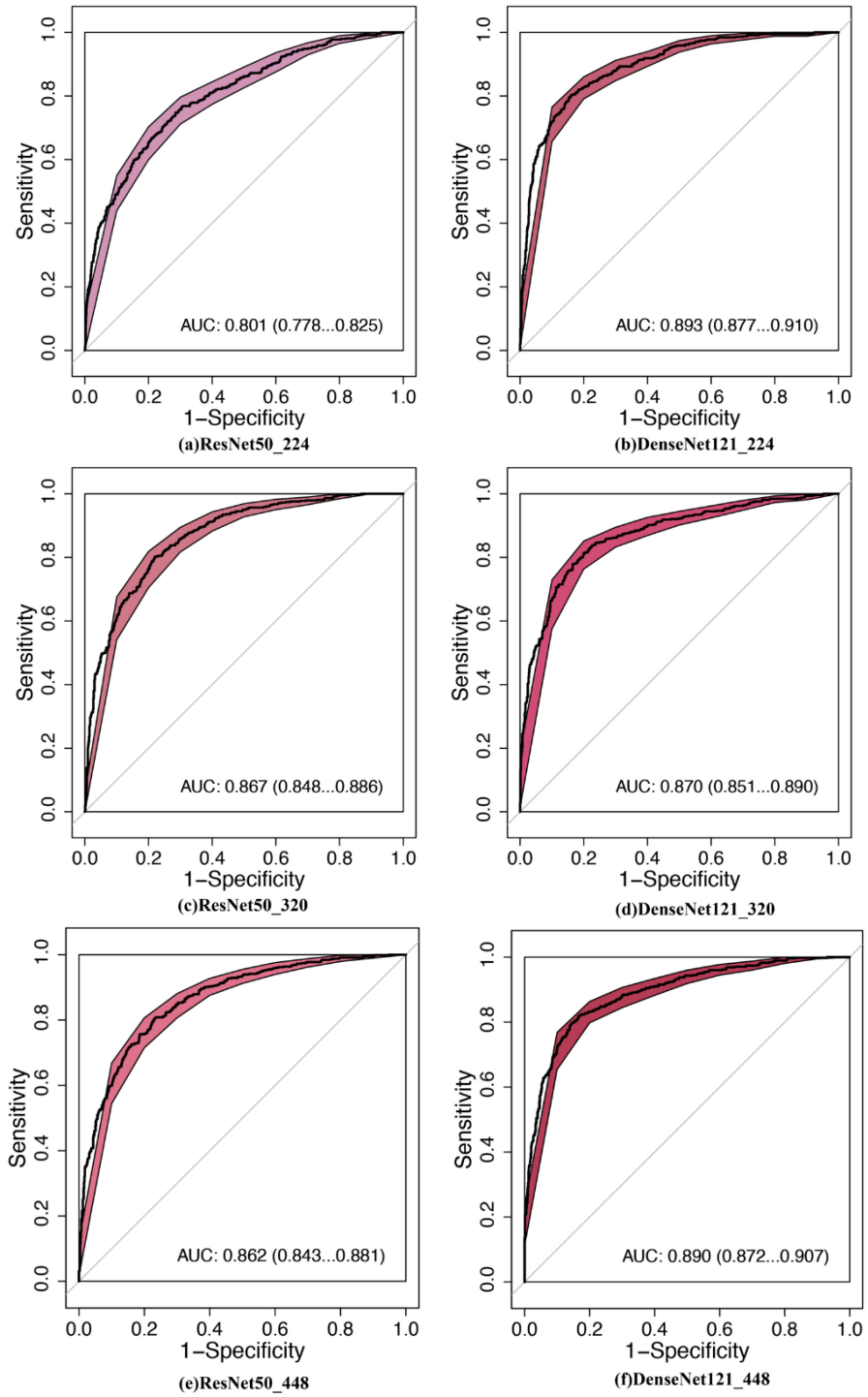


FIGURE 3
Comparison of diagnostic efficacy between DNNs in the testing set. AUC, area under the curve; 95% CI, 95% confidence interval. **(a)** ResNet50_224: ResNet50 with 224 × 224-pixel image input, **(b)** DenseNet121_224, **(c)** ResNet50_320, **(d)** DenseNet121_320, **(e)** ResNet50_448, **(f)** DenseNet121_448.

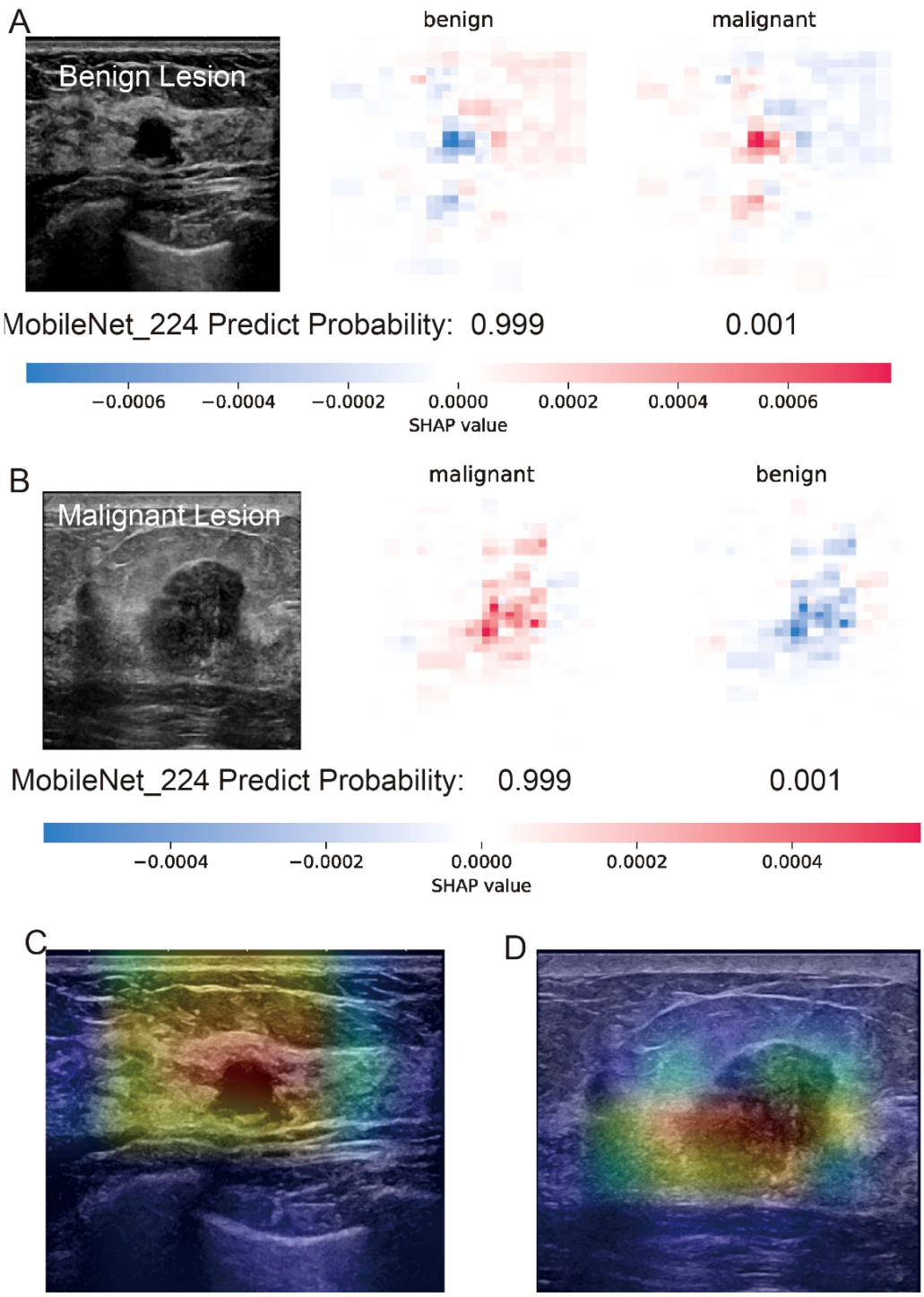


FIGURE 4
Interpretability analysis of MobileNet_224 predictions for benign and malignant breast lesions. **(A)** Benign lesion: prediction probability (0.999 for benign, 0.001 for malignant) with SHAP values highlighting key image regions contributing to the benign classification. **(B)** Malignant lesion: prediction probability (0.999 for malignant, 0.001 for benign) with SHAP values emphasizing tumor margin irregularity and microcalcifications. **(C, D)** Grad-CAM heatmaps for the benign **(C)** and malignant **(D)** lesions illustrating the model's focus on clinically relevant anatomical features (e.g., smooth margins in benign vs. spiculated regions in malignant).

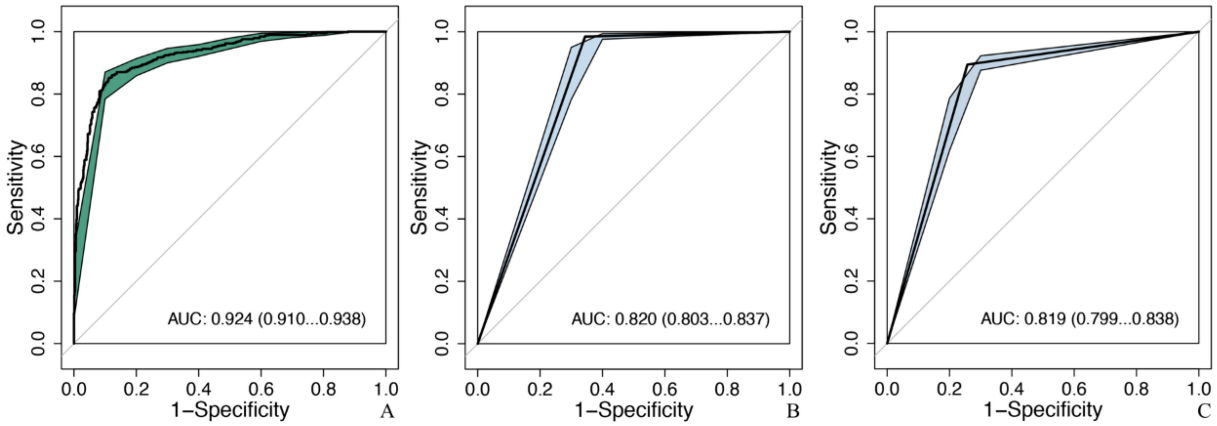


FIGURE 5
Comparison of diagnostic efficacy between the optimal model and senior doctors in the testing set. MobileNet_224, MobileNet with 224 × 224-pixel image input; AUC, area under the curve; 95% CI, 95% confidence interval. **(A)** The optimal model: MobileNet_224, **(B)** senior ultrasound doctors, **(C)** senior mammography doctors.

## Computational efficiency

MobileNet_224 exhibited the fastest inference speed (0.02 s per image), 3.8× faster than DenseNet121_448 (0.076 s) and 500× faster than manual radiologist review (~10 s per case). This efficiency did not compromise accuracy reinforcing its suitability for real-time clinical workflows (Table 4).

# Discussion

AI has demonstrated remarkable versatility across diverse domains, from anemia detection using palm and conjunctiva images (24–26) to macroeconomic forecasting via time-series models (27). In healthcare, lightweight convolutional neural networks (CNNs) are increasingly applied to resource-constrained tasks, such as MobileNet for diabetic retinopathy screening (28) and Xception for COVID-19 detection (29). Our study extends this paradigm to breast cancer ultrasound diagnosis, where optimizing existing architectures—rather than developing novel models—proves critical for clinical translation.

This study selects four models: Xception, MobileNet, DensNet121, and ResNet50, and 224 × 224-, 320 × 320-, and 448 × 448-pixel image input to explore the accuracy of breast tumors with US images. The results show that MobileNet_224 is superior to the other 11 models and the combination of input images, with an AUC of 0.924 and an accuracy of 87.3%, which are superior to those of senior US and mammography doctors (AUC: 0.820 and 0.819; accuracy: 79.1% and 83.6%).

The application of AI in medical images mainly uses convolutional neural network (CNN) to extract useful information from images. CNN has the following two characteristics: (1) can effectively reduce the dimension of images and (2) can effectively preserve features of images. There are many models derived from this, which are mainly divided into the following two categories: (1) dense neural network (DNN) such as ResNet, DenseNet, and EfficientNet (30, 31); (2) lightweight revolutionary neural networks (LW-CNNs) (32) such as MobileNet, Xception, and ShuffleNet. Large-scale network has a large amount of computation, but the processing speed is slow. LW-CNNs has designed a more efficient network computing method, which not only reduces the number of network layers and parameters but also preserves the performance. It can be used for fast reasoning of embedded and mobile systems. It has a CNN structure with high computational efficiency, adopts point-to-point grouping convolution and channel shuffling, which greatly reduce the amount of computation while maintaining accuracy, and maximize operation speed and accuracy (33, 34). In this study, the diagnostic efficiency of the two LW-CNNs is generally higher than that of the DNNs.

MobileNet (35) was based on a streamlined architecture, and a lightweight deep neural network is constructed using longitudinally separable convolution. Its core idea is that the deep separable convolution replaces the standard convolution and reduces the number of parameters (36, 37). In this study, MobileNet_224 shows the best diagnostic efficiency in different models and images.

Generally, image dimensionality reduction will not affect the final result, such as a picture of 1,000 × 1,000 pixels was reduced to 200 × 200 pixels, which has no obvious impact on the computer recognition results. Among MobileNet with different image resolutions, MobileNet_224 is superior to MobileNet_320 (AUC: 0.891) and MobileNet_448 (AUC: 0.909). The results suggest that MobileNet can still extract the information needed for diagnosis after the image dimension is reduced, which is consistent with the original intention of model design and other studies (38, 39).

A high-resolution image contains more information and larger pixel matrix, but it takes up more memory. In the convolution operation, the large size consumes more computing time than the small size. This study found that the resolution has an impact on the time consumption of the model, and the time consumption of high-resolution model analysis increases, which is consistent with other studies (40). On the contrary, small images consume less computational resources, but may lose some information and may produce misleading results. Therefore, deep learning needs to

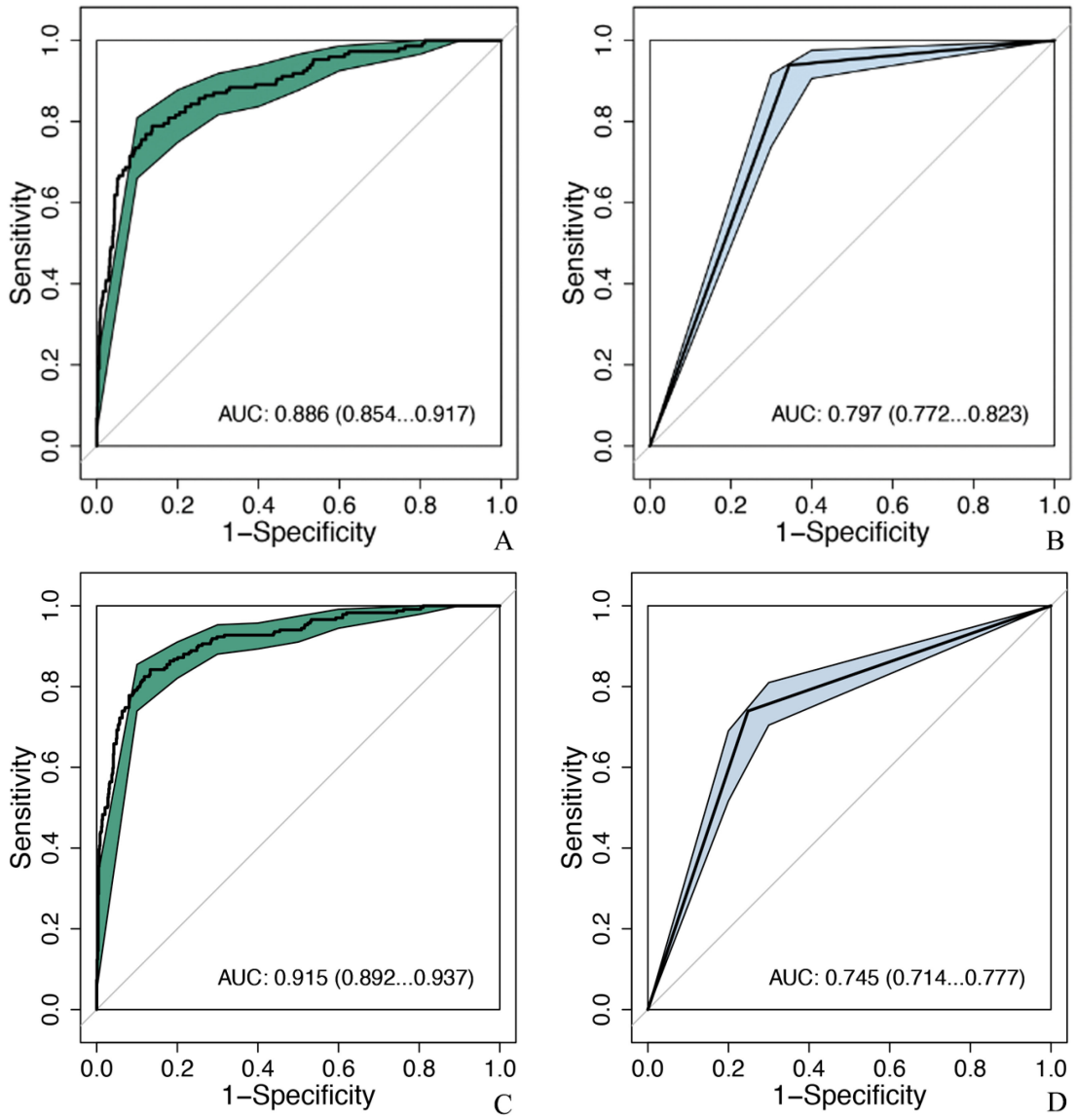


FIGURE 6
Comparison of diagnostic efficacy between the optimal model and senior doctors after excluding BIRADS 4c and 5 nodules. MobileNet_224, MobileNet with 224 × 224-pixel image input; AUC, area under the curve; 95% CI, 95% confidence interval. **(A)** MobileNet_224, **(B)** senior ultrasound doctors, **(C)** MobileNet_224, **(D)** senior mammography doctors.

compromise the contradiction between computational efficiency and recognition accuracy (41). The DNNs, such as DenseNet, ResNet50, and EfficientNetB0, have dense connections between layers and are more memory and time consuming (42). This study shows that DenseNet121_224 takes the longest time in analyzing a single picture, which is 0.07 s, while MobileNet _224 takes less than 0.02 s.

According to BI-RADS classification, Class 0 is a lesion that cannot be determined qualitatively, which has not been diagnosed but has been

TABLE 4 The average time of analyzing a single ultrasound image with different AI models (s).

| Modality | 224* | 320* | 448* | Mean ± SD | p-Value |
|---|---|---|---|---|---|
| MobileNet | 0.019 | 0.020 | 0.021 | 0.020 ± 0.001 | 0.0004 |
| Xception | 0.031 | 0.034 | 0.035 | 0.033 ± 0.002 | 0.001 |
| DenseNet121 | 0.075 | 0.076 | 0.077 | 0.076 ± 0.001 | 0.0001 |
| ResNet50 | 0.034 | 0.036 | 0.037 | 0.036 ± 0.001 | 0.0006 |

Asterisks (*) indicate the image resolution used for model input.

suspected by doctors, and the possibility of malignancy of BI-RADS 3, 4a, and 4b tumors is less than 2%, 2%–10%, and 10%–50%, respectively. According to BI-RADS 3, follow-up is recommended, and biopsy is recommended for 4a and 4b. If benign tumors can be further screened by AI method, unnecessary puncture and injury can be reduced. A study (43) reported that using the trained AI model to identify benign and malignant breast tumors was higher than the diagnostic level of doctors, the AUC of which were 0.87 (95% CI: 0.79–0.95) and 0.51 (95% CI: 0.50–0.53), respectively. In this study, the AUC of MobileNet_224 [0.886 (95% CI: 0.854–0.917)] is higher than that of senior US doctors [0.820 (95% CI: 0.803–0.837]]. Compared with senior mammography, the AUC of MobileNet_224 [0.915 (95% CI: 0.892–0.937)] is higher than that of senior mammography doctors [0.745 (95% CI: 0.714–0.777)]. To further clarify the diagnostic efficiency of AI technology, this study selected breast tumors that are difficult to diagnose using US and mammography for analysis and found that when the cut-off value of MobileNet_224 is 0.467, the diagnostic accuracy is higher than that of senior doctors in US and mammography. The model significantly reduced false positives in both ultrasound (60.1% reduction) and mammography (46.6% reduction), while improving specificity and overall accuracy (AUC increase: 6.6% for ultrasound; accuracy increase: 6.1%). The application of MobileNet_224 demonstrated significant improvements in diagnostic performance. Specifically, the number of false positives in ultrasound (US) imaging was reduced from 286 to 114 cases representing a 60.1% reduction. For mammography, the model increased the AUC and accuracy by 17% and 11.3%, respectively. Furthermore, the model reduced false positives in mammography from 204 to 109 cases, a decrease of 46.6%. These results highlight MobileNet_224's capability to diagnose early-stage breast cancer (BC), minimize false positives, and reduce unnecessary biopsies. Contrary to the assumption that higher image resolution universally improves diagnostic accuracy, our findings reveal that MobileNet_224 achieves superior performance at a 224 × 224 resolution. This challenges the prevailing trend in medical AI toward computationally intensive high-resolution frameworks.

The use of AUC, sensitivity, and specificity is widely accepted in oncology AI studies, while analysis speed addresses practical deployment needs. By excluding BI-RADS 4c/5 cases (high malignancy likelihood), we specifically tested the model's ability to resolve ambiguous diagnoses—a key clinical challenge.

Our study has several limitations. First, this study is a single-center and retrospective study. In the future, a multi-center prospective AI study should be carried out to confirm the reliability of the screening model of this study. Second, this study does not distinguish the types of US instruments and equipment, but only analyzes the static US images. The accuracy and reliability of AI technology for video data analysis need to be studied further. Last, our study focused on evaluating existing lightweight models for clinical deployment capability rather than proposing novel architectures, which limits direct comparisons with cutting-edge frameworks but prioritizes real-world practicality. Future research could expand comparisons to hybrid models, such as CNN-Transformer frameworks, to evaluate their potential for multi-scale feature extraction in breast cancer diagnosis.

## Conclusion

This study systematically evaluates the diagnostic performance of lightweight AI models (MobileNet, Xception) versus dense networks (ResNet50, DenseNet121) across ultrasound image resolutions (224 × 224, 320 × 320, 448 × 448) for breast cancer detection. Using a retrospective cohort of 4,998 patients, we demonstrate that MobileNet_224, despite its computational simplicity, achieves superior clinical utility as follows: 1) Speed–Accuracy Balance: MobileNet_224 processes images in 0.02 s—300× faster than manual review—while maintaining 87.3% accuracy addressing critical workflow bottlenecks. 2) False-Positive Reduction: The model reduces unnecessary biopsies by 60.1% in ultrasound and 46.6% in mammography directly impacting patient outcomes and healthcare costs. 3) Resolution Optimization Framework: Lower resolutions (224 × 224) suffice for accurate diagnosis challenging the need for resource-intensive high-resolution pipelines. These findings advocate for redefining clinical AI benchmarks toward deployment capability rather than theoretical performance offering a pragmatic framework for healthcare translation.

## Data availability statement

The raw data supporting the conclusions of this article will be made available by the authors, without undue reservation.

## Ethics statement

Ethical approval was not required for the study involving humans in accordance with the local legislation and institutional requirements. Written informed consent to participate in this study was not required from the participants or the participants' legal guardians/next of kin in accordance with the national legislation and the institutional requirements.

## Author contributions

YY: Conceptualization, Investigation, Writing – original draft, Writing – review & editing. JF: Data curation, Investigation, Methodology, Writing – original draft, Writing – review & editing. WZ: Funding acquisition, Project administration, Resources, Validation, Writing – review & editing. XS: Formal Analysis, Project administration, Resources, Supervision, Validation, Visualization, Writing – review & editing.

## Funding

The author(s) declare that financial support was received for the research and/or publication of this article. This project was supported by the Clinical Scientist Training Program of Shenzhen People's Hospital (SYWGSCGZH202202) and the Department of Science and Technology of Guangdong Province (Project No. 2024A0505040020).

## Conflict of interest

The authors declare that the research was conducted in the absence of any commercial or financial relationships that could be construed as a potential conflict of interest.

## Generative AI statement

The author(s) declare that no Generative AI was used in the creation of this manuscript.

## Correction note

This article has been corrected with minor changes. These changes do not impact the scientific content of the article.

## Publisher's note



## Supplementary material

The Supplementary Material for this article can be found online at: https://www.frontiersin.org/articles/10.3389/fonc.2025.1536365/full#supplementary-material

## References

1. Chen W, Zheng R, Zhang S, Zeng H, Xia C, Zuo T, et al. Cancer incidence and mortality in China, 2013. *Cancer Lett*. (2017) 401:63–71. doi: 10.1016/j.canlet.2017.04.024

2. Miller KD, Nogueira L, Devasia T, Mariotto AB, Yabroff KR, Jemal A, et al. Cancer treatment and survivorship statistics, 2022. *CA: A Cancer J For Clinicians*. (2022) 72:409–36. doi: 10.3322/caac.21731

3. Makama M, Drukker CA, Rutgers EJT, Slaets L, Cardoso F, Rookus MA, et al. An association study of established breast cancer reproductive and lifestyle risk factors with tumour subtype defined by the prognostic 70-gene expression signature (MammaPrint®). *Eur J Cancer (Oxford England: 1990)*. (2017) 75:5–13. doi: 10.1016/j.ejca.2016.12.024

4. Jin Z-Q, Lin M-Y, Hao W-Q, Jiang H-T, Zhang L, Hu W-H, et al. Diagnostic evaluation of ductal carcinoma in *situ* of the breast: ultrasonographic, mammographic and histopathologic correlations. *Ultrasound In Med Biol*. (2015) 41:47–55. doi: 10.1016/j.ultrasmedbio.2014.09.023

5. Su X, Lin Q, Cui C, Xu W, Wei Z, Fei J, et al. Non-calcified ductal carcinoma in *situ* of the breast: comparison of diagnostic accuracy of digital breast tomosynthesis, digital mammography, and ultrasonography. *Breast Cancer (Tokyo Japan)*. (2017) 24:562–70. doi: 10.1007/s12282-016-0739-7

6. Schneble EJ, Graham LJ, Shupe MP, Flynt FL, Banks KP, Kirkpatrick AD, et al. Future directions for the early detection of recurrent breast cancer. *J Cancer*. (2014) 5:291–300. doi: 10.7150/jca.8017

7. Niell BL, Freer PE, Weinfurtner RJ, Arleo EK, Drukteinis JS. Screening for breast cancer. *Radiologic Clinics*. (2017) 55:1145–62. doi: 10.1016/j.rcl.2017.06.004

8. Osako T, Takahashi K, Iwase T, Iijima K, Miyagi Y, Nishimura S, et al. Diagnostic ultrasonography and mammography for invasive and noninvasive breast cancer in women aged 30 to 39 years. *Breast Cancer (Tokyo Japan)*. (2007) 14:229–33. doi: 10.2325/jbcs.891

9. Spick C, Schernthaner M, Pinker K, Kapetas P, Bernathova M, Polanec SH, et al. MR-guided vacuum-assisted breast biopsy of MRI-only lesions: a single center experience. *Eur Radiol*. (2016) 26:3908–16. doi: 10.1007/s00330-016-4267-9

10. Aswathy M, Jagannath M. Detection of breast cancer on digital histopathology images: Present status and future possibilities. *Inf Med Unlocked*. (2017) 8:74–9. doi: 10.1016/j.imu.2016.11.001

11. Liberman L, Menell JH. Breast imaging reporting and data system (BI-RADS). *Radiologic Clinics*. (2002) 40:409–30. doi: 10.1016/S0033-8389(01)00017-3

12. Afrifa S, Varadarajan V, Appiahene P, Zhang T. A novel artificial intelligence techniques for women breast cancer classification using ultrasound images. *CEOG*. (2023) 50:271–84. doi: 10.31083/j.ceog5012271

13. Kaddes M, Ayid YM, Elshewey AM, Fouad Y. Breast cancer classification based on hybrid CNN with LSTM model. *Sci Rep*. (2025) 15:4409. doi: 10.1038/s41598-025-88459-6

14. Chung M, Calabrese E, Mongan J, Ray KM, Hayward JH, Kelil T, et al. Deep learning to simulate contrast-enhanced breast MRI of invasive breast cancer. *Radiology*. (2023) 306:e213199. doi: 10.1148/radiol.213199

15. Afrifa S, Varadarajan V, Appiahene P, Zhang T, Domfeh EA. Ensemble machine learning techniques for accurate and efficient detection of botnet attacks in connected computers. *Eng*. (2023) 4:650–64. doi: 10.3390/eng4010039

16. Wang S-R, Cao C-L, Du T-T, Wang J-L, Li J, Li W-X, et al. Machine learning model for predicting axillary lymph node metastasis in clinically node positive breast cancer based on peritumoral ultrasound radiomics and SHAP feature analysis. *J Ultrasound Med*. (2024) 43:1611–25. doi: 10.1002/jum.16483

17. Kavitha T, Mathai PP, Karthikeyan C, Ashok M, Kohar R, Avanija J, et al. Deep learning based capsule neural network model for breast cancer diagnosis using mammogram images. *Interdiscip Sciences: Comput Life Sci*. (2022) 14:113–29. doi: 10.1007/s12539-021-00467-y

18. Huang J, Mei L, Long M, Liu Y, Sun W, Li X, et al. BM-net: CNN-based mobileNet-V3 and bilinear structure for breast cancer detection in whole slide images. *Bioengineering*. (2022) 9:261. doi: 10.3390/bioengineering9060261

19. Das HS, Das A, Neog A, Mallik S, Bora K, Zhao Z. Breast cancer detection: Shallow convolutional neural network against deep convolutional neural networks based approach. *Front Genet*. (2023) 13. doi: 10.3389/fgene.2022.1097207

20. Aljuaid H, Alturki N, Alsubaie N, Cavallaro L, Liotta A. Computer-aided diagnosis for breast cancer classification using deep neural networks and transfer learning. *Comput Methods Programs Biomedicine*. (2022) 223:106951. doi: 10.1016/j.cmpb.2022.106951

21. Latha M, Kumar PS, Chandrika RR, Mahesh TR, Kumar VV, Guluwadi S. Revolutionizing breast ultrasound diagnostics with EfficientNet-B7 and Explainable AI. *BMC Med Imaging*. (2024) 24:230. doi: 10.1186/s12880-024-01404-3

22. Schnider E, Wolleb J, Huck A, Toranelli M, Rauter G, Müller-Gerbl M, et al. Improved distinct bone segmentation in upper-body CT through multi-resolution networks. *Int J Comput Assisted Radiol Surg*. (2023) 18:2091–9. doi: 10.1007/s11548-023-02957-4

23. Yousefirizi F, Klyuzhin IS, O JH, Harsini S, Tie X, Shiri I, et al. TMTV-Net: fully automated total metabolic tumor volume segmentation in lymphoma PET/CT images — a multi-center generalizability analysis. *Eur J Nuclear Med Mol Imaging*. (2024) 51:1937–54. doi: 10.1007/s00259-024-06616-x

24. Afrifa S, Appiahene P, Zhang T, Varadarajan V. Machine learning algorithms for iron deficiency anemia detection in children using palm images. *Int J Educ Manage Eng*. (2024) 14(1):1–15. doi: 10.5815/ijeme.2024.01.01

25. Appiahene P, Arthur EJ, Korankye S, Afrifa S, Asare JW, Donkoh ET. Detection of anemia using conjunctiva images: A smartphone application approach. *Med Novel Technol Devices*. (2023) 18:100237. doi: 10.1016/j.medntd.2023.100237

26. Appiahene P, Dogbe SSD, Kobina EEY, Dartey PS, Afrifa S, Donkoh ET, et al. Application of ensemble models approach in anemia detection using images of the palpable palm. *Med Novel Technol Devices*. (2023) 20:100269. doi: 10.1016/j.medntd.2023.100269

27. Adu WK, Appiahene P, Afrifa S. VAR, ARIMAX and ARIMA models for nowcasting unemployment rate in Ghana using Google trends. *J Electrical Syst Inf Technol*. (2023) 10:12. doi: 10.1186/s43067-023-00078-1

28. Huang C, Sarabi M, Ragab AE. MobileNet-V2 /IFHO model for Accurate Detection of early-stage diabetic retinopathy. *Heliyon*. (2024) 10:e37293. doi: 10.1016/j.heliyon.2024.e37293

29. Mandiya RE, Kongo HM, Kasereka SK, Kyandoghere K, Tshakwanda PM, Kasoro NM. Enhancing COVID-19 detection: an xception-based model with advanced transfer learning from X-ray thorax images. *J Imaging*. (2024) 10:63. doi: 10.3390/jimaging10030063

30. Huang G, Liu Z, van der Maaten L, Weinberger KQ. Densely connected convolutional networks. In: Proceedings of the 2017 IEEE Conference on Computer Vision and Pattern Recognition (CVPR). Honolulu, HI, USA. Piscataway, NJ: IEEE Computer Society (2017). p. 2261–9. doi: 10.1109/CVPR.2017.243

31. He K, Zhang X, Ren S, Sun J. Deep residual learning for image recognition. In: Proceedings of the 2016 IEEE Conference on Computer Vision and Pattern Recognition (CVPR). Las Vegas, NV, USA. Piscataway, NJ: IEEE (2016). p. 770–8. doi: 10.1109/CVPR.2016.90

32. Latif S, Zou Z, Idrees Z, Ahmad J. A novel attack detection scheme for the industrial internet of things using a lightweight random neural network. *IEEE Access*. (2020) 8:89337–50. doi: 10.1109/Access.6287639

33. Phan H, Liu Z, Huynh D, Savvides M, Cheng K-T, Shen Z. Binarizing MobileNet via evolution-based searching. In: Proceedings of the 2020 IEEE/CVF Conference on Computer Vision and Pattern Recognition (CVPR). (2020). p. 13417–26. doi: 10.1109/CVPR42600.2020.01343

34. Chen H-Y, Su C-Y. (2018). An enhanced hybrid MobileNet, in: *2018 9th International Conference on Awareness Science and Technology (iCAST)*, , Vol. 2018. pp. 308–12.

35. Howard AG, Zhu M, Chen B, Kalenichenko D, Wang W, Weyand T, et al. Mobilenets: Efficient convolutional neural networks for mobile vision applications. *arXiv preprint arXiv:170404861*. (2017).

36. Ansar W, Shahid AR, Raza B, Dar AH. Breast cancer detection and localization using MobileNet based transfer learning for mammograms. In: Intelligent Computing Systems: Third International Symposium, ISICS 2020, Sharjah, United Arab Emirates, March 18–19, 2020, Proceedings 3. Cham, Switzerland: Springer International Publishing (2020). p. 11–21. doi: 10.1007/978-3-030-43364-2_2

37. Gómez-Flores W, de Albuquerque Pereira WC. A comparative study of pre-trained convolutional neural networks for semantic segmentation of breast tumors in ultrasound. *Comput IN Biol AND Med*. (2020) 126:104036. doi: 10.1016/j.compbiomed.2020.104036

38. Badawy SM, Mohamed AE-NA, Hefnawy AA, Zidan HE, GadAllah MT, El-Banby GM. Automatic semantic segmentation of breast tumors in ultrasound images based on combining fuzzy logic and deep learning-A feasibility study. *PloS One*. (2021) 16:e0251899. doi: 10.1371/journal.pone.0251899

39. Chunhapran O, Yampaka T. Combination ultrasound and mammography for breast cancer classification using deep learning. In: 2021 18th International Joint Conference on Computer Science and Software Engineering (JCSSE). Lampang, Thailand. Piscataway, NJ: IEEE (2021). p. 1–6. doi: 10.1109/JCSSE53117.2021.9493840

40. Krishna ST, Kalluri HK. Deep learning and transfer learning approaches for image classification. *Int J Recent Technol Eng (IJRTE)*. (2019) 7:427–32. doi: 10.35940/ijrte.F9811.038620

41. Gao Y, Mosalam KM. Deep transfer learning for imageing7-4 structural damage recognition. *Computerion32 Civil Infrastructure Eng*. (2018) 33:748–68. doi: 10.1111/mice.2018.33.issue-9

42. Feng X, Yao H, Zhang S. An efficient way to refine DenseNet. *Signal Image Video Process*. (2019) 13:959–65. doi: 10.1007/s11760-019-01433-4

43. Kim SY, Choi Y, Kim EK, Han B-K, Yoon JH, Choi JS, et al. Deep learning-based computer-aided diagnosis in screening breast ultrasound to reduce false-positive diagnoses. *Sci Rep*. (2021) 11:395. doi: 10.1038/s41598-020-79880-0

frontiers | Frontiers in Oncology

TYPE Case Report
PUBLISHED 18 July 2025
DOI 10.3389/fonc.2025.1534112



OPEN ACCESS

EDITED BY
Raquel Diaz,
University of Genova, Italy

REVIEWED BY
Dupoiron Denis,
Institut de Cancérologie de l'Ouest (ICO), France
Cherry Bansal,
Tantia University, India

*CORRESPONDENCE
Giuseppe De Palma
g.depalma@oncologico.bari.it

†These authors have contributed equally to this work and share first authorship

RECEIVED 25 November 2024
ACCEPTED 25 June 2025
PUBLISHED 18 July 2025

CITATION
Calabrò C, Iacovelli S, De Palma G, Carravetta G, Garofalo D, Giotta F, Latorre A, Nardulli P, Ressa CM, Vitale E, De Santis V and Mastrandrea G (2025) Case Report: A successful multidisciplinary approach to doxorubicin extravasation from a PICC-port in a patient with breast cancer.
*Front. Oncol.* 15:1534112.
doi: 10.3389/fonc.2025.1534112



# Case Report: A successful multidisciplinary approach to doxorubicin extravasation from a PICC-port in a patient with breast cancer

Concetta Calabrò[1†], Serena Iacovelli[1†], Giuseppe De Palma[2*], Giuseppe Carravetta[3], Domenica Garofalo[3], Francesco Giotta[4], Agnese Latorre[4], Patrizia Nardulli[1], Cosmo Maurizio Ressa[5], Elsa Vitale[6], Valerio De Santis[5] and Giovanni Mastrandrea[3]

[1]Pharmacy Unit, IRCCS Istituto Tumori "Giovanni Paolo II" Bari, Bari, Italy, [2]Institutional BioBank, Experimental Oncology and Biobank Management Unit, IRCCS Istituto Tumori "Giovanni Paolo II" Bari, Bari, Italy, [3]Anaesthesia, Resuscitation and Postoperative Intensive Care Unit, IRCCS Istituto Tumori "Giovanni Paolo II" Bari, Bari, Italy, [4]Medical Oncology Unit, IRCCS Istituto Tumori "Giovanni Paolo II" Bari, Bari, Italy, [5]Plastic and Reconstructive Surgery Unit, IRCCS Istituto Tumori "Giovanni Paolo II" Bari, Bari, Italy, [6]Scientific Directorate, IRCCS Istituto Tumori "Giovanni Paolo II" Bari, Bari, Italy

**Background:** Infusion of chemotherapy drugs through central venous catheters in the bloodstream facilitates direct access to disseminated cancer sites to interrupt the growth and/or spread of abnormal cells. To represent the significance of a rapid, multidisciplinary intervention codified by a hospital-adopted procedure for the treatment of this specific type of extravasation.

**Methods:** A case of a 63-year-old female patient with no comorbidities but overweight who was admitted to our hospital in 2023 was discussed. The oncologist requested the placement of a long-term central venous access for chemotherapy, expected to last at least 5–6 months. This case report describes a massive anthracycline extravasation through a PICC-port. Such a serious complication requires not only the prompt administration of dexrazoxane but, more importantly, a multidisciplinary approach. Without comprehensive and timely intervention, the patient would have likely lost the upper limb.

**Clinical implications:** Following the surgical and pharmacological treatment, the patient achieved a restoration of normal limb function, thus resuming all regular activities. This outcome was made possible primarily due to the timely and professional intervention of the multidisciplinary team, which minimized the severe complications that doxorubicin extravasation can cause. Tunneling of the catheter, which moves the extravasation site (port pocket) away from the venipuncture site, is equally important. Another noteworthy element is the resumption of chemotherapy treatment, which might have been interrupted due to the severe complication resulting from the extravasation.

KEYWORDS

**breast cancer, intravenous chemotherapy drugs, doxorubicin extravasation, multidisciplinary intervention, long-term central venous access, PICC-PORT, necrosis**

# 1 Introduction

Infusion of intravenous chemotherapy drugs in the bloodstream facilitates direct access to disseminated cancer sites to interrupt the growth and/or spread of abnormal cells. To reduce complication and to facilitate this infusion, the most preferred options are central vascular access devices, including peripherally inserted central catheters (PICCs) and totally implantable vascular access devices (TIVADs) with chest insertion (chest port) or peripheral insertion (arm port or PICC port) (1, 2). Also, in economic studies published in the last 5 years, the TIVADs are starting to be considered more cost-effective than CVCs and PICCs in breast cancer chemotherapy patients (3–7).

Moreover, the cosmetic and psychological advantage has led to a more frequent use of peripherally inserted TIVADs in breast cancer: the additional scar in a hidden area of the body, the non-need to uncover and use the chest, and the non-need to carry out weekly PICC medications justify breast cancer patients preferring these devices (1). Weekly maintenance includes the use of needle-free connectors, sutureless securement devices, and transparent semipermeable dressings. In addition, PICCs require a weekly flush to ensure catheter patency and prevent occlusions (8).

In order to reduce the incidence of injury during the peripheral insertion of TIVADs, various studies close to the Italian healthcare system recommend using ultrasound guidance in real time, maximum barrier protection, the micro-Seldinger technique for the venipuncture in the proximal third of the upper arm, close to the axilla, and the tunneling up to a pocket for the port chamber located in the "green zone" of the zone insertion method (ZIM) used for PICCs (1–7, 9–13).

Extravasation is a complication related to the infusion of chemotherapy drugs in peripherally inserted TIVADs because it is clearly connected to the greater mobility of the arm compared to the chest (13).

Extravasation is one of the most feared events related to the chemotherapy drug infusion. Inadvertent administration of a solution or drug into the tissue surrounding the intravenous catheter can, in fact, result in serious complications. In particular, if it is a solution or a non-vesicant drug, it is called infiltration; when it comes to a vesicant drug, it is called extravasation. Both infiltration and extravasation can have serious consequences: the patient may require surgery that causes large scarring, experience functional limitations, or even require amputation (14). Chemotherapy extravasation remains an accidental complication of chemotherapy administration and may result in serious damage to patients (15).

A recent study evaluated a total of 739,812 infusions and identified 673 extravasation events. Incidence for all extravasation events was 0.09% (16).

More specifically, chemotherapy agents may be classified by their potential to cause tissue necrosis. Vesicants are agents that can cause blistering, sloughing of the skin, and varying degrees of localized tissue damage. Non-vesicants do not impair or destroy the tissue when they infiltrate into the tissue (17). Vesicant chemotherapy agents can be divided into two categories: DNA binding and DNA non-binding. Vesicants that bind to nucleic acids in DNA (e.g., anthracyclines) bind to the DNA in the cells of healthy tissue when they extravasate from the vein and promptly cause cell death. DNA-doxorubicin complexes are released from dead cells in the tissue and are taken up by adjacent healthy cells by endocytosis. This process of cellular uptake of extracellular substances sets up a continuing cycle of tissue damage as the anthracycline is retained in the tissue for a long period of time and recirculated in the surrounding area (18).

To prevent serious and permanent damage due to extravasations, early identification has particular importance. Generally, the optimal treatment of anthracycline extravasation includes local tissue cooling, elevation of the afflicted extremity, dexrazoxane administration, and possibly topical DMSO (19).

According to our hospital procedure, dexrazoxano must be used in case of anthracycline extravasation. Dexrazoxano works with two different mechanisms: first, the iron chelation caused by its open-ring metabolite, which can reduce iron-dependent oxidative stress that is responsible for anthracycline cardiotoxicity; second, dexrazoxano causes topoisomerase II inhibition.

The relative contribution of each mechanism to the prevention of tissue damage following anthracycline extravasation remains unclear.

Dexrazoxano must be administered once a day for three consecutive days, according to the following scheme: Day 1: 1,000 mg/m$^2$; Day 2: 1,000 mg/m$^2$; and Day 3: 500 mg/m$^2$. The first infusion must start as soon as possible and, in any case, within the first 6h of the event. Days 2 and 3 treatment should begin at the same time as Day 1 (± 3h). When extravasation involves central venous access, the hospital procedure requires the nurse to block the infusion and aspirate the utmost possible quantity of solution through the catheter.

In this case report, we want to report our experience in treating anthracycline doxorubicin extravasation related to a PICC-port in a patient with breast cancer to provide further evidence of the need for tunneling as protection of the vascular nervous axis of the arm and to save healthy tissue useful in the skin reconstruction phase. This antineoplastic chemotherapeutic agent is known to cause severe and progressive tissue necrosis. Extravasation may also produce pain and/or a burning sensation in the area where doxorubicin was administered intravenously. Doxorubicin extravasation creates a severe tissue necrosis, which is unusual because it may not appear until several weeks later and may continue to worsen for several months (20).

Furthermore, we aim to highlight the importance of a rapid, multidisciplinary intervention, as defined by a hospital-adopted procedure for the management of this specific type of extravasation. In particular, for the PICC-port, this intervention begins with the careful planning of the device placement, including appropriate tunneling.

# 2 Case description

A 63-year-old female patient was, with no comorbidities but overweight, admitted to our hospital in 2023. She had previously

undergone a left mastectomy with axillary dissection. The oncologist requested the placement of a long-term central venous access for chemotherapy, expected to last at least 5–6 months.

After a consultation and the patient examination, it was agreed to place a PICC-port. An ultrasound study of the venipuncture site was performed according to the Rapid Peripheral Vein Assessment (RaPeVA) protocol. The venipuncture site was marked with a black dermatographic pen laterally to the ultrasound probe, in the upper proximal area of the arm. At this level, it was generally possible to identify a brachio-axillary vein with a diameter of at least 0.5 cm capable of accommodating a 5 Fr PICC port catheter, which was the PICC port catheter size.

Afterwards, the feasibility of tunneling and creating a subcutaneous pocket in the "green zone" of Dawson's ZIM system to place the reservoir was evaluated. Given the size of the arm and the subcutaneous tissue, it was decided to perform tunneling parallel to the vascular-nervous bundle for about 7 cm in order to position the reservoir in the median area of the arm on the medial side.

Using maximum barrier protections, aseptic technique, and real-time ultrasound guidance, after local anesthesia with 2% lidocaine, venipuncture was performed with a micro-introduction kit and indirect Seldinger technique. Next, the venous catheter was introduced, and its length was evaluated using tip location and tip navigation systems. This was followed by the creation of the pocket for the reservoir and retrograde tunneling, still under local anesthesia. Finally, after testing the catheter's functionality, suturing was performed with separate inverted intradermal stitches using a 4–0 absorbable monofilament thread, and adhesive (cyanoacrylate) was applied. The procedure concluded with medium-pressure dressing, and the patient was given an appointment for 4–5 days later, before the first chemotherapy infusion, for reevaluation of the surgical wound and catheter functionality.

The patient presents to the chemotherapy clinic for scheduled treatment with doxorubicin and cyclophosphamide. A Huber needle was placed, and the catheter's functionality was verified. About an hour after the start of therapy, an alteration in the anatomical profile of the arm with edema and redness was noted. The patient complains of burning, and the Huber needle was found to have dislodged from the reservoir. The institutional procedure for extravasation was started immediately. The needle was removed, and the oncologist, plastic surgeon, and anesthesiologist have been contacted. The patient was taken to the operating room where the PICC-port was removed (Figure 1A), a short-term triple-lumen CVC was placed with ultrasound-guided access in the left jugular, and a diffuse extravasation with a diameter of about 20 cm was observed. Apparently, the 7 cm of tunneling was not enough to protect the vascular-nervous bundle of the arm.

The patient was properly medicated and treated with the dexrazoxano (Savene®) antidote according to institutional procedure: the extent of the lesion at the venipuncture site was reduced; lesions from vesicant chemotherapy appeared (Figure 1B); reduced venous compressibility was noted, antibiotic therapy continued, and thromboembolic prophylaxis therapy (chemical phlebitis) was initiated.

The necrotic area began to demarcate and was removed through surgical debridement; thromboembolic prophylaxis continued (Figures 2A, B). A thoracic port was placed on the left side for the continuation of therapy.

The patient continued to receive regular care, including surgical debridement; thromboembolic prophylaxis was ongoing (Figure 2C).

Continued dressings and surgical debridement were ongoing; thromboembolic prophylaxis was progressively reduced, and vacuum-assisted closure (VAC) therapy was initiated (Figures 2D, E).

After 10 months of wound healing among different pathways without any real advantage, we had a wound about 6 cm × 4 cm. The patient had a real discomfort caused by perilesional skin irritation and for continuous liquid secretions. So, in this case, we have planned a plastic surgery procedure with a local skin flap based on a safe vessel apport. This skin flap was obtained from the portion of skin that contained the venipuncture site (Figure 3). The same skin flap was saved from the necrotizing action of the extravasated drug due to the presence of tunneling. This provides further evidence of the need for tunneling as protection of the vascular nervous axis of the arm and to save healthy tissue useful in the skin reconstruction phase.

Previously, we performed an escharotomy surgery of the wound, and after that, previous to a skin marking, we made a skin incision

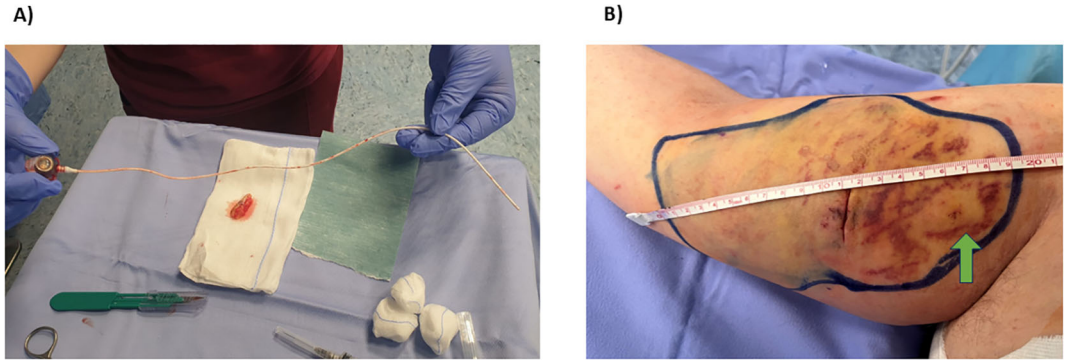


FIGURE 1
**(A)** Intact PICC-port after removal; **(B)** Edematous and reddened limb post PICC-port removal. Note the diameter of the extravasation spread and the visible venipuncture site, apparently included in the area affected by the extravasation.

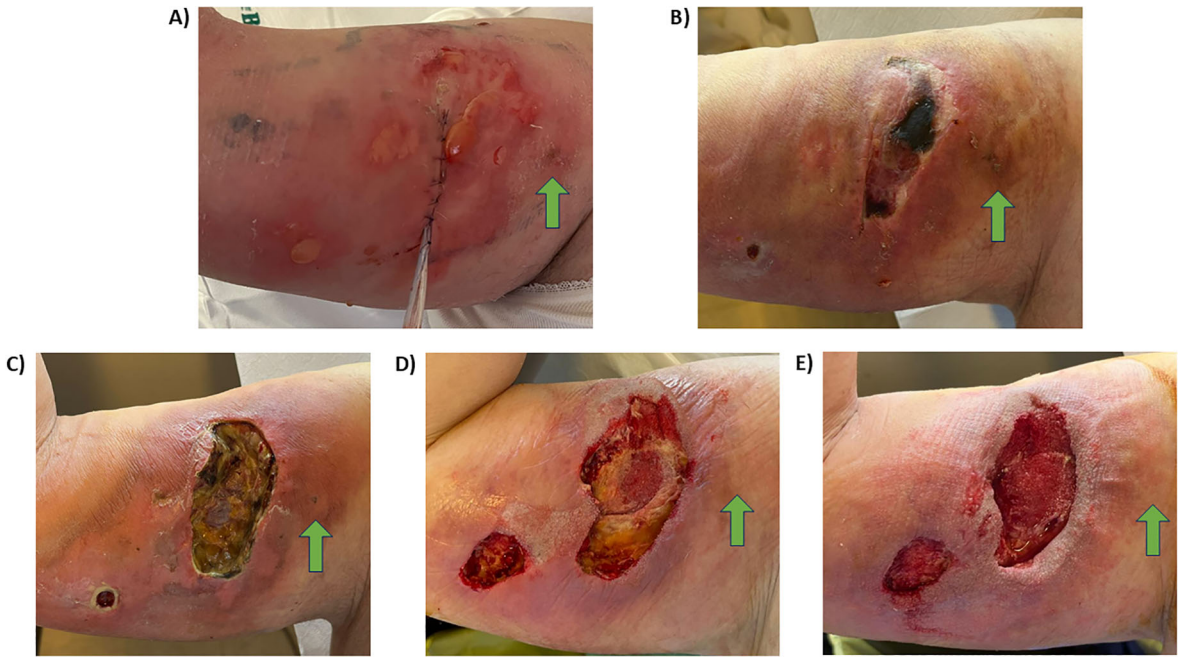


FIGURE 2
**(A)** Phase 1. About a week later, a reduction in inflammation due to the caustic properties of the vesicant chemotherapy was noted. **(B)** Phase 2. Approximately 1 month later, stabilization of the cutaneous and subcutaneous necrosis was observed. Initially, the dressing included cortisone and antibiotic creams (Clobesol and Gentamicin) and Phytostimoline. **(C)** Phase 3. Two months later, definition of the necrosis with tissue ulceration down to the muscle fascia was observed, exposing the biceps muscle. **(D)** Phase 4. Three months later, surgical cleansing and debridement were performed, followed by application of VAC Therapy for 60 days, interrupted 3 times for dressings with gauze soaked in Betadine due to allergy to the VAC patch. **(E)** Phase 5: Four months later, cleansing was performed with Noruxol and dressings with Phytostimoline in anticipation of scheduling surgical intervention for decontamination and repair with grafts or flaps. The venipuncture site is indicated.

until the muscle fascia, and we have rotated a cutaneous and subcutaneous flap. All the environment was full of scars and of cicatricial adherences, probably the result of chemotherapy extravasation. Even if we have found this obstacle, we have been provided with good tissue and good coverage of the wound with our flap (Figure 3). After the surgery, we got 15 days for final closure without any complications. We had the patient in follow-up for 6–12 months with optimal results of the scar (Figure 4).

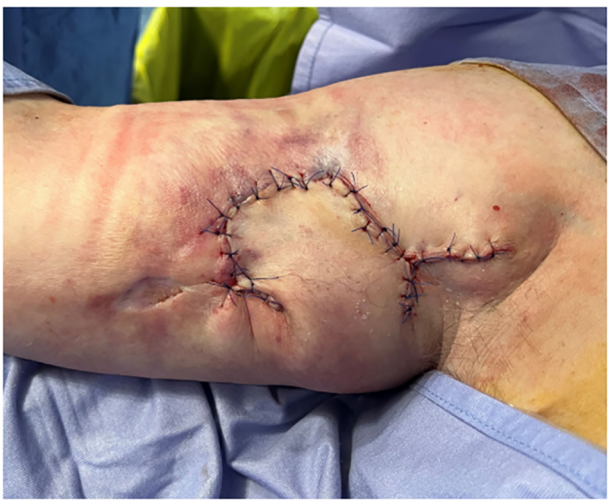

FIGURE 3
The patient has taken medication regularly. After 10 months, reconstructive plastic surgery was scheduled using a local skin flap based on the tunneling zone, including the indicated venipuncture site.

## 3 Discussion

Venous access ports positioned in the upper arm are a safe device for administering chemotherapy in breast cancer patients. This type of device is usually well accepted, especially if the positioning is done in a personalized way. In this case, it is often preferred to both the PICC and the chest port (1, 2, 6, 9).

In any case, each type of implantable device must be monitored and managed in relation to the specific placement.

As for the positioning of the PICC, a feasibility study of venipuncture with the support of the ultrasound technique must also be carried out for the PICC port in order to choose a caliber that respects the venous heritage. This evaluation allows us to prevent the thrombotic event, which is particularly related to multiple venipunctures and positioning in small-caliber vessels.

As for the positioning of the chest port, another assessment must be performed to evaluate the better surgery site and the tunnelization, which appears to play a crucial role in the successful management of extravasation, as demonstrated by our clinical experience.

In this specific case report, tunneling played a protective role at the infusion site, preventing the extravasated chemotherapeutic

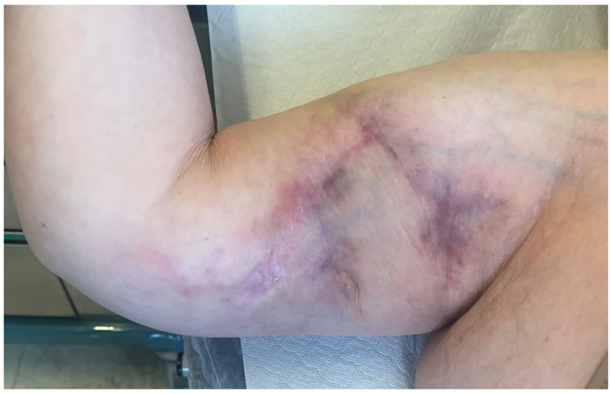

FIGURE 4
Follow up of the patient at 6 months.

agent from infiltrating deeper tissues and causing extensive damage that could have impaired function or even resulted in limb loss. The skin flap spared from exposure to the drug was later utilized by the plastic surgeon during the reconstructive phase, as shown in Figure 3.

It must be considered the reservoir size and the specific arm anatomy. The best choice of the surgery site could prevent error during the introduction of the Huber needle and the possible consequent extravasation. It is easy to understand how the Huber needle is more likely to dislocate during infusion when the reservoir is positioned at the level of the upper limb, which in itself is more mobile than the chest.

The multidisciplinary team should also pay attention to the administration phase with the PICC port. Therefore, when chemotherapy is administered, the patient must be adequately involved and motivated to keep the arm still and to report any pain or burning felt at the infusion site.

A PICC port could favor the necrotizing effect of the extravasated drug, in particular in skinny patients and in the absence of tunnelization because of the injury of the neurovascular bundle. From this perspective, early removal of the device and tunneling are recommended.

Past studies indicated that the overall estimated incidence of chemotherapy extravasation ranges from 0.01% to 7% (21). Other authors report an incidence of chemotherapy extravasation ranging from 0.1% to 6% for peripheral venous access devices and from 0.26% to 4.7% for central venous access devices (15). Data on the incidence is scant due to the absence of a centralized register of chemotherapy extravasation events.

There have been several reports of extravasation with the use of chest ports in breast cancer (22), in Ewing's sarcoma (23), and in acute lymphoblastic leukemia patients (24), in a pediatric patient receiving paclitaxel, likely for a solid tumor (25), and in a neonate requiring calcium chloride infusion through a central venous port (26).

In another study, 1,320 patients were included, with 794 in the PORT group and 526 in the PICC group. The overall complication rate was significantly lower in the PORT group ($p = 0.05$). Catheter malfunction occurred less frequently in the PORT group compared to the PICC group ($p < 0.01$). Moreover, thrombotic events were significantly less common in the PORT group ($p = 0.02$). No significant differences were observed between the two groups in terms of operative complications, catheter migration, malposition, extravasation, infections, or complications requiring catheter removal (27).

Nevertheless, to the best of our knowledge, this is the first report of a documented doxorubicin extravasation from a PICC-port in a patient with breast cancer.

The positioning technique of the arm port or PICC port changes the degree of safety in the use of the device. As well as reducing the incidence of catheter-related complications such as thrombosis and infection (1), the tunneling increases the chances of protection of the arm nerve bundle in case of overflow. In order to fulfill safe tunneling, it would be necessary to perform a feasibility assessment of the reservoir pocket prior to making the sterile field and after locating the venipuncture site using the real-time ultrasound guidance. In fact, the venipuncture site, tunnel placement, and pocket realization site should also be well identified to carry out the sterile field for performing the placement.

As placement and management of arm ports and PICC ports require the activation of a multidisciplinary team, so too does the management of extravasation complications require prompt multidisciplinary intervention. In most hospitals where chemotherapy is administered, the use of central venous catheters is now widespread to try to limit extravasation as much as possible.

The Italian Ministry of Health published the Raccomandazione 14 on the prevention of errors in treatments with antineoplastic drugs (28). In Raccomandazione 14, section 4.6.e., correct manipulation of venous access, it is recommended that for patients who have to perform a program of periodic infusions of antineoplastic drugs, implantation of central and peripheral venous catheters is considered useful to reduce the risk of extravasation. Shared procedures should be adopted among the operating units involved for the insertion of the medical device, and considering the relevance for the prevention of healthcare-related infections, it is essential to ensure proper management of venous access at all times. In any case, these medical devices are not sufficient to avoid the danger, so much so that Raccomandazione 14 itself calls for the preparation of a specific and updated procedure for the management of extravasation. This document should be immediately accessible to the health professionals involved and should indicate the first intervention measures. Therefore, it is essential to carry out training of all involved operators and to create a dedicated kit with identified antidotes for each type of chemotherapy drug. This kit should include at least cannula needles and needles of different calibers, water for injectable preparations, 10 ml vials of 25% sodium thiosulfate, hyaluronidase, vials of 99% dimethyl sulfoxide (DMSO), 1% hydrocortisone cream, sterile gauze and sterile syringes, hot and cold pack systems, and a black dermographic marker. It should be remembered that local heat treatments are used to reduce the local reaction and absorption of the infiltrate. Cooling the site (with ice packs) facilitates vasoconstriction, theoretically limiting drug dispersion.

In addition to specific antidotes, some general measures are recommended, including immediately stopping the infusion, taking

care to leave the cannula in place. This will, in fact, make it possible to aspirate as much of the extravasated drug as possible. If extravasation has involved a limb, it is advisable to elevate and immobilize it. In some cases, it may be necessary to consult a surgeon.

It would be recommended for every hospital managing oncology patients to produce local protocols that facilitate the treatment of extravasation when necessary. Collaboration and proper information for the patient and caregiver would facilitate the reduction of the magnitude of the complication of extravasation because it would allow faster secondary prophylaxis.

## 4 Patient perspective

Following the surgical and pharmacological treatments described above, the patient regained full limb functionality and was able to resume all regular activities. This favorable outcome was primarily due to the prompt and skilled intervention of the multidisciplinary team, which effectively minimized the serious complications typically associated with doxorubicin extravasation. Since the incident occurred during the first cycle of adjuvant therapy with doxorubicin and cyclophosphamide, the patient was deemed ineligible to continue with anthracycline. As a result, the treatment plan was modified, and she proceeded with the trastuzumab/Paclitaxel regimen for 12 cycles, followed by 6 additional cycles of trastuzumab monotherapy, completing a total of 18 administrations. The entire course of therapy was successfully completed.

## Data availability statement

The original contributions presented in the study are included in the article/supplementary material. Further inquiries can be directed to the corresponding author.

## Ethics statement

Written informed consent was obtained from the individual for the publication of any potentially identifiable images or data included in this article.

## Author contributions

CC: Data curation, Investigation, Writing – original draft, Writing – review & editing. SI: Visualization, Writing – original draft. GD: Project administration, Writing – original draft, Writing – review & editing. GC: Resources, Writing – review & editing. DG: Writing – review & editing. FG: Resources, Writing – review & editing. AL: Writing – review & editing. PN: Resources, Writing – review & editing. CR: Resources, Writing – review & editing. EV: Writing – review & editing. VD: Data curation, Writing – original draft, Writing – review & editing. GM: Conceptualization, Investigation, Supervision, Writing – original draft, Writing – review & editing.

## Funding

The author(s) declare that financial support was received for the research and/or publication of this article. Preparation of this report was supported by the Italian Ministry of Health (5 per mille 2021-2022, In LOVAE for BHyA study) to cover publication costs.

## Conflict of interest

The authors declare that the research was conducted in the absence of any commercial or financial relationships that could be construed as a potential conflict of interest.

## Generative AI statement

The author(s) declare that no Generative AI was used in the creation of this manuscript.

## Publisher's note

All claims expressed in this article are solely those of the authors and do not necessarily represent those of their affiliated organizations, or those of the publisher, the editors and the reviewers. Any product that may be evaluated in this article, or claim that may be made by its manufacturer, is not guaranteed or endorsed by the publisher.

## Author disclaimer

The authors affiliated to the IRCCS Istituto Tumori "Giovanni Paolo II," Bari are responsible for the views expressed in this article, which do not necessarily represent the Institute.

## References

1. Bertoglio S, Cafiero F, Meszaros P, Varaldo E, Blondeaux E, Molinelli C, et al. PICC-PORT totally implantable vascular access device in breast cancer patients undergoing chemotherapy. *J Vasc Access*. (2020) 21:460–6. doi: 10.1177/1129729819884482

2. Kim H, Kwon S, Son SM, Jeong E, Kim JY. Tailored approach to the choice of long-term vascular access in breast cancer patients. *PloS One*. (2021) 16:e0255004. doi: 10.1371/journal.pone.0255004

3. Chen N, Yang Q, Li YF, Guo Q, Huang Y, Peng JL. Cost-utility analysis of different venous access devices in breast cancer patients: a decision-based analysis model. *BMC Health Serv Res*. (2023) 23:497. doi: 10.1186/s12913-023-09517-1

4. Song X, Chen S, Dai Y, Sun Y, Lin X, He J, et al. A novel incision technique of a totally implanted venous access port in the upper arm for patients with breast cancer. *World J Surg Oncol*. (2023) 21:162. doi: 10.1186/s12957-023-03043-4

5. Tang TT, Liu L, Li CX, Li YT, Zhou T, Li HP, et al. Which is better for patients with breast cancer: totally implanted vascular access devices (TIVAD) or peripherally inserted central catheter (PICC)? *World J Surg*. (2019) 43:2245–9. doi: 10.1007/s00268-019-05022-x

6. Liu Y, Li LL, Xu L, Feng DD, Cao Y, Mao XY, et al. Comparison between arm port and chest port for optimal vascular access port in patients with breast cancer: A systematic review and meta-analysis. *BioMed Res Int*. (2020) 2020:9082924. doi: 10.1155/2020/9082924

7. Zhang P, Du J, Fan C, Mo X, Dong J, Fan Z, et al. Utility of totally implantable venous access ports in patients with breast cancer. *Breast J*. (2020) 26:333–4. doi: 10.1111/tbj.13595

8. Gorski LA, Hadaway L, Hagle ME, Broadhurst D, Clare S, Kleidon T, et al. Infusion therapy standards of practice, 8th edition. *J Infus Nurs*. (2021) 44:S1–S224. doi: 10.1097/NAN.0000000000000396

9. Xu H, Chen R, Jiang C, You S, Zhu Q, Li Y, et al. Implanting totally implantable venous access ports in the upper arm is feasible and safe for patients with early breast cancer. *J Vasc Access*. (2020) 21:609–14. doi: 10.1177/1129729819894461

10. Liu Y, Xu L, Jiang M, Chen B, Jing L, Zhang L, et al. Chinesization of the quality of life assessment, venous device-port, and its reliability and validity tests for patients with breast cancer. *J Vasc Access*. (2020) 21:983–9. doi: 10.1177/1129729820920528

11. Kamada S, Mosier R, El-Khalili T, Triantis S, Yang R. Scoping review of early intravenous infiltration and extravasation detection devices. *J InfusNurs*. (2023) 46:97–106. doi: 10.1097/NAN.0000000000000499

12. Pizzuti G, Cassani C, Bottazzi A, Ruggieri A, Della Valle A, Dionigi F, et al. Impact of totally implanted venous access port placement on body image in women with breast cancer. *J Vasc Access*. (2024) 25:673–6. doi: 10.1177/11297298221136330

13. Bertoglio S, Annetta MG, Brescia F, Emoli A, Fabiani F, Fino M, et al. A multicenter retrospective study on 4480 implanted PICC-ports: A GAVeCeLT project. *J Vasc Access*. (2022) 24(5):1114–20. doi: 10.1177/11297298211067683

14. Hadaway L. Infiltration and extravasation. *Am J Nurs*. (2007) 107:64–72. doi: 10.1097/01.NAJ.0000282299.03441.c7

15. Kreidieh FY, Moukadem HA, El Saghir NS. Overview, prevention and management of chemotherapy extravasation. *World J Clin Oncol*. (2016) 7:87–97. doi: 10.5306/wjco.v7.i1.87

16. Jackson-Rose J, Del Monte J, Groman A, Dial LS, Atwell L, Graham J, et al. Chemotherapy extravasation: establishing a national benchmark for incidence among cancer centers. *Clin J Oncol Nurs*. (2017) 21:438–45. doi: 10.1188/17.CJON.438-445

17. Schulmeister L. Extravasation management. *Semin Oncol Nurs*. (2007) 23:184–90. doi: 10.1016/j.soncn.2007.05.003

18. Cox RF. Managing skin damage induced by doxorubicin hydrochloride and daunorubicin hydrochloride. *Am J Hosp Pharm*. (1984) 41:2410–4. doi: 10.1093/ajhp/41.11.2410

19. Reeves D. Management of anthracycline extravasation injuries. *Ann Pharmacother*. (2007) 41:1238–42. doi: 10.1345/aph.1H700

20. Bowers DG Jr, Lynch JB. Adriamycin extravasation. *PlastReconstr Surg*. (1978) 61:86–92. doi: 10.1097/00006534-197801000-00015

21. Pérez Fidalgo JA, García Fabregat L, Cervantes A, Margulies A, Vidall C, Roila F, et al. Management of chemotherapy extravasation: ESMO–EONS clinical practice guidelines. *Eur J Oncol Nurs*. (2012) 16:528–34. doi: 10.1016/j.ejon.2012.09.004

22. Vasconcelos I, Schoenegg W. Massive breast necrosis after extravasation of a full anthracycline cycle. *BMJ Case Rep*. (2013) 2013:bcr2013201179. doi: 10.1136/bcr-2013-201179

23. Tom A, Joshi J, Golla MK, Lashkari HP. Doxorubicin extravasation from a port-a-cath into pleural space in a young girl: A case report and review of literature. *J Indian Assoc Pediatr Surg*. (2022) 27:648–51. doi: 10.4103/jiaps.jiaps_253_21

24. Nguyen M, Borders L, Wesolow JT, Greene J. Chemotherapy extravasation causing soft-tissue necrosis mimicking infection: A longitudinal case study. *Cureus*. (2024) 16:e55333. doi: 10.7759/cureus.55333

25. Lv DN, Xu HZ, Zheng LL, Chen LL, Ling Y, Ye AQ. Extravasation of chemotherapeutic drug from an implantable intravenous infusion port in a child: A case report. *World J Clin Cases*. (2021) 9:7840–4. doi: 10.12998/wjcc.v9.i26.7840

26. Thimmarayan G, Schmitz M, Guerrero J, Garcia X, Zhang S, Chau D. A neonate with aseptic cutaneous necrosis related to the migration of the proximal central venous catheter infusion port. *Paediatr Anaesth*. (2024) 34:86–8. doi: 10.1111/pan.14767

27. Capozzi VA, Monfardini L, Sozzi G, Armano G, Butera D, Scarpelli E, et al. Peripherally Inserted Central Venous Catheters (PICC) versus totally implantable venous access device (PORT) for chemotherapy administration: a meta-analysis on gynecological cancer patients. *Acta Biomed*. (2021) 92:e2021257. doi: 10.23750/abm.v92i5.11844

28. Ministero della Salute (Ministry of Health). Raccomandazione n. 14: Prevenzione degli errori in terapia con farmaci antineoplastici(2012). Available online at: www.salute.gov.it/imgs/C_17_pubblicazioni_1861_allegato.pdf (Accessed July 26, 2024).

frontiers | Frontiers in Oncology

TYPE Original Research
PUBLISHED 01 August 2025
DOI 10.3389/fonc.2025.1622854



OPEN ACCESS

EDITED BY
Raquel Diaz,
University of Genova, Italy

REVIEWED BY
Marco Cavaco,
Gulbenkian Institute of Science (IGC), Portugal
Harika Nagandla,
Houston Methodist Research Institute, United States

*CORRESPONDENCE
Qing Zhai
zhaiqing63@126.com
Qiong Du
dujoan-88@163.com

†These authors have contributed equally to this work

RECEIVED 04 May 2025
ACCEPTED 21 July 2025
PUBLISHED 01 August 2025

CITATION
Ye X, Wang L, Liu W, Wang M, Guo Z, Shan H, Zhai Q and Du Q (2025) Efficacy and safety of biosimilar trastuzumab (HLX02) in patients with HER2-positive advanced breast cancer: a retrospective real-world analysis. *Front. Oncol.* 15:1622854. doi: 10.3389/fonc.2025.1622854



# Efficacy and safety of biosimilar trastuzumab (HLX02) in patients with HER2-positive advanced breast cancer: a retrospective real-world analysis

Xuan Ye[1,2†], Linlin Wang[3†], Wensheng Liu[1,2], Mengmeng Wang[1,2], Zihan Guo[1,2], Han Shan[1,2], Qing Zhai[1,2*] and Qiong Du[1,2*]

[1]Department of Pharmacy, Fudan University Shanghai Cancer Center, Shanghai, China, [2]Department of Oncology, Shanghai Medical College of Fudan University, Shanghai, China, [3]Department of Pharmacy, Fudan University Shanghai Cancer Center Xiamen Hospital, Xiamen, China

**Background:** HLX02 is the first China-manufactured trastuzumab biosimilar. Few data are currently available about HLX02 in clinical practice. This study was designed to evaluate the real-world safety and efficacy of HLX02 in patients with HER2-positive metastatic breast cancer (MBC), as well as assessed the effectiveness of switching from trastuzumab originator (Herceptin®) to HLX02 during treatment.

**Methods:** Between April 2021 and October 2022, all patients with HER-2-positive MBC who received at least one cycle of HLX02 at Fudan University Shanghai Cancer Center were included in a retrospective analysis. Patients were divided into two groups: the naïve group (patients treated with HLX02 from the beginning) and the switched group (patients who switched from Herceptin® to HLX02). Efficacy evaluation and adverse events were compared between the two groups.

**Results:** A total of 124 eligible patients were finally included, with 80 patients (64.5%) in the naïve group, 44 patients (35.5%) in the switched group. The follow-up ranged from 0.7 to 40.2 months, the effectiveness rates were 57.5% in the naïve group and 54.5% in the switched group, respectively (P=0.751). The estimated median progression-free survival (PFS) were 13.70 (95% CI: 8.634–18.766) months and 14.70 (95% CI: 6.684–22.716) months in the naive and switched groups, respectively (P=0.192). Multivariate cox regression analysis suggested that brain metastasis and the current number of treatment lines were independent predictors of MBC PFS. Compared with first-line treatment, second-line treatment and third- or later-line treatment increased the disease risk by 2.095 times (95% CI: 1.043-4.210, P=0.038) and 3.035 times (95% CI:1.751-5.262, P<0.001), respectively. The incidence and distribution of treatment-emergent adverse events (TEAEs) occurrence between the two groups were relatively similar, with no significant statistical difference.

**Conclusions:** HLX02 demonstrated favorable efficacy and safety in real-world practice comparable to those observed in previous HLX02 studies. Switching between trastuzumab originator and biosimilar for MBC treatment had no impact on efficacy and did not increase safety risks.

KEYWORDS

**HLX02, trastuzumab, biosimilar, metastatic breast cancer, real-world study**

# 1 Introduction

Breast cancer remains one of the most common malignancies worldwide. In 2022, 2.3 million women were diagnosed with breast cancer, and 670,000 women died from the disease (https://www.who.int/news-room/fact-sheets/detail/breast-cancer).

Human epidermal growth factor receptor (HER2), a growth factor receptor gene, women with breast cancers that overexpress HER2 have an aggressive form of the disease, with significantly shortened disease-free survival and overall survival (1). Trastuzumab (Herceptin®, Genentech/Roche, Inc.), a humanized monoclonal antibody directed against the extracellular domain of HER2, specifically acts on HER2 on cancer cell surfaces and has significantly improved patient prognosis, was approved for treatment of HER2-positive breast cancer and for the treatment of HER2-positive metastatic gastric or gastroesophageal junction adenocarcinoma (2). However, its high cost makes it unaffordable for patients in developing countries such as China (3, 4).

The main advantages of biosimilars were cost savings and lower prices, it is essential to provide oncologists with comprehensive data on the safety and effect, and real-world evidence of biosimilars (5). Biosimilars are developed by different manufacturers, replicating the complex structures and maintaining similar therapeutic efficacy and safety profiles as the original innovator drugs is important (6). At present, many countries are committed to the development of trastuzumab biosimilars, comparing the biosimilars with trastuzumab originator (Herceptin®) (7–12). HLX02 (Zercepac®, Henlius, Inc.), launched in China in 2020, was the first China-manufactured trastuzumab biosimilar (13–16). It is more cost-effective than Herceptin® in China based on willingness-to-pay thresholds (17). A multicenter real-world has shown HLX02 and Herceptin® to have equivalent efficacy and adverse events in HER-2-positive breast cancer (18). However, real-world data on the safety and efficacy of HLX02 still remain limited, especially regarding switching from Herceptin® to HLX02.

This study aimed to evaluate HLX02's efficacy and safety based in HER2-positive metastatic breast cancer (MBC), and assess the effectiveness of switching from Herceptin® to HLX02 during treatment. It seeks to provide evidence for the clinical substitution of biosimilars in China.

# 2 Materials and methods

## 2.1 Study design and patients

This study was a retrospective, single-center, non-intervention real-world study. Patients who started therapy naïve to HLX02 and who switched from Herceptin® were collected at Fudan University Shanghai Cancer Center between April 2021 to October 2022. The major inclusion criteria were (a) patients with a pathological diagnosis of HER-2-positive metastatic breast cancer (MBC), HER2 positivity was defined as immunohistochemistry (ICH) 3+ or 2+/fluorescence *in situ* hybridization (FISH) amplification;(b) patients older than 18 years; (c) Eastern Cooperative Oncology Group (ECOG) performance score 0–2. The main exclusion criteria were (a) patients with incomplete medical records, with missing values exceeding 30%; (b) patients with prior or concurrent malignancies (other than thyroid cancer or cancer *in situ* of other organs).

This study was approved by the Ethics Committee of Fudan University Shanghai Cancer Center (No.2021-121-2424).

## 2.2 Data collection

Data variables collected from the patient's medical records included the following categories: (a) demographic and clinical characteristics, such as sex, age, menopausal status, estrogen receptor status, Ki67 level, metastasis, comorbidities and ECOG performance score; (b) drugs and outcomes, such as trastuzumab utilization patterns, efficacy evaluation; (c) abnormal clinical or laboratory findings, such as nausea, diarrhea, leukopenia, lymphopenia, thrombocytopenia etc. Data and follow-up records were updated as of September 30, 2024.

## 2.3 Treatment and dosage information

In salvage treatment of MBC, the initial loading dose of HLX02 or Herceptin® was 8mg/kg, and the maintenance dose is 6mg/kg once a time, and it is administered once every 3 weeks. The salvage

treatment regimen of HLX02 combined with other anti-tumor drugs was determined by the clinical doctor. The study did not intervene.

## 2.4 Assessments and definition of outcomes

Efficacy endpoints were assessed based on imaging reports following Response Evaluation Criteria in Solid Tumors (RECIST 1.1 version). The outcomes were effectiveness rate and the progression-free survival (PFS). In HLX02-naïve patients, if the best overall response of complete response (CR) or partial response (PR) was achieved, HLX02 was considered "effective". In patients who switched from Herceptin® to HLX02, if the best overall response remains the same as before the switch or improved somewhat, HLX02 was considered "effective" (19). PFS was defined as the time from initiation of HLX02 or Herceptin® treatment until disease progression, including any recurrence or death from any cause.

Safety endpoints were assessed and grated based on National Cancer Institute Common Terminology Criteria for Adverse Events v5.0 grading. The evaluation of adverse events included general adverse events and adverse event of special interest. The predefined adverse event of special interest was cardiotoxicity (such as palpitation, ventricular arrhythmia and reduced left ventricular function) and infusion-related reaction.

## 2.5 Statistical analysis

Normally distributed continuous variables were expressed as mean ± standard deviation, and were calculated by an independent samples t test. Non-normally distributed variables were summarized as median values, range, and were compared by Mann–Whitney U test. Differences between categorical variables were assessed using the chi-square test or Fisher's exact test. The Kaplan-Meier method was used for PFS analysis, and the log-rank test was used to determine statistically significant variables. Univariate and multivariate analyses were performed with the Cox proportional hazards regression model. Hazard ratios (HR) and 95% confidence interval (95% CI) were determined. A two-sided P-value<0.05 was considered statistically significant. Survival analysis was performed using the Kaplan-Meier method, and comparisons between groups were conducted with the log-rank test. A p-value of less than 0.05 was considered statistically significant. Statistical plotting was performed using GraphPad Prism software (version 10.1.2, GraphPad Software, San Diego, CA, USA). Statistical analyses were performed using SPSS software (version 25.0, SPSS Inc., Chicago, IL, USA).

# 3 Result

## 3.1 Patient characteristics

From April 2021 to October 2022, 359 patients received at least one dose of HLX02 were screened (Figure 1). Among them, 124

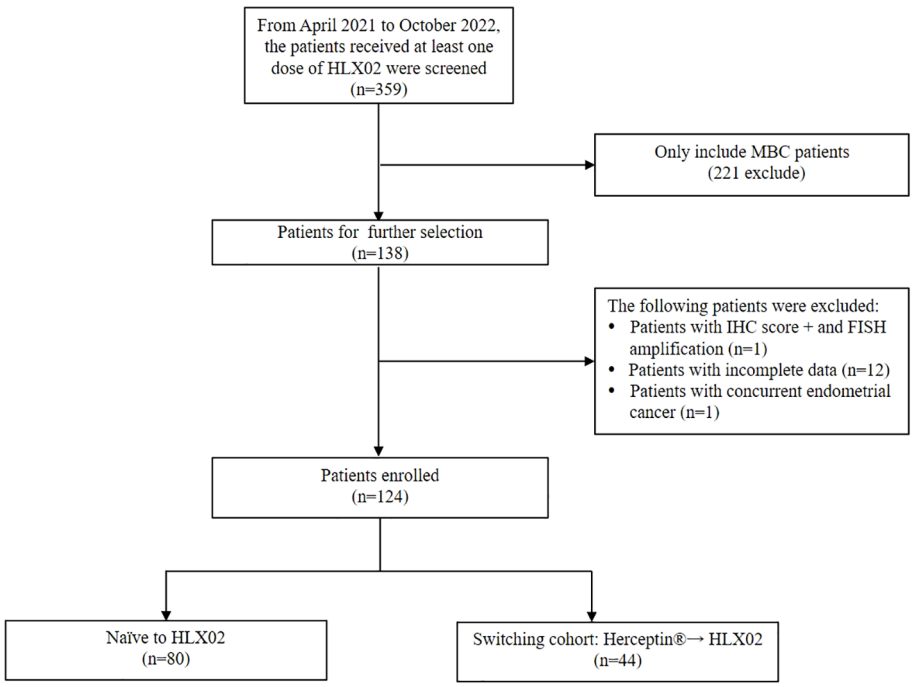


FIGURE 1
Flow-chart of patient inclusion.

MBC patients were included in our study. Patients were classified into two groups according to their prior trastuzumab treatment status: 80 patients (64.5%) were naïve to HLX02, 44 patients (35.5%) switched from the originator Herceptin® to HLX02, respectively. In the switched group, the median exposure time of Herceptin® and HLX02 was 5.4 months (range, 0.8-51.3) and 5.1 months (range, 0.8-35), respectively. The median cycles of Herceptin® and HLX02 were 7 and 7, respectively.

The demographics and clinical characteristics of the population are presented in Tables 1 and 2. All patients were female, the median age was 53 (range, 27-79) years. 78 (62.9%) patients were postmenopausal, 58 (46.8%) patients were ER positive, 46 (37.1%) patients were PR positive. Among them, 77 patients (62.1%) had 1 or 2 sites metastases, 47 patients (37.9%) had 3 or more sites metastases. 76 patients (61.3%), 16 patients (12.9%), 32 patients (25.8%) had who had previously received first-line, second-line, and third- or later-line treatments, respectively. The trastuzumab, pertuzumab and taxanes (THP) was the most commonly used dual-target therapy regimen. There were no significant statistical differences in demographics and clinical characteristic between the naïve group and switched group.

## 3.2 Efficacy results

The follow-up ranged from 0.7 to 40.2 months, based on the RECISTv1.1 criteria for clinical efficacy evaluation, no patients achieved CR, 73 patients (58.9%) achieved the best response of PR, 44 patients (35.5%) achieved SD. Among them, 7 patients (5.6%) had PD and one patient eventually died due to disease progression. HLX02 was rated as "effective" in 46 (57.5%) of naïve patients and in 24 (54.5%) of switched patients (P=0.751) (Table 3). The median PFS is shown in Figure 2, which was 14.2 months (95% CI: 10.5 - 17.9). The results of univariate analysis indicated that the number of metastases, brain metastasis, the number of current treatment lines (second-line vs. first-line, third- or later-line vs. first-line), and treatment regimens (TCbHP vs. THP) were the influencing factors for the survival period of MBC. However, trastuzumab switching during treatment had no impact on the survival period, as shown in Table 4. Multivariate Cox analysis suggested that brain metastasis and the number of current treatment lines were the independent predictors of MBC PFS. Compared with first-line treatment, second-line treatment and third- or later-line above treatment increased the disease risk by

TABLE 1 Demographic and clinical characteristics of patients.

| Characteristics | Total (n=124) | Naïve group (n=80) | Switched group (n=44) | P |
|---|---|---|---|---|
| Age, n (%) | | | | |
| <53y | 59 (47.6) | 35 (43.8) | 24 (54.5) | 0.191 |
| ≥53y | 65 (52.4) | 45 (56.2) | 20 (45.5) | |
| Menopausal status, n (%) | | | | 0.298 |
| Premenopausal | 46 (37.1) | 27 (33.8) | 19 (43.2) | |
| Postmenopausal | 78 (62.9) | 53 (66.2) | 25 (56.8) | |
| ER status, n (%) | | | | 0.239 |
| Positive | 58 (46.8) | 41 (50.6) | 17 (39.5) | |
| Negative | 66 (53.2) | 40 (49.4) | 26 (60.5) | |
| PR status, n (%) | | | | 0.249 |
| Positive | 46 (37.1) | 33 (40.7) | 13 (30.2) | |
| Negative | 78 (62.9) | 48 (59.3) | 30 (69.8) | |
| Ki-67 | | | | 0.745 |
| ≦14% | 11 (8.9) | 8 (10.0) | 3 (6.8) | |
| >14% | 113 (91.1) | 72 (90.0) | 41 (93.2) | |
| HER-2 status, n (%) | | | | 0.087 |
| IHC 3+ | 90 (72.6) | 54 (67.5) | 36 (81.8) | |
| IHC 2+ and FISH amplification | 34 (27.4) | 26 (32.5) | 8 (18.2) | |

*(Continued)*

TABLE 1 Continued

| Characteristics | Total (n=124) | Naïve group (n=80) | Switched group (n=44) | P |
|---|---|---|---|---|
| Site of metastatic disease, n (%) | | | | |
| Brain | 25 (20.2) | 14 (17.5) | 11 (25.0) | 0.319 |
| Lung | 55 (44.4) | 39 (48.8) | 16 (36.4) | 0.184 |
| Bone | 63 (50.8) | 38 (47.5) | 25 (56.8) | 0.321 |
| Liver | 40 (32.3) | 30 (37.5) | 10 (22.7) | 0.092 |
| Distant lymph node | 71 (57.3) | 42 (52.5) | 29 (65.9) | 0.149 |
| Number of metastases, n (%) | | | | 0.516 |
| 1-2 | 77 (62.1) | 48 (60.0) | 29 (65.9) | |
| ≥3 | 47 (37.9) | 32 (40.0) | 15 (34.1) | |
| Comorbidity, n (%) | | | | 0.632 |
| No | 84 (67.7) | 53 (66.2) | 31 (70.5) | |
| Yes | 40 (32.3) | 27 (33.8) | 13 (29.5) | |
| Baseline electrocardiogram, n (%) | | | | 0.405 |
| Normal | 86 (69.4) | 54 (73.0) | 32 (80.0) | |
| Abnormal | 28 (22.6) | 20 (27.0) | 8 (20.0) | |
| Missing | 10 (8.1) | / | / | |
| ECOG, n (%) | | | | 0.137 |
| 0 | 17 (13.7) | 9 (11.2) | 8 (18.2) | |
| 1 | 97 (78.2) | 62 (77.5) | 35 (79.5) | |
| 2 | 10 (8.1) | 9 (11.2) | 1 (2.3) | |
| LVEF, % | 66.5 ± 3.67 | 67.1 ± 3.66 | 65.9 ± 3.62 | 0.142 |

PR, progesterone receptor; ER, estrogen receptor; ECOG, eastern cooperative oncology group; LVEF, left ventricular ejection fraction.

2.095 times (95% CI: 1.043-4.210, P = 0.038) and 3.035 times (95% CI: 1.751-5.262, P < 0.001), respectively.

## 3.3 Safety

During the study period, a total of 375 treatment-emergent adverse events (TEAEs) were occurred, involving 112 patients (90.3%). The severity of most TEAEs was grade 1-2, and 36 patients (29.0%) occurred 120 episodes of grade 3–4 TEAEs. As shown in Table 5, the incidence of any-grade TEAEs between the naïve group and the switched group were similar, and there were no significant differences (72 patients [90.0%] vs. 40 patients [90.9%], P=0.870). The incidence of grade 3–4 TEAEs was higher in the naïve group than that in the switched group, but the difference was not statistically significant (26 patients [32.5%] vs. 10 patients [22.7%], P=0.251). The most common (≥10%) TEAEs were hematological toxicity and liver function abnormalities, exhibiting anemia (51.2% vs 65.9%, P=0.115), increased ALT (37.5% vs 36.4%, P=0.900), leukopenia (31.2% vs 18.2%, P=0.115), increased AST (28.8% vs 29.5%, P=0.926), neutropenia (25.0% vs 20.5%, P=0.660), but there was no significant difference between the two groups. One death case was occurred due to disease progression, but it was recorded as not related to HLX02. No new safety signals detected during the real-world practice.

It is worth noting that infusion-related reaction and cardiotoxicity were reported, a total of 12 patients developed infusion-related reactions, with 7 patients (8.8%) in the naïve group, and 5 patients (11.4%) in the switched group (P=0.753). A total of 5 patients reported cardiotoxicity, with 2 patients (2.5%) in the naïve group and 3 patients (6.8%) in the switched group, and there was no significant difference between the two groups (P=0.346).

# 4 Discussion

This study evaluated the efficacy and safety of HLX02 in patients with MBC based on real-world clinical data, and provided evidence for the effectiveness of trastuzumab switching during treatment.

As the first China-manufactured trastuzumab biosimilar, HLX02 is approved in Europe (EU) and China, Zhou et al. confirmed that HLX02 is bioequivalent to the originator

TABLE 2 Treatment characteristics of patients.

| Characteristics | Total (n=124) | Naïve group (n=80) | Switched group (n=44) | P |
|---|---|---|---|---|
| Current number of treatment lines, n (%) | | | | 0.600 |
| 1 | 76 (61.3) | 47 (58.8) | 29 (65.9) | |
| 2 | 16 (12.9) | 10 (12.5) | 6 (13.6) | |
| ≥3 | 32 (25.8) | 23 (28.8) | 9 (20.5) | |
| Target therapy, n (%) | | | | 0.688 |
| Single-target | 18 (14.5) | 11 (13.8) | 7 (15.9) | |
| Trastuzumab + Pertuzumab | 93 (75.0) | 59 (73.8) | 34 (77.3) | |
| Trastuzumab + Pyrotinib | 13 (10.5) | 10 (12.5) | 3 (6.8) | |
| Combined chemotherapy regimens, n (%) | | | | 0.254 |
| THP | 50 (40.3) | 27 (33.8) | 23 (52.3) | |
| TCbHP | 22 (17.7) | 17 (21.2) | 5 (11.4) | |
| HP+others | 20 (16.1) | 14 (17.5) | 6 (13.6) | |
| H+Pyrotinib+Others | 14 (11.3) | 11 (13.8) | 3 (6.8) | |
| H+Others | 18 (14.5) | 11 (13.8) | 7 (15.9) | |

T, taxanes, including albumin-bound paclitaxel and paclitaxel; H, trastuzumab; P, pertuzumab; Cb, carboplatin.

Herceptin®, with similar safety and immunogenicity profiles (16). Xu et al. shows that the objective response rate (ORR) at week 24 (71.3%), PFS (11.7 months), and OS (not reached) observed in the HLX02 treatment group (18). In addition, after a median follow-up duration of 35.0 months, 39.5% patients had died in the HLX02 group, median overall survival (OS) was 37.3 months, with a 3-year OS rate of 57.5%. Median PFS at this long-term follow-up assessment was 11.7 (95% CI 11.5, 12.1) months for the HLX02 group (15).

However, there are few studies on the real-world clinical application of HLX02 in the treatment of HER-2 positive MBC, especially in combination with other antitumor agents, such as pertuzumab. *Deng* et al. demonstrated that 32 patients (86.5%) achieved CR, 2 patients (5.4%) achieved PR in the HLX02 group (20). However, as the majority (6/96, 93.8%) of the included patients were in the early stage, this study has certain limitations for MBC. Our study focused on patients with MBC, and the results showed that 73 patients (58.9%) achieved PR, but no patients achieved CR. After a median follow-up of 0.7-40.2 month, the median PFS for HLX02 first-line treatment was 18.8 months, and the median PFS for second-line treatment was 10.3 months, the median PFS of third- or later-line treatment was 7.3 months. In previous phase III studies, the median PFS of trastuzumab or trastuzumab biosimilar combined with taxanes in first-line treatment of MBC was 10.6-12.8 months (8, 12, 18, 21, 22). At present, there are few efficacy data about second-line or later treatment of HLX02 in MBC. In the Phase II clinical trial of HLX02, 45 patients with HER-2 positive MBC were enrolled to receive HLX02, pertuzumab and physician selection chemotherapy, 12 patients (26.7%) were treated with second-line therapy, 33 patients (73.3%) were treated with third- or later-line treatment (23). Median follow-up was 1.2-43.9 months, the median PFS for second-line treatment was 6.26 months (range: 0-18.9), and the median PFS for third- or later-line treatment was 7.6 months (range: 4.8-10.3) (23). The results of our study were slightly different from the Phase II/III trial. The possible reasons are as follows: (1) the efficacy results might be affected by the characteristics of the enrolled patients, previous treatment experiences, and methodological factors (such as dosing regimens and efficacy assessment); (2) in the treatment regimen of the phase III trial, pertuzumab was not added. However, in real-world

TABLE 3 Efficacy outcomes of two groups.

| Outcome Parameter | Total (n=124) | Naïve group (n=80) | Switched group (n=44) |
|---|---|---|---|
| Best overall response, n (%) | | | |
| PR | 73 (58.9) | 46 (57.5) | 27 (61.4) |
| SD | 44 (35.5) | 28 (35.0) | 16 (36.4) |
| PD | 7 (5.6) | 6 (7.5) | 1 (2.3) |
| Effectiveness Rate | 70 (56.5) | 46 (57.5) | 24 (54.5)* |
| 95% exact CI | 50.1%-67.7% | 46.4%-68.6% | 46.4%-76.3% |
| Estimated median PFS (95% CI) | 14.2 (10.5-17.9) | 13.7 (8.63-18.77) | 14.7 (6.68-22.72) |

PR, partial response; SD, stable disease; PD, progressive disease.
*HLX02 was considered to be "ineffective" for 3 patients who reported disease progression after switched to HLX02.

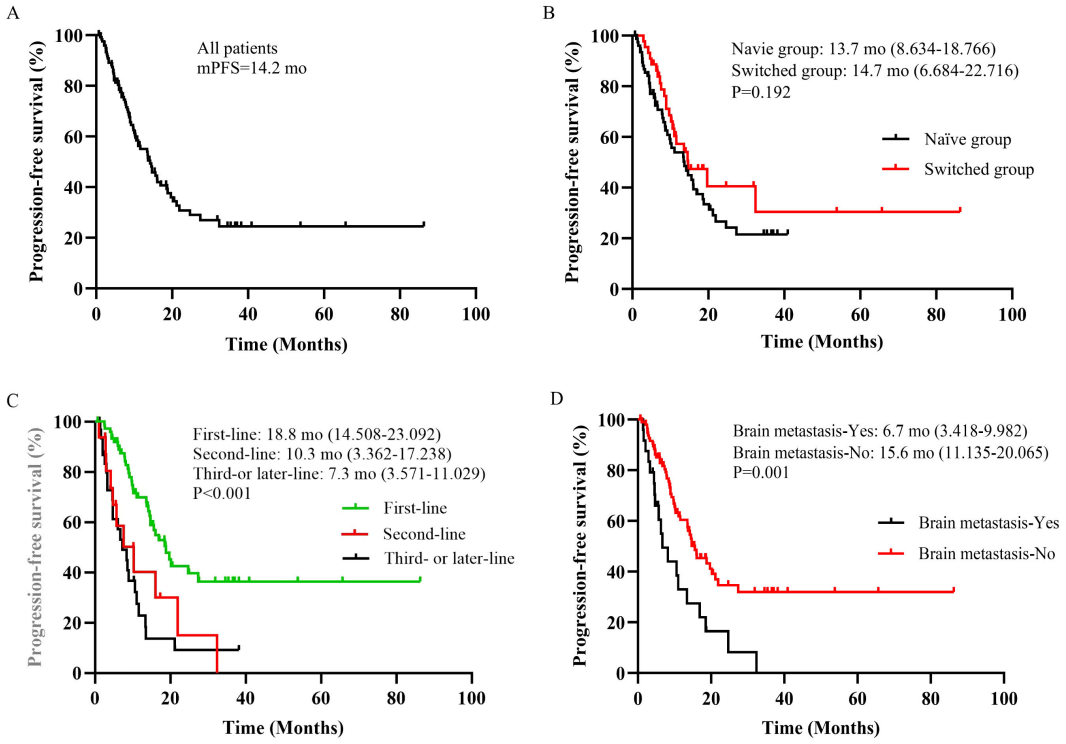


FIGURE 2
**(A)** Overall cohort. **(B)** Patients stratified by trastuzumab treatment status. **(C)** Patients stratified by current number of treatment lines. **(D)** Patients stratified by brain metastasis. mo, months.

practice, more than 75% of patients received "trastuzumab plus pertuzumab" dual-targeted therapy, which to some extent increased the PFS.

In this study, 44 patients (35.5%) MBC patients experienced switching between trastuzumab originator and biosimilar. At present, the available research data are limited regarding whether the switching between the originator and biosimilar would have an impact on efficacy and safety. The LILAC study reported that among 342 HER-2 positive EBC patients who received neoadjuvant Herceptin® treatment, 171 patients switched to trastuzumab biosimilar ABP 980 during the postoperative adjuvant treatment (24). In terms of prognosis, there was no significant statistical difference in disease progression, recurrence or mortality between the switched group and the non-switched group (HR = 0.48, 95% CI: 0.181 - 1.292); in terms of safety, there was no significant statistical difference in the overall AE incidence (26.3% vs. 22.8%, P > 0.05) and the incidence of severe AEs (7.6% vs. 6.4%, P > 0.05) between the two groups after a follow-up of 12.0 months; in terms of immunogenicity, the positive rate of anti-drug antibodies in the switched group was 1.2%, which was higher than 0.6% in the non-switched group (24). Overall, after the one-way switch (originator→biosimilar), the efficacy, safety and immunogenicity indicators of HER-2 positive breast cancer patients did not undergo significant changes. We also conducted a preliminary exploration on the impact of trastuzumab switching on outcome indicators during the research. No significant differences were observed in effectiveness rates for patients in the naïve group or in the switched group. Furthermore, the univariate analysis showed that trastuzumab switching had no impact on PFS (P=0.195).

One strength of our study is that it included the heterogeneous characteristics of clinical practice, that is more representative of entire patient population than the carefully selected individuals in clinical trials. A network meta-analysis evaluated efficacy and serious adverse reactions among various trastuzumab biosimilars and trastuzumab originator. The cumulative ranking curve (SUCRA) probability indicated that the ORR from best to worst was CT-P6, Herceptin, HLX02, PF-05280014, R-TPR-016, BCD-022, MYL-1401O, SB3. There was no statistical difference in both ORR and pathological complete response (pCR) of various trastuzumab biosimilars and Herceptin except SB3 (25). According to the result, HLX02 performs might be an optional trastuzumab biosimilar compared with others in China.

The SUCRA probability indicated that severe AEs from best to worst was MYL-1401O, Herceptin, PF-05280014, SB3, HLX02, BCD-22, CT-P6 (25). Our study showed that the safety profiles were comparable with the known safety profiles of trastuzumab in patients with breast cancer (18, 20). Anemia, increased ALT and AST, leukopenia, neutropenia, increased alkaline phosphatase and thrombocytopenia were the most common TEAEs identified in this study. These events were also consistent with previous studies of trastuzumab biosimilars (8, 12, 19, 20). There were no notable differences between the naïve group and the switched group regarding the type, incidence, or severity of TEAEs. Trastuzumab

TABLE 4 Univariate and multivariate analysis for PFS in MBC patients.

| Variables | HR | 95%CI | P |
|---|---|---|---|
| **Univariate analysis** | | | |
| Age (≥53y vs. <53y) | 1.338 | 0.831-2.155 | 0.231 |
| Menopausal status (Postmenopausal vs. Premenopausal) | 1.137 | 0.692-1.868 | 0.612 |
| ER (Negative vs. Positive) | 0.949 | 0.589-1.528 | 0.829 |
| PR (Negative vs. Positive) | 1.056 | 0.643-1.734 | 0.830 |
| Ki-67 (≦14% vs. >14%) | 0.861 | 0.372-1.990 | 0.726 |
| HER-2 status (IHC 3+ vs. IHC 2+ and FISH amplification) | 1.346 | 0.811-2.234 | 0.251 |
| Brain metastasis (Yes vs. No) | 2.354 | 1.383-4.008 | **0.002** |
| Lung metastasis (Yes vs. No) | 1.198 | 0.746-1.926 | 0.455 |
| Bone metastasis (Yes vs. No) | 1.236 | 0.770-1.984 | 0.381 |
| Liver metastasis (Yes vs. No) | 1.154 | 0.695-1.916 | 0.580 |
| Metastatic site number (≥3 vs. 1~2) | 2.372 | 1.470-3.829 | **<0.001** |
| Comorbidity (Yes vs. No) | 1.138 | 0.689-1.880 | 0.613 |
| **ECOG score** | | | |
| (1 vs 0) | 2.074 | 0.941-4.574 | 0.071 |
| (2 vs 0) | 2.593 | 0.870-7.729 | 0.087 |
| **Number of current treatment lines** | | | |
| (Second-line vs. First-line) | 2.431 | 1.232-4.798 | **0.010** |
| (Third-or later-line vs. First-line) | 3.345 | 1.955-5.723 | **<0.001** |
| **Treatment regimen** | | | |
| (TCbHP vs. THP) | 2.072 | 1.086-3.952 | **0.027** |
| (HP+Others vs THP) | 1.274 | 0.593-2.736 | 0.534 |
| (H+Others vs THP) | 1.437 | 0.701-2.944 | 0.322 |
| (H+Pyrotinib vs THP) | 1.362 | 0.629-2.950 | 0.433 |
| **Trastuzumab treatment status** | | | |
| (Naïve group vs. Switched group) | 0.715 | 0.430-1.188 | 0.195 |
| **Multivariate analysis** | | | |
| Brain metastasis (Yes vs. No) | 1.827 | 1.052-3.172 | **0.032** |
| **Number of current treatment lines** | | | |
| (Second-line vs. First-line) | 2.095 | 1.043-4.210 | **0.038** |
| (Third- or later-line vs. First-line) | 3.035 | 1.751-5.262 | **<0.001** |

PR, progesterone receptor; ER, estrogen receptor; PFS, progression-free survival; HR, hazard ratio; CI, confidence interval; T, taxanes, including albumin-bound paclitaxel and paclitaxel; H, trastuzumab; P, pertuzumab; Cb, carboplatin.
Bold values indicate P-value < 0.05, representing statistically significant differences.

has been reported in most research as related to increased risks of cardiac toxicity (26, 27). Thus, cardiotoxicity in the two groups were carefully assessed. The frequency of related events was low and similar between the two groups (2 vs. 3 patients), and without significant differences in this study.

The irrational use can be found both in resource-abundant regions and in resource-limited regions in China. A study showed the patients who lived in areas with a relatively high gross domestic product were more likely to receive trastuzumab originator than those in areas with a lower gross domestic product (28). In developing countries such as China, where biopharmaceuticals often limit patient access due to high costs, biosimilars provide an additional treatment option for enabling patient access, the introduction of biosimilars into clinical practice is necessary to

TABLE 5 Summary of adverse events.

| Adverse Events | Navie group (n=80) | Switched group (n=44) | P |
|---|---|---|---|
| TEAEs, n(%) | | | |
| Any grade | 72 (90.0) | 40 (90.9) | 0.870 |
| Grade 3-4 | 26 (32.5) | 10 (22.7) | 0.251 |
| AEs occurred in ≥10% patients in either group, n(%) | | | |
| Anemia | 41 (51.2) | 29 (65.9) | 0.115 |
| Increased ALT | 30 (37.5) | 16 (36.4) | 0.900 |
| Leukopenia | 25 (31.2) | 8 (18.2) | 0.115 |
| Increased AST | 23 (28.8) | 13 (29.5) | 0.926 |
| Neutropenia | 20 (25.0) | 9 (20.5) | 0.660 |
| Increased alkaline phosphatase | 13 (16.2) | 11 (25.0) | 0.238 |
| Thrombocytopenia | 9 (11.2) | 3 (6.8) | 0.536 |
| Hyperuricemia | 8 (10.0) | 10 (22.7) | 0.054 |
| Fatigue | 7 (8.8) | 3 (6.8) | 1.000 |
| Diarrhea | 8 (10.0) | 2 (4.5) | 0.492 |
| Decreased appetite | 5 (6.2) | 2 (4.5) | 1.000 |
| Hyperbilirubinemia | 5 (6.2) | 5 (11.4) | 0.324 |
| AEs of special interest occurring in ≥ 5% of patients, n(%) | | | |
| Infusion-related reaction | 7(8.8) | 5(11.4) | 0.753 |
| Cardiotoxic effects | 2(2.5) | 3(6.8) | 0.346 |

TEAE treatment-emergent adverse event; ALT, alanine aminotransferase, AST, aspartate aminotransferase.

sustainably reduce the healthcare burden. Treatment with biosimilars is not only a direct cost-saving approach, but also drives the clinical practice of new therapies and drugs (29). This study offers reliable real-world evidence for assessing the quality and safety of HLX02 as a crucial foundation for future evaluations. Switching to different trastuzumab combinations regimens for cancer treatment had no effects on PFS and did not increase safety risks. These real-world findings could help to optimize HER-2 therapy in advanced breast cancer, especially in regions with limited access to these expensive targeted drugs.

This study has several limitations. Firstly, as it utilizes retrospective real-world data with limited sample of patients using HLX02. Limited sample may lead to low statistical power of the association analysis, so it is necessary to expand the sample size and conduct a large-scale clinical trial with multi-center cooperation. Future studies with larger sample sizes also could validate stratified analysis based on the co-administered drugs, such as adjunctive medications, target therapy or combined with different chemotherapy. Secondly, patients are recruited from single centers and only included Chinese populations. As such, the findings are probably representative in this region, may not be generalizable globally. Finally, the patients received trastuzumab in combination with other drugs during the treatment, it may interfere whether some adverse events were caused by trastuzumab.

## 5 Conclusion

This study provided the real-world use of trastuzumab originator and its biosimilars (HLX02), the safety and efficacy of biosimilars were confirmed. These findings offered valuable information for implementation of switching from trastuzumab originator to a biosimilar.

## Data availability statement

The original contributions presented in the study are included in the article/supplementary material. Further inquiries can be directed to the corresponding authors.

## Ethics statement

This study was approved by the Ethics Committee of Fudan University Shanghai Cancer Center (No.2021-121-2424). The studies were conducted in accordance with the local legislation and institutional requirements. Without intervention in the patients' treatment, this study is a retrospective analysis.

## Author contributions

XY: Supervision, Writing – review & editing, Writing – original draft, Funding acquisition, Formal analysis, Software, Data curation, Project administration, Resources, Validation, Methodology, Conceptualization. LW: Writing – original draft, Formal analysis, Writing – review & editing, Software. WL: Software, Visualization, Data curation, Formal analysis, Resources, Writing – review & editing. MW: Supervision, Resources, Writing – review & editing, Project administration, Validation. ZG: Conceptualization, Resources, Project administration, Writing – review & editing. HS: Investigation, Writing – review & editing, Formal analysis. QZ: Funding acquisition, Resources, Validation, Project administration, Conceptualization, Visualization, Supervision, Writing – review & editing. QD: Writing – review & editing, Supervision, Funding acquisition.

## Funding

The author(s) declare that financial support was received for the research and/or publication of this article. QZ was

supported by the Clinical Research Plan of SHDC (SHDC2020CR3085B).

## Acknowledgments

We appreciated all patients who contributed to this work.

## Conflict of interest

The authors declare that the research was conducted in the absence of any commercial or financial relationships that could be construed as a potential conflict of interest.

## Generative AI statement

The author(s) declare that no Generative AI was used in the creation of this manuscript.

## Publisher's note

All claims expressed in this article are solely those of the authors and do not necessarily represent those of their affiliated organizations, or those of the publisher, the editors and the reviewers. Any product that may be evaluated in this article, or claim that may be made by its manufacturer, is not guaranteed or endorsed by the publisher.

## References

1. Chia S, Norris B, Speers C, Cheang M, Gilks B, Gown AM, et al. Human epidermal growth factor receptor 2 overexpression as a prognostic factor in a large tissue microarray series of node-negative breast cancers. *J Clin Oncol*. (2008) 26:5697–704. doi: 10.1200/JCO.2007.15.8659

2. Wyrwicz L, Rodriguez SC, Sanchez-Rovira P, Lewis S, Sandschafer D, San T. Real-world clinical scenarios during introduction of trastuzumab biosimilar for HER2-positive breast cancer in the European Union. *Future Oncol*. (2024) 20:821–32. doi: 10.2217/fon-2023-0421

3. Lammers P, Criscitiello C, Curigliano G, Jacobs I. Barriers to the use of trastuzumab for HER2+ Breast cancer and the potential impact of biosimilars: A physician survey in the United States and emerging markets. *Pharm (Basel)*. (2014) 7:943–53. doi: 10.3390/ph7090943

4. Cherny N, Sullivan R, Torode J, Saar M, Eniu A. ESMO European Consortium Study on the availability, out-of-pocket costs and accessibility of antineoplastic medicines in Europe. *Ann Oncol*. (2016) 27:1423–43. doi: 10.1093/annonc/mdw213

5. Bas TG, Duarte V. Biosimilars in the era of artificial intelligence-international regulations and the use in oncological treatments. *Pharm (Basel)*. (2024) 17(7):925. doi: 10.3390/ph17070925

6. Cazap E, Jacobs I, McBride A, Popovian R, Sikora K. Global acceptance of biosimilars: importance of regulatory consistency, education, and trust. *ONCOLOGIST*. (2018) 23:1188–98. doi: 10.1634/theoncologist.2017-0671

7. Mamori T, Tanioka M, Takada K, Hamano H, Tsukioki T, Takahashi Y, et al. Real-World comparative analysis of trastuzumab originator and biosimilars: safety, efficacy, and cost effectiveness. *BIODRUGS*. (2025) 39:131–42. doi: 10.1007/s40259-024-00686-x

8. Rugo HS, Barve A, Waller CF, Hernandez-Bronchud M, Herson J, Yuan J, et al. Effect of a proposed trastuzumab biosimilar compared with trastuzumab on overall response rate in patients with ERBB2 (HER2)-Positive metastatic breast cancer: A randomized clinical trial. *JAMA*. (2017) 317:37–47. doi: 10.1001/jama.2016.18305

9. Stebbing J, Baranau YV, Baryash V, Manikhas A, Moiseyenko V, Dzagnidze G, et al. Long-term efficacy and safety of CT-P6 versus trastuzumab in patients with HER2-positive early breast cancer: final results from a randomized phase III trial. *Breast Cancer Res Treat*. (2021) 188:631–40. doi: 10.1007/s10549-021-06240-5

10. Pivot X, Bondarenko I, Nowecki Z, Dvorkin M, Trishkina E, Ahn JH, et al. Phase III, randomized, double-Blind study comparing the efficacy, safety, and immunogenicity of SB3 (Trastuzumab biosimilar) and reference trastuzumab in patients treated with neoadjuvant therapy for human epidermal growth factor receptor 2-Positive early breast cancer. *J Clin Oncol*. (2018) 36:968–74. doi: 10.1200/JCO.2017.74.0126

11. Stebbing J, Baranau Y, Baryash V, Manikhas A, Moiseyenko V, Dzagnidze G, et al. CT-P6 compared with reference trastuzumab for HER2-positive breast cancer: a randomised, double-blind, active-controlled, phase 3 equivalence trial. *Lancet Oncol*. (2017) 18:917–28. doi: 10.1016/S1470-2045(17)30434-5

12. Pegram MD, Bondarenko I, Zorzetto M, Hingmire S, Iwase H, Krivorotko PV, et al. PF-05280014 (a trastuzumab biosimilar) plus paclitaxel compared with reference trastuzumab plus paclitaxel for HER2-positive metastatic breast cancer: a randomised, double-blind study. *Br J Cancer*. (2019) 120:172–82. doi: 10.1038/s41416-018-0340-2

13. Xie L, Zhang E, Xu Y, Gao W, Wang L, Xie MH, et al. Demonstrating analytical similarity of trastuzumab biosimilar HLX02 to herceptin((R)) with a panel of sensitive and orthogonal methods including a novel fcgammaRIIIa affinity chromatography technology. *BIODRUGS*. (2020) 34:363–79. doi: 10.1007/s40259-020-00407-0

14. Zhu X, Ding Y, Yu Y, Wang M, Zhou W, Wang J, et al. A Phase 1 randomized study compare the pharmacokinetics, safety and immunogenicity of HLX02 to reference CN- and EU-sourced trastuzumab in healthy subjects. *Cancer Chemother Pharmacol*. (2021) 87:349–59. doi: 10.1007/s00280-020-04196-9

15. Xu B, Zhang Q, Sun T, Li W, Teng Y, Hu X, et al. Updated efficacy and safety of HLX02 versus reference trastuzumab in metastatic HER2-positive breast cancer: A randomized phase III equivalence trial. *BREAST*. (2025) 80:104413. doi: 10.1016/j.breast.2025.104413

16. Zhou W, Wang M, Yu Y, Wang J, Wu Y, Yang G, et al. Comparing the pharmacokinetics, safety, and immunogenicity of HLX02 to US- and EU-approved trastuzumab in healthy Chinese male subjects: A Phase I, randomized, double-blind, parallel-group study. *Expert Opin Biol Ther*. (2023) 23:717–25. doi: 10.1080/14712598.2023.2183117

17. Deng W, Hu J, Li M, Yang S, Xie Z, Chen J. Trastuzumab biosimilar HLX02 versus reference trastuzumab in patients with recurrent or metastatic HER2-positive breast cancer: a model-based economic evaluation for China. *Expert Rev Pharmacoecon Outcomes Res*. (2022) 22:1117–26. doi: 10.1080/14737167.2022.2107506

18. Xu B, Zhang Q, Sun T, Li W, Teng Y, Hu X, et al. Efficacy, safety, and immunogenicity of HLX02 compared with reference trastuzumab in patients with recurrent or metastatic HER2-Positive breast cancer: A randomized phase III equivalence trial. *BIODRUGS*. (2021) 35:337–50. doi: 10.1007/s40259-021-00475-w

19. Park MH, Seo JH, Park JH, Seong MK, Park KU, Kim MK, et al. Efficacy and safety of biosimilar trastuzumab (CT-P6) in routine clinical practice in the Republic of Korea: a real-world post-marketing surveillance study. *Expert Opin Biol Ther*. (2024) 24:305–12. doi: 10.1080/14712598.2024.2334386

20. Deng W, Hu J, Yang S, Xie Z, Li M, Li J, et al. A multicenter real-world study comparing the clinical equivalence of trastuzumab biosimilar HLX02 and reference trastuzumab in the treatment of HER-2-positive breast cancer. *Am J Cancer Res*. (2023) 13:3113–22.

21. Marty M, Cognetti F, Maraninchi D, Snyder R, Mauriac L, Tubiana-Hulin M, et al. Randomized phase II trial of the efficacy and safety of trastuzumab combined with docetaxel in patients with human epidermal growth factor receptor 2-positive metastatic breast cancer administered as first-line treatment: the M77001 study group. *J Clin Oncol*. (2005) 23:4265–74. doi: 10.1200/JCO.2005.04.173

22. Baselga J, Cortes J, Kim SB, Im SA, Hegg R, Im YH, et al. Pertuzumab plus trastuzumab plus docetaxel for metastatic breast cancer. *N Engl J Med*. (2012) 366:109–19. doi: 10.1056/NEJMoa1113216

23. Zhang R, Liu X, Song G, Zhang Y, Li H. Trastuzumab biosimilar (HLX02), pertuzumab plus chemotherapy in patients with HER2-positive metastatic breast cancer after progression of trastuzumab: A prospective, phase II study. *Cancer Res Treat*. (2024) 56:795–801. doi: 10.4143/crt.2023.1151

24. von Minckwitz G, Colleoni M, Kolberg HC, Morales S, Santi P, Tomasevic Z, et al. Efficacy and safety of ABP 980 compared with reference trastuzumab in women with HER2-positive early breast cancer (LILAC study): a randomised, double-blind, phase 3 trial. *Lancet Oncol*. (2018) 19:987–98. doi: 10.1016/S1470-2045(18)30241-9

25. Liu T, Liu D, Jin Y, Dong M. Trastuzumab biosimilars vs trastuzumab originator in the treatment of HER2-positive breast cancer: a systematic review and network meta-analysis. *Immunopharmacol Immunotoxicol*. (2022) 44:809–15. doi: 10.1080/08923973.2022.2090956

26. Pei J, Feng L, Mu Q, Wang Q, Wu Z, Wang Z, et al. Exploring an novel diagnostic gene of trastuzumab-induced cardiotoxicity based on bioinformatics and machine learning. *Sci Rep*. (2024) 14:30067. doi: 10.1038/s41598-024-81335-9

27. Wang Y, Xu J, Xie Y, Zhou D, Guo M, Qin Y, et al. Interventions for prevention and treatment of trastuzumab-induced cardiotoxicity: an umbrella review of systematic reviews and meta-analyses. *Front Pharmacol*. (2024) 15:1479983. doi: 10.3389/fphar.2024.1479983

28. Li J, Wang S, Wang Y, Wang X, Wang H, Feng J, et al. Disparities of trastuzumab use in resource-Limited or resource-Abundant regions and its survival benefit on HER2 positive breast cancer: A real-World study from China. *ONCOLOGIST*. (2017) 22:1333–8. doi: 10.1634/theoncologist.2017-0088

29. Giuliani J, Fiorica F, Albanese V, Bonetti A. Financial toxicity and cancer treatments: Help from biosimilars - The explanatory case of bevacizumab. *Eur J Cancer*. (2021) 143:40–2. doi: 10.1016/j.ejca.2020.11.004

frontiers | Frontiers in Oncology

TYPE Original Research
PUBLISHED 13 August 2025
DOI 10.3389/fonc.2025.1525114



OPEN ACCESS

EDITED BY
Sharon R. Pine,
University of Colorado Anschutz Medical Campus, United States

REVIEWED BY
Zhengyu Lin,
First Affiliated Hospital of Fujian Medical University, China
Hong-Tao Hu,
Henan Provincial Cancer Hospital, China

*CORRESPONDENCE
Kaixian Zhang
kaixianzhangtz@163.com

†These authors have contributed equally to this work

RECEIVED 08 November 2024
ACCEPTED 17 July 2025
PUBLISHED 13 August 2025

CITATION
Xing C, Li P, Yang S, Man Q, Zhang X, Yuan Q, Hu M, Bai Y and Zhang K (2025) Investigation of the efficacy and safety of lung biopsy plus microwave ablation for a solitary suspected malignant pulmonary nodule after radical mastectomy.
*Front. Oncol.* 15:1525114.
doi: 10.3389/fonc.2025.1525114



# Investigation of the efficacy and safety of lung biopsy plus microwave ablation for a solitary suspected malignant pulmonary nodule after radical mastectomy

Chao Xing†, Peishun Li†, Sen Yang, Qirong Man, Xusheng Zhang, Qianqian Yuan, Miaomiao Hu, Yunling Bai and Kaixian Zhang*

Department of Oncology, Tengzhou Central People's Hospital, Tengzhou, Shandong, China

**Purpose:** To evaluate the safety and efficacy of CT-guided lung biopsy combined with microwave ablation (MWA) for solitary suspected malignant pulmonary nodules in post-radical surgery breast cancer patients.

**Materials and methods:** This retrospective study included 37 post-radical surgery breast cancer patients with solitary suspected malignant pulmonary nodules, treated with CT-guided lung biopsy and MWA between January 2014 and December 2018. Institutional review board approval was obtained. Clinical outcomes and complications were analyzed.

**Results:** Pathological results identified primary lung cancer in 5 patients (13.5%, 5/37) and metastatic invasive ductal carcinoma (breast origin) in 30 patients (81.1%, 30/37). Major complications included pneumothorax (n=8, 21.6%), chest pain (n=6, 16.2%), and hemoptysis (n=4, 10.8%). For metastatic cases, 2-, 3-, and 5-year survival rates were 86.2%, 58.3%, and 35.3%, respectively. The median progression-free survival after MWA was 35 months (range: 4–72; 95% CI: 24.53–46.48), and median overall survival was 44 months (95% CI: 32.55–55.45).

**Conclusion:** CT-guided lung biopsy combined with MWA is a safe and effective approach for managing solitary suspected malignant pulmonary nodules in post-radical surgery breast cancer patients.

KEYWORDS

**lung biopsy, microwave ablation (MWA), pulmonary nodule, breast cancer, lung metastases**

# Introduction

Breast cancer is one of the most common prevalent tumors among women, with a mortality-to-incidence ratio of 15% (1). Lung metastases are frequently witnessed in breast cancer patients (2). As a result, when intrapulmonary nodules are detected in breast cancer patients, they are frequently misdiagnosed as lung metastases. Nevertheless, studies have indicated that the incidence of primary lung cancer in breast cancer patients is approximately 1% (3–5), while the incidence of concurrent double primary cancer (with a time difference between diagnoses of no more than 6 months) is about 0.6% in breast cancer patients (4). Identifying a solitary pulmonary nodule in patients with breast cancer poses a diagnostic challenge. For such nodules, surgical resection is a feasible option. However, many patients are either unable or unwilling to undergo surgery due to factors such as advanced age, poor cardiopulmonary function, or other reasons. Recent studies (6–10) have demonstrated that lung biopsy combined with microwave ablation (MWA) for the solitary pulmonary nodule can yield outcomes similar to surgical resection.

However, there is scarce research exploring the application of this technology in breast cancer patients who have undergone radical surgery and subsequently developed a solitary pulmonary nodule. To fill this gap, we conducted a retrospective study to assess the efficacy of a concurrent diagnostic and therapeutic approach. This approach entailed conducting a CT-guided biopsy, immediately followed by MWA of the solitary pulmonary nodule suspected of malignancy in patients with a history of radical breast cancer surgery.

# Materials and methods

## Subjects

This retrospective study included 37 patients who underwent CT-guided lung biopsy combined with microwave ablation for suspected malignant solitary pulmonary nodules after radical mastectomy from January 2014 to December 2018. All patients had histopathologically confirmed invasive ductal carcinoma and underwent radical mastectomy. Chest computed tomography (CT) imaging demonstrated the existence of a newly identified solitary pulmonary nodule. The baseline imaging comprised chest and abdominal computed tomography (CT), enhanced cranial MRI, whole-body bone scan ECT, and, if accessible, positron-emission tomography (PET) CT. All patients were regarded as ineligible for reoperation or declined to undergo surgical resection.

Exclusion criteria encompassed the following: (1) Uncontrolled infectious inflammation around the lesion; (2) Skin infection or ulceration at the puncture site; (3) Severe pulmonary fibrosis, especially drug-induced fibrosis (11, 12); (4) Patients with a marked bleeding propensity and coagulation disorders; (5) Cachexia; (6) Severe cardiopulmonary insufficiency.

All cases were reviewed by an interdisciplinary oncology committee consisting of thoracic surgeons, respiratory physicians, medical oncologists, radiation oncologists, diagnostic and interventional radiologists, pathologists, and anesthesiologists. The flow chart is shown in Figure 1.

## Instrumentation

A Siemens Light Speed 64V spiral CT scanner (Germany) guided biopsy and MWA. Under CT guidance, transthoracic core biopsies used an 18G Argon coaxial system (MCXS1820LX semi-automatic). MWA employed an ECO-100A1 system (SFDA 20172011470; Nanjing ECO) with 2,450 ± 20 MHz frequency and 0-150W adjustable power. The 16G-20G microwave antenna (150-200mm length) featured a 15-mm active tip and water-cooled system to reduce surface temperature.

## Procedure of the operation

Prior to treatment, patients underwent thorough clinical evaluation, including laboratory tests, imaging, and pulmonary function assessments. Blood work included coagulation studies. Anticoagulants were held 1 week pre-procedure to minimize bleeding risk.

Patients were positioned supine or prone based on nodule location, secured with a vacuum-negative pressure pad, and the puncture site was marked on the skin.

An 18-gauge biopsy core needle was inserted into the center of the tumor through a coaxial cannula before initiating MWA. A biopsy was performed first to obtain two or three specimens from a single core needle. The tissue samples were preserved in 10% formalin and later evaluated pathologically after H&E staining. All biopsy specimens underwent immunohistochemical testing (including ER, PR, and HER-2). A CT scan was done to monitor for biopsy-related complications.

Under CT guidance, the MWA probe was accurately positioned in the pulmonary tumor. Limited pneumothorax without progression during MWA was acceptable. However, chest tube insertion was required for progressive pneumothorax interfering with probe placement or causing clinical symptoms. Ablation power was typically 30-50W for 3-10 minutes. CT scans monitored probe targeting, adjusted depth/angle, and ensured the intended ablation zone. Continuous monitoring of vital signs (BP, HR, ECG, $SpO_2$) was performed throughout the procedure.

An immediate post-MWA CT scan frequently displayed ground-glass opacity (GGO) 0.5 to 1.0 cm in width at the periphery of the pulmonary nodule, indicating complete ablation (13, 14). The CT scan was also employed to assess for complications such as pneumothorax, hemothorax, or pleural effusion. If a progressive pneumothorax was detected, chest tube insertion would be indicated to manage the situation.

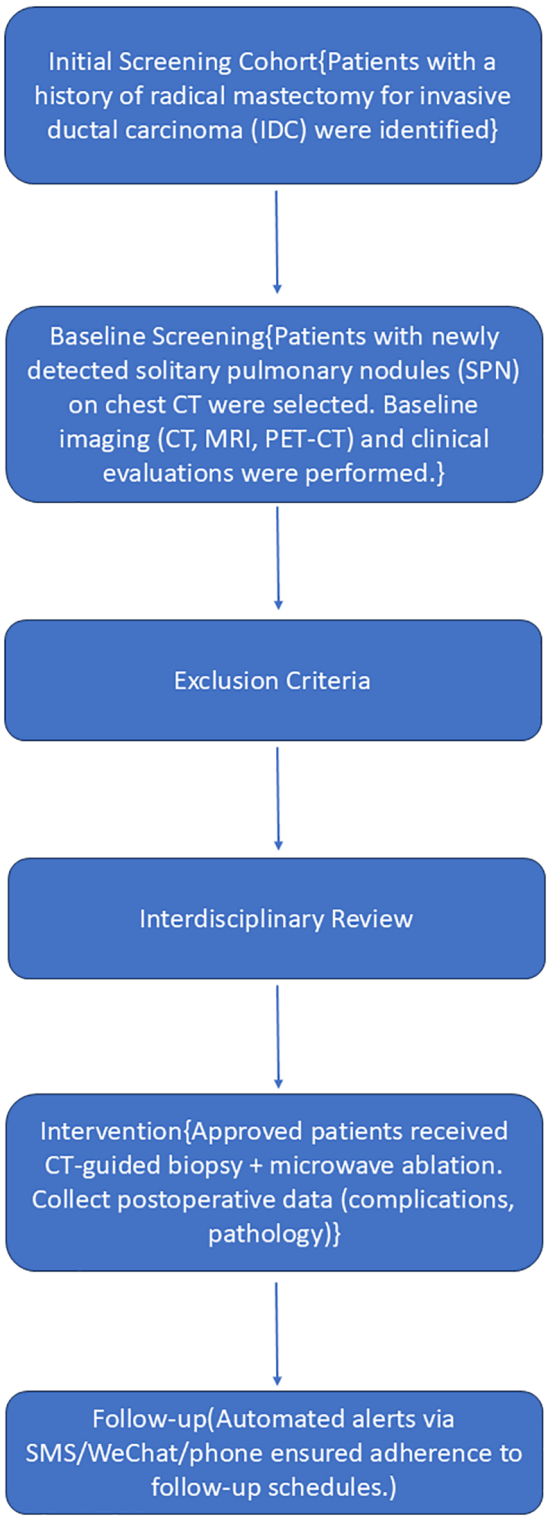


FIGURE 1
Flow chart of the eligibility process for the study.

This retrospective study was approved by the Ethics Committee of Tengzhou Central People's Hospital (Ethics Review No. 2018-Ethics Review-08). All participants provided written informed consent after detailed explanation of the procedures.

## Assessment of therapeutic efficacy and follow-up

Patients underwent enhanced CT scans at 1, 3, 6, and 12 months after MWA in the first year, and then every 6 months thereafter. Enhancement at the lesion site was considered indicative of incomplete treatment. Regions that remained unenhanced and were larger than the treated metastases were regarded as representing complete ablative necrosis and thus considered fully effective for the treatment.

The primary response rate was defined as the percentage of target tumors successfully eliminated during the initial ablation session. The assessment of the local efficacy of MWA was conducted by a single oncologist and two radiologists.

Survival outcomes included progression-free survival (the time from MWA until the recurrence of other metastases or death, PFS) and overall survival (the time from MWA until death, OS).

## Statistical analysis

IBM SPSS 26.0 was used for statistical analysis. Data are presented as the total count (percentage) and mean values. The Chi-square test was utilized for categorical variables. The Kaplan-Meier method was used to determine the survival rate and local progression-free survival rate. In all statistical assessments, results were regarded as significant if $p < 0.05$.

# Results

## General information

From January 2014 to December 2018, 37 female patients with a solitary suspected malignant pulmonary nodule after radical breast cancer surgery were treated with CT-guided lung biopsy combined with MWA in our hospital. All patients were female and had undergone modified radical mastectomy with pathologically confirmed invasive ductal carcinoma. The median age was 53 years (range: 27 to 73 years). HER-2 was detected by immunohistochemistry in all patients, and 10 were strongly positive (verified by FISH). 34 patients received adjuvant chemotherapy, 11 received adjuvant radiotherapy, 10 received adjuvant targeted therapy, and 22 received adjuvant endocrine therapy. The pulmonary nodules ranged in size from 6 to 28 mm (15.65 ± 6.13) (Table 1).

All patients underwent technically successful lung biopsy combined with MWA. One month after the operation, a CT scan showed that 37 lesions were completely covered by the tumor coagulation area after ablation, and the primary effective rate was 100% (37/37).

## Pathological results of puncture biopsy

Among the 37 patients, 35 cases (35/37, 94.6%) were pathologically diagnosed as malignant tumors, among which 5

TABLE 1 Characteristics of patients.

| Characteristics | n (%) |
|---|---|
| Total number of patients | 37 |
| Age (years) | |
| <60 | 27 (73.0%) |
| ≥60 | 10 (27.0%) |
| Previous chemotherapy | |
| No | 3 (8.1%) |
| Yes | 34 (91.9%) |
| Previous radiotherapy | |
| No | 26 (70.3%) |
| Yes | 11 (29.7%) |
| Previous endocrine therapy | |
| No | 15 (40.5%) |
| Yes | 22 (59.5%) |
| ER | |
| Negative | 15 (40.5%) |
| Positive | 22 (59.5%) |
| PR | |
| Negative | 16 (43.2%) |
| Positive | 21 (56.8%) |
| HER-2 over-expression | |
| No | 27 (73.0%) |
| Yes | 10 (27.0%) |
| Maximum tumor diameter (cm) | |
| ≤ 1.0 | 10 (27.0%) |
| 1.0<~≤2.0 | 17 (46.0%) |
| 2.0<~≤3.0 | 10 (27.0%) |

ER, estrogen receptor; PR, progesterone receptor; HER-2: human epidermal growth factor receptor2.

cases (5/37, 13.5%) were diagnosed as primary lung cancer (Figure 2). The biopsy pathology of 30 cases (30/37, 81.1%) was invasive ductal carcinoma (Table 2, Figure 3). The remaining 2 cases (2/37, 5.4%) were diagnosed as atypical adenomatous hyperplasia (AAH) (Table 2). A separate subgroup analysis was conducted for the clinical treatment of the 30 cases with lung metastases from breast cancer.

## Postoperative complications

The major complications were pneumothorax, chest pain, and hemoptysis. Pneumothorax occurred in 11 of 37 cases (29.7%). Severe (lung compression >50%) and moderate (lung compression 20%-50%) pneumothorax occurred in two cases, and these patients underwent catheter drainage. The other nine patients' pneumothorax was gradually absorbed without special treatment. The incidence of chest pain was 73.0% (27/37), and that of hemoptysis was 27.0% (10/37). Among the 10 hemoptysis cases, three were moderate (hemoptysis volume 10-100 mL), seven were mild (hemoptysis volume <10 mL), and there was no severe hemoptysis (hemoptysis volume >100 mL). No other complications such as needle implantation metastases, pulmonary embolism, or bronchopleural fistula were observed (Table 3).

## Postoperative PFS of lung metastases subgroup

During follow-up, local progression at the ablation site (Local Tumor Progression, LTP) occurred in 16.7% (5/30) of cases during a median follow-up of 44 months. These five lesions were from five different patients, two of whom underwent a second ablation treatment and the other three who opted for medical therapy. The 1-year, 2-year, and 3-year cumulative LTP rates were 3.3%, 10.0%, and 16.7%, respectively.

The median time from MWA of lung metastases to disease progression was 35 months (ranged 4-72 months, 95% confidence interval 24.53–46.48). Univariate analysis indicated that the PFS after MWA was related to time from primary tumor to lung metastases, HER-2 over-expression, and histological grade (P<0.05) (Table 4). Cox regression analysis demonstrated that time from the primary tumor to lung metastases and histological grade had a significant effect on PFS (P<0.05).

## Postoperative OS of lung metastases subgroup

The 2-year, 3-year and 5-year survival rates were 86.2%, 58.3% and 35.3% respectively. The median OS time in the lung metastases subgroup was 44 months (95% confidence interval 32.55–55.45). Univariate analysis revealed that OS was related to the time from primary tumor to lung metastases, HER-2 over-expression and histological grade (P<0.05) (Table 5). Cox regression analysis demonstrated that HER-2 over-expression and histological grade had a significant effect on OS (P<0.05) (Table 6).

# Discussion

In the context of a history of breast cancer, a solitary pulmonary nodule could potentially be lung metastases, primary lung cancer, or benign lung lesions (15). According to a review (16), the incidence of metastatic lesions ranged from 34% to 75%, that of primary lung cancer varied from 12% to 48%, and for benign lesions, it was from 14% to 18%. This study, focusing on CT-guided lung biopsy combined with MWA for suspected malignant nodules, found primary lung cancer in 13.5% (5/37) and breast cancer metastases in 81.1% (30/37), yielding a 94.6% malignancy rate

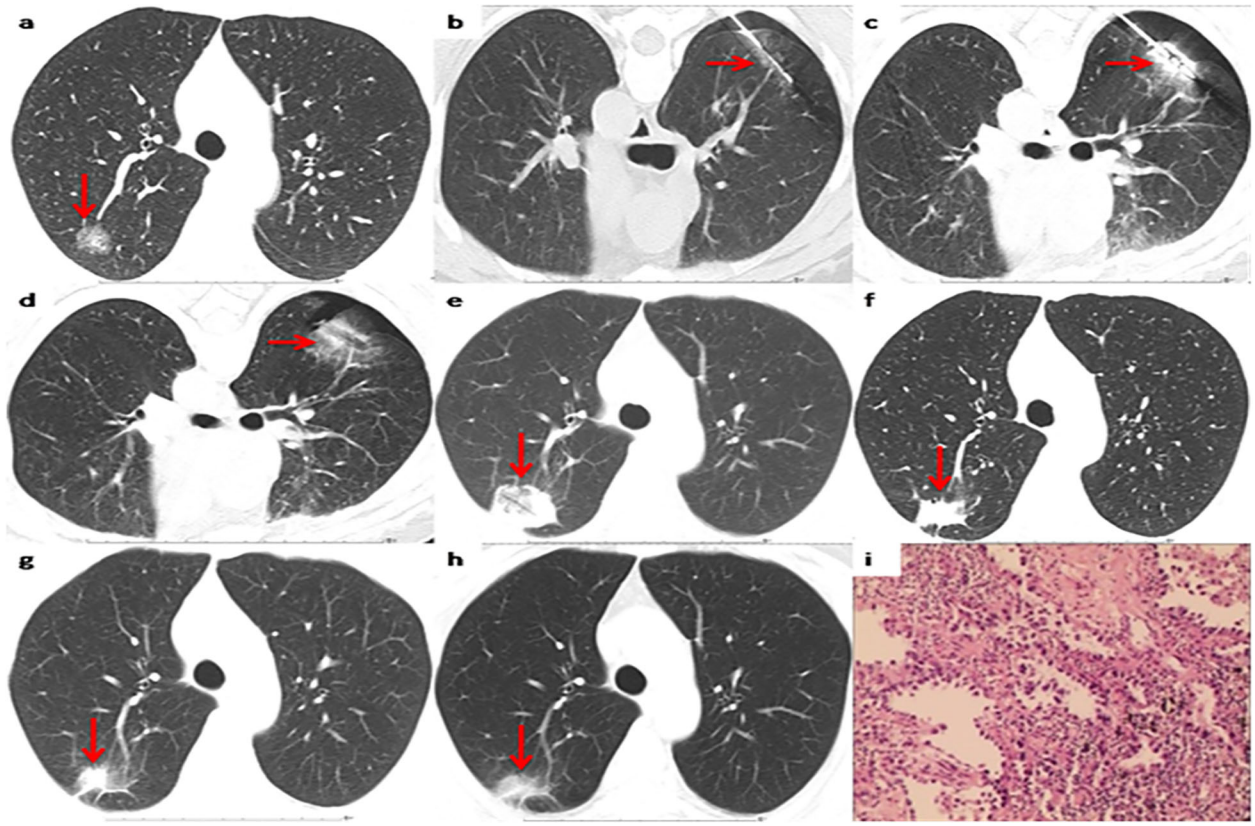


FIGURE 2
Representative CT scans of a patient with primary lung invasive adenocarcinoma after breast cancer surgery. **(a)** Preoperative image. **(b)** The biopsy needle has been inserted into the nodule center to complete the biopsy sectioning. **(c)** The MWA antenna has been inserted into the nodule center. **(d)** Postoperative image immediately after MWA. **(e)** 1 month after MWA. **(f)** 12months after MWA. **(g)** 36 months after MWA. **(h)** 60 months after MWA. **(i)** Pathological results of primary lung invasive adenocarcinoma biopsy.

(35/37)—higher than historical data. This phenomenon may be related to the following reasons: (1) The breast cancer TNM stage of the patient group included in this study at the initial treatment was relatively late; (2) tissue sampling via biopsy improving diagnostic accuracy; (3) Small sample size with selection bias; (4) The included patients had a longer follow-up time and regular periodic examinations, enabling earlier detection of malignant lesions and increasing the detection rate of malignant tumors.

TABLE 2 Pathological results of puncture biopsy.

| Histopathology results | Number | % |
|---|---|---|
| Total | 37 | |
| Invasive Ductal Carcinoma | 30 | 81.1% |
| Atypical Adenomatous Hyperplasia | 2 | 5.4% |
| Adenocarcinoma In Situ | 1 | 2.7% |
| Invasive Adenocarcinoma | 3 | 8.1% |
| Minimally Invasive Adenocarcinoma | 1 | 2.7% |

In 2021, WHO histological classification of lung tumors defined atypical adenomatous hyperplasia and adenocarcinoma *in situ* (AIS) as glandular prodromal lesions (17). Asymptomatic slow-growing glandular prodromal lesions can be managed conservatively with careful observations and regular follow-up. Even after surgical treatment, the 5-year disease-free survival rate of patients after complete surgical resection of AIS is 100% or close to 100% (18). In this study, 3 cases of glandular prodromal lesions were not only pathologically diagnosed but also inactivated by thermal ablation after synchronous diagnosis and treatment. While conservative observation is typical for such lesions, the protocol's synchronous biopsy-ablation approach prioritized timely intervention, aligning with the patients' high-risk profile and the procedure's demonstrated safety.

For patients with advanced lung metastases of breast cancer, systemic treatment such as chemotherapy, hormonal therapy, and anti-HER2 are main methods of therapy. There is currently no consensus on whether solitary lung metastases need surgery. Friedel et al. (19) reported 467 patients with lung metastases from breast cancer, of which 84% patients underwent complete resection, and the 5 -, 10 -, and 15-year survival rates were 38%, 22%, and 20%, respectively. According to the International Lung Metastases Registry

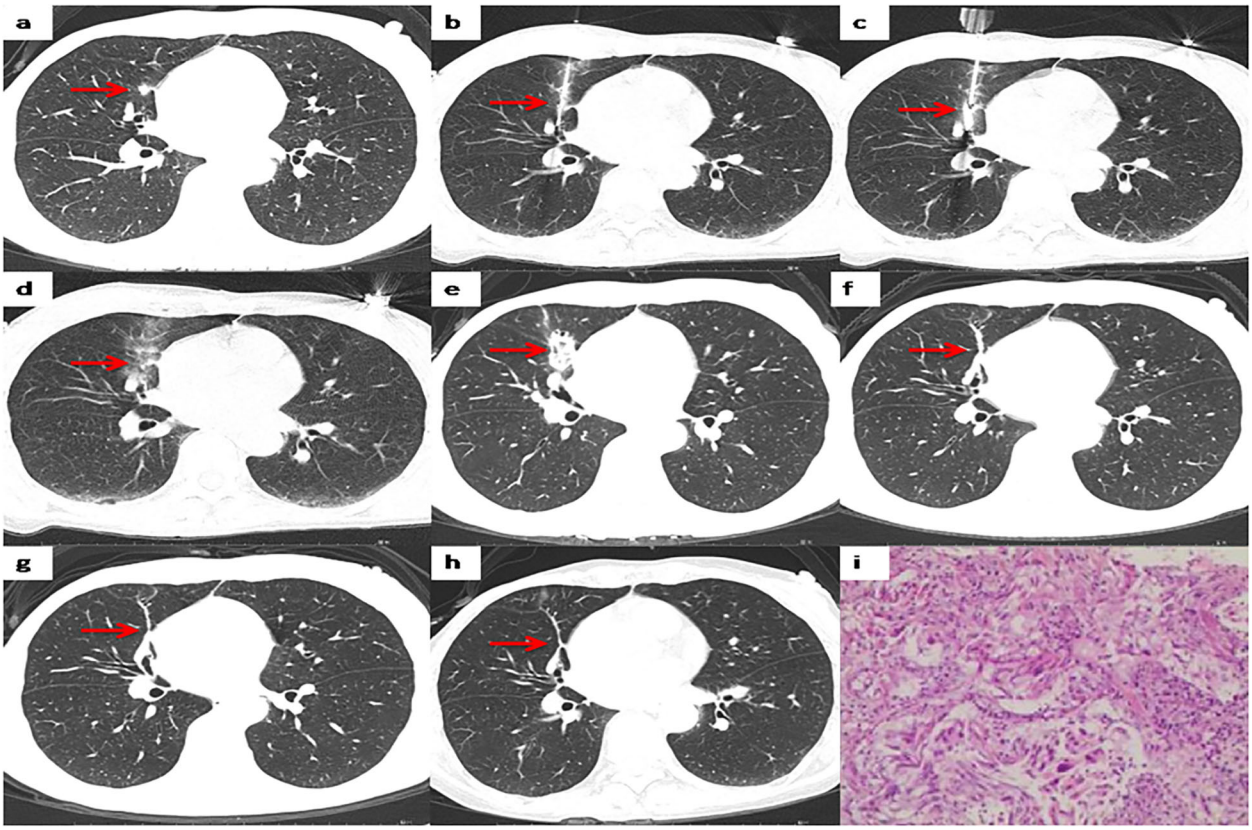


FIGURE 3
Representative CT scans of a patient with right lung metastases after breast cancer surgery. **(a)** Preoperative image. **(b)** The biopsy needle has been inserted into the nodule center to complete the biopsy sectioning. **(c)** The MWA antenna has been inserted into the nodule center. **(d)** Postoperative image immediately after MWA. **(e)** 1 month after MWA. **(f)** 12months after MWA. **(g)** 36 months after MWA. **(h)** 60 months after MWA. **(i)** Pathological results of lung metastases biopsy.

(20), the median OS and 5-year OS rates in patients undergoing surgical resection of lung metastases from breast cancer were 37 months and 38% in the R0 group. As a minimally invasive technique, local thermal ablation has been applied to the treatment of early lung cancer, and the number of lung cancer patients treated each year is rapidly increasing (21–24). It has been proved that percutaneous thermal ablation can also effectively treat lung metastases (25–28). In this study, the 5-year survival rate of patients with lung metastases who underwent needle biopsy combined with MWA was 35.3%, which was similar to that reported in previous studies. These findings may be explained by three key factors. First, all breast cancer patients with lung metastases received personalized multimodal therapy post-MWA, integrating chemotherapy, endocrine therapy, targeted agents, and immunotherapy as indicated. Second, MWA effectively debulked local tumors, reducing the risk of systemic spread. Third, comprehensive pre-treatment staging excluded extrapulmonary disease in all enrolled patients.

In this study, the median time from MWA of lung metastases to disease progression was 35 months (range 4–72 months, 95% CI 24.53–46.48). Univariate analysis revealed that post-MWA PFS correlated significantly with time from primary tumor to lung metastases, HER-2 overexpression, and histological grade (P<0.05,

TABLE 3 Side effects and complications during and after microwave ablation procedure*.

| Side effects and complications | n (%) |
|---|---|
| Pneumothorax | |
| Grade 1 | 9 (24.3%) |
| Grade 3 | 2 (5.4%) |
| Chest pain | |
| Grade 1 | 23 (62.6%) |
| Grade 2 | 4 (10.8%) |
| Hemoptysis | |
| Grade 1 | 7 (18.9%) |
| Grade 2 | 3 (8.1%) |
| Fever | |
| Grade 1 (38°C-39°C) | 2 (5.4%) |
| Fatigue | |
| Grade 1 | 4 (10.8%) |

*(Continued)*

TABLE 3 Continued

| Side effects and complications | n (%) |
|---|---|
| Pleural effusion | |
| Grade 1 | 8 (21.6%) |
| Nausea | |
| Grade 1 | 9 (24.3%) |
| Vomiting | |
| Grade 1 | 3 (8.1%) |
| Cough | |
| Grade 1 | 11 (29.7%) |

*Complications were graded according to the Common Terminology Criteria for Adverse Events (CTCAE) version 5.0.

Table 4). Cox regression showed time from primary to lung metastases and histological grade significantly affected PFS (P<0.05, Table 6), confirming them as independent prognostic factors for local control in breast cancer patients with lung metastases. The median overall survival (OS) time in the lung metastases subgroup was 44 months (95% confidence interval 32.55–55.45). Univariate analysis showed that OS was related to the time from primary tumor to lung metastases, HER-2 over-expression, and histological grade (P<0.05, Table 5). Cox regression showed HER-2 overexpression and histological grade significantly impacted OS (P<0.05, Table 6), confirming them as independent prognostic factors for breast cancer patients with lung metastases. This study identified time from primary to lung metastases, histological grade, and HER-2 status as key prognostic factors in breast cancer lung metastases. These findings warrant validation in larger studies.

Needle biopsy and MWA have similar procedures and complications (pneumothorax, bleeding, etc.) (29–31). Complications are closely related to the physiological conditions of lung tissue and the times of pleural puncture (32). Chi et al. (33) reported that the incidence of pneumothorax was 25%in coaxial biopsy combined with MWA for ground-glass nodes. In this study, the incidence of pneumothorax was 29.7%, which was higher than previously reported in the literature. Wang et al. (34) reported that the incidence of hemoptysis following pulmonary nodule ablation

TABLE 4 PFS after MWA according to lung metastatic tumor and treatment.

| Prognostic factors | N | Median PFS (months) | 95% CI | χ 2 | p value |
|---|---|---|---|---|---|
| The size of lung metastatic tumor (cm) | | | | 2.195 | 0.334 |
| 0 ≤ 1 | 8 | 35 | 24.84-45.16 | | |
| 1.0<~≤2.0 | 14 | 30 | 14.32-45.68 | | |
| 2.0<~≤3.0 | 8 | 17 | | | |
| Initial TNM staging | | | | 0.194 | 0.908 |
| I | 3 | 34 | 0-70.81 | | |
| II | 15 | 39 | 20.08-57.92 | | |
| III | 12 | 35 | 21.60-48.40 | | |
| ER | | | | 0.589 | 0.443 |
| Positive | 16 | 35 | 26.84-43.16 | | |
| Negative | 14 | 30 | 24.00-36.00 | | |
| Time from primary tumor to lung metastases (months) | | | | 5.445 | 0.020 |
| <60 | 18 | 27 | 15.63-38.37 | | |
| ≥60 | 12 | 45 | 40.22-49.78 | | |
| HER-2 over-expression | | | | 5.849 | 0.016 |
| Yes | 9 | 45 | 33.05-56.95 | | |
| No | 21 | 27 | 10.85-43.15 | | |
| Histological grade | | | | 10.267 | 0.006 |
| I | 8 | 45 | 39.15-50.85 | | |
| II | 12 | 34 | 24.10-43.91 | | |
| III | 10 | 15 | 10.00-20.00 | | |

CI, confidence interval.

TABLE 5 OS after MWA according to lung metastatic tumor and treatment.

| Prognostic factors | N | Median OS (months) | 95% CI | χ 2 | p value |
|---|---|---|---|---|---|
| The size of lung metastatic tumor (cm) | | | | 3.034 | 0.219 |
| 0 ≤ 1 | 8 | 63 | 35.28-90.72 | | |
| 1.0<~≤2.0 | 14 | 39 | 26.87-51.13 | | |
| 2.0<~≤3.0 | 8 | 28 | 25.91-30.09 | | |
| Initial TNM staging | | | | 0.955 | 0.620 |
| I | 3 | 64 | 0.00-148.82 | | |
| II | 15 | 39 | 24.54-53.46 | | |
| III | 12 | 44 | 17.40-70.61 | | |
| ER | | | | 0.932 | 0.334 |
| Positive | 16 | 44 | 35.58-52.42 | | |
| Negative | 14 | 35 | 12.65-57.35 | | |
| Time from primary tumor to lung metastases (months) | | | | 5.932 | 0.015 |
| <60 | 18 | 35 | 22.86-47.14 | | |
| ≥60 | 12 | 63 | 49.68-76.32 | | |
| HER-2 over-expression | | | | 9.009 | 0.003 |
| Yes | 9 | 65 | 42.19-87.81 | | |
| No | 21 | 35 | 21.01-48.99 | | |
| Histological grade | | | | 11.173 | 0.004 |
| I | 8 | 63 | 24.45-101.55 | | |
| II | 12 | 39 | 27.31-50.69 | | |
| III | 10 | 25 | 2.49-47.51 | | |

was 22%. In this study, the incidence of hemoptysis was 27%, which was higher than previously reported in the literature. These differences may be because most patients in this study had pulmonary nodules with a maximum diameter less than 2cm (73.0%). Due to small nodule size, multiple adjustments of the biopsy needle are needed for accuracy, and all patients require 2-3 biopsies. These multiple operations increase the risk of damage to lung tissues and blood vessels, raising the incidence of hemoptysis.

This study has inherent limitations. As a retrospective analysis, it relies on pre-existing records, susceptible to incomplete data, inaccuracies, and selection bias. The small sample size compromises statistical power, limiting generalizability. Notably, no comparative analysis was performed with alternative modalities (surgical resection, SBRT, RFA). The lack of head-to-head comparisons hinders definition of MWA's clinical role. Prospective, multicenter randomized controlled trials with larger cohorts are needed to rigorously assess MWA's efficacy and safety profile.

TABLE 6 Multivariate analysis of PFS.

| Prognostic factors | PFS | | | OS | | |
|---|---|---|---|---|---|---|
| | Odds ratio | 95% CI | p | Odds ratio | 95% CI | p |
| Time from primary tumor to lung metastases (months) | 3.864 | 1.014-14.726 | 0.048 | 3.590 | 0.941-13.694 | 0.061 |
| HER-2 over-expression | 2.586 | 0.791-8.454 | 0.116 | 7.090 | 1.399-35.936 | 0.018 |
| Histological grade | 2.418 | 1.044-5.600 | 0.039 | 3.142 | 1.239-7.971 | 0.016 |

In conclusion, this study shows that concurrent lung biopsy with MWA demonstrates significant clinical value for suspected malignant pulmonary nodules, enabling simultaneous diagnosis and therapeutic intervention. However, patient selection and optimal treatment timing remain key challenges in clinical implementation.

## Data availability statement

The original contributions presented in the study are included in the article/supplementary material. Further inquiries can be directed to the corresponding author.

## Ethics statement

The Ethics Committee of Tengzhou Central People's Hospital granted approval for this retrospective study (Ethics Review Number 2018-Ethics Review-08). The studies were conducted in accordance with the local legislation and institutional requirements. The participants provided their written informed consent to participate in this study. Written informed consent was obtained from the individual(s) for the publication of any potentially identifiable images or data included in this article.

## Author contributions

CX: Writing – original draft, Writing – review & editing, Conceptualization. PL: Writing – original draft, Writing – review & editing, Conceptualization, Data curation, Formal Analysis. SY: Data curation, Writing – review & editing, Resources, Visualization. QM: Methodology, Supervision, Writing – review & editing. XZ: Formal Analysis, Writing – review & editing. QY: Investigation, Writing – review & editing. MH: Software, Visualization, Writing – review & editing. YB: Resources, Validation, Writing – review & editing. KZ: Writing – original draft, Writing – review & editing.

## Funding

The author(s) declare that no financial support was received for the research and/or publication of this article.

## Acknowledgments

We would like to express our sincere gratitude to the local institutional review board for approving this study. We also appreciate the efforts of the interdisciplinary oncology committee, including thoracic surgeons, respiratory physicians, medical oncologists, radiation oncologists, diagnostic and interventional radiologists, pathologists, and anesthesiologists, for their comprehensive review of all cases.

## Conflict of interest

The authors declare that the research was conducted in the absence of any commercial or financial relationships that could be construed as a potential conflict of interest.

## Generative AI statement

The author(s) declare that no Generative AI was used in the creation of this manuscript.

## Publisher's note

All claims expressed in this article are solely those of the authors and do not necessarily represent those of their affiliated organizations, or those of the publisher, the editors and the reviewers. Any product that may be evaluated in this article, or claim that may be made by its manufacturer, is not guaranteed or endorsed by the publisher.

## References

1. Siegel RL, Miller KD, Jemal A. Cancer statistics, 2020. *CA Cancer J Clin*. (2020) 70:7–30. doi: 10.3322/caac.21590

2. Winer EP, Morrow M, Osbourne CK, Harris JR. Malignant tumors of the breast. In: De Vita VT Jr., Hellman S, Rosenberg SA, editors. *Cancer. Principles & practice of oncology, 6th*. Lippincott Williams & Wilkins, Philadelphia (2001). p. 1651–716.

3. Schonfeld SJ, Curtis RE, Anderson WF, de González AB. The risk of a second primary lung cancer after a first invasive breast cancer according to estrogen receptor status. *Cancer Causes Control*. (2012) 23:1721–8. doi: 10.1007/s10552-012-0054-3

4. Shoji F, Yamashita N, Inoue Y, Kozuma Y, Toyokawa G, Hirai F, et al. Surgical resection and outcome of synchronous and metachronous primary lung cancer in breast cancer patients. *Anticancer Res*. (2017) 37:5871–6. doi: 10.21873/anticanres.12032

5. Wang R, Yin Z, Liu L, Gao W, Li W, Shu Y, et al. Second primary lung cancer after breast cancer: A population-based study of 6,269 women. *Front Oncol*. (2018) 8:427–37. doi: 10.3389/fonc.2018.00427

6. Gao F, Han X, Dou W, Li Z. CT-guided microwave ablation and biopsy of highly suspected Malignant ground-glass nodule of lung with co-axle technique. *Chin J Interv Imaging Ther*. (2020) 17:464–7. doi: 10.13929/j.issn.1672-8475.2020.08.004

7. Chi J, Ding M, Wang Z, Hu H, Shi Y, Cui D, et al. Pathologic diagnosis and genetic analysis of sequential biopsy following coaxial low-power microwave thermal coagulation for pulmonary ground-glass opacity nodules. *Cardiovasc InterventRadiol*. (2021) 44:1204–13. doi: 10.1007/s00270-021-02782-9

8. Yao W, Lu M, Fan W, Huang J, Gu Y, Gao F, et al. Comparison between microwave ablation and lobectomy for stage I non-small cell lung cancer: A propensity score analysis. *Int J Hyperthermia*. (2018) 34:1329–36. doi: 10.1080/02656736.2018.1434901

9. Wei Z, Wang Q, Ye X, Yang X, Huang G, Li W, et al. Microwave ablation followed by immediate biopsy in the treatment of non-small cell lung cancer. *Int J Hyperthermia*. (2018) 35:262–8. doi: 10.1080/02656736.2018.1494856

10. Zhong L, Sun S, Shi J, Cao F, Han X, Bao X, et al. Clinical analysis on 113 patients with lung cancer treated by percutaneous CT-guided microwave ablation. *J Thorac Dis*. (2017) 9:590–7. doi: 10.21037/jtd.2017.03.14

11. Alexander ES, Dupuy DE. Lung cancer ablation: technologies and techniques. *Semin InterventRadiol*. (2013) 30:141–50. doi: 10.1055/s-0033-1342955

12. Bhatia S, Pereira K, Mohan P, Narayanan G, Wangpaichitr M, Savaraj N, et al. Radiofrequency ablation in primary non-small cell lung cancer: what a radiologist needs to know. *Indian J Radiol Imaging*. (2016) 26:81–91. doi: 10.4103/0971-3026.178347

13. Kuroki M, Nakada H, Yamashita A, Sawaguchi A, Uchino N, Sato S, et al. Loss of cellular viability in areas of ground-glass opacity on computed tomography images immediately after pulmonary radiofrequency ablation in rabbits. *Jpn J Radiol*. (2012) 30:323–30. doi: 10.1007/s11604-012-0054-y

14. Bojarski JD, Dupuy DE, Mayo-Smith WW. CT imaging findings of pulmonary neoplasms after treatment with radiofrequency ablation: results in 32 tumors. *AJR Am J Roentgenol*. (2005) 185:466–71. doi: 10.2214/ajr.185.2.01850466

15. Yoshimoto M, Tada K, Nishimura S, Makita M, Iwase T, Kasumi F, et al. Favourable long-term results after surgical removal of lung metastases of breast cancer. *Breast Cancer Res Treat*. (2008) 110:485–91. doi: 10.1007/s10549-007-9747-9

16. Rashid OM, Takabe K. The evolution of the role of surgery in the management of breast cancer lung metastases. *J Thorac Dis*. (2012) 4:420–4. doi: 10.3978/j.issn.2072-1439.2012.07.16

17. WHO Classification of Tumours Editorial Board. WHO classification of tumours. In: *Thoracic tumours, 5th*. IARC Press, Lyon (2021).

18. Liu Q, Zeng Y, Liu B, Wang Y, Li XF, Zhou DQ, et al. Clinical and CT radiomic features for predicting pulmonary nodules in adenocarcinoma. *Chin Comput Med Imag*. (2022) 28:245–50. doi: 10.19627/j.cnki.cn31-1700/th.2022.03.020

19. Friedel G, Pastorino U, Ginsberg RJ, Goldstraw P, Johnston M, Pass H, et al. Results of lung metastasectomy from breast cancer: prognostic criteria on the basis of 467 cases of the International Registry of lung metastases. *Eur J Cardiothorac Surg*. (2002) 22:335–44. doi: 10.1016/S1010-7940(02)00331-7

20. Pagani O, Senkus E, Wood W, Colleoni M, Cufer T, Kyriakides S, et al. International guidelines for management of metastatic breast cancer: can metastatic breast cancer be cured? *J Natl Cancer Inst*. (2010) 102:456–63. doi: 10.1016/j.diii.2016.08.016

21. De Baere T, Tselikas L, Catena V, Buy X, Deschamps F, Palussière J, et al. Percutaneous thermal ablation of primary lung cancer. *DiagnInterv Imaging*. (2016) 97:1019–24. doi: 10.1016/j.diii.2016.08.016

22. Healey TT, March BT, Baird G, Dupuy DE. Microwave ablation for lung neoplasms: a retrospective analysis of long-term results. *J VascIntervRadiol*. (2017) 28:206–11. doi: 10.1016/j.jvir.2016.10.030

23. Yang X, Ye X, Zheng A, Huang G, Ni X, Wang J, et al. Percutaneous microwave ablation of stage I medically inoperable non-small cell lung cancer: clinical evaluation of 47cases. *J Surg Oncol*. (2014) 110:758–63. doi: 10.1002/jso.23701

24. Han X, Yang X, Ye X, Liu Q, Huang G, Wang J, et al. Computed tomography-guided percutaneous microwave ablation of patients 75 years of age and older with early-stage non-small cell lung cancer. *Indian J Cancer*. (2015) 52:e56–60. doi: 10.4103/0019-509X.172514

25. Ferguson J, Izahrani N, Zhao J, Glenn D, Power M, Liauw W, et al. Long term results of RFA to lung metastases from colorectal cancer in 157 patients. *Eur J Surg Oncol*. (2015) 41:690–5. doi: 10.1016/j.ejso.2015.01.024

26. Mat Sui Y, Hiraki T, Gobara H. Long-term survival following percutaneous radiofrequency ablation of colorectal lung metastases. *J Vasc Interv Radiol*. (2015) 26:303. doi: 10.1016/j.jvir.2014.11.013

27. de Baère T, Aupérin A, Deschamps F. Radiofrequency ablation is a valid treatment option for lung metastases: experience in 566 patients with 1,037 metastases. *Ann Oncol*. (2015) 26:987–91. doi: 10.1093/annonc/mdv037

28. Vogl TJ, Eckert R, Naguib NN. Thermal ablation of colorectal lung metastases: retrospective comparison among laser-induced thermotherapy, radiofrequency ablation, and microwave ablation. *AJRAm J Roentgenol*. (2016) 207:1340–9. doi: 10.2214/AJR.15.14401

29. Gould MK, Donington J, Lynch WR, Mazzone PJ, Midthun DE, Naidich DP, et al. Evaluation of individuals with pulmonary nodules: When is it lung cancer? Diagnosis and management of lung cancer, 3rd ed; American College of Chest Physicians evidence-based clinical practice guidelines. *Chest*. (2013) 143:e93S–e120S. doi: 10.1378/chest.12-2351

30. Maxwell AW, Healey TT, Dupuy DE. Percutaneous thermal ablation for small-cell lung cancer: Initial experience with ten tumors in nine patients. *J VascInterv Radiol*. (2016) 27:1815–21. doi: 10.1016/j.jvir.2016.09.009

31. Chassagnon G, Gregory J, Al Ahmar M, Magdeleinat P, Legmann P, Coste J, et al. Risk factors for hemoptysis complicating 17–18-gauge CT-guided transthoracic needle core biopsy: Multivariate analysis of 249 procedures. *DiagnIntervRadiol*. (2017) 23:347–53. doi: 10.5152/dir.2017.160338

32. Wei Y, Xiao Y, Zhang X, He X, Zhang X, Zhang X, et al. Clinical application of CT-guided percutaneous RFA combined with halfway biopsy for pulmonary nodule and management for prevention of intraoperative bleeding. *Chin J Interv Imaging Ther*. (2021) 18:8–12. doi: 10.13929/j.issn.1672-8475.2021.01.003

33. Chi J, Wang Z, Ding M, Hu H, Zhai B. Technical safety and efficacy of a blunt-tip microwave ablation electrode for CT-guided ablation of pulmonary ground-glass opacity nodules. *EurRadiol*. (2021) 31:7484–90. doi: 10.1007/s00330-021-07774-4

34. Wang D, Li B, Bie Z, Li Y, Li X. Synchronous core-needle biopsy and microwave ablation for highly suspicious Malignant pulmonary nodule via a coaxial cannula. *J Cancer Res Ther*. (2019) 15:1484–9. doi: 10.4103/jcrt.JCRT_721_18

frontiers | Frontiers in Oncology

TYPE Case Report
PUBLISHED 10 September 2025
DOI 10.3389/fonc.2025.1593952



OPEN ACCESS

EDITED BY
Raquel Diaz,
University of Genova, Italy

REVIEWED BY
Yigit Ali Üncü,
Akdeniz University, Türkiye
Cherry Bansal,
Tantia University, India

*CORRESPONDENCE
Jin Hu
hujin4444@whu.edu.cn

RECEIVED 14 March 2025
ACCEPTED 23 July 2025
PUBLISHED 10 September 2025

CITATION
Yang Q, Gong Y and Hu J (2025)
A rare case of mammary hamartoma presenting as malignant on radiological assessment and benign on pathological examination: a case report.
*Front. Oncol.* 15:1593952.
doi: 10.3389/fonc.2025.1593952



# A rare case of mammary hamartoma presenting as malignant on radiological assessment and benign on pathological examination: a case report

Qingfeng Yang, Yiping Gong and Jin Hu*

Department of Breast and Thyroid Surgery, Renmin Hospital, Wuhan University, Wuhan, China

Breast hamartomas are rare, benign, and encapsulated lesions composed of a combination of fatty, glandular, muscular, and fibrous tissue. Mammography provides an overview of the breast's structure and can identify the characteristic "breast within a breast" appearance typical of hamartomas. Ultrasound is useful for determining the echogenicity and vascularization of hamartomas, thereby helping to differentiate them from potential malignancies. Magnetic Resonance Imaging (MRI) is another indispensable tool in the diagnostic arsenal for breast hamartomas. One of the major challenges in differential diagnosis is distinguishing hamartomas from fibroadenomas, which typically occur in young women. Here, we present a case of a 21-year-old female with a highly suspicious lesion based on radiological features, which was ultimately diagnosed histologically as a breast hamartoma.

KEYWORDS

**breast, hamartoma, case report, breast hamartoma, mammary hamartoma**

## Introduction

Breast hamartomas are uncommon, benign, and encapsulated lesions with unclear etiology and pathogenesis (1). They are characterized by an exceptionally low clinical incidence, accounting for approximately 4.8% of all benign breast masses (2). These lesions are composed of a mixture of glandular, fatty, fibrous, and muscular tissues (3). Although typically benign, their clinical presentation and diagnostic features pose unique challenges to clinicians, making their study significant for medical practice. Breast hamartomas

usually occur in middle-aged, perimenopausal women but can develop at any age (3). Although these tumors are uncommon, they can grow to substantial sizes and may co-occur with malignant tumors. Surgical resection is the first-line treatment. In this report, we describe a rare case of a breast hamartoma that exhibited discordant pathological and radiological findings.

## Case presentation

A 21-year-old woman presented to our hospital with a palpable lump in her right breast. She reported that the mass had been present for approximately two months, during which it had gradually increased in size, accompanied by a mild discomfort but without significant pain or other symptoms. Her family medical history was unremarkable, and she denied any history of tobacco use. Physical examination revealed a painless, hard, ill-defined, poorly mobile mass in the upper lateral part of the right breast. A dimpling sign was observed in the breast.

Breast ultrasound revealed a hypoechoic mass in the right breast with indistinct borders, classified as BI-RADS IVc (Figures 1A, B). Bilateral mammography showed an oval, well-circumscribed, predominantly fatty mass measuring approximately 3.3×3.7 cm in the upper outer quadrant of the right breast (Figure 2), which was assigned a BI-RADS IVa score. Given the atypical appearance of the mass, further evaluation with magnetic resonance imaging (MRI) was performed. MRI demonstrated a mass-like lesion with mixed T1 signal and prolonged T2 signal in the upper quadrant of the right breast, measuring about 2.8 cm×3.1 cm×2.3 cm. The lesion exhibited heterogeneous enhancement during the contrast-enhanced scan (Figure 3), and a BI-RADS IVc score was reaffirmed. After discussion in our multidisciplinary team, the patient underwent surgical excision of the right breast mass. Fine-needle aspiration cytology (FNAC) was initially considered, but due to the patient's young age and the clinical presentation of a mass with a dimpling sign, the multidisciplinary team opted for surgical excision to obtain a more definitive diagnosis and to address the patient's concerns about potential malignancy. The patient underwent surgical excision of the right breast mass under general anesthesia, with careful dissection and removal of the mass while preserving the surrounding breast tissue. During the surgery, a rapid frozen section pathology was performed on the right breast mass. The frozen section pathology report indicated a benign lesion of the right breast, with a consideration of breast hamartoma. The interior of the resected tumor appeared yellow and white. Postoperative pathology revealed a mammary hamartoma in the right breast, measuring 3.5×3.3×3 cm. The tumor was well-defined and composed of randomly arranged glandular and stromal components, as well as adipose tissue and smooth muscle fibers (Figure 4). Immunohistochemistry results showed Desmin (focal +), ER (-), Ki-67 (+, approximately 5%), and SMA (+). The patient was followed up after three months, and an ultrasound report showed no recurrence.

## Discussion

The average age of patients with breast hamartomas ranges from 19 to 56 years, with a mean age of 41.8 years (4). Alran et al. reported a median age of 40 years (3). In our case, the patient was a 23-year-old young woman. Similarly, Aminpour N et al. reported a case of a 23-year-old female with myoid hamartoma of the breast (5). Therefore,

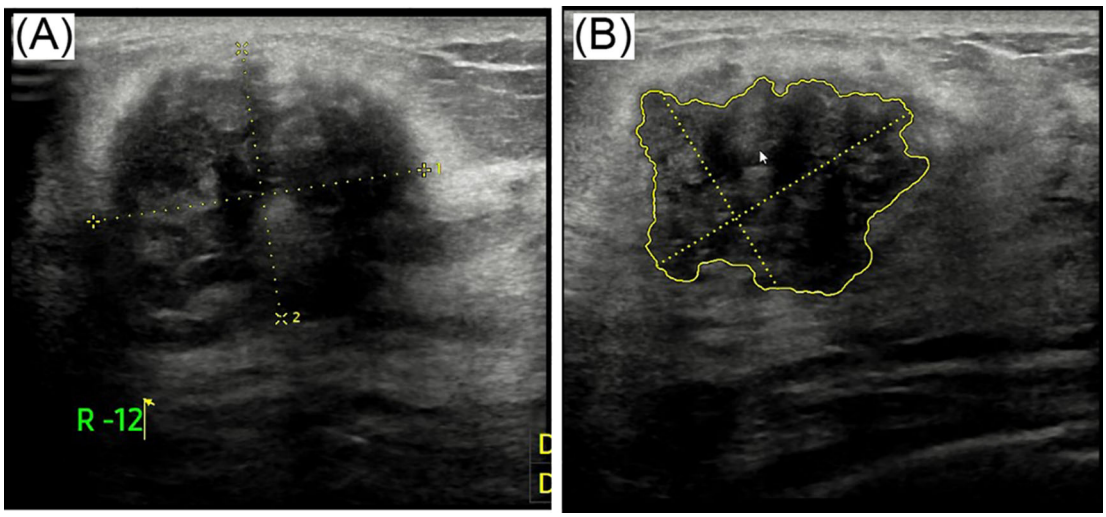


FIGURE 1
Ultrasound images labeled **(A)** and **(B)**. Image **(A)** shows a mass with dotted yellow lines indicating measurements. Image **(B)** highlights an irregularly shaped area outlined in yellow, also marked with measurement lines.

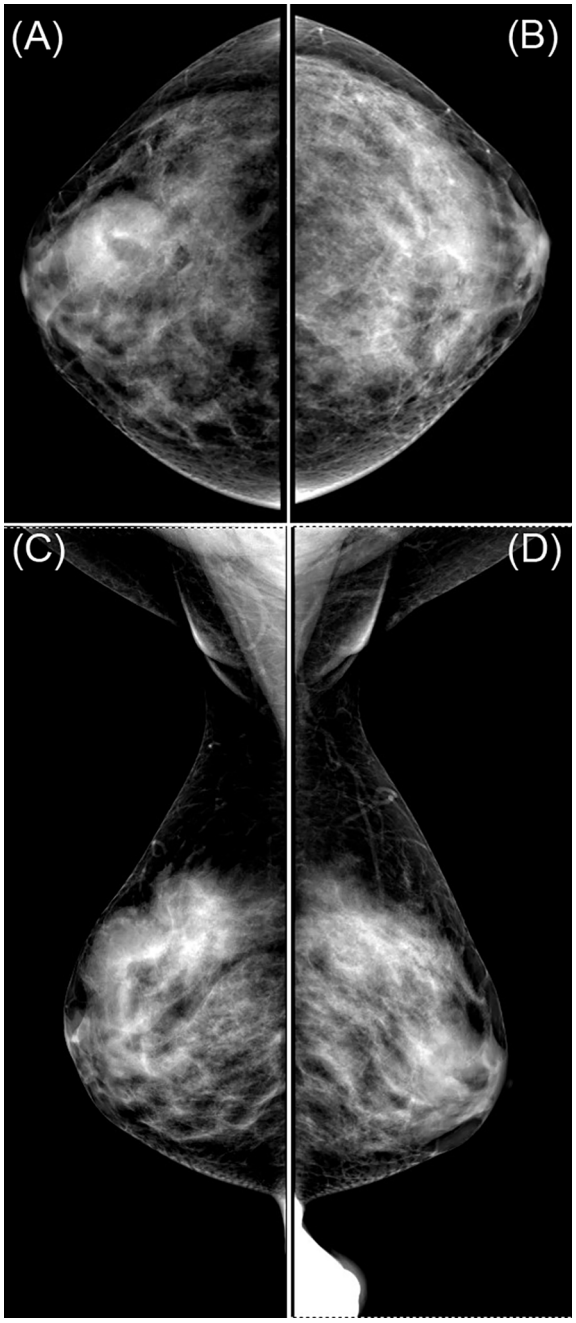


FIGURE 2
Mammogram images labeled **(A–D)** show different views of a breast, highlighting dense areas. Panels **(A, B)** are craniocaudal views, while **(C)** and **(D)** are mediolateral oblique views. The images display varying tissue densities, useful for medical analysis.

when a young woman presents with a large, hard, slow-growing breast mass, and core-needle biopsy based on breast ultrasound suggests fibroadenoma, differentiation from breast hamartoma is necessary.

Breast hamartoma is rarely occurs in men. Gupta SS et al. reported a case in a 13-year-old boy (6).

Although breast hamartomas are generally slow-growing, the gradual growth observed in this case may be attributed to the patient's young age and hormonal factors.

Hamartomas are rarely associated with malignancies. However, a few studies have reported invasive breast cancer coexisting with breast hamartoma. Sevim Y et al. identified invasive ductal carcinoma in one case and lobular carcinoma *in situ* in another (4). To our knowledge, there have been two reported cases of breast parenchymal hamartoma with synchronous contralateral breast cancer (7, 8). This association may be related to PTEN hamartoma tumor syndrome (PHTS), characterized by mutations in the PTEN tumor suppressor gene (8).

Mammary hamartoma is a relatively rare benign breast lesion composed of an abnormal mixture of adipose, glandular, and fibrous tissue, often forming a well-circumscribed mass. As slow-growing, benign entities, these lesions are distinct for their heterogeneous composition and generally favorable prognosis (1). Despite their benign nature, accurate recognition and diagnosis of mammary hamartomas are vital due to their potential to be confused with other, potentially malignant breast masses (9, 10). Such lesions are typically detected incidentally during routine breast imaging performed for other clinical indications.

Mammography is often the first-line imaging modality for evaluating breast lesions, including mammary hamartomas. Its ability to provide a detailed overview of the breast's structure helps identify the classic "breast within a breast" appearance characteristic of hamartomas (11). However, mammography's sensitivity is limited in dense breast tissue, where lesions can be obscured, making diagnosis challenging and often necessitating additional imaging.

Ultrasound is a non-invasive diagnostic tool that significantly supplements mammography by providing detailed information on the internal structure of breast masses. It offers real-time imaging and is particularly useful for differentiating solid from cystic lesions. Ultrasound also aids in assessing the echogenicity and vascularization of hamartomas, which can help distinguish them from malignancies (12, 13). Elastography, often combined with ultrasound, assesses tissue stiffness, a key feature differentiating benign from malignant lesions.

Magnetic Resonance Imaging (MRI) is another essential diagnostic tool for breast lesions. MRI offers high contrast resolution, making it ideal for imaging complex breast structures and revealing atypical vascular patterns (14). Its sensitivity to changes in tissue composition makes it a valuable adjunct when mammography and ultrasound results are inconclusive. Techniques like contrast-enhanced MRI can highlight regions with increased vascularity or unusual enhancement patterns suggestive of malignancy, thereby enhancing diagnostic accuracy (11, 15).

Clinically, hamartomas typically present as movable, well-circumscribed masses with a rubbery texture, similar to fibroadenomas (3).

In our clinical experience, the diagnostic prevalence of breast hamartoma appears lower than that reported in the literature. Diagnosis is typically established by core-needle biopsy combined with appropriate correlation of clinical and radiologic features. Breast hamartomas may be underdiagnosed because pathologists might categorize these lesions as fibroadenomas rather than hamartomas (4).

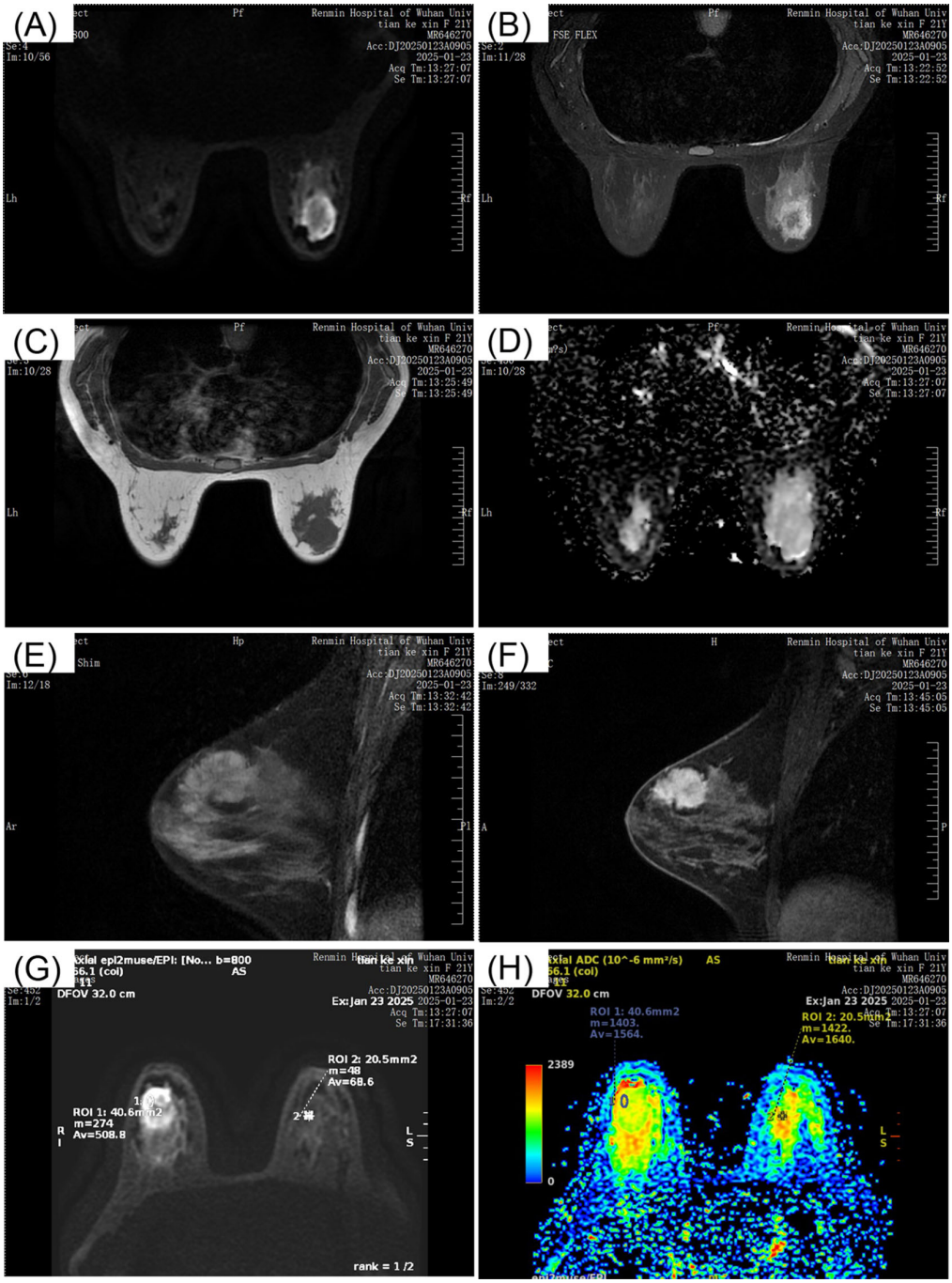


FIGURE 3
MRI breast scans depicting different views. Image **(A)** shows a coronal section with a visible mass. Image **(B)** presents another coronal view. Image **(C)** is a transverse section. Image **(D)** displays a diffusion-weighted image. Image **(E)** and **(F)** are sagittal views with noticeable lesions. Image **(G)** and **(H)** contain color maps indicating apparent diffusion coefficients, with regions of interest marked. All images are labeled with patient information and scan details from Renmin Hospital of Wuhan University, dated January 23, 2025.

Differential diagnosis is crucial to ensure hamartomas are not misclassified, preventing potentially incorrect treatment. This requires integrated assessment of clinical, radiological, and histopathological data (16).

Differential diagnosis can be particularly challenging when distinguishing hamartomas from fibroadenomas, which share a similar imaging appearance (17). Both can appear as well-circumscribed, hypoechoic masses on ultrasound; however,

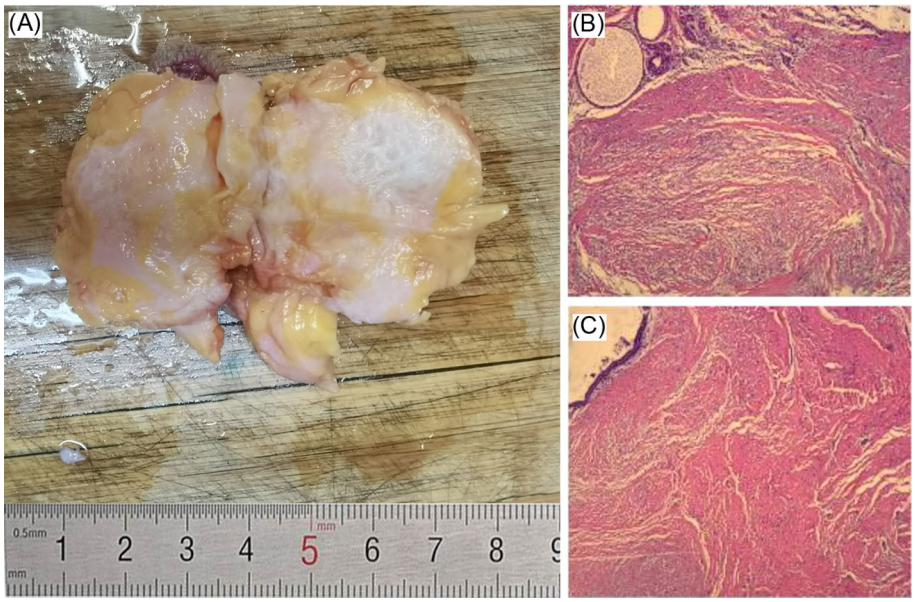


FIGURE 4
**(A)** Excised tissue sample on a cutting board with a ruler indicating size in centimeters. **(B)** and **(C)** Microscopic views of tissue sections displaying fibrous structures in shades of pink, red, and yellow.

hamartomas usually exhibit greater internal heterogeneity due to their composition of both fat and fibrous tissue (18). MRI is superior for delineating internal composition, enhancement patterns, and tissue characteristics compared to other modalities (12).

Management strategies for mammary hamartomas range from active surveillance to surgical excision, tailored to individual patient factors. Understanding the clinical relevance of treatment approaches is crucial, especially since many cases remain asymptomatic. While surgery is indicated in some cases, non-invasive management remains a viable alternative for most patients, underscoring the need for personalized treatment plans.

In summary, we describe an unusual case of breast hamartoma that presented with radiological features concerning for a highly malignant lesion. Surgical excision was the treatment of choice. Given the rarity of such presentations and the limited number of previously reported cases, this case provides valuable insights and warrants further investigation.

## Data availability statement

The original contributions presented in the study are included in the article/supplementary material. Further inquiries can be directed to the corresponding authors.

## Ethics statement

Written informed consent was obtained from the individual(s) for the publication of any potentially identifiable images or data included in this article.

## Author contributions

QY: Writing – review & editing, Writing – original draft. YG: Supervision, Conceptualization, Writing – review & editing. JH: Data curation, Writing – review & editing.

## Funding

The author(s) declare that no financial support was received for the research, and/or publication of this article.

## Conflict of interest

The authors declare that the research was conducted in the absence of any commercial or financial relationships that could be construed as a potential conflict of interest.

## Generative AI statement

The author(s) declare that no Generative AI was used in the creation of this manuscript.

Any alternative text (alt text) provided alongside figures in this article has been generated by Frontiers with the support of artificial intelligence and reasonable efforts have been made to ensure accuracy, including review by the authors wherever possible. If you identify any issues, please contact us.

## Publisher's note



## References

1. Tazeoğlu D, Dağ A, Arslan B, Berkeşoğlu M. Breast hamartoma: clinical, radiological, and histopathological evaluation. *Eur J Breast Health*. (2021) 17:328–32. doi: 10.4274/ejbh.galenos.2021.2021-3-6

2. Charpin C, Mathoulin MP, Andrac L, Barberis J, Boulat J, Sarradour B, et al. Reappraisal of breast hamartomas. A morphological study of 41 cases. *Pathol Res Practice*. (1994) 190:362–71. doi: 10.1016/S0344-0338(11)80408-5

3. Alran L, Chamming's F, Auriol-Leizagoyen S, Velasco V, Deleau F, Brouste V, et al. Breast hamartoma: reassessment of an under-recognised breast lesion. *Histopathology*. (2022) 80:304–13. doi: 10.1111/his.14544

4. Sevim Y, Kocaay AF, Eker T, Celasin H, Karabork A, Erden E, et al. Breast hamartoma: a clinicopathologic analysis of 27 cases and a literature review. *Clinics (Sao Paulo Brazil)*. (2014) 69:515–23. doi: 10.6061/clinics/2014(08)03

5. Aminpour N, Sogunro O, Towfighi P, Park BU, Boisvert M. Clinical management of myoid hamartomas of the breast: A case report and literature review. *Heliyon*. (2022) 8:e11723. doi: 10.1016/j.heliyon.2022.e11723

6. Gupta SS, Singh O, Hastir A, Arora G, Sabharwal G, Mishra H. Breast hamartoma with intrathoracic extension in a 13-year-old boy. *J Cancer Res Ther*. (2010) 6:86–8. doi: 10.4103/0973-1482.63559

7. Cho JS, Ryu HS, Ro HW, Lim HS, Park MH, Lee JS, et al. Myoid hamartoma of the breast with synchronous contralateral breast cancer: report of a case. *J Breast Cancer*. (2010) 13:120–3. doi: 10.4048/jbc.2010.13.1.120

8. El Yousfi Z, El Mansoury FZ, El Bakkari A, Omor Y, Latib R. Breast hamartoma with synchronous contralateral breast cancer: A case report. *Cureus*. (2024) 16:e66534. doi: 10.7759/cureus.66534

9. Wu J, Gong W, Li Q, Han X, Zhang T. Multi modality radiomics diagnosis of breast cancer based on MRI, ultrasound, and mammography. *BMC Med Imaging*. (2025) 25(1):265. doi: 10.1186/s12880-025-01767-1

10. Amir RA, Sheikh SS. Breast hamartoma: A report of 14 cases of an under-recognized and under-reported entity. *Int J Surg Case Rep*. (2016) 22:1–4. doi: 10.1016/j.ijscr.2016.03.007

11. He Z, Chen Z, Tan M, Elingarami S, Liu Y, Li T, et al. A review on methods for diagnosis of breast cancer cells and tissues. *Cell Prolif*. (2020) 53:e12822. doi: 10.1111/cpr.12822

12. Gerami R, Sadeghi Joni S, Akhondi N, Etemadi A, Fosouli M, Eghbal AF, et al. A literature review on the imaging methods for breast cancer. *Int J Physiol Pathophysiol Pharmacol*. (2022) 14:171–6. doi: 10.14740/ijppp-v14-9301184

13. Lebron-Zapata L, Jochelson MS. Overview of breast cancer screening and diagnosis. *PET Clin*. (2018) 13:301–23. doi: 10.1016/j.cpet.2018.02.001

14. Eskreis-Winkler S, Sung JS, Dixon L, Monga N, Jindal R, Simmons A, et al. High-temporal/high-spatial resolution breast magnetic resonance imaging improves diagnostic accuracy compared with standard breast magnetic resonance imaging in patients with high background parenchymal enhancement. *J Clin Oncol: Off J Am Soc Clin Oncol*. (2023) 41:4747–55. doi: 10.1200/JCO.22.00635

15. Vaidya TP, Ramani SK. Imaging evaluation of male breast masses with histopathologic correlation: A case series. *Indian J Radiol Imaging*. (2021) 31:360–5. doi: 10.1055/s-0041-1734358

16. Garmpis N, Psilopatis I, Dimitroulis D, Garmpi A, Nikolettos K, Vrettou K. A proposed cytodiagnosistic approach for breast lesions. *Maedica*. (2023) 18:376–9. doi: 10.26574/maedica.2023.18.2.376

17. Shahan CL, Layne GP. Advances in breast imaging with current screening recommendations and controversies. *Obstet Gynecol Clinics North America*. (2022) 49:1–33. doi: 10.1016/j.ogc.2021.11.001

18. Kurtoğlu Özçağlayan T, Öznur M. Digital mammography, ultrasound and magnetic resonance imaging characteristics in differential diagnosis of papillary carcinoma subtypes of the breast and diagnostic challenges. *Eur J Breast Health*. (2022) 18:172–81. doi: 10.4274/ejbh.galenos.2022.2021-9-4

frontiers | Frontiers in Oncology

TYPE Methods
PUBLISHED 10 September 2025
DOI 10.3389/fonc.2025.1577591



OPEN ACCESS

EDITED BY
Raquel Diaz,
University of Genova, Italy

REVIEWED BY
Giovanni Tazzioli,
University of Modena and Reggio Emilia, Italy
Matteo Bardelli,
Pisana University Hospital, Italy

*CORRESPONDENCE
Jiannan Wu
king8702@163.com

†These authors have contributed equally to this work

RECEIVED 16 February 2025
ACCEPTED 28 August 2025
PUBLISHED 10 September 2025

CITATION
Cao R, Zhang J, Su A, Bao H, He Z and Wu J (2025) An effective four-step approach in treating refractory seroma after mastectomy for breast cancer.
*Front. Oncol.* 15:1577591.
doi: 10.3389/fonc.2025.1577591



# An effective four-step approach in treating refractory seroma after mastectomy for breast cancer

Rui Cao[1†], Jing Zhang[2†], An Su[1†], Haoshi Bao[1], Zhou He[1] and Jiannan Wu[1*]

[1]Breast Tumor Center, Sun Yat-Sen University, Guangzhou, China, [2]Anesthesiology Department, Sun Yat-Sen Memorial Hospital, Sun Yat-Sen University, Guangzhou, China

**Background:** Postoperative chest wall seroma is a common complication following modified radical mastectomy. When persistent, it can lead to the formation of a dense fibrous capsule (pseudobursa), resulting in a refractory seroma that is unresponsive to conventional treatments and may delay essential adjuvant therapies. Surgical excision of the capsule carries significant risks. This study introduces a less invasive surgical technique to manage this challenging condition.

**Methods:** From 2018 to 2021, 20 patients with refractory seroma after modified radical mastectomy were included in this retrospective study. Inclusion required seroma persistence for over one month despite repeated aspirations, with the presence of a fibrous capsule confirmed by ultrasonography. A minimally traumatic, four-step technique was employed under local anesthesia, involving capsule scraping, "cross-hatch" scoring, and flap fixation. A drainage tube was inserted post-procedure. Color Doppler ultrasound was used for pre- and post-procedural assessment.

**Results:** The study included 20 female patients with a median age of 57.5 years. All patients had node-positive breast cancer. The "cross-hatch" capsular scoring technique was successfully performed in all cases. The median postoperative drainage time was 7 days (range 6–12 days). During a median follow-up of 3 months, no seroma recurrence was observed. The procedure was well-tolerated with minimal pain, and no significant complications such as hematoma or infection occurred.

**Conclusion:** The "cross-hatch" capsular scoring technique is a safe, effective, and less invasive method for managing refractory post-mastectomy seroma. This approach minimizes patient trauma, reduces recovery time, and helps maintain the continuity of adjuvant therapies, thereby offering a valuable alternative to more aggressive surgical interventions.

KEYWORDS

**breast cancer, refractory seroma, fibrous capsule, minimally traumatic surgery, flap fixation, local anesthesia**

# Introduction

Postoperative chest wall seroma is one of the most common complications after modified radical mastectomy for breast cancer, characterized by the abnormal subcutaneous accumulation of plasma and lymphatic fluid in a dead space (1–3). Its incidence ranges from 15% to 85%, varying by diagnostic criteria and detection methods (4, 5). In some cases, the seroma persists or recurs despite conservative treatments like repeated aspiration or compression, evolving into a refractory seroma. This condition can impede recovery by causing skin necrosis, wound infection, and delays in crucial adjuvant therapies (6), thereby impacting patient outcomes and quality of life.

A key pathological feature of a refractory seroma is the formation of a dense, smooth-walled fibrous capsule, known as a pseudobursa, around the fluid collection (7). This capsule's avascular, secretory inner lining prevents the adherence of the skin flap to the chest wall, perpetuating the fluid accumulation and rendering conventional treatments ineffective. While complete surgical excision of the capsule (capsulectomy) combined with negative pressure suction has been shown to be effective (8–10), this procedure presents significant challenges. For patients who have undergone axillary lymph node dissection, the capsule often extends into the axilla, in close proximity to vital nerves and vessels. A formal capsulectomy in this region requires extensive dissection, often under general anesthesia, and carries substantial risks of neurovascular injury, intraoperative bleeding, and significant postoperative pain.

Given these risks, there is a clear clinical need for a safer, less invasive alternative. In this study, we developed and evaluated a minimally traumatic surgical technique performed under local anesthesia. The procedure involves scraping and scoring the capsule ("cross-hatch" capsulotomy) without removing it, followed by flap fixation to obliterate the dead space. We herein report our experience, demonstrating the effectiveness and safety of this novel approach in a series of 20 patients.

# Patients and methods

## Patient selection

Between 2018 and 2021, 20 consecutive female patients with refractory seroma following modified radical mastectomy at our institution were included in this retrospective study. The inclusion criteria were: 1) persistence of seroma for over one month despite conventional management (including repeated percutaneous aspirations); and 2) the presence of a distinct, organized fibrous capsule confirmed by preoperative ultrasound examination. All patients had been pathologically diagnosed with breast cancer and had undergone axillary lymph node dissection as part of their initial surgery. Of these 20 patients, 10 underwent a standard Level I and II axillary lymph node dissection, while the remaining 10, who presented with clinically enlarged Level III lymph nodes, underwent a complete Level I-III dissection. The refractory seromas in this cohort developed after the removal of the initial surgical drains, which were typically kept in place for a period of 7 to 14 days.

The choice of modified radical mastectomy (MRM) for the initial surgery was based on clinical indications at the time of diagnosis, such as multicentric disease, large tumor-to-breast ratio, or patient preference, reflecting the clinical practice at our institution during the study period. Patients were excluded if they had an active infection, severe coagulation disorders, or declined the procedure. Since this study was conducted retrospectively based on a modification of an established clinical technique, formal ethical committee approval was not required by our institutional guidelines.

## The cross-hatch capsular scoring technique

The surgical procedure was performed in an outpatient setting and comprises four essential steps (Figure 1).

1. Incision and Exposure: After routine ultrasonography to map the extent of the seroma, the area was sterilized. Using 0.5% lidocaine for local anesthesia, an incision of 7–10 cm was made along the original mastectomy scar to access the seroma cavity. The seroma fluid was completely aspirated with a suction device, revealing the dense, smooth-walled fibrous capsule (pseudobursa) lining the cavity (Figure 1A). The aspirated fluid was visually inspected; as all cases presented with clear, serous fluid without signs of infection (e.g., purulence or turbidity), routine microbiological cultures were not performed.
2. Capsular Scoring: The key step involves altering the capsule surface. Using a No. 22 scalpel blade, the entire inner surface of the capsule on the skin flap and chest wall was methodically scraped to de-epithelialize the secretory lining. Following this, multiple "cross-hatch" scores or shallow incisions were made through the capsule down to the subcutaneous tissue or muscle layer (Figure 1B). Care was taken in the axillary region to avoid deep incisions that could injure the axillary vein or surrounding nerves. The fibrous capsule itself was left *in situ*.
3. Flap Fixation and Drainage: To obliterate the dead space, the skin flap was anchored to the underlying pectoral or serratus anterior muscle fascia using multiple interrupted 2–0 absorbable sutures (Figure 1C). A single closed-suction drainage tube was then placed within the cavity.
4. Closure and Compression: The skin incision was closed in layers. A sterile dressing and a multi-layer elastic compression bandage were applied to the chest wall to ensure firm apposition of the flaps (Figure 1D). The drain was connected to a low-pressure suction bottle. A single

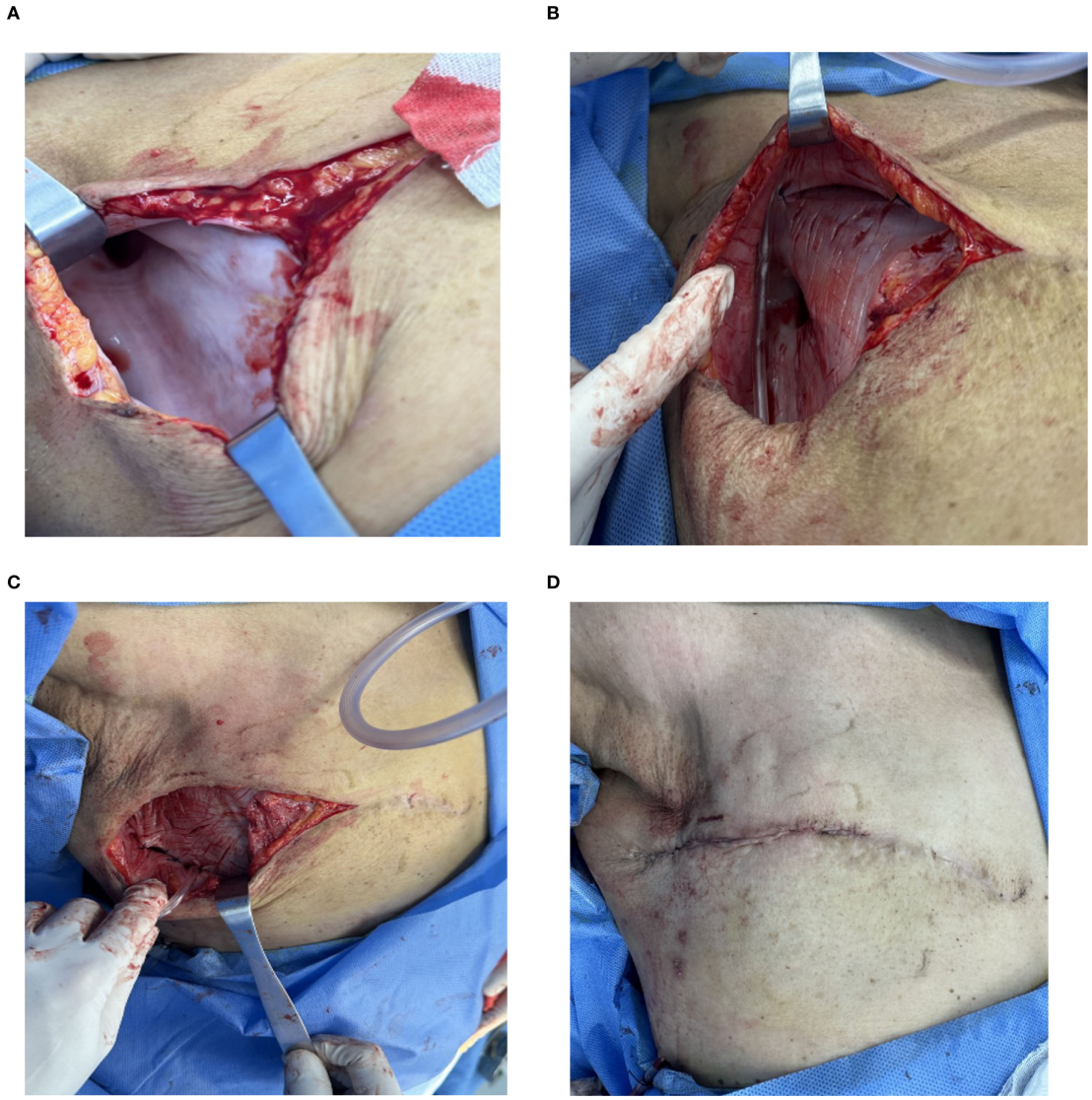


FIGURE 1
Key Steps of the Minimally Traumatic Surgical Procedure. **(A)** Exposure of the Pseudobursa: Following incision and complete fluid aspiration, the characteristic smooth, white fibrous capsule is visualized covering the chest wall and extending into the axilla. **(B)** Capsular Scoring: A scalpel is used to create multiple shallow, crisscrossing incisions ("cross-hatch" pattern) across the entire inner surface of the capsule, promoting an inflammatory healing response. The capsule itself is preserved. **(C)** Flap Fixation and Drainage: To ensure apposition, the skin flap is sutured to the underlying muscle fascia using 2–0 absorbable sutures. A drainage tube is placed to manage initial exudate. **(D)** Wound Closure: The incision is re-approximated with absorbable sutures, completing the procedure before compression bandaging is applied.

dose of a first-generation cephalosporin was administered preoperatively for surgical prophylaxis in all cases.

## Post-procedure management and follow-up

The drainage tube was removed when the daily output was consistently less than 20 ml for two consecutive days. The compression dressing remained in place until after drain removal. All patients underwent a color Doppler ultrasound examination one week after drain removal to confirm the absence of fluid re-accumulation. Follow-up was conducted at 1 and 3 months post-procedure to assess for seroma recurrence and any late complications.

# Results

## Patient and tumor characteristics

A total of 20 female breast cancer patients with refractory seroma were included. The median age was 57.5 years (range: 47-78), and the mean Body Mass Index (BMI) was 24.6 kg/m $^2$ (range: 19.4-35.5 kg/m $^2$). Comorbidities included diabetes mellitus in 4

patients (20%) and hypertension in 8 patients (35%). Six patients (30%) had received neoadjuvant chemotherapy.

Postoperative histopathology from the initial mastectomy revealed stage IIB in 8 patients (40%), IIIA in 6 patients (30%), and IIIC in 6 patients (30%). The median number of total lymph nodes removed was 17 (range: 7-30). All 20 patients had positive lymph nodes, with a median of 3 affected nodes (range: 1-25). Patient characteristics are summarized in Table 1.

## Procedural outcomes

The "cross-hatch" capsular scoring technique was successfully performed on all 20 patients under local anesthesia.

The median postoperative drainage time was 7 days (range 6–12 days). No major perioperative complications such as hematoma, surgical site infection, or flap necrosis were observed. Patients reported minimal postoperative pain, which was well-managed with oral analgesics.

During a median follow-up of 3 months, no recurrence of seroma was observed in any patient. Post-procedural ultrasound examinations confirmed complete resolution of the fluid collection and adherence of the skin flaps to the chest wall.

TABLE 1 Clinicopathlogical characteristics of the patients.

| Item | Results |
|---|---|
| Median age | 57.5 yrs (rang 47-78 yrs) |
| Body mass index (Mean standard deviation, kg/$m^2$) | 24.6 (±3.98) |
| Hypertension (Cases) | 8/20 |
| Neoadjuvant chemotherapy | 6/20 |
| adjuvant chemotherapy | 14/20 |
| Diabetes (Cases) | 4/20 |
| Number of dissected lymph nodes | |
| <10 | 1 |
| 10-20 | 11 |
| >=20 | 9 |
| Number of metastatic lymph nodes | |
| <4 | 7 |
| 4-9 | 7 |
| >=10 | 6 |
| Post opertive Stage | |
| 2B | 8 |
| 3A | 6 |
| 3C | 6 |

# Discussion

Managing postoperative refractory seroma in breast cancer surgery remains a significant clinical challenge. Our study demonstrates that the "cross-hatch" capsular scoring technique is a highly effective and safe method for treating this condition.

The rationale behind our technique is not merely to drain fluid but to fundamentally alter the pathophysiology of the non-healing seroma cavity. The pseudobursa's smooth, avascular inner lining prevents natural tissue adherence and perpetuates fluid secretion. By mechanically scraping and scoring this surface, we create a controlled inflammatory response. This, combined with meticulous flap fixation and external compression, promotes fibrin deposition and granulation, leading to the permanent obliteration of the dead space. The temporary drain serves only to manage the initial reactive exudate while this crucial adherence process occurs. Our results, showing no recurrences in 20 consecutive patients, provide strong preliminary evidence that this method offers a durable solution.

The standard surgical alternative for an encapsulated seroma is a formal capsulectomy. Unlike this procedure, which requires extensive and often high-risk dissection under general anesthesia, our technique is minimally traumatic. By leaving the capsule's outer layer intact and avoiding deep dissection, especially in the axilla, we minimize the risk of bleeding and neurovascular injury. Other innovative approaches, such as ultrasound-guided scraping with Negative Pressure Wound Therapy (NPWT), have been described (11). Our method, however, offers distinct advantages in its simplicity and accessibility, as it utilizes standard surgical instruments and does not require specialized equipment. The limited incision allows for direct visualization, ensuring thorough treatment of the capsule surface while protecting vital structures.

A key strength of our approach is its performance under local anesthesia. This makes it suitable for a wider range of patients, including the elderly or those with comorbidities who may be poor candidates for general anesthesia. The minimal postoperative pain reported by our patients, combined with the outpatient nature of the procedure, enhances patient comfort, reduces healthcare costs, and lessens the psychological burden associated with recurrent clinic visits.

This study has several limitations. Firstly, it is a retrospective, single-arm study with a relatively small sample size. Therefore, it should be considered a proof-of-concept series demonstrating the technique's feasibility and initial efficacy. Secondly, the follow-up period is limited to three months, although this is generally sufficient to detect early seroma recurrence. Future research should focus on larger, prospective, and potentially comparative studies to further validate these findings and assess long-term outcomes.

# Conclusion

The "cross-hatch" capsular scoring technique represents a significant advancement in the management of postoperative

refractory seroma. Its minimally traumatic nature, high efficacy, and excellent safety profile make it a valuable option for surgeons and patients alike. By adopting this method, clinicians can effectively resolve a challenging postoperative complication, improve recovery times, reduce morbidity, and ensure the timely continuation of essential adjuvant therapies, ultimately enhancing the quality of care in breast cancer surgery.

## Data availability statement

The original contributions presented in the study are included in the article/Supplementary Material. Further inquiries can be directed to the corresponding author.

## Author contributions

RC: Conceptualization, Data curation, Formal Analysis, Writing – original draft, Writing – review & editing, Investigation, Methodology, Validation. JZ: Investigation, Writing – original draft, Writing – review & editing, Formal Analysis, Resources, Software, Validation. AS: Methodology, Writing – original draft, Investigation, Project administration. HB: Resources, Software, Validation, Writing – original draft, Methodology, Conceptualization, Data curation, Formal Analysis, Funding acquisition, Investigation, Project administration, Supervision, Visualization. ZH: Investigation, Validation, Visualization, Writing – review & editing. JW: Data curation, Funding acquisition, Project administration, Supervision, Writing – original draft, Writing – review & editing, Conceptualization.

## Funding

The author(s) declare that no financial support was received for the research and/or publication of this article.

## Conflict of interest

The authors declare that the research was conducted in the absence of any commercial or financial relationships that could be construed as a potential conflict of interest.

## Generative AI statement

The author(s) declare that no Generative AI was used in the creation of this manuscript.

Any alternative text (alt text) provided alongside figures in this article has been generated by Frontiers with the support of artificial intelligence and reasonable efforts have been made to ensure accuracy, including review by the authors wherever possible. If you identify any issues, please contact us.

## Publisher's note

All claims expressed in this article are solely those of the authors and do not necessarily represent those of their affiliated organizations, or those of the publisher, the editors and the reviewers. Any product that may be evaluated in this article, or claim that may be made by its manufacturer, is not guaranteed or endorsed by the publisher.

## References

1. Agrawal A, Ayantunde AA, Cheung KL. Concepts of seroma formation and prevention in breast cancer surgery. *ANZ J Surg.* (2006) 76:1088–95. doi: 10.1111/j.1445-2197.2006.03949.x

2. Kuroi K, Shimozuma K, Taguchi T, Imai H, Yamashiro H, Ohsumi S, et al. Effect of mechanical closure of dead space on seroma formation after breast surgery. *Breast Cancer (Tokyo Japan).* (2006) 13:260–5. doi: 10.2325/jbcs.13.260

3. van Bemmel AJ, van de Velde CJ, Schmitz RF, Liefers GJ. Prevention of seroma formation after axillary dissection in breast cancer: a systematic review. *Eur J Surg Oncol: J Eur Soc Surg Oncol Br Assoc Surg Oncol.* (2011) 37:829–35. doi: 10.1016/j.ejso.2011.04.012

4. Kuroi K, Shimozuma K, Taguchi T, Imai H, Yamashiro H, Ohsumi S, et al. Evidence-based risk factors for seroma formation in breast surgery. *Japanese J Clin Oncol.* (2006) 36:197–206. doi: 10.1093/jjco/hyl019

5. Vinton AL, Traverso LW, Jolly PC. Wound complications after modified radical mastectomy compared with tylectomy with axillary lymph node dissection. *Am J Surg.* (1991) 161:584–8. doi: 10.1016/0002-9610(91)90905-s

6. Tejler G, Aspegren K. Complications and hospital stay after surgery for breast cancer: a prospective study of 385 patients. *Br J Surg.* (1985) 72:542–4. doi: 10.1002/bjs.1800720714

7. Fosheim K, Bojesen S, Troestrup H, Laenkholm AV. Capsulectomy can successfully treat chronic encapsulated breast seroma: A case report. *Cureus.* (2022) 14:e21677. doi: 10.7759/cureus.21677

8. Bi H, Fang S, Jiang D, Xing X, Zhu J, Wang X, et al. Ultrasound-guided scraping of fibrous capsule plus bilayered negative pressure wound therapy for treatment of refractory postmastectomy seroma. *J Plast Reconstr Aesthet Surg: JPRAS.* (2015) 68:403–9. doi: 10.1016/j.bjps.2014.11.007

9. Marangi GF, Segreto F, Morelli Coppola M, Arcari L, Gratteri M, Persichetti P. Management of chronic seromas: A novel surgical approach with the use of vacuum assisted closure therapy. *Int Wound J.* (2020) 17:1153–8. doi: 10.1111/iwj.13447

10. Esen E, Saydam M, Guler S, Akinci M, Bahcecioglu IB, Gulcelik MA, et al. Successful use of minimal invasive debridement plus negative pressure wound therapy under skin flap and axillary region for refractory postmastectomy seroma: A STROBE-compliant retrospective study. *Medicine*. (2022) 101:e31634. doi: 10.1097/md.0000000000031634

11. Stanczyk M, Grala B, Zwierowicz T, Maruszynski M. Surgical resection for persistent seroma, following modified radical mastectomy. *World J Surg Oncol.* (2007) :5:104. doi: 10.1186/1477-7819-5-104

frontiers | Frontiers in Oncology

TYPE Case Report
PUBLISHED 29 September 2025
DOI 10.3389/fonc.2025.1602732



OPEN ACCESS

EDITED BY
Sharon R. Pine,
University of Colorado, United States

REVIEWED BY
Bilgin Kadri Aribas,
Bülent Ecevit University, Türkiye
Nektarios I. Koufopoulos,
University General Hospital Attikon, Greece
Cherry Bansal,
Tantia University, India

*CORRESPONDENCE
Jianyong Zhang
zhangjy92@126.com
Yunsong Peng
pys@mail.ustc.edu.cn

RECEIVED 30 March 2025
ACCEPTED 09 September 2025
PUBLISHED 29 September 2025

CITATION
Ding T, Zheng Y, Zhang J and Peng Y (2025) Benign tumor mimicking cancer in breast: a case report.
*Front. Oncol.* 15:1602732.
doi: 10.3389/fonc.2025.1602732



# Benign tumor mimicking cancer in breast: a case report

Tingting Ding[1], Yu Zheng[2], Jianyong Zhang[3]* and Yunsong Peng[4]*

[1]Department of Pathology, Affiliated Hospital of Guizhou Medical University, Guiyang, Guizhou, China, [2]Department of Breast Surgery, Affiliated Hospital of Guizhou Medical University, Guiyang, China, [3]Department of Vascular and Thyroid Surgery, Guizhou Provincial People's Hospital, Guiyang, Guizhou, China, [4]Department of Medical Imaging, Guizhou Provincial People's Hospital, Guiyang, Guizhou, China

Breast granular cell tumor (BGCT) is a rare neoplasm that typically presents as a benign lesion but is frequently misdiagnosed as breast cancer prior to biopsy. Herein, we report a case of BGCT that was initially suspected to be breast cancer based on preoperative physical examination and imaging findings. A 39-year-old Asian woman presented with a firm and painless mass in the right breast. Color Doppler ultrasonography revealed a 15 mm × 15 mm × 14 mm nodule in the upper inner quadrant of the right breast without obvious blood flow signal. On magnetic resonance imaging (MRI), dynamic contrast-enhanced sequences demonstrated homogeneous enhancement. Both ultrasonography and MRI reported the lesion as the Breast Imaging Reporting and Data System (BI-RADS) Category 4B. Based on these findings, the patient was clinically suspected to be an early breast cancer. A surgical plan was formulated, beginning with an excisional frozen section with negative margins and proceeding to breast-conserving surgery if necessary. Frozen section analysis confirmed the presence of a tumor but could not determine whether the lesion was benign, malignant, or borderline. Histopathological examination with hematoxylin-eosin staining and immunohistochemistry ultimately established the diagnosis of BGCT. Early and accurate diagnosis is crucial for developing appropriate treatment plans for breast neoplasms. Given the unique characteristics and rarity of these tumors, clinicians, radiologists and pathologists should remain vigilant and consider the possibility of BGCT in the differential diagnosis.

KEYWORDS

**breast granular cell tumor, breast cancer, misdiagnosis, radiology, histopathology**

## 1 Introduction

Granular cell tumor (GCT) is a rare neoplasm (1), typically benign, with malignancy occurring in fewer than 1% of cases (2). It is currently widely believed to originate from Schwann cells of peripheral nerves (3). GCTs can arise in virtually any part of the body and may present as multicentric lesions (4). They most commonly occur in the head and neck

region, with breast involvement being relatively rare, accounting for approximately 6–8% of all cases (5). A breast granular cell tumor (BGCT) prevalence of 1:1000 to 1:600 among breast malignancies has been widely reported (6). Notably, BGCT can coexist with breast carcinoma (6). Definitive diagnosis of BGCT relies on histopathological examination and immunohistochemistry (7). Complete surgical excision remains the most effective treatment strategy (1, 7). This case is of particular interest because BGCT can closely mimic invasive breast carcinoma on clinical and radiologic evaluation. Its rarity and overlapping features with malignancy may lead to misdiagnosis and potentially inappropriate treatment.

Clinically, when a breast lesion is suspected to be malignant, mammography, ultrasonography, and magnetic resonance imaging (MRI) are all recommended imaging modalities (8, 9). Additionally, several derivative imaging techniques have been developed to differentiate breast lesions, such as ultrasonography contrast imaging and digital breast tomosynthesis (10, 11). In Asia, ultrasonography is routinely used as the initial imaging modality for premenopausal patients with breast lesions. In cases of fatty breast tissue, mammography is also recommended. If physical examination or ultrasonography suggests a high likelihood of malignancy, mammography and MRI are directly added. Herein, we report a case of BGCT that mimicked carcinoma on ultrasonography and MRI. The diagnosis was confirmed by histological examination, and this case is presented to enhance readers' understanding of BGCT.

## 2 Case presentation

A 39-year-old woman presented to our department with a 10-day history of a right breast mass, initially detected during a routine health check-up. She had no known personal or family history of breast cancer. Physical examination revealed a palpable and firm and painless mass in the upper inner quadrant of the right breast, with unclear margins. No enlarged lymph nodes were palpable in the right axilla. Color Doppler ultrasonography of the right breast identified a hypoechoic nodule at the 2–3:00 position at the edge of the glandular tissue in the right breast (Figure 1A). The nodule measured approximately 15 mm × 15 mm × 14 mm, with an irregular shape, angulated and spiculated margins, uniform internal echoes, significant posterior acoustic shadowing, and no obvious blood flow signal. It was classified as the Breast Imaging Reporting and Data System (BI-RADS) Category 4B. Breast MRI showed a mass in the upper inner quadrant of the right breast, measuring approximately 15 mm × 13 mm × 8 mm. The mass exhibited low signal intensity on T1-weighted imaging (T1WI), slightly high signal intensity on T2-weighted imaging (T2WI) (Figure 1B), central low signal intensity, and slightly high signal intensity on diffusion-weighted imaging (DWI). Apparent diffusion coefficient (ADC) mapping revealed reduced signal intensity, and dynamic contrast enhancement demonstrated homogeneous enhancement. The time-intensity curve (TIC) exhibited a slow-rising pattern, and the lesion was classified as BI-RADS 4B (Figure 1C). Mammography was not performed due to the lesion's small size, its location in the upper-inner quadrant of the right breast edge, and its proximity to the chest wall, which rendered mammography unsuitable for evaluation. Computed tomography (CT) of chest and abdominal ultrasonography showed no abnormalities. There was no evidence of axillary lymph node enlargement according to her imaging findings.

Given the suspicion of early breast cancer, a surgical plan was made to perform a wide excision first because of the infiltrative pattern of the lesion under general anesthesia for pathological investigations. If intraoperative frozen section analysis indicated malignancy, a breast-conserving surgery with radical resection would be considered. During surgery, frozen section analysis suggested that the lesion was likely a benign tumor, and that there were no tumor cells at the surgical margins. Postoperative histopathological examination with hematoxylin-eosin staining revealed disrupted normal breast tissue architecture with nests of large polygonal tumor cells with abundant eosinophilic granular cytoplasm infiltrating the surrounding breast parenchyma (Figure 2A), consistent with a tumor. Immunohistochemical staining results were as follows: S100 (+), CK (−), Vimentin (+), CD68 (+), CK7 (−), CK5/6 (−), PAS (+), NSE (+), Ki-67 (1%+), E-cadherin (+), P120 (+), Calretinin (+), α-Inhibin (+), SOX10 (+), P53 (wild-type), HER2 (0), GATA3 (−), ER (−), PR (−), GCDFP-15 (−), Mammaglobin (−), Desmin (−), SMA (−), PAX8 (−), P63 (−) and AR (−). Several of these markers are shown in Figures 2B-F. The final diagnosis was a benign BGCT.

## 3 Discussion

BGCTs typically present as firm, painless palpable masses (1). While imaging may occasionally reveal well-circumscribed lesions suggestive of benign pathology (4, 12), BGCTs often appear spiculated or poorly defined, mimicking the radiological features of breast carcinoma and thus are frequently misdiagnosed preoperatively (2, 13–16). These tumors are most commonly located in the upper inner quadrant, as in the case we report. This distribution is currently attributed to their origin from the intramammary branches of the supraclavicular nerve, whereas primary breast carcinomas more frequently arise in the upper outer quadrant (13). Surgeons, radiologists and pathologists should remain vigilant and consider these tumors as part of the differential diagnosis when evaluating breast masses.

Radiologic imaging has limited sensitivity in detecting BGCTs (17, 18). Ultrasonographically, benign BGCTs may display malignant features such as a solid, heterogeneous mass with indistinct margins and a high depth-to-width ratio (19), as demonstrated in our case. However, some cases may show benign characteristics with well-defined margins (4, 12). On mammography, BGCTs typically appear as small lesions (<3 cm), though lesions up to 6 cm have been reported (7). They may present as circumscribed masses or indistinct, spiculated

**Abbreviations:** BGCT, breast granular cell tumor; MRI, magnetic resonance imaging; BI-RADS, Breast Imaging Reporting and Data System; GCT, granular cell tumor; T1WI, T1-weighted images; T2WI, T2-weighted images; DWI, diffusion-weighted imaging; ADC, apparent diffusion coefficient; TIC, time-intensity curve; CT, computed tomography; CEUS, contrast-enhanced ultrasonography; NSE, neuron-specific enolase; PAS, periodic acid–Schiff.

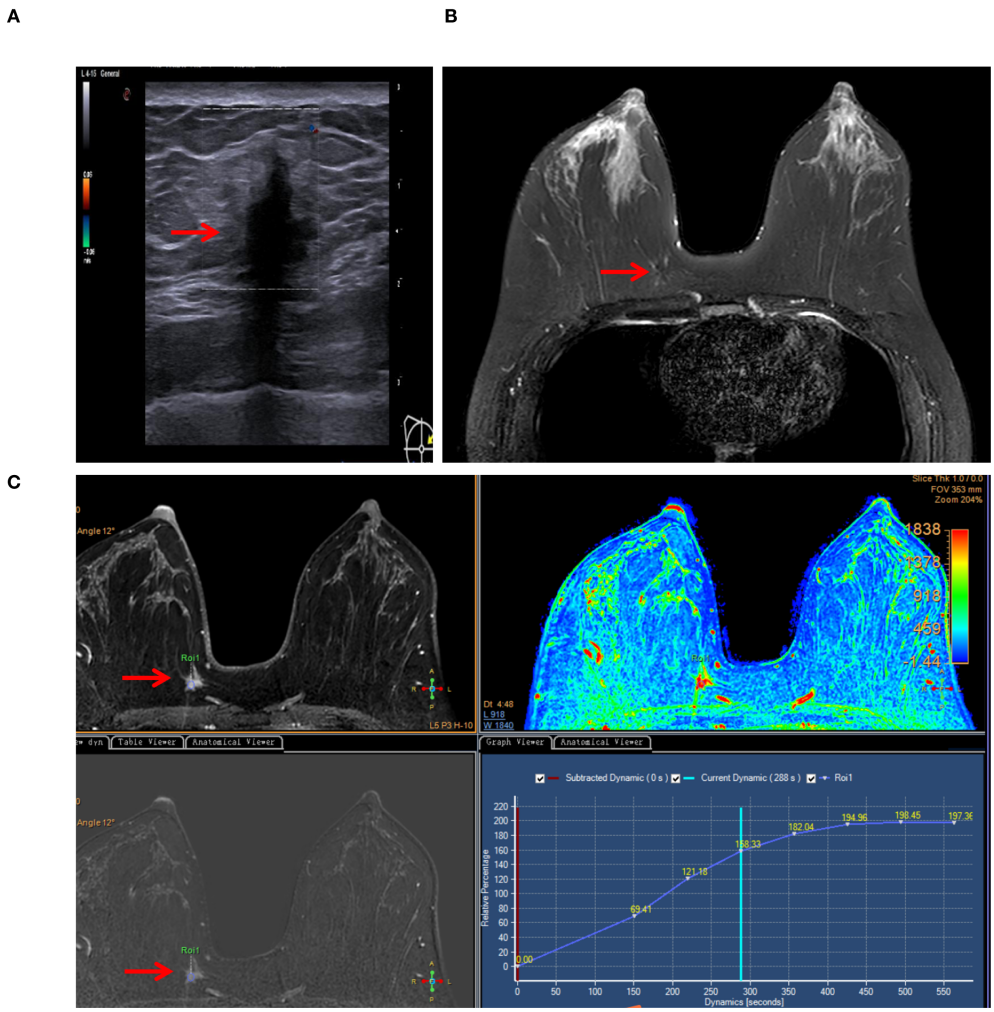


FIGURE 1
Typical imaging findings (lesion marked by arrows). **(A)** Color Doppler ultrasonography detected a noncapsular mass in the upper inner quadrant of the right breast (15×15×14 mm). **(B)** Breast MRI revealed a mass in the right breast (15×13×8 mm), exhibiting slightly high signal intensity on T2-weighted imaging (T2WI). **(C)** MRI dynamic contrast enhancement, silhouette image, Apparent diffusion coefficient (ADC) mapping (pseudo-color image), dynamic contrast enhancement and the time-intensity curve (TIC).

lesions without calcification, further complicating differentiation from malignancy (20). MRI, including dynamic contrast-enhanced sequence, has limited sensitivity for diagnosing BGCTs but remains valuable for assessing lesion extent and multifocality (21, 22). Some studies report low-to-intermediate signal intensity on T1WI and a lack of hyperintensity on T2WI, consistent with our case. Although dynamic MRI kinetic curves and enhancement patterns may aid in distinguishing between benign and malignant lesions, the role of DWI and ADC values in assessing tumor aggressiveness remains controversial (23). To date, no specific imaging features have been definitively associated with BGCTs. Some authors reported homogeneous enhancement on T1WI images and ring-like enhancement on T2WI sequences. T1WI signals are typically low to intermediate, while T2WI signals can be variable (24). For breast masses in which malignancy cannot be excluded, we believe that contrast-enhanced ultrasonography (CEUS) serves as an important supplementary diagnostic tool (25). CEUS can further reveal the blood perfusion characteristics and dynamic changes of the lesion, thereby aiding in the evaluation of its nature, particularly for those classified as BI-RADS 4 based on Doppler ultrasonography findings.

Grossly, BGCTs appear as small, firm, grayish-white nodules with a dense cut surface. Microscopically, the tumor is characterized by aggregates of loosely infiltrating large round or polygonal cells with abundant eosinophilic granular cytoplasm and variable amounts of collagenous stroma. Nuclei are generally small and centrally located (1). The infiltrative nature of these tumors, combined with prominent nucleoli, necessitates distinction from scirrhous carcinoma and apocrine carcinoma (13). The hallmark histologic feature aiding in differential diagnosis is the presence of granular cytoplasm within the tumor cells.

Immunohistochemically, BGCTs are negative for estrogen receptor, progesterone receptor, and human epidermal growth factor receptor 2. They are believed to originate from Schwann cells of neural origin, which explains their strong positivity for S100 protein, vimentin, and neuron-specific enolase (NSE), and negativity for pan-cytokeratin. Additionally, BGCTs often express

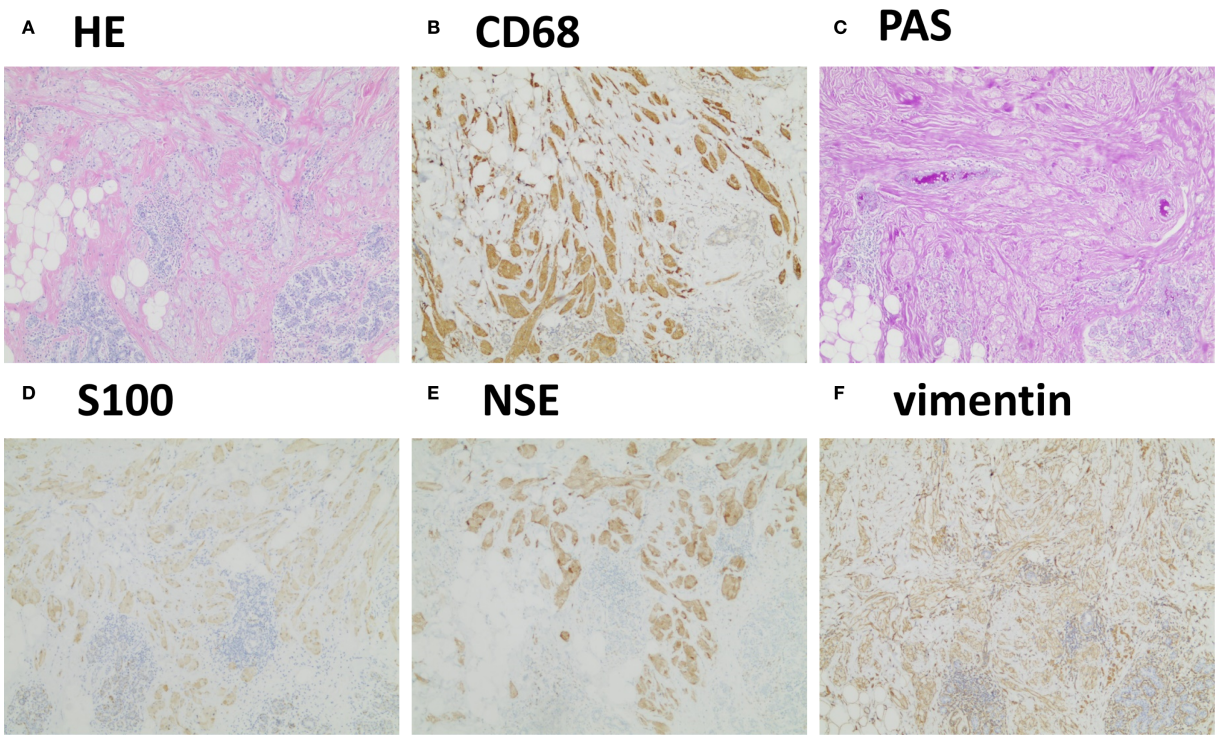


FIGURE 2
Typical histopathological findings. **(A)** Hematoxylin–eosin staining revealed disrupted normal breast tissue architecture with nests of atypical cells featuring abundant cytoplasm. **(B-F)** Immunohistochemistry showed positivity for CD68, PAS, S100, NSE, and vimentin (4×).

CD68 and stain positive for periodic acid–Schiff (PAS), indicative of lysosomal activity in approximately 90% of cases (6). The Ki-67 proliferation index is an important marker of tumor aggressiveness (26). Given their typically benign nature, most of them exhibit a Ki-67 index of <2%. In evaluating potential malignancy, Ki-67 index must be considered in conjunction with clinical course and mitotic activity (26).

Malignant transformation is rare, accounting for <1% of all GCTs, including those of the breast (3). Nevertheless, cases of malignant BGCT have been reported. Malignant GCTs are classified as high-grade sarcomas, with high metastatic potential and poor prognosis (26). Features suggestive of malignancy include: tumor size ≥ 4 cm, increased mitotic rate (≥2 mitoses per 10 high-power fields at 400× magnification), rapid growth, evidence of local invasion, marked cellular pleomorphism (1).

Histopathologic confirmation should be obtained prior to treatment for suspected malignant lesions. Although diagnosis via fine-needle aspiration or intraoperative frozen section has been reported (12), this approach depends heavily on the expertise of the pathologist. Core needle biopsy (1, 3, 27), excisional biopsy (7, 16), and vacuum-assisted breast biopsy are considered more reliable methods. Histopathologic examination and immunohistochemistry remain the gold standard for diagnosis. Inappropriate pathological assessment may lead to overtreatment (2, 28, 29).

Complete surgical excision with negative margins remains the only treatment of choice (1). Wide local excision is the most widely accepted surgical strategy and is essential for further pathological evaluation after biopsy. Recurrence of benign BGCTs is extremely rare. Even in cases with positive margins, the risk of long-term recurrence is low (30). In the event of lymph node metastasis from malignant BGCTs, axillary lymph node dissection is warranted. Long-term follow-up (up to 10 years) is recommended (30).

This case is of particular interest due to the rarity of BGCTs in the breast. A thorough understanding of their clinicopathologic and radiologic features is critical for the accurate differentiation from breast carcinoma.

## Data availability statement

The original contributions presented in the study are included in the article/supplementary material. Further inquiries can be directed to the corresponding authors.

## Ethics statement

The studies involving humans were approved by Ethics Committee of the Affiliated Hospital of Guizhou Medical University. The studies were conducted in accordance with the local legislation and institutional requirements. The participants provided their written informed consent to participate in this study. Written informed consent was obtained from the individual(s) for the publication of any potentially identifiable images or data included in this article.

## Author contributions

TD: Data curation, Writing – original draft, Writing – review & editing. YZ: Funding acquisition, Methodology, Validation, Writing – original draft, Writing – review & editing. JZ: Funding acquisition, Resources, Writing – original draft, Writing – review & editing. YP: Funding acquisition, Writing – original draft, Writing – review & editing.

## Funding

The author(s) declare financial support was received for the research and/or publication of this article. This work was supported by the National Natural Science Foundation of China under Grand 82460590 (YP), 82302286 (YZ), 82060390 (JZ) and the health research project of Guizhou Province gzwkj2025-302 (JZ).

## Acknowledgments

We thank the patient for granting permission to publish this information.

## Conflict of interest

The authors declare that the research was conducted in the absence of any commercial or financial relationships that could be construed as a potential conflict of interest.

## Generative AI statement

The author(s) declare that no Generative AI was used in the creation of this manuscript.

Any alternative text (alt text) provided alongside figures in this article has been generated by Frontiers with the support of artificial intelligence and reasonable efforts have been made to ensure accuracy, including review by the authors wherever possible. If you identify any issues, please contact us.

## Publisher's note



## References

1. De Simone N, Aggon A, Christy C. Granular cell tumor of the breast: clinical and pathologic characteristics of a rare case in a 14-year-old girl. *J Clin Oncol*. (2011) 29: e656–7. doi: 10.1200/JCO.2011.35.9448

2. Akbari A, Behravan P, Moradi A, Akbari ME. Case report of a benign granular cell tumor resembling breast carcinoma in a young woman: A diagnostic challenge. *Case Rep Oncol*. (2024) 17:608–13. doi: 10.1159/000538771

3. James NE, Guan Y, Musa F, Cuffolo G. Granular cell tumour of the breast. *BMJ Case Rep*. (2024) 17(8):e258326. doi: 10.1136/bcr-2023-258326

4. Adeniran A, Al-Ahmadie H, Mahoney MC, Robinson-Smith TM. Granular cell tumor of the breast: a series of 17 cases and review of the literature. *Breast J*. (2004) 10:528–31. doi: 10.1111/j.1075-122X.2004.21525.x

5. Miller JA, Karcnik TJ, Karimi S. Granular cell tumor of the breast: definitive diagnosis by sonographically guided percutaneous biopsy. *J Clin Ultrasound*. (2000) 28:89–93. doi: 10.1002/(SICI)1097-0096(200002)28:2<89::AID-JCU6>3.0.CO;2-N

6. Brown AC, Audisio RA, Regitnig P. Granular cell tumour of the breast. *Surg Oncol*. (2011) 20:97–105. doi: 10.1016/j.suronc.2009.12.001

7. Albasri AM, Ansari IA, Aljohani AR, Alhujaily AS. Granular cell tumour of the breast in a young female: A case report and literature review. *Niger J Clin Pract*. (2019) 22:742–4. doi: 10.4103/njcp.njcp_282_18

8. Luo L, Wang X, Lin Y, Ma X, Tan A, Chan R, et al. Deep learning in breast cancer imaging: A decade of progress and future directions. *IEEE Rev Biomed Engineering*. (2025) 18:130–51. doi: 10.1109/RBME.2024.3357877

9. Kong X, Zhang Q, Wu X, Zou T, Duan J, Song S, et al. Advances in imaging in evaluating the efficacy of neoadjuvant chemotherapy for breast cancer. *Front Oncol*. (2022) 12:816297. doi: 10.3389/fonc.2022.816297

10. Pötsch N, Vatteroni G, Clauser P, Helbich TH, Baltzer PAT. Contrast-enhanced mammography versus contrast-enhanced breast MRI: A systematic review and meta-analysis. *Radiology*. (2022) 305:94–103. doi: 10.1148/radiol.212530

11. van Nijnatten TJA, Morscheid S, Baltzer PAT, Clauser P, Alcantara R, Kuhl CK, et al. Contrast-enhanced breast imaging: Current status and future challenges. *Eur J Radiol*. (2024) 171:111312. doi: 10.1016/j.ejrad.2024.111312

12. El Aouni N, Laurent I, Terrier P, Mansouri D, Suciu V, Delaloge S, et al. Granular cell tumor of the breast. *Diagn Cytopathol*. (2007) 35:725–7. doi: 10.1002/dc.20736

13. Hammas N, El Fatemi H, Jayi S, Hafid I, Fikri G, El Houari A, et al. Granular cell tumor of the breast: a case report. *J Med Case Rep*. (2014) 8:465. doi: 10.1186/1752-1947-8-465

14. Ito M, Amari M, Sato A, Hikichi M. Granular cell tumor mimicking breast carcinoma: A report of two cases. *Cureus*. (2024) 16:e57500. doi: 10.7759/cureus.57500

15. Leo C, Briest S, Pilch H, Schütz A, Horn LC, Leinung S. Granular cell tumor of the breast mimicking breast cancer. *Eur J Obstet Gynecol Reprod Biol*. (2006) 127:268–70. doi: 10.1016/j.ejogrb.2006.01.026

16. Gogas J, Markopoulos C, Kouskos E, Gogas H, Mantas D, Antonopoulou Z, et al. Granular cell tumor of the breast: a rare lesion resembling breast cancer. *Eur J Gynaecol Oncol*. (2002) 23:333–4.

17. Akatsu T, Kobayashi H, Uematsu S, Tamagawa E, Shinozaki H, Kase K, et al. Granular cell tumor of the breast preoperatively diagnosed by fine-needle aspiration cytology: report of a case. *Surg Today*. (2004) 34:760–3. doi: 10.1007/s00595-004-2784-7

18. Corines MJ, Krystel-Whittemore M, Murray M, Mango V. Uncommon tumors and uncommon presentations of cancer in the breast. *Curr Breast Cancer Rep*. (2021) 13:331–46. doi: 10.1007/s12609-021-00435-x

19. Irshad A, Pope TL, Ackerman SJ, Panzegrau B. Characterization of sonographic and mammographic features of granular cell tumors of the breast and estimation of their incidence. *J Ultrasound Med*. (2008) 27:467–75. doi: 10.7863/jum.2008.27.3.467

20. Iglesias A, Arias M, Santiago P, Rodríguez M, Mañas J, Saborido C. Benign breast lesions that simulate Malignancy: magnetic resonance imaging with radiologic-pathologic correlation. *Curr Probl Diagn Radiol*. (2007) 36:66–82. doi: 10.1067/j.cpradiol.2006.12.001

21. Abreu N, Filipe J, André S, Marques JC. Granular cell tumor of the breast: correlations between imaging and pathology findings. *Radiol Bras*. (2020) 53:105–11. doi: 10.1590/0100-3984.2019.0056

22. Scaranelo AM, Bukhanov K, Crystal P, Mulligan AM, O'Malley FP. Granular cell tumour of the breast: MRI findings and review of the literature. *Br J Radiol*. (2007) 80:970–4. doi: 10.1259/bjr/95130566

23. Aydin H, Guner B, Esen Bostanci I, Bulut ZM, Aribas BK, Dogan L, et al. Is there any relationship between adc values of diffusion-weighted imaging and the histopathological prognostic factors of invasive ductal carcinoma? *Br J Radiol*. (2018) 91:20170705. doi: 10.1259/bjr.20170705

24. Moffa G, Galati F, Panzironi G, Rizzo V, Kripa E, Pediconi F. Granular cell tumor of the breast: Tip and tricks on conventional and magnetic resonance imaging. *Breast J*. (2020). doi: 10.1111/tbj.14113

25. Zhu M, Xu H, Chen Y, Peng Y. Multimodal ultrasonography findings of extramammary granular cell tumors: Two case reports. *Front Oncol*. (2023) 13:1136770. doi: 10.3389/fonc.2023.1136770

26. Akahane K, Kato K, Ogiso S, Sakaguchi K, Hashimoto M, Ishikawa A, et al. Malignant granular cell tumor of the breast: case report and literature review. *Breast Cancer*. (2015) 22:317–23. doi: 10.1007/s12282-012-0362-1

27. Corso G, Di Nubila B, Ciccia A, De Camilli E, Vicini E, Trentin C, et al. Granular cell tumor of the breast: Molecular pathology and clinical management. *Breast J*. (2018) 24:778–82. doi: 10.1111/tbj.13036

28. Ohnishi H, Nishihara K, Tamae K, Mitsuyama S, Abe R, Toyoshima S, et al. Granular cell tumors of the breast: a report of two cases. *Surg Today*. (1996) 26:929–32. doi: 10.1007/BF00311799

29. Bauerfeind I, Ditsch N, Sittek H, Diebold J. Reduction mammaplasty in granular cell tumour of the breast. *Br J Plast Surg*. (2004) 57:458–61. doi: 10.1016/j.bjps.2003.12.019

30. Papalas JA, Wylie JD, Dash RC. Recurrence risk and margin status in granular cell tumors of the breast: a clinicopathologic study of 13 patients. *Arch Pathol Lab Med*. (2011) 135:890–5. doi: 10.5858/2010-0430-OAR.1

# Frontiers in Oncology

**Advances knowledge of carcinogenesis and tumor progression for better treatment and management**

The third most-cited oncology journal, which highlights research in carcinogenesis and tumor progression, bridging the gap between basic research and applications to imrpove diagnosis, therapeutics and management strategies.

---

## Discover the latest Research Topics

See more →


**Frontiers**

Avenue du Tribunal-Fédéral 34
1005 Lausanne, Switzerland
frontiersin.org

**Contact us**

+41 (0)21 510 17 00
frontiersin.org/about/contact